CONTROL OF KEY POLYMER PROPERTIES VIA REVERSIBLE ADDITION-FRAGMENTATION CHAIN TRANSFER IN EMULSION POLYMERIZATION

By

Ibrahem Suleiman Altarawneh

B.Sc (Chemical Engineering) Hons,
M.Sc (Engineering Studies) Hons

A thesis submitted in fulfillment of the requirements for the degree of

Doctor of Philosophy in
Process Systems Engineering

School of Chemical and Bio-Molecular Engineering

The University of Sydney, NSW, 2006

AUSTRALIA

August 2008

Declaration

I declare that the entire contents of this thesis are, to the best of my knowledge and belief, original, unless otherwise acknowledged in the text. It should be noted that the experimental data used in Chapter 3 were taken from the literature, and the original sources of these data were clearly stated and acknowledged. This thesis contains no material that has been presented for a degree or diploma at this or any other institute of higher education.

Ibrahem Suleiman Altarawneh

August 2008

Acknowledgment

My heartfelt and sincere thanks go to A/Prof. Vincent Gomes who has been more than just a supervisor over the course of this Ph.D. Your support, advice, and wise counsel are greatly appreciated. It was a great pleasure for me to study under a well knowledgeable and highly skilled supervisor, and I hope to be able to provide the same in return.

I would like to thank A/Prof. Fariba Dehghani, my associate supervisor, for her continuous support during my PhD. I also acknowledge Dr. Mourtada Srour for his insightful suggestions and for sharing his knowledge in emulsion polymerization kinetics. I would be remiss without noting the technical and administrative staff in the school, especially, Dr. Jeffrey Shi, Annette, Regina, Katharyn, Dennis Trevaskis who made my daily activities run smoothly. I also gratefully acknowledge the generous financial support from Al-Hussein Bin Talal University.

My closest friends, Dr. Moamar Aljefout and Saleh Rawadieh, are considered as a part of my family, and members of family do not forget each other. We had nice times and memories that will never be forgotten. I would also like to express my great appreciation to the Arabic community in Sydney, especially my dear friends Dr. Ahamd khwaldeh, Ali Alhaj, Mustafa Sowan, Dr. Fayez Wahwah, Mohamed Saleh Altarawneh and many others, who had alleviated the pain and agony of being away from home.

I would like to hand my special thanks to my wife Dr. Maysa Khadra for her continuous support, encouragement and love. Finally, I would like to thank my mother, brothers and sisters for their effort, encouraging words, cheering and love feelings.

To everyone who helped in this project… thank you!

TO MY PARENTS, SISTERS AND BROTHERS

Summary

Free radical emulsion polymerization (FRP) is widely adopted in industry due to its applicability to a wide range of monomers. Despite its many benefits and wide spread use, the fast chain growth and the presence of rapid irreversible termination impose limitations with respect to the degree of control in FRP. Furthermore, producing block copolymers and polymers with complex structures via FRP is not feasible. Closer control of macromolecular chain structure and molar mass, using novel polymerization techniques, is required to synthesize and optimize many new polymer products. Reversible addition fragmentation chain transfer (RAFT)-mediated polymerization is a novel controlled living free radical technique used to impart living characters in free radical polymerization. In combination with emulsion polymerization, the process is industrially promising and attractive for the production of tailored polymeric products. It allows for the production of particles with specially-tailored properties, including size, composition, morphology, and molecular weights.

The mechanism of RAFT process and the effect of participating groups were discussed with reviews on the previous work on rate retardation. A mathematical model accounting for the effect of concentrations of propagating, intermediate, dormant and dead chains was developed based on their reaction pathways. The model was combined with a chain-length dependent termination model in order to account for the decreased termination rate. The model was validated against experimental data for solution and bulk polymerizations of styrene. The role of the intermediate radical and the effect of RAFT agent on the chain length dependent termination rate were addressed theoretically. The developed kinetic model was used with validated kinetic parameters to assess the observed retardation in solution polymerization of styrene with high active RAFT agent (cumyl dithiobenzoate). The fragmentation rate coefficient was used as a model parameter, and a value equal to 6×10^{4} s^{-1} was found to provide a good agreement with the experimental data. The model predictions indicated that the observed retardation could be attributed to the cross termination of the intermediate radical and, to some extent, to the RAFT effect on

increasing the average termination rate coefficient. The model predictions showed that to preserve the living nature of RAFT polymerization, a low initiator concentration is recommended. In line with the experimental data, model simulations revealed that the intermediate radical prefers fragmentation in the direction of the reactant.

The application of RAFT process has also been extended to emulsion polymerization of styrene. A comprehensive dynamic model for batch and semi-batch emulsion polymerizations with a reversible addition-fragmentation chain transfer process was developed. To account for the integration of the RAFT process, new modifications were added to the kinetics of zero-one emulsion polymerization. The developed model was designed to predict key polymer properties such as: average particle size, conversion, particle size distribution (PSD), and molecular weight distribution (MWD) and its averages. The model was checked for emulsion polymerization processes of styrene with O-ethylxanthyl ethyl propionate as a RAFT based transfer agent. By using the model to investigate the effect of RAFT agent on the polymerization attributes, it was found that the rate of polymerization and the average size of the latex particles decreased with increasing amount of RAFT agent. It was also found that the molecular weight distribution could be controlled, as it is strongly influenced by the presence of the RAFT based transfer agent.

The effects of RAFT agent, surfactant (SDS), initiator (KPS) and temperature were further investigated under semi-batch conditions. Monomer conversion, MWD and PSD were found to be strongly affected by monomer feed rate. With semi-batch mode, Mn and <r> increased with increasing monomer flow rate. Initiator concentration had a significant effect on PSD. The results suggest that living polymerization can be approached by operating under semi-batch conditions where a linear growth of polymer molecular weight with conversion was obtained.

The lack of online instrumentation was the main reason for developing our calorimetry-based soft-sensor. The rate of polymerization, which is proportional to the heat of reaction, was estimated and integrated to obtain the overall monomer conversion. The calorimetric model developed was found to be capable of estimating polymer molecular weight via

simultaneous estimation of monomer and RAFT agent concentrations. The model was validated with batch and semi-batch emulsion polymerization of styrene with and without RAFT agent. The results show good agreement between measured conversion profiles by calorimetry with those measured by the gravimetric technique. Additionally, the number average molecular weight results measured by SEC (GPC) with double detections compare well with those calculated by the calorimetric model. Application of the offline dynamic optimisation to the emulsion polymerization process of styrene was investigated for the PSD, MWD and monomer conversion. The optimal profiles obtained were then validated experimentally and a good agreement was obtained.

The gained knowledge has been further applied to produce polymeric particles containing block copolymers. First, methyl acrylate, butyl acrylate and styrene were polymerized separately to produce the first block. Subsequently, the produced homopolymer attached with xanthate was chain-extended with another monomer to produce block copolymer under batch conditions. Due to the formation of new particles during the second stage batch polymerization, homopolymer was formed and the block copolymer produced was not of high purity. The process was further optimized by operating under semi-batch conditions. The choice of block sequence was found to be important in reducing the influence of terminated chains on the distributions of polymer obtained. It has been found that polymerizing styrene first followed by the high active acrylate monomers resulted in purer block copolymer with low polydispersity confirmed by GPC and H-NMR analysis.

Author publications

Publications generated from this work:

1. Altarawneh, I. S.; Gomes, V. G.; Srour, M. H. Polymer Chain Extension in Semi-Batch Emulsion Polymerization with RAFT Based Transfer Agent: The Influence of Reaction Conditions on Polymerization Rate and Product Properties. Journal of Applied polymer Science (accepted, May 2008).

2. Altarawneh, I. S.; Gomes, V. G.; Srour, M. H. The Influence of Xanthate Based Transfer Agents on Styrene Emulsion Polymerization: Mathematical Modelling and Model Validation. Macromolecular Reaction Engineering, (2008), **2**(1): p. 58-79.

3. Altarawneh, I. S.; Srour, M. H. and Gomes, V. G. RAFT with Bulk and Solution Polymerization: An Approach to Mathematical Modelling and Validation. Polymer-Plastics Technology and Engineering, (2007), **46**(11): p. 1103-1115

4. Altarawneh, I. S., Jung, J., Srour, M. H and Gomes, V.G., Controlled Living Emulsion Polymerization. Australasian Chemical Engineering Conference CHEMECA, 28-Septemper – 1 October, 2008, Newcastle, Australia

5. Altarawneh, I. S.; Srour, M. H.; Gomes, V. G. Manipulating Polymer Mass via Reversible Addition-Fragmentation Chain Transfer in Emulsion Polymerization Process. The Second Jordanian International Conference of Materials Science and Engineering, 4-6 September, 2007, Al-Salt Jordan.

6. Altarawneh, I. S.; Srour, M. H; Gomes, V. G. Kinetic considerations in RAFT-mediated homogenous polymerization. 17th International Congress of Chemical and Process Engineering, 27-31 August, 2006, Prague-Czech Republic

Related publications:

7. Srour, M. H.; Gomes, V. G.; Altarawneh, I. S.; Romagnoli, J. A. Inferential Conversion and Composition Monitoring via Microcalorimetric Measurements in Emulsion Terpolymerization. Polymer-Plastics Technology and Engineering, (2008), **47**(1): p. 13 - 22.

8. Srour, M. H., Gomes, V. G. & Altarawneh, I. S. Optimal operating strategies for emulsion terpolymerisation. Chemical Engineering Science, (2008), 63, 4257.

9. Srour, M. H.; Gomes, V. G.; Altarawneh, I. S.; Bhushan, B.; Romagnoli, J. A, Online Control of Emulsion Terpolymerisation Process Using Multivariable Model Predictive Control, Chemical Engineering Science **(Submitted)**

Publications In progress:

Altarawneh, I. S.; Gomes, V. G; Srour, M. H. Synthesis of Di-and Tri-block copolymers via RAFT process in emulsion polymerization

Altarawneh, I. S.; Gomes, V. G; Srour, M.H. Inferential monitoring of monomer conversion and polymer molecular weight in RAFT-emulsion polymerisation through calorimetric measurements

Table of Contents

Chapter 4: Modelling of RAFT in Emulsion Polymerization

Chapter 5: Experimental Setup and Model Validation

Chapter 6: Polymer Chain Extension

Chapter 7: Calorimetry and Process Optimization

Chapter 8: Block Copolymerization

Chapter 9: Conclusions and Future Directions

List of Figures

List of Schemes

List of Tables

Glossary of Symbols and Abbreviations

symbol	definition	typical units
a_s	Minimum area occupied by a single surfactant molecule on a particle surface	dm^2
A	Heat transfer area	m^2
AA	Acrylic acid	dm^2
A_B	Base area of the reactor	m^2
A_p	Particles surface area	dm^2
AR	Initial RAFT agent	
AR_o	Initial RAFT agent concentration	mol/l
$AIBN$	Azobisisobutyronitrile, Oil soluble initiator	
$ATRP$	Atom transfer radical polymerization	
AP	Polymeric RAFT agent (macro-RAFT agent)	
$B(V,V^{'})$	Rate coefficient of coagulation of two particles of volume V and V'	1/mol.s
BA	Butyl acrylate	
cmc	Critical micelle concentration	mol/l
$C_{micelle}$	Micelles concentration	mol/l
C_p^{AR}	Initial RAFT agent concentration in the latex particles	mol/l
$C_{p\_sat}^{AR}$	Saturated initial RAFT agent concentration in the latex particles	mol/l
C_p^{AP}	Polymeric RAFT agent concentration in the latex particles	mol/l
C_p^{M}	monomer concentration in the latex particles	mol/l
C_p^{Rad}	concentration of all radicals inside the particle	
C_{tr}	Transfer constant to RAFT agent	
$C_{p\_sat}^{M}$	Saturated monomer concentration in the latex particles	mol/l
C_w^{AR}	Initial RAFT agent concentration in the aqueous phase	mol/l
$C_{w\_sat}^{AR}$	Saturated initial RAFT agent concentration in the aqueous phase	mol/l
C_w^{M}	monomer concentration in the aqueous phase	mol/l
$C_{w\_sat}^{M}$	Saturated monomer concentration in the aqueous phase	mol/l
CLD	Chain length dependent	
$CSIRO$	Commonwealth Scientific and Industrial Research Organization	
$CLFRP$	Controlled living free radical polymerization	
CDB	Cumyl-dithiobenzoate RAFT agent	

CPDB	2-(2-cyanopropyl) Dithiobenzoate RAFT agent	
CTA	Chain transfer agent	
C_{tr}^{M}	Transfer constant to monomer	
C_{tr}^{I}	Transfer constant to Initiator	
C_{tr}^{CTA}	Transfer constant to transfer agent	
d_{AR}	Density of RAFT agent	kg/l
d_m	Density of monomer	kg/l
d_p	Density of polymer	kg/l
d_R	Reactor diameter	m^2
D	Dead polymer generated from termination between two radicals	mol/l
D_R	Diffusion coefficient for monomer in water	dm^2/s
D_{rd}	Diffusion coefficient for monomer radical	dm^2/s
D_w	Diffusion coefficient for RAFT radical in water	dm^2/s
D_i	Diffusion rate coefficients of chain of length ‘i’	dm^2/s
D_j	Diffusion rate coefficients of chain of length ‘j’	dm^2/s
D_{mon}	Monomer diffusion rate coefficient	dm^2/s
DT	Degenerative transfer	
$[E^{\bullet}]$	Aqueous phase concentration of desorbed radicals	mol/l
EMA	2-(ethoxylcarbonyl)propyl-2-yl dithiobenzoate RAFT agent	
ESP	Electron spin resonance	
f	Initiator efficiency	
F_{AR}	RAFT agent flow rate	g/min
F_I	Initiator flow rate	g/min
F_m	Monomer flow rate	g/min
FRP	Free radical polymerization	
GC	Gas chromatography	
GPC	Gel permeation chromatography	
h_R	Hight of the reaction mixture	m
ΔH_p	Heat of polymerization	
i	Number average degree of polymerization	
I_2	Undecomposed initiator molecule	
$I^{\bullet}$	Decomposed initiator fragment	
$[I]$	Initiator concentration	mol/l
$[I^{\bullet}]$	Initiator fragment concentration	mol/l
IUPAC	International Union of Pure and Applied Chemistry	

j_{crit}	Critical degree of polymerization for homogenous nucleation	
K	Rate of propagation growth per particle	l/s
K'	Equilibrium constant (k_{add} / k_{frag})	
k_{add}	Addition rate coefficient to RAFT agent	1/mol.s
k_{-add}	Inverse addition rate coefficient to RAFT agent	1/mol.s
k_d	First-order rate coefficient for the dissociation of initiator	1/s
k_{diff}	Diffusion controlled rate coefficient	
k_{ct}	Rate coefficient for the cross termination of the intermediate radical	l/mol.s
k_{dM}	Rate coefficient for desorption of monomeric radicals from particles	1/s
k_{dR}	Rate coefficient for desorption of RAFT radicals from particles	1/s
k_e^i	Entry rate coefficient for oligomeric radical	1/mol.s
k_{eE}	Re-entry rate coefficient of desorbed radicals	1/mol.s
k_e^R	Entry rate coefficient for RAFT derived radical	1/mol.s
$k_{e,micelle}^i$	Rate coefficient for entry of an oligomeric radical into a micelle	1/mol.s
$k_{e,micelle}^R$	Rate coefficient for entry of a RAFT radical into a micelle	1/mol.s
K_{frag}	Overall fragmentation rate coefficient	1/mol.s
k_{frag}^{PAP}	Forward fragmentation rate coefficients of the intermediate radical PAP in the latex particles, respectively	1/s
k_{-frag}^{PAP}	Backward fragmentation rate coefficients of the intermediate radical PAP in the latex particles, respectively	1/s
k_{frag}^{RAR}	Forward fragmentation rate coefficients of the intermediate radical RAR in the latex particles, respectively	1/s
k_{-frag}^{RAR}	Backward fragmentation rate coefficients of the intermediate radical RAR in the latex particles, respectively	1/s
k_{frag}^{RAP}	Forward fragmentation rate coefficients of the intermediate radical RAP in the latex particles, respectively	1/s
k_{-frag}^{RAP}	Backward fragmentation rate coefficients of the intermediate radical RAP in the latex particles, respectively	1/s
k_{frag}^{PAR}	Forward fragmentation rate coefficients of the intermediate radical PAR in the latex particles, respectively	1/s
k_{-frag}^{PAR}	Backward fragmentation rate coefficients of the intermediate radical PAR in the latex particles, respectively	1/s
k_p	Propagation rate coefficient	1/mol.s
k_p^i	Propagation rate coefficient of oligomeric radical with degree of polymerization i	1/mol.s
$k_{p,aq}^i$	Propagation rate coefficient of the aqueous phase oligomeric radicals of degree ‘i’	1/mol.s
k_p^R	Propagation rate coefficient of the RAFT radical in the latex phase	1/mol.s

KPS	Potassium per sulfate (water soluble initiator)	
k_{st}	Rate coefficient for the self termination of the intermediate radical	1/mol.s
$< k_t >$	Average second-order rate coefficient for the termination	1/mol.s
$k_{t,aq}$	Aqueous phase termination rate coefficient	1/mol.s
$k_t^{i,j}$	Microscopic termination coefficient between two chains	l/mol.s
k_{tr}	Transfer rate coefficient	1/mol.s
k_{-tr}	Inverse transfer rate coefficient	1/mol. s
$k_{tr,aq}^{AR}$	Transfer rate coefficient to RAFT agent in the aqueous phase	1/mol. s
k_{tr}^{AR}	Transfer rate coefficient to the initial RAFT agent in the latex phase	1/mol. s
k_{tr}^{CTA}	Transfer rate coefficient to transfer agent	1/mol. s
k_{tr}^{I}	Transfer rate coefficient to Initiator	1/mol. s
k_{tr}^{M}	Transfer rate coefficient to monomer	1/mol. s
k_{tc}	Rate coefficient for the termination by combination	1/mol. s
k_{tc}	Rate coefficient for the termination by disproportionation	1/mol. s
$LFRP$	Living free radical polymerization	
m_j	Mass of the jacket content	kg
m_M	Mass of monomer	g
m_p	Mass of polymer	g
M	Monomer molecule	
$M^{\bullet}$	Monomeric radical	
$[M]$	Monomer concentration in homogenous systems	mol/l
$[M_{aq}^{\bullet}]$	Monomeric radical concentration in the aqueous phase	
MA	Methyl acrylate	
Mn	Number average molecular weight	g/mol
MMA	Methyl methacrylate	
Mw	Weight average molecular weight	g/mol
M_w^{AR}	RAFT agent molecular weight	kg/mol
M_w^{M}	Monomer molecular weight	g/mol
MWD	Molecular weight distribution	
n	Particles molar concentration density	mol/l.dm
$\bar{n}$	Average number of radicals per particle	mol/l.dm
n_{agg}	Agglomeration number of surfactant	
$\overline{n_{Int}}$	Average number of intermediate radicals per particle	mol/l.dm
n_o	Molar concentration density of Particles containing no radicals	mol/l.dm

n_1^R	Molar concentration density of Particles containing one R- radical	mol/l.dm
n_1^{RAR}	Molar concentration density of Particles containing RAR intermediate radical	mol/l.dm
n_1^{RAP}	Molar concentration density of Particles containing RAP intermediate radical	mol/l.dm
n_1^P	Molar concentration density of Particles containing one polymeric- radical	mol/l.dm
n_1^{PAR}	Molar concentration density of Particles containing PAR intermediate radical	mol/l.dm
n_1^{PAP}	Molar concentration density of Particles containing PAP intermediate radical	mol/l.dm
N_A	Avogadro's number	
N_{AR}	Number of moles of initial RAFT agent	mol
N_{AP}	Number of moles of polymeric RAFT agent	mol
N_m	Number of moles of monomer	mol
NMP	Nitroxide mediated polymerization	
NMR	Nuclear magnetic resonance	
N_{tot}	Total number of particles	
PAP	Intermediate radical generated from the addition of P to AP	mol/1
PAR	Intermediate radical generated from the addition of P to AR	mol/1
$P_1^\bullet$	Polymeric radical with one monomer unit	
$P_2^\bullet$	Polymeric radical with two monomer units	
$P_3^\bullet$	Polymeric radical with three monomer units	
$P_{aq}^\bullet$	Concentration of the oligomeric radicals in the aqueous phase	mol/1
PBEs	Population balance equations	
PEPDTA	1-phenylethylphenyl dithioacetate RAFT agent	
PEDP	1-phenylethyl Dithiobenzoate RAFT agent	
P_{ij}	Probability of termination	
$P_{j_{crit}}^\bullet$	Polymeric radical with degree of polymerization j_{crit}	
$P_n^\bullet$	Polymeric radical with degree of polymerization n	
$P_m^\bullet$	Polymeric radical with degree of polymerization m	
PPPDTA	2-phenylprop-2-yl Phenyldithioacetate RAFT agent	
PSD	Particle size distribution	
PSPI	Particle size polydispersity index	
$PSt^\bullet$	Polystyrene radical	
q_p	Heat capacity of the reactor content	j/kg.K
q_p^w	Heat capacity of	j/kg.K

Q_f	Heat flow through the reactor wall	j/s
Q_{loss}	Heat loss to the surroundings	j/s
Q_r	Heat of reaction	j/s
Q_{stir}	Heat added by the stirrer	j/s
r	Radius of unswollen latex particle	nm
r	Monomer to RAFT agent molar ratio	
Δr	size of radial interval	nm
$< r >$	number mean particle radius	nm
$< r^2 >$	number mean squared radius	nm^2
R	Leaving group of the RAFT agent	
R	universal gas constant	
$R^{\bullet}$	RAFT leaving group radical	
RAP	Intermediate radical generated from the addition of R to AP	
RAR	Intermediate radical generated from the addition of R to AR	
RI	Refractive index detector used in GPC for molecular weight determination	
R_i	Rate of initiation	l/mol. s
R_p	Rate of polymerization in the RAFT free system	l/mol. s
$R_p^{'}$	Rate of polymerization in the presence of RAFT agent	l/mol. s
R_p^{AR}	Rate of consumption of the initial RAFT agent	mol/l. s
R_p^{AP}	Rate of production of the polymeric RAFT agent	mol/l. s
R_p^M	Polymerization rate in emulsion polymerization	mol/l. s
R_t	Rate of termination	1/mol. s
r_s	Radius of Swollen latex particles	nm
S_{ads}	Amount of surfactant per unit volume adsorbed onto the polymer surface	mol/1
S_{tot}	Total concentration of the added surfactant	mol/1
SEC	Size exclusion chromatography, see GPC	
SDS	Sodium dodecyl sulfate (surfactant)	
St	Styrene monomer	
t	Time of the reaction measured from	s
T	Temperature	K or ^oC
$T^{\bullet}$	Total radical concentration in bulk and solution polymerizations	mol/l
$T_{aq}^{\bullet}$	Total radical concentration in the aqueous phase	mol/l
T_{amb}	Ambient temperature	^oC
TAT	Overall intermediate radical concentration	mol/l

$T_{j,in}$	Jacket inlet temperature	^{o}C
$T_{j,out}$	Jacket outlet temperature	^{o}C
THF	Tetrahydrofuran, the solvent used for GPC molecular weight determination	
TPEs	Thermoplastic elastomers	
T_r	Reaction temperature	^{o}C
U	Overall heat transfer coefficient	W/m^2.K
UV	Ultra violate detector	
V_d	Volume of the droplets phase	dm^3
V_M	Volume of the monomer in the system	dm^3
V_p	Volume of the polymer in the system	dm^3
V_r	Total reaction volume	dm^3
V_w	Volume of the water phase	dm^3
w_p	Weight fraction of the polymer	
x	Fractional conversion	
Xanthate, I	O-ethylxanthyl ethyl propionate RAFT agent	
Xanthate, II	O-ethylxanthyl ethyl benzene RAFT agent	
z	Critical degree of polymerization	
Z	Activation group of the RAFT agent	
α	Root-mean-square end-to-end distance per square root of the number of monomer units in a polymer chain	dm
γ	Interfacial tension between the latex particles and aqueous phase	dyn/cm
γ_o	Initial molar ratio of monomer to RAFT agent	
ν	partial molar volume of the monomer	
χ	Flory-Huggins interaction parameter between the monomer and polymer	
χ_s	Interfacial tension between the particle and the surfactant	dyn/cm
Γ_{wp}^{i}	Water-particle partitioning coefficient of species i	
Γ_{dp}^{i}	Droplet-particle partitioning coefficient of species i	
Γ_{dw}^{i}	Droplet-water partitioning coefficient of species i	
δ	Total concentration of chains	mol/l
$\delta(V-V_o)$	Dirac delta function	
ρ	First order pseudo rate coefficient for all entry events	1/s
ρ_{init}	First order pseudo entry rate coefficient	1/s
ε	Entry efficiency	

σ	Van der Waals radius of a monomer unit	dm
Φ	Polymer volume fraction	

Chapter One

Introduction

Chapter 1
Introduction

1.1 Polymers

Polymers have been with us since the beginning of time. Though the word sounds complicated, they are a part of everyday life. Natural polymers include such things as tar and shellac, tortoise shell and horns, as well as tree saps that produce amber and latex. The synthetic polymers we are familiar with range from the plastic bags and bottles used daily to the Kevlar and Mylar used to protect astronauts while they are in space. Polymers are large molecules built up by covalent linking of a large number of much smaller molecules. The term is derived from the Greek words: *polys* meaning *many*, and *meros* meaning *parts*. A polymer may consist of hundreds, thousands, tens of thousands or more monomer molecules (IUPAC., 1996). Hence, its molecular weight is very large, giving it interesting and useful mechanical and chemical properties. The volume of synthetic polymers produced worldwide is greater than the volume of steel. At present, polymer industry is a multi-billion dollar business, and still is growing at a rate faster than most other industries.

As their children were found of playing with balls made from local rubber trees, the Mayans are assumed to be among the first to find applications for polymers. The development of vulcanization by Charles Goodyear in 1839 improved the durability of natural rubber, signifying the first popularized semi-synthetic polymer. The first truly synthetic polymer, called bakelite, was fabricated by Leo Bakeland in 1909 and was used as insulation for electric wires. A major milestone in the history of polymer science was the ‘macromolecular hypothesis’ by Hermann Staudinger in 1922, which proposed that both natural and synthetic polymers are large molecules that consist of long chains of atoms held together by covalent bonds. Since then, the molecular structure of polymers started to emerge and nowadays, almost 90 years later, a knowledge base of respectable size has been built by the contributions of thousands of researchers.

Prior to World War II, natural substances were generally available; therefore, synthetic polymers that were being developed were not a necessity. During World War II, the natural resources of rubber, wool, silk, and other materials were cut off, making the use of synthetic polymers critical. Since then, polymer industry has experienced a rapid development and has evolved into one of the fastest growing industries worldwide. Until the mid-1980s, the main emphases of polymer research were linked directly with macromolecules, relating to their formation by polymerization and their physical, mechanical, and chemical properties. Since then, there has been a significant broadening of research areas and polymer technology is now interacting with many other modern scientific and technological disciplines (Stepto *et al.*, 2003).

1.2 Free radical polymerization

Free radical polymerization is one of the processes of polymer formation in which polymer grows by successive addition of the monomer units. It takes place via the breaking of a double bond of the monomer unit, converting it into an active propagating radical (Moad *et al.*, 2002). Free radical polymerization (FRP) is one of the most widely implemented processes for the production of commercial high molecular weight polymers. Despite its many benefits and wide spread use, the fast chain growth and the presence of the rapid irreversible termination impose some limitation with respect to the degree of control that can be asserted over polymer molecular weight distribution and polymer structure (Moad *et al.*, 2000). Further more, producing block copolymers, and polymers with complex structure via FRP is impractical.

The necessity to have good control in polymerization systems led to the development of living free radical polymerization (LFRP). LFRP describes polymerization where the propagating chains have no fate except propagation, and termination reactions are absent or substantially suppressed. Polymers are called “living” when they preserve their active site (end functionality) and continue to grow by further addition of monomer in the absence of termination reactions. Polymerization is “controlled” when the polymer chains are protected from termination by a capping agent, resulting in the number average molecular weight increases linearly with increasing monomer

conversion and the polymer polydispersity index decreases gradually and approach one at high conversion (Ando *et al.*, 1996; Fischer, 2003).

Very late in the twentieth century several new methods were discovered which allowed the development of living polymerization using free radical chemistry. These techniques involved nitroxide mediated polymerization (Schulte *et al.*, 2004; Solomon *et al.*, 1985), atom transfer radical polymerization (Wang, 1995) and reversible addition–fragmentation chain transfer (Chiefari *et al.*, 1998). These techniques belong to a new technological discipline known as controlled/living free radical polymerization (CLFRP) which combines the advantages of free radical polymerization and those of living polymerizations. The significant advantages of these techniques permit the preparation of a wide range of different materials which are either difficult to prepare, or not available via other polymerization processes.

1.3 Thesis motivations

Controlling polymerization products through the use of new monomers and oligomers, catalysts, and polymerization mechanisms has become one of the most active research areas in polymer science and technology. Closer control of macromolecular chain structure and molar mass, using novel polymerization techniques, is required to synthesize and optimize many new polymer products.

The flexibility of FRP and its applicability to a wide range of monomers under different reaction conditions makes it a widely adopted industrial technique for the production of commercial polymeric materials. The mechanical properties of the produced polymers depend on their chemical structure and molecular weight distribution (MWD). The major effects of increasing chain length are increased toughness, creep resistance and melt temperature. Higher molecular weight polymers are seen as providing a greater number of the chains, thus giving the polymer product a higher tensile strength. In fact, not all polymer molecules can be manufactured to an exact specified molecular weight, so each batch will have an average molecular weight distribution. There can be either a broad or a narrow spread between molecular weights of the largest and smallest molecules, and yet the polymer could still have the same average. As the molecular

weight distribution increases, or broadens, it means that there are more molecules with differing molecular weights, while a narrow molecular weight distribution means that there is a higher proportion of molecules of similar length and weight. A narrow distribution provides more uniform and well-defined mechanical properties.

Emulsion polymerization is one of the FRP techniques and is an important process for the polymer industry as it has significant advantages over bulk and solution polymerizations. Furthermore, emulsion polymerization is a water based system and hence it is an environmentally friendly process. Particle size distribution (PSD) in emulsion is also an important factor in determining the properties of the final product; for example a narrow PSD is required for a glossy finish to latex paints, while a broad PSD will result in a matt finish. On the other hand, adhesives require a broad PSD to enhance their strength. The controlled particle sizes that characterize the controlled polymer emulsions provide a number of benefits in many applications. Emulsions of smaller particles are generally very stable and have useful process advantages such as faster reaction kinetics and more scalable and reproducible preparations. Such emulsions have useful optical properties (e. g., lower turbidity), high viscosity, greater surface area, and easier coalescence to form more uniform or thinner films, all of which may be advantageous in typical applications such as adhesives, dispersants, coatings and separation media.

Desirable properties of large-particle emulsions include opacity, low viscosity, and ease of polymer isolation. Emulsions with uniform or broad particle size distribution can result by manipulating reaction conditions; for example, broad particle size distribution may result from properly chosen polymerization conditions, or may be obtained by blending particles of narrow size distribution obtained from several different polymerizations. If these factors (MWD and PSD) can be controlled, then it is possible to develop a relationship between polymer architecture, particle morphology and film properties.

Although FRP is a very dominant, fast and economical technique for polymer synthesis, it permits very little control over the molecular weight distribution and the structure of the polymer chain. Also the synthesis of sophisticated macromolecular architectures, such as block copolymers, star polymers or comb polymers, is not possible with FRP. A

suitable way to control the polymer structure efficiently during its synthesis is by a living process in which almost all of the growing radicals are protected from termination reactions. In terms of polymer structure, there is a large interest in architectures such as block copolymers, which cannot be made via conventional free-radical polymerization. Block copolymers have a wide range of applications. The production of such polymers is possible via what is so called controlled/living free radical polymerizations. A novel controlled/living free radical polymerization technique was invented in 1998, offering the production of novel polymers in a manner that their structure and their molecular weight can be brought under control. Such a technique is known as living free radical polymerization with reversible addition-fragmentation chain transfer agent (RAFT mediated polymerization) (Chiefari *et al.*, 1998).

A successful living free radical polymerization requires at least a negligible radical-radical termination. Therefore, radical flux must be minimized via reducing the initiator concentration to ensure this criterion. Such reduction results in low polymerization rate in homogenous systems such as bulk and solution polymerizations. This problem can be overcome in principle by operating in emulsion polymerization, so as to take advantage of radical segregation to decrease terminations without significantly reducing the polymerization rate with respect to the corresponding nonliving processes. Thus, combining RAFT process with emulsion polymerization will offer an ideal route for polymers production, in a manner such that the polymer properties (MWD, PSD, PDI, polymer structure, etc) can be controlled. In addition, the living nature of the polymerization processes allow for novel means for controlling particle size and distribution of the resulting polymer latex.

Many problems encountered in industrial polymerization reactors or processes are associated with inherent complexities in polymerization kinetics and mechanisms. Moreover, many of the process variables that affect important product quality indices are difficult (if not impossible) to measure online; or they can be measured at low sampling frequencies with time delays, making product quality monitoring and control difficult. The control of PSD and MWD, which is critical for manipulating the end-use properties of the produced polymer, suffers from both of these aspects. Furthermore, the offline measurement of these properties is expensive, difficult and time consuming. Mathematical modeling is a powerful tool for the development of process

understanding and advanced reactor technology in the polymer industry. Modeling of polymerization processes, especially modeling of polymer architectural properties (PSD and MWD), is of enormous industrial importance because it plays a key role in achieving the industry's goal of speedy introduction of new products into markets. Therefore, a comprehensive kinetic mathematical model for RAFT mediated emulsion polymerization will provide a good tool to understand the relationship between process variables and product characteristics via understanding the interaction between the events that take place in the system.

1.4 Thesis aims

RAFT polymerization has been recognised as one of the most versatile methods for the production of well-defined homopolymers, block copolymers and triblock copolymers. RAFT is an important process that can be directly applied to polymerization either in homogenous or heterogeneous systems. In combination with emulsion polymerization, the process is industrially promising and attractive for the production of tailored polymeric products. It, however, involves a plethora of complex kinetic events which indicate that the application of RAFT is more complicated than conventional emulsion polymerization.

This thesis aims to investigate RAFT polymerization as a suitable method to control polymer molecular weight, polydispersity and structure, focusing on its application in emulsion systems. Such an investigation would help in providing crucial understanding of the RAFT systems and the prevailing mechanisms, and hence developing an integrated framework that is industrially attractive especially for dispersed media. This knowledge will be applied to produce homo/co-polymers with controlled architecture in emulsion systems. The components of this investigation are:

- To develop a comprehensive dynamic reactor model for a batch homogeneous (solution and bulk) RAFT polymerization that is capable of accurately predicting the polymerization process and product attributes (conversion, number average molecular weight and polymer polydispersity).

- To validate the homogenous RAFT polymerization model for selected RAFT-homogenous polymerization systems.
- To build a comprehensive dynamic reactor model for RAFT heterogeneous polymerization that is capable of accurately predicting polymerization properties such as: monomer conversion, particle size distribution (PSD), number average molecular weight (Mn) and polymer polydispersity (PDI) over a wide range of operating conditions.
- To setup a state-of-the-art reactor facility to assist in validating the RAFT-emulsion model predictions under different process conditions.
- To investigate the operation of emulsion polymerization reactor using the monomer feed as a primary variable to control particle size distribution (PSD), and RAFT agent concentration to control molecular weight distribution (MWD) of the produced polymer.
- To develop an adaptive reactor calorimetry that makes use of a detailed reactor energy/mass balance to infer monomer conversion and polymer molecular weight, for RAFT emulsion polymerizations, which will be used as an online soft sensor.
- To incorporate our *ab initio* model within an optimal control policy to produce desired polymer PSD and MWD for both offline and online applications.
- To develop a method to synthesize block copolymers of desired composition.

1.5 Thesis contributions

The main contributions in this work are as follows:

- Developing a comprehensive mathematical model accounting for RAFT-homogenous free radical polymerization. The model was validated by using the published experimental data for selected RAFT-homogenous polymerization systems, and may be used as a tool to investigate the reasons behind the observed retardation.

- Developing a comprehensive mathematical model accounting for RAFT-heterogeneous free radical polymerization. This model was validated against experimental results and found to be capable of accurately predicting monomer conversion, PSD, MWD and other properties at many different reaction conditions.
- Investigating the effect of changing reaction temperature and the amount of RAFT agent, initiator and surfactant on the polymer key properties. Based on this investigation, the manipulating variables that had a significant effect on the polymerization rate, MWD, and PSD were determined and their effects were quantified.
- Developing an online calorimetry-based soft-sensor for use as a soft sensor for the prediction of monomer conversion, rate of reaction and molecular weight.
- The use of the dynamic RAFT-heterogeneous model for generating offline optimal trajectories and for online soft sensing of the PSD and MWD within the model based control structure.
- Producing new composite polymeric materials (block copolymers) via RAFT emulsion polymerization.

1.6 Thesis structure

This thesis is organized as follows:

- **In Chapter 2,** the basic principles of free radical polymerization (FRP) and living free radical polymerization (LFRP) occurring in either homogeneous or heterogeneous systems are reviewed with an emphasis on the development of molecular mass and rate of polymerization.
- **In Chapter 3,** the detailed mechanism of RAFT process in homogenous systems is discussed along with reviewing the previous work in this area. The development of a comprehensive dynamic reactor model for a batch homogeneous (solution and bulk) RAFT polymerization which is capable of accurately predicting the polymerization attributes (conversion, number average molecular weight and polymer polydispersity) is presented. The role of the intermediate radical is investigated using the developed model. Finally, the

homogenous RAFT polymerization model is validated using the published experimental data for selected RAFT-homogenous polymerization systems.

- **In Chapter 4,** the knowledge of RAFT process is moved forward toward its application in emulsion systems. First the mechanism of conventional emulsion polymerization is discussed. The common problems associated with the application of RAFT in emulsion polymerization are introduced. Consequently, the mechanism of RAFT process is incorporated in emulsion polymerization mechanism to build a comprehensive dynamic reactor model for RAFT heterogeneous polymerization that is capable of accurately predicting polymerization properties such as: monomer conversion, particle size distribution (PSD), number average molecular weight (Mn) and polymer polydispersity (PDI) over a wide range of operating conditions.
- A state-of-the-art reactor facility to assist in validating the RAFT-emulsion model predictions under different process conditions is discussed **in Chapter 5**. This is followed by a through investigation of the application of RAFT in batch emulsion polymerization, with the results compared with the model predictions.
- The use of RAFT agent in semi-batch emulsion polymerization of styrene is experimentally presented **in Chapter 6**. The results of the chain extension experiments demonstrating the living nature of the dormant chains formed in the batch reactor are presented and compared with model simulations. The significant kinetic difference between batch and semi-batch reactors is highlighted in terms of living nature of the polymerization.
- The first part of **Chapter 7** focuses on the development of an adaptive reactor calorimetry model that makes use of a detailed reactor energy/mass balance to infer monomer conversion and polymer molecular weight for RAFT emulsion polymerizations. In the second part the incorporation of the sophisticated model, developed in Chapter 4 within an optimal control policy to produce desired polymer PSD and MWD for both offline and online applications is discussed.
- In **Chapter 8,** the knowledge is further extended toward employing the low active RAFT agent in emulsion polymerization to produce well-defined block copolymers. First, homopolymerization of methyl acrylate, butyl acrylate and styrene with low active RAFT agent to produce the first block is discussed. The effect of changing monomer type in the polymerization with low active RAFT

agent is rationalized. Then the first homopolymer block is chain extended with another monomer under both batch and semi-batch conditions. The importance of operation mode and blocking sequence is discussed.

Finally a number of conclusions and recommendations are included in **Chapter 9**, where the applications of high active RAFT agent in emulsion and miniemulsion polymerizations are recommended for future studies.

1.7 References

Ando, T.; Kato, M.; Kamigaito, M. and Sawamoto, M., 1996. Living Radical Polymerization of Methyl Methacrylate with Ruthenium Complex: Formation of Polymers with Controlled Molecular Weights and Very Narrow Distributions. *Macromolecules*, 29(3): 1070.

Chiefari, J.; Chong, Y.K.; Ercole, F.; Krstina, J.; Jeffery, J.; Le, T.P.T.; Mayadunne, R.; Meijs, G.F.; Moad, C.L.; Moad, G.; Rizzardo, E. and Thang, S.H., 1998. Living Free-Radical Polymerization by Reversible Addition-Fragmentation Chain Transfer: The RAFT Process. *Macromolecules*, 31(16): 5559.

Fischer, H. (Editor), 2003. Criteria for Livingness and Control in Nitroxide-Mediated and Related Radical Polymerization. American Chemical Society, 854, Washinghton, DC.

IUPAC., 1996. Glossary of Basic Terms in Polymer Science. *Pure Appl. Chem.*, 68: 2287.

Moad, G.; Chiefari, J.; Chong, Y.K.; Krstina, J.; Mayadunne, R.T.A.; Postma, A.; Rizzardo, E. and Thang, S.H., 2000. Living free radical polymerization with reversible addition-fragmentation chain transfer (the life of RAFT). *Polymer International*, 49(9): 993.

Moad, G.; Chiefari, J.; Mayadunne, R.T.A.; Moad, C.L.; Postma, A.; Rizzardo, E. and Thang, S.H., 2002. Initiating free radical polymerization. *Macromolecular Symposia*, 182(3): 65.

Schulte, T.; Knoop, C.A. and Studer, A., 2004. Nitroxide-mediated living free-radical polymerization of styrene: A systematic study of the variation of the alkoxyamine concentration. *Journal of Polymer Science Part a-Polymer Chemistry*, 42(13): 3342.

Solomon, D.H.; Rizzardo, E. and Cacioli, P., 1985. Free radical polymerization and the produced polymers. Eur. Pat. Appl, EP 135280

Stepto, R.; Horie, K.; Kitayama, T. and Abe, A., 2003. Mission and challenges of polymer science and technology. *Pure and Applied Chemistry*, 75(10): 1359.

Wang, J., Matyjaszewski, K., 1995. Controlled/Living Radical Polymerization. Halogen Atom Transfer Radical Polymerization Promoted by a Cu(I)/Cu(II) Redox Process. *Macromolecules*, 28(23): 7901.

Chapter Two

Background

Chapter 2
Background

Abstract

In this chapter the basic principles of free radical polymerization (FRP) and living free radical polymerization (LFRP) occurring in either homogeneous or heterogeneous systems are reviewed with an emphasis on development of molecular mass and rate of polymerization. The aim of this concise revision is to gain an adequate knowledge that is required for the development of the homogeneous and heterogeneous living free radical polymerizations mathematical models in the subsequent chapters.

2.1 Free radical polymerization

Free-radical polymerization (FRP) is a chain-growth polymerization process and one of the most practical techniques used for polymer synthesis. In free radical polymerization, an initiator is used to generate free radicals that can initiate polymerization by addition of monomer units. Thermal dissociation of the initiator is the most widely used means of radical generation (Moad, 1995). Addition of monomer units to the propagating chain, initiated by the initiator fragment, continues until chain growth is terminated. The termination occurs when two propagating chains meet and undergo bimolecular termination or when the propagating chain transfers its radical to another specie (e.g. to monomer, polymer, solvent, chain transfer agent, etc.) resulting in the formation of dead chains. The term “dead” stems from the fact that these chains have lost their active center, and cannot add monomer units anymore, unless chain transfer to these dead polymer chains takes place (Odian, 2004; Stevens., 1999).

In FRP, each chain grows very fast in the early stages of polymerization, and this eventually leads to the formation of dead polymer as one of the chain stoppage events take place. The timescale for chain growth may be in the order of seconds or even less. Therefore, variation of polymerization conditions over this short timescale for chain

growth is very difficult, resulting in a poor or very limited control over the molecular weight distribution and polymer architecture.

2.1.1 Mechanism and kinetics of FRP

The mechanism of FRP belongs to the class of chain reactions. Fast growth via subsequent addition of monomers to an active centre (initiator fragment) at the end of the chain is the main characteristic of chain reactions. Free radical polymerization consists of a sequence of five steps: radical formation, initiation, propagation, termination and chain transfer.

The initiator-derived free radicals that initiate polymerization are generated by thermal or photochemical homolytic cleavage of covalent bonds, or by a redox process. These initiator-derived radicals add to carbon–carbon double bond of monomer unit resulting in chain initiating radicals, which in turn propagate further. The homolytic decomposition of the initiator molecule (I_2) into two active primary radicals $(I^\bullet)$ is described by:

$$I_2 \xrightarrow{k_d} 2I^\bullet \qquad \textbf{(2-1)}$$

Initiation step involves the addition of the initiator-derived radical (dissociated radical) to the first monomer molecule to produce the chain initiating radical $P_1^\bullet$:

$$I^\bullet + M \xrightarrow{k_p^i} P_1^\bullet \qquad \textbf{(2-2)}$$

where M represents a monomer molecule and k_p^i is the rate constant for the initiation step. The initiator-derived radicals do not always react with monomer and side reactions are known to occur in many cases. Thus the initiator efficiency, *f,* is not 100% and depends on a number of factors (Odian, 2004). The decomposition of the initiator is the rate determining step since it is slower than the initiation step. The rate of initiation (R_i) is given by:

$$R_i = -\frac{d[I^\bullet]}{dt} = 2fk_d[I] \qquad \textbf{(2-3)}$$

where k_d is the rate constant for the initiator dissociation and $[I]$ is the initiator concentration.

Propagation is the successive addition of monomer molecules to the active centre at the end of the chain-initiating radical. Each addition generates a new radical that has the same characteristics as the pre-existing one, except that it is larger by one monomer unit. In order for a high molecular weight polymer to be formed, the propagation step must occur at a sufficiently high rate in comparison with the other elementary reactions. However, several factors may prevent propagation to form high molecular weight polymer, such as polar, resonance, and steric factors resulting from the substituents bound to the reacting carbon–carbon double bond and the radical center. The successive addition is represented by:

$$P_1^\bullet + M \xrightarrow{k_p^i} P_2^\bullet \qquad \textbf{(2-4)}$$

$$P_2^\bullet + M \xrightarrow{k_p^i} P_3^\bullet \qquad \textbf{(2-5)}$$

$$P_n^\bullet + M \xrightarrow{k_p} P_{n+1}^\bullet \qquad \textbf{(2-6)}$$

where k_p is the rate constant for propagation and (n) is the number of the added monomers. The reaction rates of primary propagating radicals have been separately determined for some monomers in specially designed experiments (Zetterlund *et al.*, 1999). The results of these experiments indicate that the rate constants decrease with increasing chain length for the first few addition steps, and remain almost constant for longer radicals ($k_p^i > k_p$) . Recent data from pulsed-laser polymerization (PLP) indicated a weak long chain-length dependence of the propagation rate constant k_p extending over several hundred degrees of polymerization (Olaj *et al.*, 2000).

Termination of growing chains takes place through the bimolecular reaction between two growing chains. Termination occurs by combination resulting in one dead polymer chain and/or by disproportionation when a hydrogen atom (atom abstraction) transfers

from one growing chain to the other, thereby resulting in two polymeric chains, one of which is saturated while the other is unsaturated. The two different modes of termination can be represented in general terms by:

$$P_n^{\bullet} + P_m^{\bullet} \xrightarrow{k_{tc}} P_{n+m} \qquad \textbf{(2-7)}$$

$$P_n^{\bullet} + P_m^{\bullet} \xrightarrow{k_{td}} P_n + P_m \qquad \textbf{(2-8)}$$

where k_{tc} and k_{td} are the rate constants for termination by coupling and disproportionation, respectively; P_n, P_m and P_{n+m} are the produced dead polymers. Typical termination rate constants are in the range of 10^6–10^8 L mol^{-1} s^{-1} or orders of magnitude greater than the propagation rate constants (Odian, 2004). The much greater value of k_t compared to k_p does not prevent propagation because the radical species are present in very low concentrations. The termination process in a polymerizing system is usually diffusion-controlled with a rate constant significantly lower than that for small radicals (Kobatake and Yamada, 1995; Russell, 1994). The rate of monomer consumption can be described by the rate of propagation:

$$R_p = -\frac{d[M]}{dt} = k_p[T^{\bullet}][M] \qquad \textbf{(2-9)}$$

where $[T^{\bullet}]$ is the total concentration of all chain radicals, that is, all radicals of size $P_1^{\bullet}$ and larger. When the free radical polymerization is first started, the number of chains increases from zero as the initiator begins to decompose. Accordingly, the frequency of termination events increases from the early stages of the polymerization as the total radical concentration increases. The termination rate is given by:

$$R_t = 2 < k_t > [T^{\bullet}]^2 \qquad \textbf{(2-10)}$$

Equation (2-10) shows that the rate of termination (R_t) is of second order with respect to the radical concentration. Thus, a change in radical concentration affects the rate of termination more than the rate of polymerization. This means that a high radical concentration dramatically increases the rate of termination reactions and thus reduces the average degree of polymerization.

Radicals are continuously produced from the decomposition of the initiator and consumed by the termination reactions. Eventually, the rate of radical generation is balanced by the rate at which radicals undergo mutual annihilation. Consequently the concentration of radicals reaches a steady-state value, and hence the rate of termination is equal to the rate of initiation. Typical polymerizations reach steady-state after a period, which may be at most a minute (Odian, 2004). Rearrangement of equations (2-3) and (2-10) gives the steady state concentration of radicals:

$$[T^{\bullet}] = \left(\frac{fk_d[I]}{< k_t >} \right)^{1/2} \quad \textbf{(2-11)}$$

Similarly, by assuming that the rate of radical generation is equal to the rate of initiation, the steady state concentration of the initiator fragments is given by:

$$[I^{\bullet}] = \frac{2fk_d[I]}{k_{pi}[M]} \quad \textbf{(2-12)}$$

Substituting equation (2-11) into equation (2-9) yields:

$$R_p = -\frac{d[M]}{dt} = k_p[M] \left(\frac{fk_d[I]}{< k_t >} \right)^{1/2} \quad \textbf{(2-13)}$$

Equation (2-13) gives the polymerization rate in terms of monomer concentration and overall active radical concentration. Equation (2-13) indicates that the polymerization rate is first order with respect to the monomer concentration and one half order with respect to the initiator concentration.

Transfer reactions can occur between a propagating chain and a molecule of monomer, transfer agent, initiator, and solvent. The transfer reaction produces one dead chain and a new small radical that may or may not be efficient in reinitiating the polymerization. Transfer reaction can be represented by:

$$P_n^{\bullet} + X \xrightarrow{k_{tr,X}} P_n + X^{\bullet} \quad \textbf{(2-14)}$$

where $k_{tr,X}$ is the rate constant of transfer to species X (X could be monomer, initiator, transfer agent or dead polymer) while $X^{\bullet}$ is a small radical generated from the transfer reaction. The number average kinetic chain length is defined by the ratio of propagation rate to chain stoppage rate. By including the effect of chain transfer in the free radical mechanism, the number average kinetic chain length is given by:

$$i = \frac{k_p[M][T^{\bullet}]}{k_{tr}^{M}[M][T^{\bullet}] + k_{tr}^{I}[I][T^{\bullet}] + k_{tr}^{CTA}[CTA][T^{\bullet}] + 2 < k_t > [T^{\bullet}]^2} \qquad \textbf{(2-15)}$$

The chain-transfer constants for monomer, initiator and chain-transfer agent, are given by:

$$C_{tr}^{M} = \frac{k_{tr}^{M}}{k_p}, C_{tr}^{I} = \frac{k_{tr}^{I}}{k_p}, C_{tr}^{CTA} = \frac{k_{tr}^{CTA}}{k_p} \qquad \textbf{(2-16)}$$

Dividing the numerator and the denominator in equation (2-15) by $k_p[M][T^{\bullet}]$ and taking the reciprocal yields:

$$\frac{1}{i} = \frac{1}{i_o} + C_{tr}^{M} + C_{tr}^{I}\frac{[I]}{[M]} + C_{tr}^{CTA}\frac{[CTA]}{[M]} \qquad \textbf{(2-17)}$$

Equation (2-17) is known as the Mayo equation and shows the quantitative effect of the various chain transfer reactions on the number average degree of polymerization (kinetic chain length), where i and i_o are the number-average degrees of polymerization with and without chain transfer, respectively.

2.1.2 Free radical polymerization methods

The reactions by which free radical polymerizations are carried out are of two main types, namely homogeneous and heterogeneous reactions (Odian, 2004). Solution and bulk polymerizations are homogeneous processes, while emulsion polymerization is a heterogeneous process. These are described in more details next.

2.1.2.1 Bulk and solution polymerizations

In bulk polymerization (also referred to as mass polymerization), the only ingredient are a monomer-soluble initiator, a monomer and a polymer, these are all present in a single phase (homogenous polymerization), without solvents or dispersion media. Bulk polymerization offers the simplest polymerization technique among the others with minimum of contamination of the product. However, the highly exothermic nature of the free radical addition reaction and the tendency toward the gel effect combine to make heat dissipation difficult. As such a careful temperature control is required. Furthermore, the conversion of monomer into polymer increases the viscosity of the reaction at relatively low conversion, thereby making stirring and heat transfer inefficient. This may cause an auto-acceleration and reactor thermal runaway, which requires strong and elaborate stirring equipment to overcome such problems. Due to these difficulties, bulk polymerization is not, commercially, a widely used technique for chain polymerization. However, these difficulties can be circumvented by reducing the reaction conversion with separation and recycling of unreacted monomer.

Polymerization in solvent overcomes many of the disadvantages of the bulk polymerization. Solution polymerization occurs with a solvent which acts as a diluent, reducing the viscosity of the reactions and aiding in the transfer of the heat of polymerization, thereby ensuring better heat removal and mixing. On the other hand, the presence of the solvent may induce new difficulties; as an example, chain transfer to the solvent may occur, leading to reduce the degree of polymerization. As such, careful selection of the appropriate solvent is crucial. In addition, further processing is required in order to extract the solvent from the final products, where complete extraction of the solvent is difficult and economically impractical. Solution polymerization is, thus, commercially unattractive.

2.1.2.2 Emulsion polymerization

Emulsion polymerization is based on a system consisting of water as the continuous phase, a water-soluble initiator, a slightly water-soluble monomer, and an emulsifier (surfactant). Initially, the surfactant is in the form of micelles (ca. 5–10 nm in diameter, 10^{19}–10^{21} dm^{-3} in number) which are spherical or rodlike aggregates of 50-100

surfactant molecules with their hydrophobic 'tails' oriented inward and their hydrophilic 'heads' outward. These micelles form when the surfactant concentration exceeds the critical micelle concentration. As shown in Scheme 2-1, the water-insoluble monomer droplets (ca. 1–10 μm in diameter, 10^{12}–10^{14} dm^{-3} in number) are stabilized with the micelle-forming surfactant. Since, the monomer being used in emulsion polymerization has low water solubility, it is clear that there will be three phases, referred to the monomer phase, aqueous phase and micellar phase.

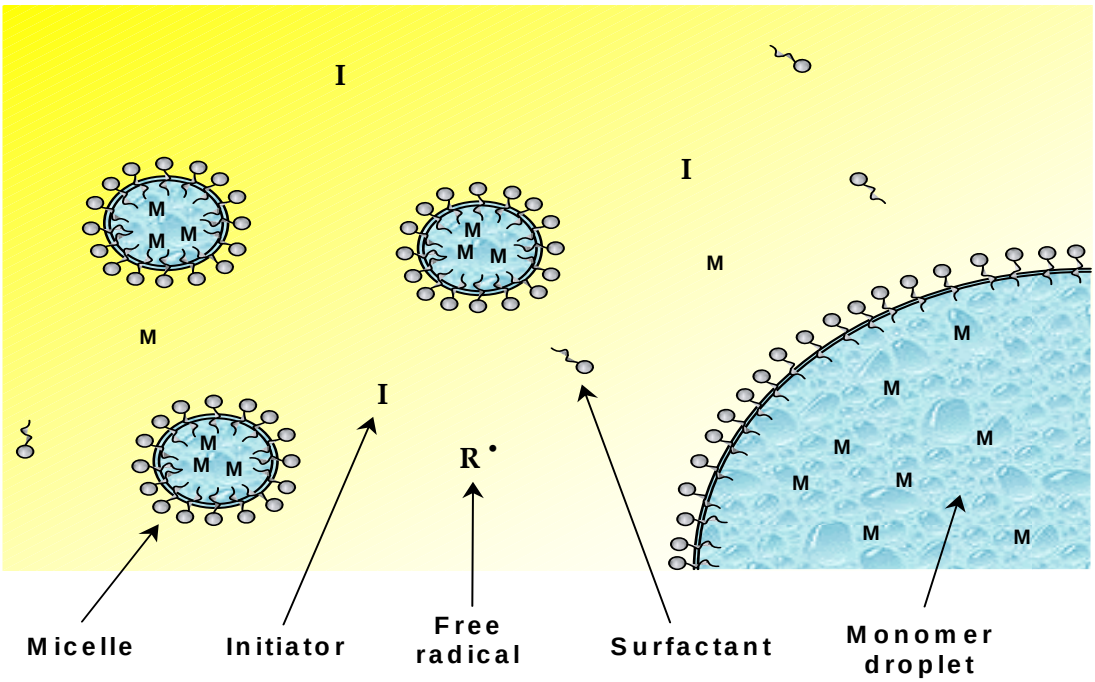

Scheme 2-1: Emulsion polymerization system.

The water soluble initiator initiates the polymerization reaction by producing highly reactive radicals in the aqueous phase, which in turn initiate polymerization in monomer swollen micelles, converting them into monomer-swollen polymer particles (ca. 0.05–1 μm in diameter, 10^{16}–10^{18} dm^{-3} in number). Finally a dispersion of polymer particles is obtained. In general, monomer droplets are not effective in competing with micelles in capturing free radicals generated in the aqueous phase due to their relatively small surface area. However, monomer droplets may become the predominant particle nucleation loci if the droplet size is reduced to the submicron range. This technique is referred to as miniemulsion polymerization.

The unique feature of kinetics in emulsion polymerization results from the compartmentalization of the growing radicals within separate particles. Thus, the polymerization rate and conversion are high, resulting in high production rate. Heat transfer is facilitated by the presence of the water phase which insures high control level of temperature. Since polymerization occurs inside the particles the viscosity can be maintained at the lowest level, and as a result the system is easy to be handled. Due to these advantages, emulsion polymerization is one of the widely adopted free radical polymerization techniques on an industrial scale.

2.2 Living free radical polymerization

In conventional polymerization processes, as discussed above, the initiator decomposes into two fragments in which each one of them reacts with the monomer. The propagation step then takes place with more monomer molecules to produce a polymeric radical denoted by (P_n^*), while termination occurs when two active propagating chains encounter each other producing a dead polymeric chain. Under such conditions polymeric chains form rapidly in the early stages of polymerization, that is, the individual chains grow, typically, for 0.01-10 s before terminating. The fast chain growth and the presence of the rapid irreversible termination impose some limitation with respect to the degree of control that can be asserted over polymer molecular weight and structure (Moad *et al.*, 2000).

Living polymerization describes polymerization in which propagating chains have no fate except propagation, and chain polymerization proceeds without the occurrence of irreversible chain breaking processes, i.e. chain transfer and termination (Chiefari *et al.*, 1998; Moad *et al.*, 2000). In conventional FRP, in fact, bimolecular termination limits the chain lifetime to a small fraction of the entire process time and, therefore, changes in the operating conditions (monomer concentration and composition, viscosity, temperature, etc.) affect the structure of the polymer chains produced at different stages of the process. In a living polymerization, instead, these changes are equally distributed over all the polymer chains, which grow uniformly during the whole duration of the reaction. Moreover, the living chains are still able to restart propagation when the

monomer is completely depleted, and hence the production of block copolymers by simple addition of the co-monomer is possible. This is clearly not possible in FRP.

Ionic polymerization is considered as a pure living free radical polymerization due to the absence of termination reactions (Penczek, 1997; Szwarc, 1956). The nature of the reaction media in ionic polymerizations is often not clear since heterogeneous inorganic initiators are often involved. Further, it is extremely difficult in most instances to obtain reproducible kinetic data because ionic polymerizations proceed at very rapid rates and are extremely sensitive to the presence of small concentrations of impurities. The formation of ions with sufficiently long lifetimes for propagation to yield high-molecular-weight products generally requires stabilization of the propagating centers by solvation. Relatively low or moderate temperatures are also needed to suppress termination, transfer, and other chain-breaking reactions which destroy propagating centers. Although solvents of high polarity are desirable to solvate the ions, they cannot be employed for several reasons. The highly polar hydroxylic solvents (water, alcohols) react with and destroy most ionic initiators. Thereby, emulsion polymerization is not suitable for ionic polymerization. Other polar solvents such as ketones prevent initiation of polymerization by forming highly stable complexes with the initiators. Ionic polymerizations are, therefore, usually carried out in solvents of low or moderate polarity such as tetrahydrofuran, ethylene dichloride, and pentane, although moderately high polarity solvents such as nitrobenzene are also used (Odian, 2004).

Unfortunately, because of the monomers that can be polymerized via this technique are limited, the stringent reaction conditions and the high sensitivity of the carbon-centered anion toward the impurities, the application of ionic free radical polymerization is industrially restricted (Souaille and Fischer, 2000).

2.3 Controlled/living free radical polymerization

Controlled living free radical polymerization (CLFRP) is different from ionic radical polymerization; the latter is termination-free polymerization, while CLFRP is distinguished by the presence of bimolecular termination and chain transfer. By considering the nature of ionic polymerization, to establish living polymerization the

initiator should be consumed at the beginning of polymerization. In addition there should be a rapid exchange between the species involved in the system compared with their propagation rate, and irreversible termination reactions should be maintained at the lowest level.

In the last three decades some techniques that combine the versatility of free radical polymerization with the advantages of living free radical polymerization have been developed. Generally, the basic principle for these techniques is based on the dynamic equilibrium developed between the active and dormant species, which implies an alternating activation of the capped polymer chains and deactivation of the active chains. Such conditions become possible in the presence of reagents (capping agents) that react with the propagating radicals by *reversible deactivation* or *reversible chain transfer*.

In reversible termination (deactivation), the deactivation of the active radicals takes place by termination reaction with a capping agent to form a dormant polymer chain which can be activated by a reversible homolytic cleavage. The activated polymer chain can then add monomer units until it is deactivated again. This technique can be best represented by nitroxide mediated polymerization (NMP) (Li *et al.*, 1995; Ravve, 2000; Solomon *et al.*, 1985) and atom transfer radical polymerization (ATRP) (Matyjaszewski *et al.*, 2000; Wang, 1995). In these techniques, the equilibrium is shifted strongly towards the dormant species so that the active radical concentration is lower than that in conventional FRP. As propagation is first order with respect to radical concentration and irreversible termination is second order, the lower radical concentration results in a significantly reduced termination rate that maintains the living character of the chains (Cunningham, 2002). On the other hand, reversible chain transfer requires active chains to undergo transfer reactions with the dormant chains. Reversible transfer can be best represented by the reversible addition-fragmentation chain transfer (RAFT) (Chong *et al.*, 1999; Donovan *et al.*, 2002; Feldermann *et al.*, 2004) and degenerative transfer (DT). As with reversible termination, some irreversible termination occurs resulting in dead chains and broadening the molecular weight distribution. Unlike reversible termination, the rate is not suppressed because the reversible step is transfer, not termination, and hence the concentration of radicals is not altered (Cunningham, 2002).

2.3.1 Nitroxide mediated polymerization

Nitroxide mediated polymerization (NMP) was first reported by Solomon *et al.* (1985). NMP technique is based on the reversible activation of the dormant polymer $P-X$ to an active radical $P^{\bullet}$ and the so-called persistent radical species $X^{\bullet}$ as shown in Scheme 2-2. The reaction can be initiated by using an alkoxyamine P-X, where P is an alkyl and X a nitroxide group. The reaction is controlled by the effect of the nitroxide persistent radical $X^{\bullet}$, which is the build-up of free nitroxide (Fischer, 2001).

Once the initiation takes place, equilibrium will be established between the active and dormant species. The probability of termination reactions is very low since the nitroxide and carbon-centered radical (alkyl) diffuse away from each other, which allows stepwise growth of the polymer chains. However, termination between two carbon-centered radicals is probable, resulting in the formation of a dead polymer and excess of free nitroxide. As more terminations between the carbon-centered radicals take place the propagating species will be taken out from the equilibrium and the amount of free nitroxide will increase, thereby making the equilibrium presented in Scheme (2-2) shifts to the lift. The equilibrium shift increases the control level over the reaction, while the polymerization rate slows down. The polydispersity of the produced polymer via NMP technique is not as narrow as that obtained in ionic polymerization (Li *et al.*, 1995; Ravve, 2000)

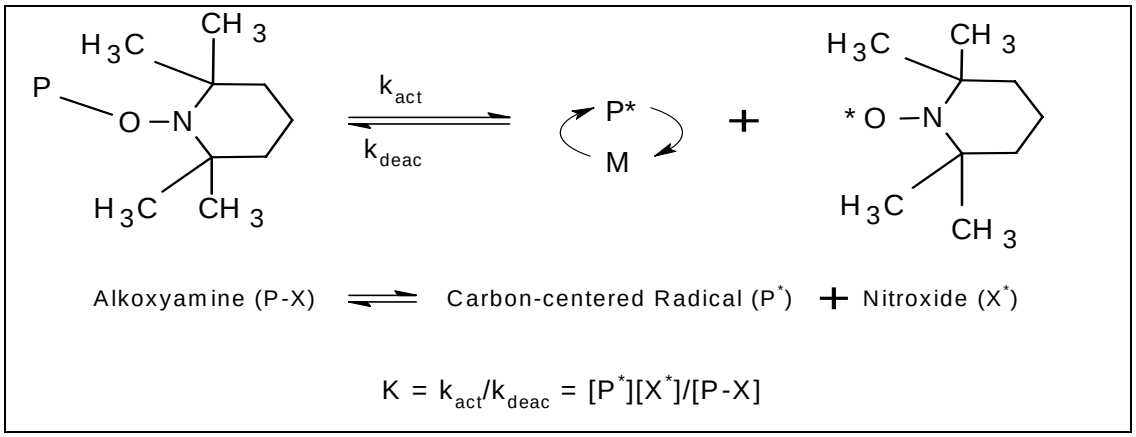

Scheme 2-2: Mechanism of nitroxide mediated polymerization.

It has to be noted that the NMP technique was successfully used for making homopolymers and block copolymers from styrene and its derivatives. However it

failed in the other systems, while the only exception known so far has been reported by Beniot *et al.,* (1998), i.e. the successful polymerization of styrene and n-butyl acrylate in the presence of a novel nitroxyl radical containing a diethyl phosphonate group in the β-position of the nitrogen atom. In addition, the temperature required for control of the MWD in this system is as high as 125 ^{o}C. Poor colloidal stability and the greater partitioning of the hydrophobic species into the aqueous phase are major drawbacks regarding its application in heterogeneous systems (e.g. emulsion polymerization)

2.3.2 Atom transfer radical polymerization

Unlike NMP, ATRP has been used successfully to prepare well-defined polymers and copolymers of styrene, acrylate, methacrylate, and acrylonitrile (Matyjaszewski *et al.*, 2000; Wang, 1995). Controlled living polymerization via atom transfer radical polymerization (ATRP) was first reported in 1995 by the Matyjaszewski research group (Wang, 1995). In ATRP, the lifetime of the active species is very short such that only a few monomer units are added during each active cycle, giving the reaction its living character.

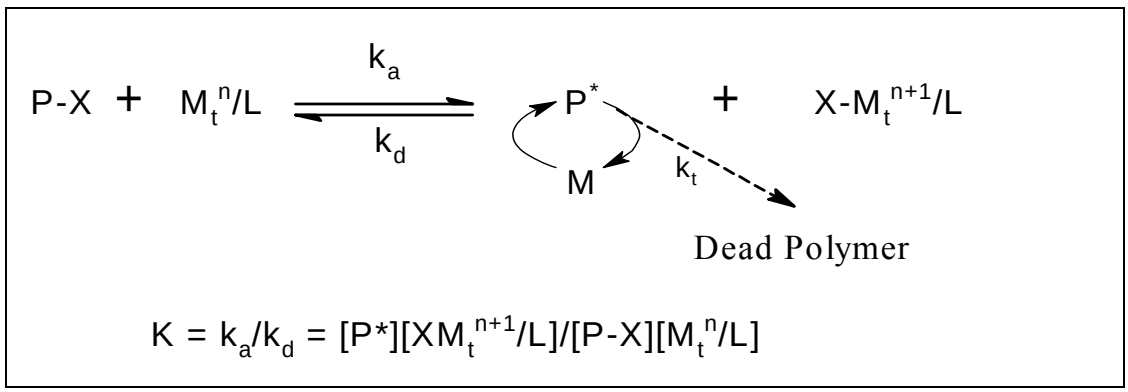

Scheme 2-3: Activation/deactivation (ka/k$_d$) equilibrium in atom transfer radical polymerization, the metal is usually cupper and the halide is chlorine or bromine.

Although ATRP behaves differently from conventional free radical polymerization, the fundamental reactions involved are very similar and include initiation, propagation, transfer and termination. Since in a truly living polymerization, chain termination does not occur, the "living" character of the chains in ATRP derives from the fact that chain propagation is first order with respect to radical concentration and irreversible bi-

molecular termination is second order. As such, the concentration of the radicals is kept very low resulting in the rate of bi-molecular termination being greatly reduced.

As depicted in Scheme (2-3), the radical formation occurres via a transition metal catalyst (M_t^n / L) that activates the organic dormant species $(P-X)$ by abstracting the halide (X) at the chain end. The transition metal catalyst M_t^n / L (where M_t^n is the transition metal in the lower oxidation state "n" complexed with an appropriate ligand) reacts reversibly with the added initiator molecule and produces an oxidized transition metal halide complex $(X-M_t^{n+1} / L)$ and a radical $P^{\bullet}$ as a propagating polymer chain. That is, the polymer chain is activated by the removal of a transferable atom or group X from the end of the polymer chain $P-X$ and deactivated by the return of a transferable atom or group in the reverse reaction where the returning atom or group may not necessarily be the same. This process repeats itself, until desired consumption of the monomer is reached, where reactivation of the dormant species allows the polymer chains to grow and deactivate again, resulting in a polymer chain that grows slowly and steadily with predetermined molecular weights because under appropriate conditions the contribution of termination is small. The basic kinetics of ATRP resembles that of NMP. Thus, adjusting the concentration of the transition metal catalyst allows for shifting the equilibrium in the direction of the deactivation, and hence keeps the radical concentration low.

ATRP is suitable for polymerization of a wide variety of monomers, and tolerates the presence of impurities. Thereby, ATRP is readily applicable to industrial processes (Matyjaszewski and Xia, 2001; Patten and Matyjaszewski, 1998). However, the major disadvantage of this method is the contamination of the polymer with a ligand/metal complex which needs more processing in order to separate it from the final product, thereby increasing the production cost. In addition, ATRP needs unconventional initiating system that often have poor compatibility with polymerization media (Moad *et al.*, 2000). Furthermore, in emulsion polymerization the partitioning of the small deactivating species between the particle and aqueous phases slows down the growth of the aqueous phase radical, thereby reducing the radical entry and hence reducing the reaction rate (Michael J. Monteiro, 2002) along with poor control of the particle size distribution.

2.3.3 Reversible addition-fragmentation chain transfer polymerization

Reversible addition–fragmentation chain transfer (RAFT) was invented in 1998 by Rizzardo and co-workers (Chiefari *et al*., 1998). The mechanism of RAFT free radical polymerization is given in Scheme 2-4.

Like degenerative transfer, RAFT process employs a chain transfer agent that reacts with the propagating radicals. Initially, the addition of monomer units onto the active radicals leads to the initiation of the propagating chains (Pn^*) that are able to further propagate with monomer. The reversible reaction is between a dormant chain (*AR*) and an active radical (Pn^*), in which an end group (capping moiety A: *S=C-Z-S*) originating from the transfer agent is exchanged between the two chains (Cunningham, 2002).

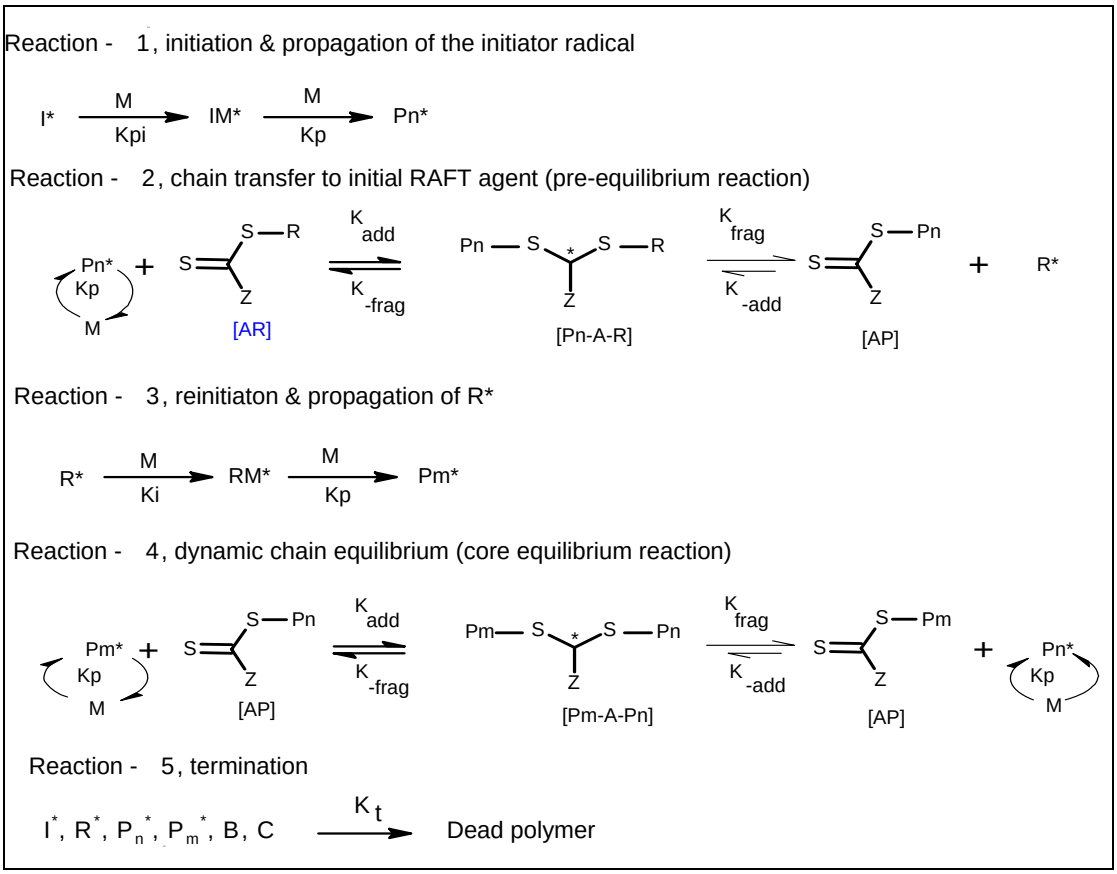

Scheme 2-4: Mechanism of the RAFT process.

The exchange occurs via the formation of the intermediate radical (*Pn-A-R*) that can fragment to produce a propagating radical (R^*) and a dormant chain (*AP*) carrying the chain transfer end group. The produced reinitiating radical (R^*) adds monomer forming a polymeric radical (Pm^*) which can add to either (*AR*) or (*AP*). In degenerative chain transfer (*DT*) the transfer occurs directly without the formation of an intermediate species. The capping agent used in DT is an atom or a simple group without, for instance, a double bond. In this case, the capping moiety is simply transferred from radical to radical without forming any kinetically important intermediate species. The so-called iodide-mediated polymerization, in which A is iodine, is a well-known example.

In the RAFT process a rapid equilibrium between the active propagating radicals (Pn^* *and* Pm^*) and the dormant polymeric chain (*AP*) provides equal probability for all chains to grow, and allows for the production of polymers with narrow polydispersity. Additionally, most of the polymeric chains carry the RAFT moiety (Scheme 2-5), and hence block copolymers can be produced by adding another batch of the second monomer.

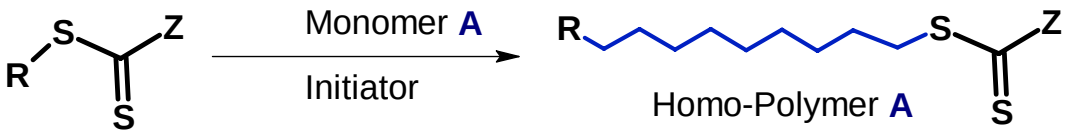

Scheme 2-5: End groups in the polymeric chain produced by RAFT polymerization.

Among the above mentioned techniques for controlled/living radical polymerization (NMP, ATRP), RAFT is the most flexible technique which is able to induce living behaviour for a wide range of monomers via a range of initiation methods and at a varying reaction temperatures (Chong *et al.*, 1999; Donovan *et al.*, 2002; Feldermann *et al.*, 2004). Moreover, the RAFT process is able to control polymerization in bulk, solution and emulsion polymerizations (Chiefari *et al.*, 1998; Moad *et al.*, 2000). In addition, several studies have been reported for the application of RAFT process in mini-emulsion systems (Butte *et al.*, 2001; Chiefari *et al.*, 1998; Moad *et al.*, 2000; Monteiro and Charleux, 2005; Russum *et al.*, 2005; Uzulina *et al.*, 2000). As RAFT process is the method of choice in this work, a complete and detailed description of the

process is provided in Chapter 3 for its application in bulk and solution polymerizations and in the subsequent Chapters for its application in emulsion polymerization.

2.3.3.1 RAFT agents

The general form of the thiocarbonylthio RAFT agents is shown in Scheme (2-6). Such compounds can be designed with structural variety involving the leaving group, *R*, and the stabilizing group, *Z*. The effectiveness of RAFT agents strongly depends on the monomer being polymerized, polymerization conditions, and on the nature of RAFT agent that is determined by the properties of the leaving group (*R*) and activating group (*Z*) (Adamy *et al.*, 2003; Chiefari *et al.*, 1998; Mayadunne *et al.*, 1999). The role of RAFT agent can be expressed in terms of the *Z* and *R* groups. The Z group does not directly involve in the polymerization reaction, but it significantly influences the stability of the non propagating thiocarbonylthio intermediate radical.

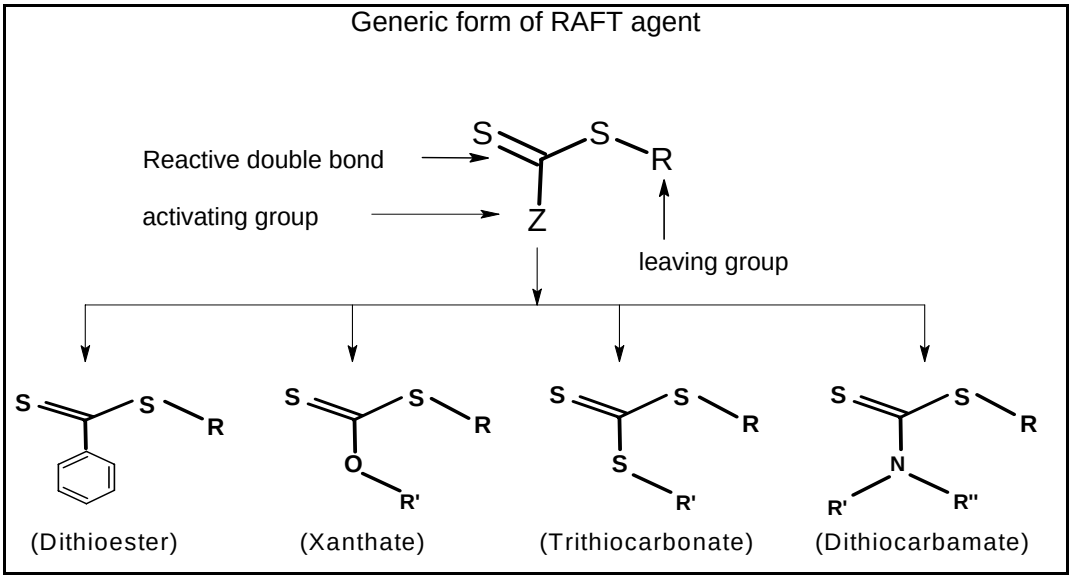

Scheme 2-6: Generic structure of the different RAFT agents.

A strong stabilizing group favours the production of the intermediate radical by enhancing the reactivity of the C=S double bond toward radical addition (high k_{add}). In styrene polymerization, for example, if Z is a phenyl group (e.g. dithioesters), the polymeric radical reacts with the RAFT agent at an addition rate coefficient close to 1×10^{6} dm^{3} $mol^{-1}.s^{-1}$ (Kwak *et al.*, 2004; Monteiro and de Brouwer, 2001; Wang *et al.*, 2003). If Z is substituted with ethoxide moiety (e.g. xanthates) the addition rate

coefficient decreases to 1×10^3(dm^3 mol^{-1}. s^{-1}) (Adamy *et al.*, 2003; Smulders, 2002). The significant difference (~3 orders of magnitude) between these two Z groups, illustrates that this segment of RAFT agent is of great importance. Phenyl as a Z group has been found to be the best candidate for most monomers as it improves the reactivity of RAFT agent and balances the stability of the intermediate radical and its reactivity toward fragmentation (Chiefari *et al.*, 2003; Perrier, 2005).

This type of RAFT agent includes dithioacetates and dithiobenzoates, in which the R group is usually a tertiary alkyl moiety substituted with an electron- withdrawing group. The activity of Dithioesters is higher than the other RAFT agents, and they provide a good control over the molecular weight and structure of the polymer in homogenous polymerization. However, some drawbacks associate with this class of RAFT agents, such as the significant rate retardation in styrene polymerization (Barner-Kowollik *et al.*, 2002; Kwak *et al.*, 2004; Kwak *et al.*, 2002; Monteiro and de Brouwer, 2001).

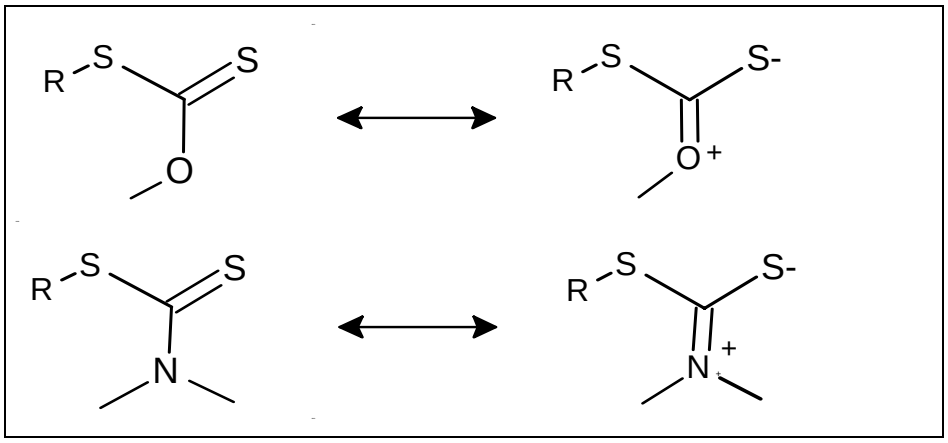

Scheme 2-7: Canonical forms of xanthates and dithiocarbamates.

Experimental data (Chiefari *et al.*, 2003; Chong *et al.*, 2003; Destarac, 2002; Mayadunne *et al.*, 1999) suggest that the chain transfer coefficients ($k_{tr} = k_pC_{tr}$) of the RAFT agents decrease in the series where Z is Ph (C_6H_5) > SCH_2Ph ~ SMe ~ Me ~ N-pyrrolo >> OC_6H_5 > O(alkyl) >> $N(alkyl)_2$, and more general in terms of RAFT agent compounds, the chain transfer coefficient decreases in the series when the RAFT agent is dithiobenzoates > trithiocarbonates ~ dithioalkanoates > dithiocarbonates (xanthates) > dithiocarbamates. R group enables reinitiation, even if its effect is mainly restricted to the first transfer. Therefore, the R group must be a good homolytic leaving group *(k_{frag} ≥ k_{-frag})* relative to the propagating polymeric radical (*Pn**). Experimentally, a tertiary

alkyl moiety substituted with an electron- withdrawing group was found to be the ideal candidate for the R group.

In the case of Z group has O or N attached to the carbon centered atom, the nonbonded electron pair on the heteroatom is delocalized with the S=C double bound, resulting in reducing the reactivity of the double bond toward radical addition, and hence decreasing the addition rate of the propagating radical on the sulfur atom, leading to poor control over the molecular weight (scheme 2-7). This case is best represented by xanthates and dithiocarbamates**.** Xanthates are specified by having alkyl-O- as the Z group, while R group is usually a tertiary alkyl moiety substituted with an electron-withdrawing group. Its activity is low and the polymerization with this kind of RAFT agent usually results in no retardation and a broad polydispersity polymer with a controlled molar mass.

However, xanthates are an important class of RAFT agents, as they are the only RAFT agents that can be successfully used in a conventional *ab initio* emulsion polymerization (Altarawneh *et al.*, 2008; Charmot *et al.*, 2000; Monteiro *et al.*, 2005; Monteiro and De Barbeyrac, 2001; Simms *et al.*, 2005; Smulders *et al.*, 2003; Smulders and Monteiro, 2004). In addition, xanthates are colourless, have a less offensive smell and easier to synthesis. Dithiocarbamates have R_1R_2-N as the Z group, where R_1 is an alkyl group, and R_2 is an electron withdrawing group. An example of this class of RAFT agent is N,N-dialkyl dithiocarbamates. This RAFT agent is inactive in controlling radical polymerization, due to the delocalization of the non-bonded electron pair on the nitrogen with the thiocarbonyl group (scheme 2-7), leading to reduction in the C=S double bond reactivity toward radical addition. On the other hand, this class of RAFT agents have been shown to be effective, if the nitrogen is part of an aromatic system, or substituted by an electron withdrawing group (Chiefari *et al.*, 2003; Destarac, 2000).

2.3.3.2 Transfer constant

The most important parameter that can characterize the ability of a RAFT agent to provide a successful control over the molecular weight is the transfer constant (C_{tr}), which is a measure of the transfer rate to RAFT agent to the propagation rate of the monomer being polymerized. In order to preserve the living nature of the

polymerization, the frequency of the termination reaction should be, as much as possible, maintained at the lowest level. Such a criterion can be achieved by ensuring that the contribution of the initiator derived radical in RAFT polymerization is very low compared to the contribution of RAFT derived radical **(R^*)**. Thus, the vast majority of the polymeric chains are produced by RAFT agent derived radicals. It is, therefore, worth noting that the leaving group **(R^*)** will constitute the end group in the majority of the dormant chains. These features further increase the possibilities of controlling the living free radical polymerization along with increasing the possibilities of producing block copolymer (Smulders *et al.*, 2003).

The overall transfer rate coefficient can be represented as a composite of the addition-fragmentation rate coefficients. From the pre and/or core-equilibrium reactions (Scheme 2-4), the backward (k_{-tr}) and forward (k_{tr}) transfer rate coefficients can be calculated as:

$$k_{tr} = k_{add} \frac{k_{frag}}{k_{frag} + k_{-frag}} \qquad \textbf{(2-18a)}$$

$$k_{-tr} = k_{-add} \frac{k_{-frag}}{k_{frag} + k_{-frag}} \qquad \textbf{(2-18b)}$$

From equation 2-18a it is clear that, in order to achieve a high transfer rate to the initial RAFT agent, k_{-frag} should not be orders of magnitude greater than k_{frag}, or in other words, R should be a good 'leaving' group, preferably better than the added polymeric radical (Smulders, 2002). This means that the intermediate radical fragments in the forward direction. At very low conversions reaction (2) in scheme 2-4 is the dominate one. Once all the initial RAFT agent has been consumed, this reaction will be no longer present and the transfer will then be between the polymeric propagating radicals and the dormant polymeric RAFT agent (***AP***) leading to the production of symmetrical intermediate bi-polymeric radical **(*Pm-A-Pn*).** The value of k_{frag} is assumed to be equal to k_{-frag} due to the symmetrical structure of the intermediate radical, and hence equation 2-18a reduces to:

$$k_{tr} = k_{add} / 2 \qquad \textbf{(2-18c)}$$

To achieve a low polydispersity polymer the growing radical center needs to be transferred quickly so that the propagating radical will not grow too rapidly to too long chain length. This requires that the transfer rate should be higher than the propagation rate or the transfer constant should be greater than one.

2.4 Block copolymers via RAFT process

Block copolymers are macromolecules composed of sequences, or blocks, of chemically distinct repeating units. Block copolymers are useful in many applications where a number of different polymers are connected together to yield a material with hybrid properties. The most important and popular application of block copolymers is their use as thermoplastic elastomers (TPEs). These materials are so versatile that they can be used for wine bottle stoppers, jelly candles, outer coverings for optical fiber cables, adhesives, bitumen modifiers, or in artificial organ technologies and drug delivery systems.

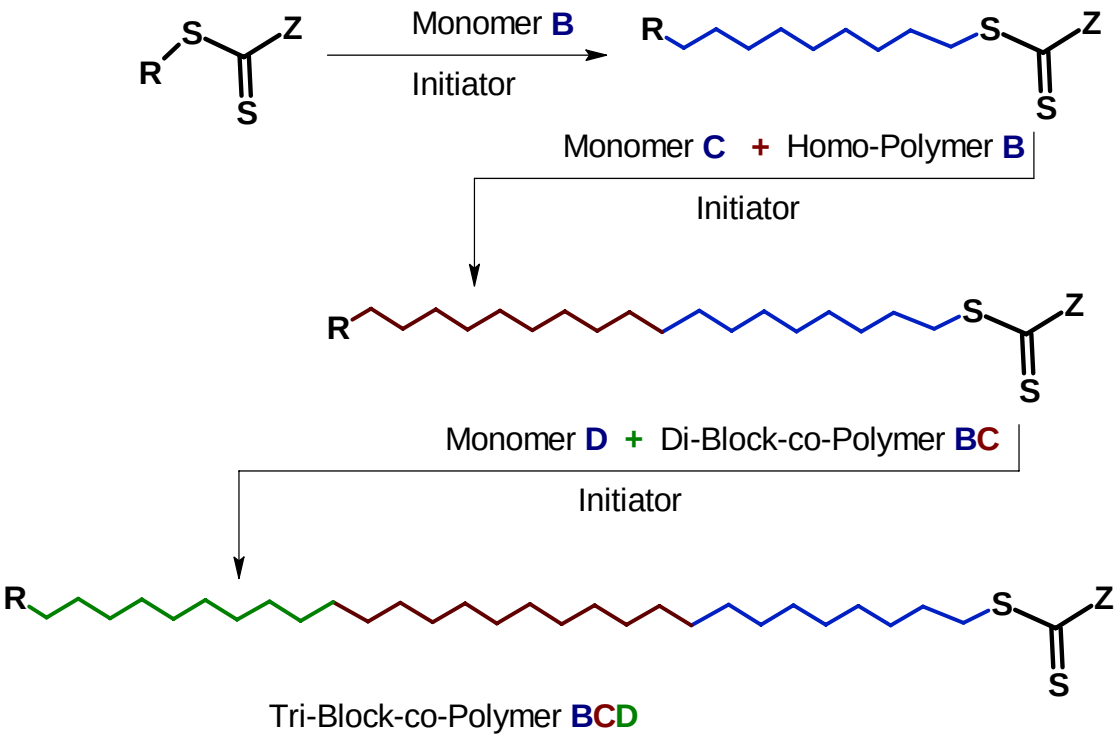

Scheme 2-8: Illustration of the linear Di- and Tri-block copolymers produced by RAFT polymerization.

The importance of block copolymers stems from the fact that a single molecule contains two (or more) different polymers, and therefore may in some sense exhibit the characteristics of both components. This offers the possibility of tuning properties, or combinations of properties, between the extremes of the pure components. However, a random or statistical copolymer could also perform this function without the effort required to prepare the block architecture. The important difference is that, two different polymers will usually not mix as they tend to phase separate into almost pure components. The architecture of a block copolymer defeats this macroscopic phase separation, because of the covalent linkages between the different blocks.

A key feature of RAFT polymerization is that the RAFT moiety (A: thiocarbonylthio end group) present in the initial RAFT agent is retained in the polymeric product. The retention of this group is responsible for polymers' living nature and the product acts as macro RAFT agent (Scheme 2-8). Thus, one of the major straight forward applications of RAFT-mediated living polymerization is the synthesis of block copolymers by simply adding another monomer once the first polymerization stage finishes (Scheme 2-8). The first block consisting of monomer B is initially polymerized in the presence of RAFT agent (AR) forming a macro-RAFT agent or polymeric RAFT agent (AP_B), where P_B is the polymer produced from monomer B. In the second stage of polymerization, the polymeric RAFT agent (AP_B) is used to mediate the polymerization of monomer C resulting in the AP_B-P_C block copolymer.

Triblock copolymers AP_B-P_C-P_B and AP_B-P_C-P_D can be synthesized by adding monomer B or monomer D to the pre-prepared AP_B-P_C block copolymer (Perrier, 2005). If monomer C is added directly to the system when the polymerization of monomer B has reached a high conversion, the final polymeric chain will show a middle section composed of a gradient polymer between B and C, thereby separating the block rich in monomer B from the block rich in monomer C. The difference between copolymers produced by RAFT copolymerization and those produced by conventional copolymerization is that copolymers formed by RAFT copolymerization are gradient copolymers whereas those formed by conventional process are blends (Chiefari *et al.*, 1998; Moad *et al.*, 2005).

The production of block copolymers from sequential monomer addition requires that the first block retains its chain-end functionality, and this is generally achieved by the polymerization of the first monomer being stopped at a conversion below 90%. In RAFT/MADIX polymerization, the radical source introduced to the system to trigger the degenerative chain transfer also leads to the formation of homopolymer side products with uncontrolled chain lengths. Therefore, a low concentration of the radical source should be used to maintain a high ratio of living chains to dead uncontrolled chains. The sequence of the monomer addition also needs careful consideration. One requirement for forming a narrow-polydispersity AP_B-P_C block copolymer is that the first formed polymeric thiocarbonylthio compound should have a high transfer constant to the monomer in the subsequent polymerization. This requires that the leaving ability of the first block should be comparable to, or greater than, that of the propagating radical of the second block (Rizzardo *et al.*, 2000).

2.5 References

Adamy, M.; van Herk, A.M.; Destarac, M. and Monteiro, M.J., 2003. Influence of the Chemical Structure of MADIX Agents on the RAFT Polymerization of Styrene. *Macromolecules*, 36(7): 2293.

Altarawneh, I.S.; Gomes, V.G. and Srour, M.S., 2008. The Influence of Xanthate-Based Transfer Agents on Styrene Emulsion Polymerization: Mathematical Modeling and Model Validation. *Macromolecular Reaction Engineering*, 2(1): 58.

Barner-Kowollik, C.; Vana, P.; Quinn, J.F. and Davis, T.P., 2002. Long-lived intermediates in reversible addition-fragmentation chain-transfer (RAFT) polymerization generated by g radiation. *Journal of Polymer Science, Part A: Polymer Chemistry*, 40(8): 1058.

Benoit, D.; Grimaldi, S.; Finet, J.P.; Tordo, P.; Fontanille, M. and Gnanou, Y., 1998. Controlled/living free-radical polymerization of styrene and n-butyl acrylate in the presence of a novel asymmetric nitroxyl radical. *ACS Symposium Series*, 685(Controlled Radical Polymerization): 225.

Butte, A.; Storti, G. and Morbidelli, M., 2001. Miniemulsion living free radical polymerization by RAFT. *Macromolecules*, 34(17): 5885.

Charmot, D.; Corpart, P.; Adam, H.; Zard, S.Z.; Biadatti, T. and Bouhadir, G., 2000. Controlled radical polymerization in dispersed media. *Macromolecular Symposia*, 150(Polymers in Dispersed Media): 23.

Chiefari, J.; Chong, Y.K.; Ercole, F.; Krstina, J.; Jeffery, J.; Le, T.P.T.; Mayadunne, R.; Meijs, G.F.; Moad, C.L.; Moad, G.; Rizzardo, E. and Thang, S.H., 1998. Living Free-Radical Polymerization by Reversible Addition-Fragmentation Chain Transfer: The RAFT Process. *Macromolecules*, 31(16): 5559.

Chiefari, J.; Mayadunne, R.T.A.; Moad, C.L.; Moad, G.; Rizzardo, E.; Postma, A.; Skidmore, M.A. and Thang, S.H., 2003. Thiocarbonylthio Compounds (S:C(Z)S-R) in Free Radical Polymerization with Reversible Addition-

Fragmentation Chain Transfer (RAFT Polymerization). Effect of the Activating Group Z. *Macromolecules*, 36(7): 2273.

Chong, Y.K.; Krstina, J.; Le, T.P.T.; Moad, G.; Postma, A.; Rizzardo, E. and Thang, S.H., 2003. Thiocarbonylthio Compounds [S:C(Ph)S-R] in Free Radical Polymerization with Reversible Addition-Fragmentation Chain Transfer (RAFT Polymerization). Role of the Free-Radical Leaving Group (R). *Macromolecules*, 36(7): 2256.

Chong, Y.K.; Le, T.P.T.; Moad, G.; Rizzardo, E. and Thang, S.H., 1999. A More Versatile Route to Block Copolymers and Other Polymers of Complex Architecture by Living Radical Polymerization: The RAFT Process. *Macromolecules*, 32(6): 2071.

Cunningham, M.F., 2002. Living/controlled radical polymerizations in dispersed phase systems. *Progress in Polymer Science (Oxford)*, 27(6): 1039.

Destarac, M.B., W.; Taton, D.; Gauthier-Gillaizeau, I.; Zard, S. Z. , 2002. Xanthates as Chain-Transfer Agents in Controlled Radical Polymerization (MADIX): Structural Effect of the O-Alkyl Group. *Macromolecular Rapid Communications*, 23(17): 1049.

Destarac, M.C., D.; Franck, X.; Zard, S. Z. , 2000. Dithiocarbamates as universal reversible addition-fragmentation chain transfer agents. *Macromolecular Rapid Communications*, 21(15): 1035.

Donovan, M.S.; Sanford, T.A.; Lowe, A.B.; Sumerlin, B.S.; Mitsukami, Y. and McCormick, C.L., 2002. RAFT polymerization of N,N-dimethylacrylamide in water. *Macromolecules*, 35(12): 4570.

Feldermann, A.; Toy, A.A.; Phan, H.; Stenzel, M.H.; Davis, T.P. and Barner-Kowollik, C., 2004. Reversible addition fragmentation chain transfer copolymerization: influence of the RAFT process on the copolymer composition. *Polymer*, 45(12): 3997.

Fischer, H., 2001. The Persistent Radical Effect: A Principle for Selective Radical Reactions and Living Radical Polymerizations. *Chem. Rev.*, 101(12): 3581.

Kobatake, S. and Yamada, B., 1995. Severely Hindered Propagation and Termination Allowing Radical Polymerization of .alpha.-Substituted Acrylate Bearing a Bis(carbomethoxy)ethyl Group. *Macromolecules*, 28(12): 4047.

Kwak, Y.; Goto, A. and Fukuda, T., 2004. Rate Retardation in Reversible Addition-Fragmentation Chain Transfer (RAFT) Polymerization: Further Evidence for Cross-Termination Producing 3-Arm Star Chain. *Macromolecules*, 37(4): 1219.

Kwak, Y.; Goto, A.; Tsujii, Y.; Murata, Y.; Komatsu, K. and Fukuda, T., 2002. A kinetic study on the rate retardation in radical polymerization of styrene with addition-fragmentation chain transfer. *Macromolecules*, 35(8): 3026.

Li, I.; Howell, B.A.; Ellaboudy, A.; Kastl, P.E. and Priddy, D.B., 1995. Synthesis, characterization, and evaluation of initiators for living free radical polymerization: Synthesis of polystyrene with controlled structure. *Polymer Preprints (American Chemical Society, Division of Polymer Chemistry)*, 36(1): 469.

Matyjaszewski, K.; Shipp, D.A.; Qiu, J. and Gaynor, S.G., 2000. Water-Borne Block and Statistical Copolymers Synthesized Using Atom Transfer Radical Polymerization. *Macromolecules*, 33(7): 2296.

Matyjaszewski, K. and Xia, J., 2001. Atom Transfer Radical Polymerization. *Chem. Rev.*, 101(9): 2921.

Mayadunne, R.T.A.; Rizzardo, E.; Chiefari, J.; Chong, Y.K.; Moad, G. and Thang, S.H., 1999. Living Radical Polymerization with Reversible Addition-

Fragmentation Chain Transfer (RAFT Polymerization) Using Dithiocarbamates as Chain Transfer Agents. *Macromolecules*, 32(21): 6977.

Michael J. Monteiro, J.d.B., 2002. Preparation of Reactive Composite Latexes by ?Living? Radical Polymerization Using the RAFT Process. A New Class of Polymer Materials. *Macromolecular Rapid Communications*, 23(5-6): 370.

Moad, G.; Chiefari, J.; Chong, Y.K.; Krstina, J.; Mayadunne, R.T.A.; Postma, A.; Rizzardo, E. and Thang, S.H., 2000. Living free radical polymerization with reversible addition-fragmentation chain transfer (the life of RAFT). *Polymer International*, 49(9): 993.

Moad, G.; Rizzardo, E. and Thang, S.H., 2005. Living radical polymerization by the RAFT process. *Australian Journal of Chemistry*, 58(6): 379.

Moad, G., Solomon, D. H., 1995. The Chemistry of Free Radical Polymerization;. Pergamon Press, New York.

Monteiro, M.J.; Adamy, M.M.; Leeuwen, B.J.; van Herk, A.M. and Destarac, M., 2005. A "living" radical ab initio emulsion polymerization of styrene using a fluorinated xanthate agent. *Macromolecules*, 38(5): 1538.

Monteiro, M.J. and Charleux, B., 2005. Living radical polymerisation in emulsion and miniemulsion. *Chemistry and Technology of Emulsion Polymerisation*: 111.

Monteiro, M.J. and De Barbeyrac, J., 2001. Free-radical polymerization of styrene in emulsion using a reversible addition - Fragmentation chain transfer agent with a low transfer constant: Effect on rate, particle size, and molecular weight. *Macromolecules*, 34(13): 4416.

Monteiro, M.J. and de Brouwer, H., 2001. Intermediate radical termination as the mechanism for retardation in reversible addition-fragmentation chain transfer polymerization. *Macromolecules*, 34(3): 349.

Odian, G.G., 2004. Principles of polymerization. Wiley, Hoboken, N.J.

Olaj, O.F.; Vana, P.; Zoder, M.; Kornherr, A. and Zifferer, G., 2000. Is the rate constant of chain propagation kp in radical polymerization really chain-length independent? *Macromolecular Rapid Communications*, 21(13): 913.

Patten, T.E. and Matyjaszewski, K., 1998. Atom-transfer radical polymerization and the synthesis of polymeric materials. *Advanced Materials (Weinheim, Germany)*, 10(12): 901.

Penczek, S., 1997. Ionic polymerization fundamentals Polymer International, 44.

Perrier, S.T., P., 2005. Macromolecular design via reversible addition-fragmentation chain transfer (RAFT)/xanthates (MADIX) polymerization. *Journal of Polymer Science Part A: Polymer Chemistry*, 43(22): 5347.

Ravve, A., 2000. Principles of Polymer Chemistry. Klumer Academic, New York.

Rizzardo, E.; Chiefari, J.; Mayadunne, R.T.A.; Moad, G. and Thang, S.H., 2000. Synthesis of defined polymers by reversible addition-fragmentation chain transfer: The RAFT process. *ACS Symposium Series*, 768: 278.

Russell, G.T., 1994. On exact and approximate methods of calculating an overall termination rate coefficient from chain length dependent termination rate coefficients. *Macromolecular Theory and Simulations*, 3(2): 439.

Russum, J.P.; Barbre, N.D.; Jones, C.W. and Schork, F.J., 2005. Miniemulsion reversible addition fragmentation chain transfer polymerization of vinyl acetate. *Journal of Polymer Science, Part A: Polymer Chemistry*, 43(10): 2188.

Simms, R.W.; Davis, T.P. and Cunningham, M.F., 2005. Xanthate-mediated living radical polymerization of vinyl acetate in miniemulsion. *Macromolecular Rapid Communications*, 26(8): 592.

Smulders, W.W., 2002. Macromolecular architecture in aqueous dispersions: 'living' free-radical polymerization in emulsion. Ph.D. Thesis, Technische Universiteit Eindhoven, Eindhoven, Neth.

Smulders, W.W.; Gilbert, R.G. and Monteiro, M.J., 2003. A kinetic investigation of seeded emulsion polymerization of styrene using reversible addition-fragmentation chain transfer (RAFT) agents with a low transfer constant. *Macromolecules*, 36(12): 4309.

Smulders, W.W. and Monteiro, M.J., 2004. Seeded emulsion polymerization of block copolymer core-shell nanoparticles with controlled particle size and molecular weight distribution using xanthate-based RAFT polymerization. *Macromolecules*, 37(12): 4474.

Solomon, D.H.; Rizzardo, E. and Cacioli, P., 1985. Free radical polymerization and the produced polymers. Eur. Pat. Appl, EP 135280

Souaille, M. and Fischer, H., 2000. Kinetic Conditions for Living and Controlled Free Radical Polymerizations Mediated by Reversible Combination of Transient Propagating and Persistent Radicals: The Ideal Mechanism. *Macromolecules*, 33(20): 7378.

Stevens., M.P., 1999. Polymer chemistry : an introduction. Oxford University Press, New York.

Szwarc, M., 1956. Living Polymers. *Nature*, 178: 1168

Uzulina, I.; Kanagasabapathy, S. and Claverie, J., 2000. Reversible addition fragmentation transfer (RAFT) polymerization in emulsion. *Macromolecular Symposia*, 150: 33.

Wang, A.R.; Zhu, S.; Kwak, Y.; Goto, A.; Fukuda, T. and Monteiro, M.S., 2003. A difference of six orders of magnitude: A reply to the magnitude of the fragmentation rate coefficien. *Journal of Polymer Science, Part A: Polymer Chemistry*, 41(18): 2833.

Wang, J., Matyjaszewski, K., 1995. Controlled/"Living" Radical Polymerization. Halogen Atom Transfer Radical Polymerization Promoted by a Cu(I)/Cu(II) Redox Process *Macromolecules*, 28(23): 7901.

Zetterlund, P.B.; Busfield, W.K. and Jenkins, I.D., 1999. Free Radical Polymerization of Acrylonitrile: Mass Spectrometric Identification of the Nitroxide-Trapped Oligomers Formed in and Estimated Rate Constants for Each of the First Eight Propagation Steps. *Macromolecules*, 32(24): 8041.

Chapter Three

Modelling of RAFT in Bulk and Solution Polymerizations

Chapter 3

Modeling of RAFT in Bulk and Solution Polymerizations

Abstract

This chapter focuses on the mechanism of RAFT process and the effect of R and Z groups, along with a review of the previous work on rate retardation. A mathematical model accounting for the concentrations of the propagating, intermediate, dormant and dead chains is developed based on their reaction pathways. The kinetic scheme employed includes initiation, propagation, pre-equilibrium, core-equilibrium and termination of the propagating radicals, along with termination reactions of the carbon-centered intermediate radical. This model is combined with a chain-length dependent termination model in order to account for the decreased termination rate. The model has been validated against experimental data for both solution and bulk polymerizations of styrene.

The model predictions indicate that the observed retardation can be attributed to the cross termination of the intermediate radical and, to some extent, to the RAFT effect on increasing the average termination rate coefficient. The model predictions suggest that, in order to preserve the living nature of RAFT polymerization, a low initiator concentration is required.

3.1 Introduction

Living free radical polymerization techniques allow for the production of complex architecture polymers such as block, comb, and star copolymers with controlled molecular weight distributions. The most prominent techniques capable of inducing living characteristics in free radical polymerization are atom transfer free radical polymerization (ATRP) (Matyjaszewski and Xia, 2001), nitroxide-mediated polymerization (NMP) (Schulte *et al.*, 2004; Solomon *et al.*, 1985) and reversible addition-fragmentation chain transfer polymerization (RAFT) (Chiefari *et al.*, 1998;

Moad *et al.*, 2005). The principle of these techniques is based on the dynamic equilibrium developed between the active and dormant species by either reversible termination or reversible transfer, which implies an alternating activation of the dormant polymer chains and deactivation of the active chains (Moad *et al.*, 2005). In reversible termination, i.e. NMP and ATRP, the end-capped chain can be activated through undergoing a reversible homolytic cleavage, resulting in the activated polymer chain adds monomer units until it is deactivated again by a capping agent. Such activation-deactivation reactions lower the free radical concentration and hence significantly decrease termination events whereby a pseudo living polymer is obtained.

In reversible addition-fragmentation chain transfer (RAFT), the exchange between the dormant species (carrying RAFT moiety) and the active propagating polymeric chains is rapid and offers an equal probability for the end-capped polymeric chains to activate via the fragmentation of the intermediate radical and add more monomer units, while deactivation of the polymeric radicals proceeds via the addition to the dormant agent. Polymers with predictable molecular weights and narrow polydispersity ($1.05<PDI<1.4$) can be produced for a wide range of monomers, while their end group can be maintained active at the end of the reaction (Chiefari *et al.*, 1998; Moad *et al.*, 2005). The RAFT process resembles the degenerative transfer (DT), in which there is a fast exchange between growing radical and dormant species via transfer reactions. In RAFT this exchange takes place via an intermediate radical, while in DT a direct exchange occurs without the formation of an intermediate radical.

3.2 The RAFT process

3.2.1 Mechanism of RAFT polymerization

The RAFT mechanism is facilitated by compounds having a structure such as (S=C(Z)S-R, reagent AR scheme 3-1) (Chiefari *et al.*, 1998). Such compounds can be designed with structural variety involving the leaving group **R** and the stabilizing group **Z**. A polymerization reaction using a RAFT agent is postulated to proceed according to the kinetic events given in scheme 3-1 (Chiefari *et al.*, 1998; Goto *et al.*, 1999; Moad *et al.*, 2005). As in free radical polymerization, the decomposition of a conventional free-radical initiator generates free radicals. The initiator derived radical may terminate, add

to the RAFT agent, AR, and add to monomer. In typical RAFT polymerization the concentrations of the initiator and the RAFT agent are much lower than the monomer concentration, and as a result the probability that the initiator derived radical reacts with monomer is much higher. Addition of the initiator derived radical to monomer produces a polymeric propagating radical $Pn^{\bullet}$.

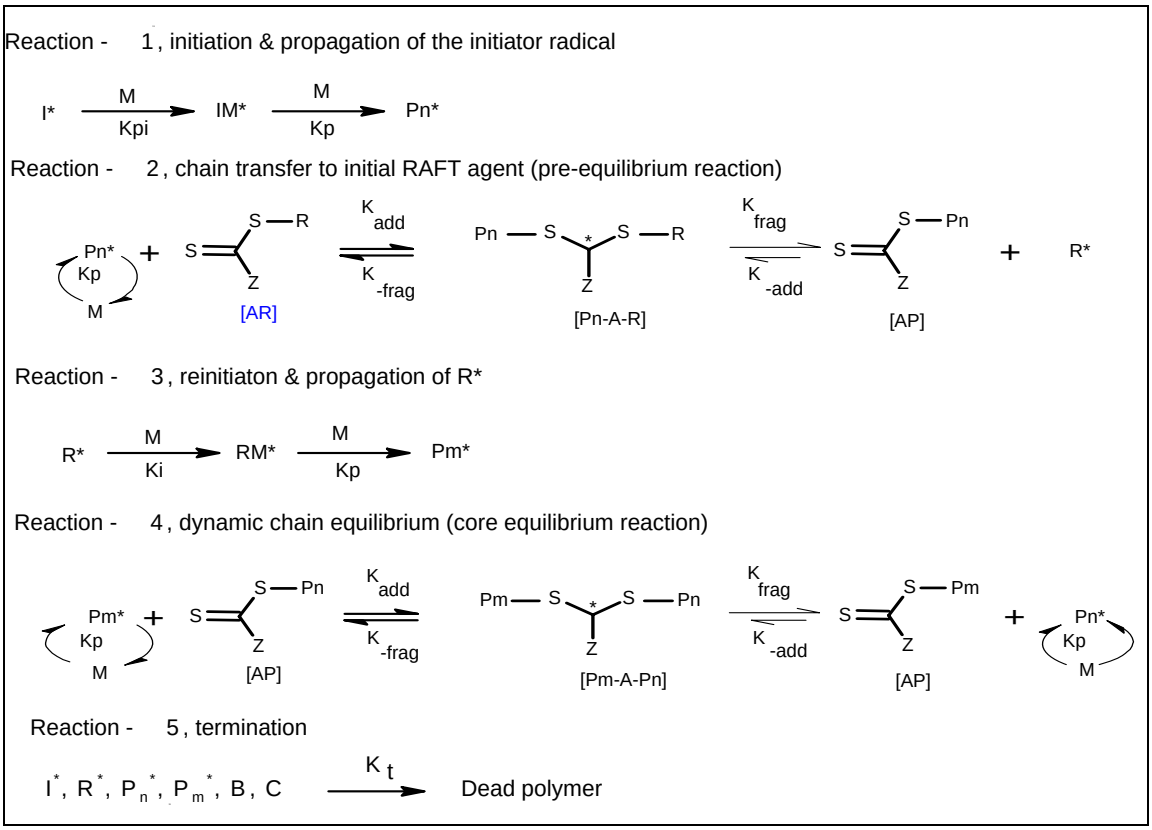

Scheme 3- 1: Detailed mechanism of RAFT free radical polymerization.

During the pre-equilibrium stage, addition of the propagating radical $Pn^{\bullet}$ to the thiocarbonylthio reagent (compound AR) followed by forward fragmentation of the intermediate radical (compound Pn-A-R), gives rise to a temporarily deactivated dormant polymer species (a polymeric RAFT agent, compound AP) and a new reinitiating radical $R^{\bullet}$. The intermediate radical may collapse into its originating species resulting in rate retardation and poor control of the molecular weight, unless R is a good homolytic leaving group. Generally, higher alkyl substitution of the α-carbon of the R group enhances the leaving character of this moiety. Thus, a tertiary alkyl leaving group generally offers better control over molecular architecture than primary or secondary alkyl leaving groups. Also further substitution with moieties that can stabilize the

expelled radical through resonance increases the leaving character of the **R** group. Another key feature regarding the **R** group is its ability to reinitiate polymerization. If the leaving radical $\mathbf{R}^{\bullet}$ slowly adds to monomer then inhibition and retardation may occur, mainly during the early stages of the polymerization resulting in broadening of the molecular weight distribution.

The intermediate polymeric radical **Pn-A-R** is linked on one side with a polymer chain and on the other side with the **R** group; this intermediate radical can then fragment forward with a rate coefficient , k_{frag} , or undergoes a reverse fragmentation reaction governed by the reverse fragmentation coefficient , k_{-frag} ,. The fragmentation direction depends on the stability of the attached radicals **($\mathbf{Pn}^{\bullet}$** and **$\mathbf{R}^{\bullet}$).** Preferably, larger chains attached to the intermediate radicals (unsymmetrical radicals) have a greater tendency to break, which suggests that the equilibrium is even shifted toward the starting materials. Therefore, a critical selection of the R group is definitely essential to properly start the RAFT reaction.

The reinitiating radical $\mathbf{R}^{\bullet}$ propagates with monomer forming a new propagating radical $\mathbf{Pm}^{\bullet}$ which can add either to the RAFT agents AR or AP. The back addition of the reinitiating radical $\mathbf{R}^{\bullet}$ to the polymeric RAFT agent **AP** is kinetically insignificant since the propagation rate of $\mathbf{R}^{\bullet}$ with monomer is much higher than the back addition rate ($k_i[M] >> k_{-add}[AP]$) and thus the back addition reaction can be neglected from the kinetic equations. Due to the retention of the RAFT moiety (A: S=C(Z)S-) the dormant polymeric RAFT agent **AP** acts similar to a RAFT agent **AR.** As in reaction 2 (pre-equilibrium reaction) a propagating radical $\mathbf{Pm}^{\bullet}$ reacts with the polymeric RAFT agent **AP**, thereby forming a symmetrical intermediate radical **Pm-A-Pn**. The symmetrical intermediate radical **Pm-A-Pn** has an equal probability of undergoing either forward or backward fragmentation; hence there is no preference regarding which direction the fragmentation would take place. The chain length of the two attached polymeric radicals to the both sides of the intermediate radical **Pm-A-Pn** may not be exactly of the same length; this may have no effect on the fragmentation direction, unless one of the two polymeric radicals is extremely short.

Reaction 4 in Scheme 3-1 is the core of the RAFT process, and is described by the equilibrium constant **K** ($K = k_{add} / k_{frag}$), representing the quotient of the rate coefficient of addition and the rate coefficient of fragmentation. Through the core-equilibrium reaction (reaction 4) a propagating radical $\mathbf{Pm^{\bullet}}$ is transformed into a dormant chain, while the retained polymeric radical $\mathbf{Pn^{\bullet}}$ which is release is capable of further growth. The process of radical addition and release repeats itself continuously throughout the core-equilibrium stage, thereby, providing an equal probability for all polymeric radicals to grow simultaneously. In addition, the vast majority of chains retain the thiocarbonylthio moiety **(A: S=C(Z)S)** when the reaction is completed (Kubo *et al.*, 2005; Mayadunne *et al.*, 2000; Smulders *et al.*, 2003), thus block copolymers synthesis by polymerizing another monomer is possible. It is important to realize that equilibrium takes place between the whole population of propagating radicals and the whole population of the dormant chains. The concentration of the RAFT agent (AR and AP) is constant, unless the thiocarbonylthio moiety is destroyed in the reaction. The radical concentration in a typical polymerization is usually five to six orders of magnitude lower than the concentration of the RAFT agent (Monteiro and de Brouwer, 2001; Wang *et al.*, 2003). This indicates that a very small number of radicals are exchanged amongst a large number of polymer chains at any given moment.

Bimolecular termination reactions take place when two growing radicals encounter each other. Termination between polymeric radicals and initiator-derived radicals, $\mathbf{I^{\bullet}}$, or chain transfer agent derived radicals, $\mathbf{R^{\bullet}}$, can usually be neglected due to their low concentrations in the polymerization system (Monteiro and de Brouwer, 2001; Schilli *et al.*, 2002). In RAFT systems the occurrences of the termination reactions are relatively suppressed because the probability that two radicals meet each other is much lower than that in conventional free radical polymerization systems. It is believed that the intermediate radicals formed in RAFT polymerizations may undergo self termination with each other or cross termination with propagating radicals. The existence of such terminations is still a subject of much debate (Kwak *et al.*, 2004a; Monteiro and de Brouwer, 2001). However, experimental results reported by Kwak *et al*. (2004b) and de Brouwer *et al*. (2000), suggest the formation of a 3-arm star polymer which is a possible product of the cross termination of the intermediate radicals. Furthermore, such termination is believed to be irreversible, because at 60^{o}C no decay of the 3-arm star polymer concentration was observed. Evidence supporting the above discussed RAFT

mechanism was reported by Hawthorn *et al.* (1999), where the formation of the intermediate polymeric (**Pn-A-R**) and bipolymeric (**Pm-A-Pn**) RAFT radicals were experimentally verified by direct ESR observation, and by the end group analysis of the polymer products using NMR and UV-vis spectroscopy conducted by Chiefari *et al.*(1998).

3.2.2 Retardation in RAFT homogeneous polymerization

The activation-deactivation equilibrium in RAFT polymerization is a chain transfer reaction, in which for each radical consumed via reversible termination, a new radical forms and sustains the radical flux. Theoretically, from the kinetics of free radical polymerization, the polymerization rate is strongly related to the concentration of propagating radicals and their termination rate coefficients. Therefore, the addition of a RAFT agent should not affect the concentration of the free radicals. However, experimental data shows that RAFT polymerization, under the same conditions as in a conventional process, experiences decreasing rate of polymerization (retardation effect).

This phenomena is more pronounced when using highly active RAFT agents, such as dithiobenzoates (Barner-Kowollik *et al.*, 2006; Barner-Kowollik *et al.*, 2001; Barner-Kowollik *et al.*, 2002; Chiefari *et al.*, 2003; Coote, 2004; Kwak *et al.*, 2004a; Kwak *et al.*, 2004b; Kwak *et al.*, 2002; Luo *et al.*, 2006; Vana *et al.*, 2002b), and very little or even negligible when using low active RAFT agents such as xanthates (Adamy *et al.*, 2003; Smulders, 2002; Smulders *et al.*, 2003). Nevertheless, in bulk and solution polymerization of styrene with cumyl-dithiobenzoate (CDB), a linear growth of molecular weight with conversion, and polydispersity index (PDI) values lower than 1.1 were reported for different CDB concentrations and monomer conversions (Kwak *et al.*, 2004a; Saricilar *et al.*, 2003; Vana *et al.*, 2002c). These experimental findings indicate that the retardation rate has no effect on the polydispersity and molecular weight, but dramatically influences the overall kinetics.

The causes of the inhibition and rate retardation were investigated and the proposed reasons are: (i) slow fragmentation of the intermediate radical (Barner-Kowollik *et al.*, 2005; Barner-Kowollik *et al.*, 2001; Barner-Kowollik *et al.*, 2002; Feldermann *et al.*, 2004; Vana *et al.*, 2002b); and, (ii) additional side reactions such as termination of the

intermediate RAFT radical with either growing polymeric radicals (cross-termination) or among themselves (self-termination) (Monteiro and de Brouwer, 2001; Wang *et al.*, 2003). The latter explanation is the most widely accepted one, as investigations with polymeric 3-armed stars polymer formed in RAFT process indicate intermediate radical cross termination (Kwak *et al.*, 2004a; Kwak *et al.*, 2004b; Venkatesh *et al.*, 2004). Other factors that may also affect the polymerization rate are: increasing termination rate and slow reinitiation by the expelled radical $\mathbf{R}^{\bullet}$ (Chiefari *et al.*, 1998; Moad *et al.*, 2000).

In the work of Perrier *et al*.(2002), the effect of the slow re-initiation on the inhabitation period was investigated by considering the re-initiation rate coefficient for Cumyl and Cyanoisopropyl radicals generated from two different RAFT agents. Since the Cumyl radical has a re-initiation rate coefficient higher than that for the Cyanoisopropyl radical, it may be concluded that the Cumyl radical would undergo fast re-initiation and induce less inhabitation period. However, experimental data suggests that the Cumyl radical induces the longest inhabitation period followed by Phenylethyl and then Cyanoisopropyl. For this reason, the observed inhabitation period is not caused by slow re-initiation, and the stability of the intermediate radical has a significant role in the inhabitation effect, which for Cumyl is higher than that for Phenylethyl, while that for Phenylethyl is also higher than that for Cyanoisopropyl. Thus, slow reinitiation may not significantly influence the polymerization rate, especially with highly active RAFT agents (transfer constant $C_{tr} > 10$), since its effect is restricted to the first transfer.

Several studies were conducted to investigate the effect of the intermediate radical and the leaving group on polymerization processes (Chiefari *et al.*, 1998; Chiefari *et al.*, 2003; Donovan *et al.*, 2002; Perrier *et al.*, 2002). A RAFT agent like CPDB (2-(2-cyanopropyl) Dithiobenzoate) has a leaving group similar to the initiating species generated by the initiator. This RAFT agent was reported to be an effective agent in the polymerization of styrene in bulk polymerization. In these systems no significant inhabitation at low RAFT agent concentration was observed. Yet, the inhabitation period was found to increase with increasing the RAFT agent concentration. In addition, rate retardation was observed and was found to be almost similar in magnitude to that reported in 1-phenylethyl Dithiobenzoate (1-PEDP) mediated polymerization. As

both (CPDB) and (1-PEDP) RAFT agents have the same Z-group (phenyl), both systems shows the same degree of retardation (Perrier *et al.*, 2002).

For polymerization of styrene mediated by CDB, Barner-Kowollik *et al.* (Barner-Kowollik *et al.*, 2001; Barner-Kowollik *et al.*, 2002) assumed that the intermediate radical is stable enough to cause no polymerization and no termination with a propagating radical; thus the slow fragmentation of the intermediate radical was postulated to be the main reason behind the observed retardation. A fragmentation rate coefficient of the order of $10^{-2}s^{-1}$ was estimated using conversion-molecular weight data and was used to fit their experimental data. However, based on ESR measurements for the same system, Kwak *et al*. (2002) concluded that the fragmentation is fast with a relevant rate constant of the order of $10^{4}s^{-1}$, thereby leading to bring about a quick equilibrium with the addition, and that the slow fragmentation is not the key reason for the retardation in the styrene/CDB. On the other hand, Monteiro *et al.* (2001), noticed the formation of tripled molecular weight species with UV-irradiated polystyryl dithiobenzoate (PSt-SCSPh) in a monomer-free experiment. These authors then assumed that the intermediate RAFT radical undergoes cross termination with the propagating polymeric radical (Polystyryl radical, $PSt^{\bullet}$).

In the polymerizations of styrene with O-ethylxanthyl ethyl propionate (xanthate I) and O-ethylxanthyl ethyl benzene (xanthate II) conducted by Smulders (2002), no retardation was observed. It has been pointed out that, due to the lower resonance of the ethoxide (on the xanthate) compared with the phenyl (on the CDB), the intermediate radical formed in the polymerization with xanthates is less stable and may have a fragmentation rate higher than the reported one for the intermediate radical formed in the polymerization with CDB ($\sim 10^{5}\ s^{-1}$).

3.3 Modelling RAFT polymerization

For a better understanding of the process, a model based on the proposed polymerization mechanism (Scheme 3-1) has been developed. The repeated RAFT reaction cycles, which induce the equilibrium between active and dormant radicals via the formation of the intermediate radicals, are implemented directly according to their

reaction pathways. This model does not account for the chain lengths but shows the time evaluation of the species generation and consumption.

In this work, the initiator-derived radicals (P_n^*) are considered to be similar to the RAFT-derived radicals ($P_m^\bullet$). This assumption is likely to be valid, since in a typical recipe involving RAFT polymerization, a small amount of initiator compared with the RAFT agent is applied. Hence the vast majority of the propagating species are derived from the RAFT agent. The dormant polymeric RAFT agent (**AP)** acts as the initial RAFT agent (**AR)** due to the retention of the thiocarbonylthio fragment (A: S=C(Z)S-), and therefore all propagating radicals are assumed to have the same addition rate coefficient to the initial RAFT agent or to the polymeric RAFT agent. Once the initial RAFT compound is consumed, the carbon-centered intermediate radical (species **Pm-A-Pn**, Scheme 3-1) produced is attached with two polymeric chains ($P_n^\bullet$ and $P_m^\bullet$) of approximately the same length and identical stability. Hence the symmetrical intermediate radical has no preference with respect to the direction of the fragmentation ($k_{frag} \approx k_{\_frag}$) (Butté, 2000; Smulders, 2002). Unless one of the two polymeric radicals is extremely short, there is no effect on the fragmentation direction (Smulders, 2002). The intermediate radical is assumed to terminate with another intermediate radical (self termination) and any other propagating radical (cross termination).

3.3.1 Species concentrations

In RAFT polymerization there are two kinds of initiating radicals, these are: radicals generated from the initiator known as initiator-derived radicals; and radicals generated from the RAFT agent, known as RAFT-derived radicals. The propagation of these radicals results in two kinds of propagating polymeric chains with two different end groups. A mass balance over the active and dormant species gives:

$$\frac{d[I^\bullet]}{dt} = 2fk_d[I] \qquad \textbf{(3-1)}$$

$$\begin{aligned}\frac{d[P^\bullet]}{dt} = {} & 2fk_d[I] + k_{pi}[R^\bullet][M] + k_{\_frag}[PAR] + k_{frag}[RAP] + 2k_{frag}[PAP] \\ & - k_{add}[P^\bullet][AR] - k_{add}[P^\bullet][AP] - k_{\_add}[P^\bullet][AP] - k_{\_add}[P^\bullet][AR] \\ & - k_t[P^\bullet]([P^\bullet]+[R^\bullet]) - k_{ct}[P^\bullet]([PAP]+[PAR]+[RAP]+[RAR])\end{aligned} \qquad \textbf{(3-2)}$$

$$\frac{d[R^\bullet]}{dt} = -k_{pi}[R^\bullet][M] + k_{frag}[PAR] + k_{-frag}[RAP] + 2k_{frag}[RAR] + k_{-frag}[RAP] - k_{add}[R^\bullet][AR] - k_{add}[R^\bullet][AP] - k_{-add}[R^\bullet][AR] - k_{-add}[R^\bullet][AP] - k_t[R^\bullet]([P^\bullet]+[R^\bullet]) - k_{ct}[R^\bullet]([PAP]+[PAR]+[RAP]+[RAR]) \quad \textbf{(3-3)}$$

Four intermediate radicals are expected to be formed in RAFT polymerization, these are:

1- RAR type intermediate radical resulted from the addition of $R^\bullet$ type radicals to the initial RAFT agent AR:

$$\frac{d[RAR]}{dt} = k_{add}[R^\bullet][AR] + k_{-add}[R^\bullet][AR] - 2k_{frag}[RAR] - k_{ct}[RAR]([P^\bullet]+[R^\bullet]) - k_{st}[RAR]\cdot([PAP]+[PAR]+[RAP]+[RAR]) \quad \textbf{(3-4)}$$

2- PAR type intermediate radical resulted from the addition of $P^\bullet$ type radicals to the initial RAFT agent AR:

$$\frac{d[PAR]}{dt} = k_{add}[P^\bullet][AR] + k_{-add}[P^\bullet][AR] - k_{frag}[PAR] - k_{-frag}[PAR] - k_{ct}[PAR]([P^\bullet]+[R^\bullet]) - k_{st}[PAR]\cdot([PAP]+[PAR]+[RAP]+[RAR]) \quad \textbf{(3-5)}$$

3- RAP type intermediate radical resulted from the addition of $R^\bullet$ type radicals to the polymeric RAFT agent AP:

$$\frac{d[RAP]}{dt} = k_{add}[R^\bullet][AP] + k_{-add}[R^\bullet][AP] - k_{frag}[RAP] - k_{-frag}[RAP] - k_{ct}[RAP]([P^\bullet]+[R^\bullet]) - k_{st}[PAR]\cdot([PAP]+[PAR]+[RAP]+[RAR]) \quad \textbf{(3-6)}$$

4- PAP type intermediate radical resulted from the addition of $P^\bullet$ type radicals to the polymeric RAFT agent AP:

$$\frac{d[PAP]}{dt} = k_{add}[P^\bullet][AP] + k_{-add}[P^\bullet][AP] - 2k_{frag}[PAP] - k_{ct}[PAP]([P^\bullet]+[R^\bullet]) - k_{st}[PAP]\cdot([PAP]+[PAR]+[RAP]+[RAR]) \quad \textbf{(3-7)}$$

The concentrations of the dormant species AR and AP are given by:

$$\frac{d[AR]}{dt} = -k_{add}[P^{\bullet}][AR] - k_{add}[R^{\bullet}][AR] - k_{-add}[P^{\bullet}][AR] - k_{-add}[R^{\bullet}][AR] + k_{-frag}[PAR] + 2k_{frag}[RAR] + k_{frag}[RAP] \quad \textbf{(3-8)}$$

$$\frac{d[AP]}{dt} = -k_{add}[P^{\bullet}][AP] - k_{add}[R^{\bullet}][AP] - k_{-add}[P^{\bullet}][AP] - k_{-add}[R^{\bullet}][AP] + k_{-frag}[RAP] + 2k_{frag}[PAP] + k_{frag}[PAR] \quad \textbf{(3-9)}$$

The overall concentration of the propagating radicals $[T^{\bullet}]$ is given by the total concentration of the propagating radicals $P^{\bullet}$ and $R^{\bullet}$:

$$\frac{d[T^{\bullet}]}{dt} = 2fk_d[I] + k_{frag}[TAT] + k_{-frag}[TAT] - k_{add}[T^{\bullet}]([AR]+[AP]) - k_{-add}[T^{\bullet}]([AR]+[AP]) - k_t'[T^{\bullet}]^2 - k_{ct}[T^{\bullet}][TAT] \quad \textbf{(3-10)}$$

The overall concentration of the intermediate radicals $[TAT]$ is given by the total concentration of the intermediate radicals PAP, PAR, RAP and RAR:

$$\frac{d[TAT]}{dt} = k_{add}[T^{\bullet}]([AR]+[AP]) + k_{-add}[T^{\bullet}]([AR]+[AP]) - k_{frag}[TAT] - k_{-frag}[TAT] - k_{ct}[T^{\bullet}][TAT] - k_{st}[TAT]^2 \quad \textbf{(3-11)}$$

The summation of the concentrations of $[AR]$ and $[AP]$ gives the total concentration of the dormant chains, and this is equal to the concentration of the initial RAFT agent at the beginning of the reaction, $[AR_o]$; fk_d is the effective dissociation rate coefficient of the initiator, which is the product of the initiator efficacy and the coefficient of thermally induced initiator decomposition. Both quantities are available from literature for a wide range of temperatures (Buback, 1994; Moad *et al.*, 1984) . The parameters k_{add} and k_{-add} are the forward and backward addition rate coefficients, respectively; k_{frag} , k_{-frag} are the forward and backward fragmentation rate coefficients of the intermediate radical, respectively; k_t' is the chain length dependent termination rate coefficient for the termination between two propagating radicals; k_{ct} and k_{st} are the cross and self termination rate coefficients of the intermediate radicals, respectively.

Using the steady state assumption, the summation of Equations **(3-10)** and **(3-11)** gives the overall initiation rate which is equal to the rate at which the radicals undergo mutual annihilation. The steady state initiation is given by:

$$2fk_d[I] = k_t[T^\bullet]^2 + 2k_{ct}[T^\bullet][TAT] + k_{st}[TAT]^2 \qquad \textbf{(3-12)}$$

Substituting Equation **(3-12)** into Equation **(3-10)** gives:

$$\begin{aligned} 0 = {} & k_{frag}[TAT] + k_{-frag}[TAT] + k_{ct}[T^\bullet][TAT] + k_{st}[TAT]^2 \\ & - k_{add}[T^\bullet]([AR]+[AP]) - k_{-add}[T^\bullet]([AR]+[AP]) \end{aligned} \qquad \textbf{(3-13)}$$

The typical values of the radical concentration ($[T^\bullet]$ and/or $[TAT]$) are of the order of 1×10^{-9} to 1×10^{-8} (Monteiro and de Brouwer, 2001), so that it is safe to assume that both cross and self termination terms are negligible relative to the addition and fragmentation terms. Hence, Equation **(3-13)** becomes:

$$[TAT](k_{frag} + k_{-frag}) - [T^\bullet]([AR]+[AP])(k_{add} + k_{-add}) = 0 \qquad \textbf{(3-14)}$$

This equation expresses the equilibrium between the propagating radicals and dormant species. The concentration of the dormant species is assumed to be constant over the entire reaction period. This may not be the case, however, because of the irreversible cross termination between an intermediate radical and a propagating radical resulting in a 3-armed star dead polymer that contains the RAFT moiety, and hence a very small amount of the dormant species will be destroyed. The loss of a small or even negligible amount of RAFT moiety may not significantly affect the dynamic equilibrium and hence Equation (3-14) is still valid. Due to the high monomer concentration relative to the RAFT agent concentration, and assuming that the leaving radicals $\mathbf{R}^\bullet$ and $\mathbf{P}^\bullet$ have a high reactivity to monomer, the reverse addition reaction can be neglected from the kinetic study ($k_{pi}[M] >> k_{-add}[AP]$) (Smulders, 2002). Under the steady state conditions, the equilibrium constant **K** can be given by:

$$K = \frac{k_{add}}{k_{frag}} = \frac{2\cdot[TAT]}{[T^\bullet]([AR]+[AP])} = \frac{2\cdot[TAT]}{[T^\bullet][AR_o]} \qquad \textbf{(3-15)}$$

Assuming that the addition-fragmentation equilibrium is achieved, and by taking the intermediate radicals' side reactions into account, the steady-state concentration of the propagating radical can be estimated by solving Equations (3-12) and (3-15) for [T$^\bullet$]:

$$[T^\bullet]^2 = \frac{4 \cdot f \cdot k_d \cdot k_{frag} \cdot [I]}{2 \cdot k_{frag} \cdot k_t + 2 \cdot k_{add.} k_{ct} \cdot [AR_o] + 0.5 \cdot k_{st} \cdot (k_{add} / k_{frag}) \cdot k_{add} \cdot [AR_o]^2} \quad \textbf{(3-16)}$$

3.3.2 Chain length dependent termination rate

Most often the growth of a polymer chain is halted by the termination reaction. In ideal RAFT polymerization, assuming that the concentration of radicals remains constant, the repeated reversible transfer events during the polymerization induce equilibrium between dormant and living chains; thus the overall rate of polymerization and the rate of individual reaction steps remain unaltered. Consequently, all chains will grow together at the same time. However, this behaviour cannot be completely achieved in RAFT polymerization systems because of the termination reactions that alter radical concentrations and hence affect the livingness nature of the polymerization, leading to a reduction in the polymerization rate (retardation effect) (Kwak *et al.*, 2004a; Kwak *et al.*, 2004b; Moad *et al.*, 2005; Monteiro and de Brouwer, 2001; Vana *et al.*, 2002a).

In the RAFT polymerization mechanism presented in Scheme 3-1, there are four types of radicals involved in the system where each radical can undergo self termination with a radical of the same kind and cross termination with the other different radicals. The termination rate coefficient $(k_t^{'})$, which controls the termination reactions between the propagating radicals (P_n^*) and (P_m^*) is known to be chain-length dependent (Russell, 1993). The presence of the RAFT agent in the polymerization system affects the chain-length distribution and hence the termination rate coefficient will be influenced. The termination rate coefficient can be calculated from the microscopic termination coefficient $(k_t^{i,j})$ between two chains having length '*i*' and '*j*' using the Smoluchowski equation:

$$k_t^{i,j} = 2 \cdot \pi \cdot P_{ij} \cdot (D_i + D_j) \cdot r \cdot N_A \quad \textbf{(3-17)}$$

where P_{ij} is the probability that a radical-radical encounter will result in termination; N_A is Avogadro's number; r is van der Waals radii of the monomer; D_i, D_j are the diffusion rate coefficients of chains of length '*i*' and '*j*'. The diffusion coefficient is a function of the weight fraction of the polymer and can be calculated according to the following expression (Piton *et al*., 1993):

$$D_i(w_p) = \frac{D_{mon}(w_p)}{i^n} \quad \textbf{(3-18)}$$

where D_{mon} is the monomer diffusion coefficient; D_i is the diffusion coefficient of a propagating chain of length '*i*'. The exponent *n* is equal to (0.49) for $(w_p = 0.0)$ and $(0.66 + 2w_p)$ for $(w_p > 0.0)$. In RAFT polymerization, the chain length '*i*' can be approximated by the ratio of the polymerized monomer to the chains number as follows:

$$i = \frac{x \cdot M_o}{\delta} \quad \textbf{(3-19)}$$

$$\delta = [AR]_o + 2fk_d[I] \quad \textbf{(3-20)}$$

The second term in equation (3-20) describes the number of chains that are derived from the decomposed initiator. In the absence of the RAFT agent, the average degree of polymerization *'i'* can be estimated from the average kinetic chain length ($i = k_p[M]/\sqrt{2fk_dk_t[I]}$). For the polymerization of styrene at 60°C with dithiobenzoate as a RAFT agent, Kwak *et al.* (2004a) estimated the ratio of cross termination rate coefficient to propagating radical termination rate coefficient to be 0.4. In addition, Monteiro (2005) has estimated the intermediate-intermediate termination rate coefficient, based on the data presented in the works of Kwak *et al*. (2004a) and Fukuda *et al*. (2003) to be approximately equal to $(kct/1000)$. From these ratios the cross and self termination rate coefficients of the intermediate radical can be modelled as a function of the chain length dependent termination rate coefficient $(k_t^{'})$.

3.3.3 Polymerization rate and rate retardation

In this work the initiator-derived radicals (P_n^*) are considered to be similar to the RAFT-derived radicals (P_m^*), thus the model does not discriminate between these propagating radicals. Practically, this assumption seems to be valid, since in any typical recipe of RAFT polymerization a small amount of initiator compared to RAFT agent is applied in order to preserve the living nature of the polymerization, and hence the vast majority of the propagating species are derived from the RAFT agent. The polymerization rate of the RAFT and RAFT free systems can be calculated by:

$$R_p^{'} = \frac{dx^{'}}{dt} = k_p[M^{'}]\sqrt{\frac{4fk_d[I]}{2k_t^{'} + 2K(k_{ct}([AR]+[AP])) + 0.5K^2(k_{st}([AR]+[AP])^2)}} \qquad \textbf{(3-21)}$$

$$R_p = \frac{dx}{dt} = k_p[M]\sqrt{\frac{2fk_d[I]}{k_t}} \qquad \textbf{(3-22)}$$

where $R_p^{'}$ and R_p are polymerization rates with and without RAFT agent, respectively; $[M]$ is monomer concentration for RAFT-free polymerization; $[M^{'}]$ is monomer concentration for polymerization with RAFT agent; $x^{'}$ and x are monomer fractional conversions for the polymerization with and without RAFT agent, respectively; k_t is the chain length dependent termination rate coefficient for the polymerization without RAFT agent and $k_t^{'}$ is that for the polymerization with RAFT agent.

The differences between k_t and $k_t^{'}$ comes from the effect of the RAFT agent in reducing the molar masses of the growing polymeric chains. Such reduction in molar masses results in increasing the average termination rate and hence reducing the polymerization rate. The polymerization ratio (Y) of any polymerization system using RAFT agent can be defined as the ratio of the RAFT-polymerization rate $(R_p^{'})$ to that for the polymerization without RAFT (R_p); this ratio is given by the following expression (Altarawneh *et al.*, 2007):

$$Y = \frac{R_p^{'}}{R_p} = \frac{dx^{'}}{dx} = \frac{[M^{'}]}{[M]} \frac{1}{\sqrt{(k_t^{'}/k_t) + K(k_{ct}/k_t)[AR_o] + 0.25K^2(k_{st}/k_t)[AR_o]^2}} \quad \textbf{(3-23)}$$

Equation (3-23) indicates that the polymerization ratio depends on the equilibrium constant K, cross and self termination of the intermediate radical (k_{ct}, k_{st}), initial concentration of RAFT agent $[AR_o]$, and the gel effect reduction factor $(k_t^{'}/k_t)$. Kwak *et al*. (2004a), derived an expression to predict the polymerization ratio for a bulk RAFT polymerization relative to a bulk free RAFT polymerization as:

$$Y = \frac{R_p^{'}}{R_p} = \frac{dx^{'}}{dx} = \frac{1}{\sqrt{(1 + 2K(k_{ct}/k_t)[AR_o] + K^2(k_{st}/k_t)[AR_o]^2}} \quad \textbf{(3-24)}$$

The difference between Equations (3-23 and 3-24) is that Equation (3-23) accounts for the increased termination rate $(k_t^{'}/k_t)$ and for the monomer concentration history $([M^{'}]/[M])$, while Equation (3-24) does not. The polymerization retardation rate is defined as $1-Y$, which decreases as polymerization proceeds. Consequently, Equation (3-23) predicts the polymerization rate retardation factor at any time, while Equation (3-24) predicts a constant value for rate retardation over the entire period of polymerization. The prediction of Equation (3-24) is about the same as that predicted by Equation (3-23) at (t $\rightarrow$0), where $k_t^{'} \cong k_t$ and $[M^{'}] \cong [M]$.

3.3.4 Polymer MW and PDI

The number of chains is determined by the amount of the consumed RAFT agent and the amount of the decomposed initiator. The targeted number (*Mn*) and weight (*Mw*) average molecular weights can then be described by the equation for degenerative chain transfer (Mueller *et al.*, 1995):

$$Mn = \frac{xM_o}{\delta} M_w^M = \frac{x[M_o]M_w^M}{([AR]_o - [AR]) + 2f([I]_o(1 - e^{-k_d t}))} \quad \textbf{(3-25)}$$

where $[AR] \approx [AR_o](1-x)^{C_{tr}}$

The weight average molecular weight is given by:

$$Mw = \gamma_o \left(2 + \frac{(2-x)(1-C_{tr})}{C_{tr}} \right) M_w^M \qquad \textbf{(3-26)}$$

The ratio of weight average molecular weight to number average molecular weigh is known as polymer polydispersity and given by:

$$PDI = \frac{Mw}{Mn} \qquad \textbf{(3-27)}$$

where M_w^M is the molecular weight of the monomer; Mw and PDI are the weight average molecular weight and polydispersity index, respectively. Chains number (δ) is determined by the concentration of the consumed RAFT agent $[AR]$ and the concentration of the initiator that has been decomposed.

3.4 Results and discussions

The complexity of the RAFT process with its multitude coupled elementary reactions has been resolved via modelling strategies. A simple approach to determine the coefficients, i.e. the pulsed-laser polymerization technique for assessing propagation and termination rate coefficients (Buback *et al.*, 1995), has not yet been used for the RAFT kinetic parameters, i.e. k_{add} and k_{frag}. These kinetic coefficients, however, can be deduced from experimental data, such as rate of polymerization and average molecular weight in combination with an applicable kinetic scheme. Thus, the data obtained is model-dependent, which explains the remarkable difference in the reported values of k_{add} and k_{frag} (Kapfenstein-Doak *et al.*, 2001; Monteiro and de Brouwer, 2001). In this section, model simulations are presented along with experimental data obtained from literature for selected styrene solution polymerizations with high and low active RAFT agents and for styrene bulk polymerization with a high active RAFT agent.

3.4.1 Styrene solution polymerization with a high active RAFT agent

Bulk and solution styrene polymerization with a high active RAFT agent (e.g., 2-phenylprop-2-yl dithiobenzoate (CDB)) exhibits a pronounced retardation effect. This strong retardation makes the CDB/St system a good candidate for investigating RAFT kinetics. Experimental data for the solution polymerization of styrene at 80^{o}C with CDB as a RAFT agent and AIBN as the initiator have been reported eleswhere (Monteiro and de Brouwer, 2001). The recipe is given in Table 3-1 and kinetic parameters are given in Table 3-2.

3.4.1.1 RAFT effect on termination rate

Due to the nature of the RAFT polymerization, the molar mass of the growing polymeric species is controlled via the repeated addition-fragmentation cycles in a way that the monomer units distribute almost equally over the growing polymer chains. Consequently, all growing polymer chains have approximately the same length with a low degree of polymerization compared with the polymeric chain species produced in conventional free radical polymerization. Thus, the gel effect in RAFT polymerization is lower than that in conventional free radical polymerization. Hence the effective termination rate is higher. Simulation results with experimental data are shown in Fig. 3-1. In these simulations, the fragmentation rate coefficient is of the same order of magnitude as the addition rate coefficient, and the cross and self termination rates of the intermediate radical were set to zero so that their contributions to the polymerization rate can be eliminated, as indicated by Equation (3-23). Therefore, any predicted retardation in the simulation would be due to an increase in the average termination rate.

The solid curve (1a) in Figure 3-1b shows the calculated termination rate coefficient (k_t) used to fit experimental data for polymerization without RAFT agent, while the dashed curve (1b) represents the calculated termination rate coefficient $(k_t^{`})$ with 0.06 M RAFT agent. From figure 3-1b it seems that the RAFT agent increases the average termination rate via reducing the average chain length which results in faster diffusion relative to the longer chains and hence higher termination. The calculated termination

rate ($k_t^{'}$) is higher and decreases with time as the chain length of the propagating radicals increases, whereas the conventional termination rate coefficient (k_t) decreases with time at a rate faster than that for ($k_t^{'}$). The termination reaction in conventional free radical polymerization is dominated by long-short termination; that is the long immobile chains are terminated by short mobile species. On the other hand, in RAFT polymerization all chains are approximately of the same length and have the same probability to terminate with each other and with short radicals formed from initiator decomposition. Therefore, the termination rate in the RAFT system is higher.

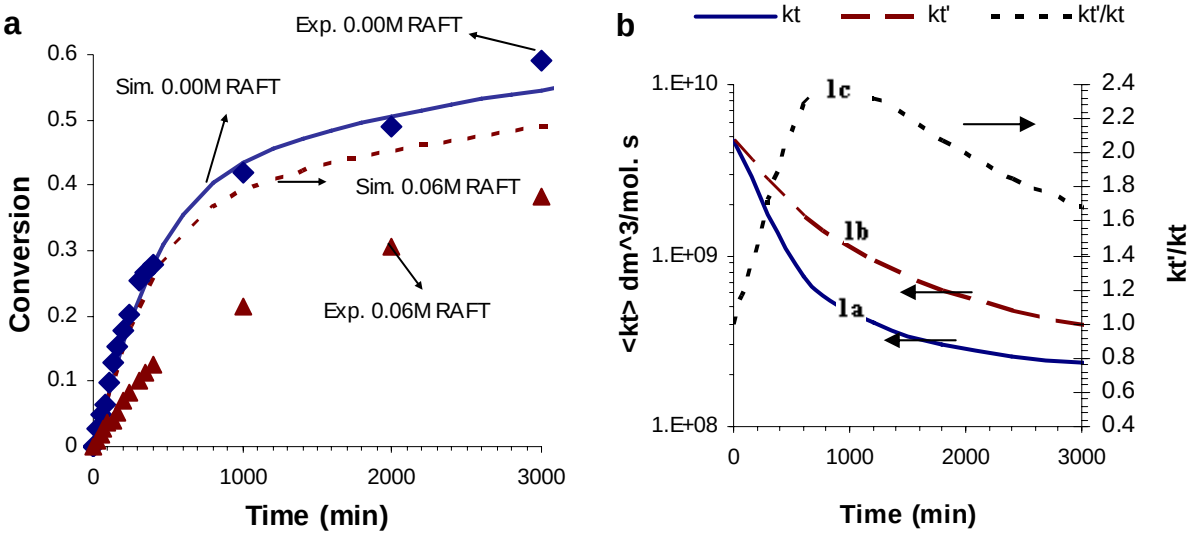

Figure 3-1: Experimental (symbols) and simulated (lines) solution polymerization of 3M styrene: (a) Styrene conversion with 0.06M RAFT agent (▲) and without RAFT agent (■); (b) Calculated termination rate coefficients $k_t^{'}$, k_t and their ratio as a function of time.

The increase in the effective termination rate due to the RAFT agent used can not be sustained for the entire period of the reaction. That is, at longer polymerization times, when almost all propagating radicals are longer, the RAFT termination rate ($k_t^{'}$) gets close to the conventional termination rate (k_t), and the effect of RAFT agent on the termination rate almost vanishes. The termination ratio ($k_t^{'}/k_t$) in Equation (3-23) accounts for the effect of RAFT agent in reducing the gel effect (increasing the termination rate). This ratio is predicted to increase from unity at the very beginning of the reaction, where the polymer fraction weight is almost zero, to reach a maximum value after some time, and then decreases with time as chains become longer and less mobile (curve 1c in Fig. 3-1b). This effect causes the rate to be initially slightly lower

and diminishes as the chains grow. Such effect could lead to an unavoidable retardation as demonstrated by the dotted curve in Fig. 3-1a. The effect of an increase in the average termination rate can not by itself explain the observed retardation, since the predicted conversion profile (dotted curve in Fig. 3-1b) does not agree well with experimental data. Hence other mechanisms must be invoked.

3.4.1.2 Slow fragmentation effect

To investigate the effect of slow fragmentation, simulations were carried out in which the value of the fragmentation rate coefficient was reduced stepwise from 10^{7} s^{-1} to 10^{-2} s^{-1}. The simulation results presented in Fig. 3-2 show that slow fragmentation alone has no effect on the observed retardation unless an unrealistic value (10^{-2} s^{-1}) is used. As a very low fragmentation rate is used, the results show that slow fragmentation alone can not explain the observed retardation, even at the beginning of the polymerization reaction (Fig. 3-3a). The predicted low polymerization rate at the beginning is due to radical retention, where each intermediate radical retains two propagating radicals resulting in the reduction of the active radical concentrations. However, the retained radicals will be eventually released and will participate in the polymerization, thereby resulting in an increase in the polymerization rate later.

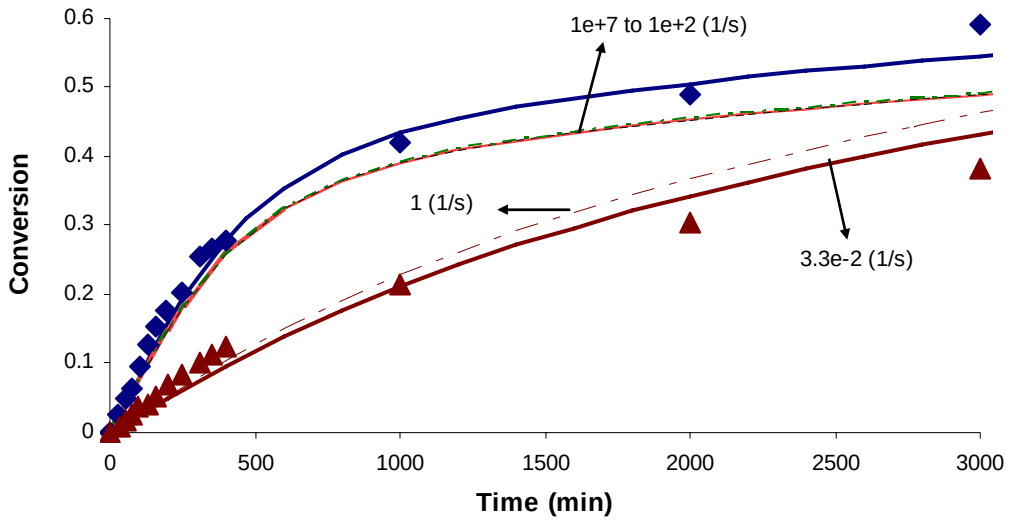

Figure 3-2: Effect of slow fragmentation on the polymerization rate. Legend: polymerization with 0.06M RAFT agent (▲); polymerization without RAFT agent (■).

For polymerization with 60 m*M* dithiobenzoate, the model predicts a high intermediate radical concentration, on the order of 4×10^{-3} mol. l^{-1} (Fig. 3-3b), when using a fragmentation rate coefficient equal to 3.3×10^{-2} s^{-1} without intermediate radical termination. This value is about four orders of magnitude greater than the experimentally reported electron spin resonance (ESR) value of 0.8μM (Hawthorne *et al.*, 1999).

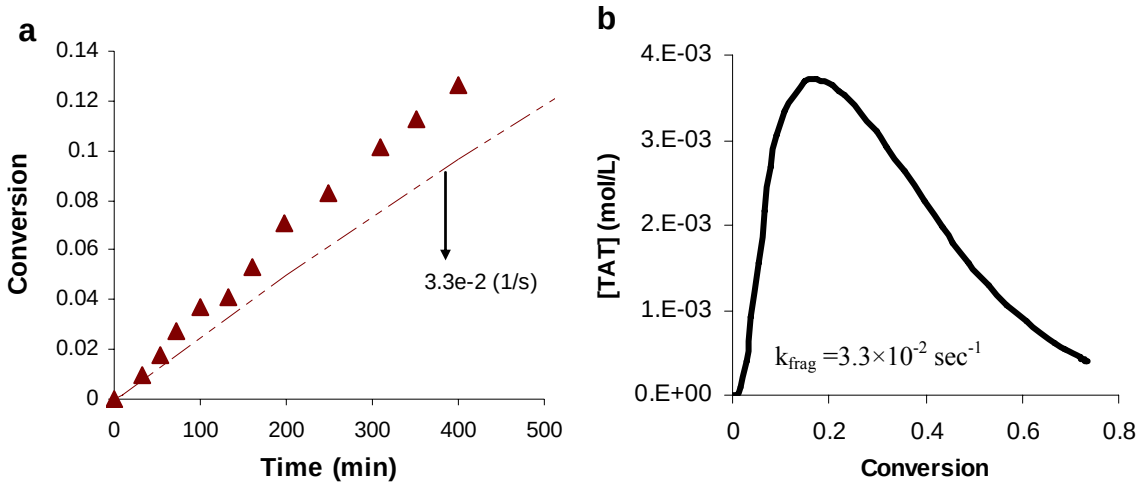

Figure 3-3: Experimental (symbols) and simulated (lines) solution polymerization of 3M styrene: (a) Detail of (Fig. 3-2) focusing on the initial period of the polymerization with 0.06M RAFT agent; (b) Simulated intermediate radical concentration at high and low fragmentation rate coefficients (k_{frag} =3×10^{-2} s^{-1}).

In this context, two points should be taken into account: (a) slow fragmentation leads to intermediate radical accumulation and retaining of sufficient amounts of propagating radicals. This implies that the intermediate radical concentration is greater than the propagating radical concentration, and (b) the high concentration of the intermediate radicals serves to greatly increase the intermediate radical side reactions, such that the probability of the termination of other radicals by an intermediate radical is high. Based on this, it is concluded that such side-reactions (intermediate radical termination) are a consequence of slow fragmentation, rather than its primary cause. The low fragmentation rate coefficient (3.3×10^{-2} s^{-1}) is experimentally infeasible. Thus, the observed retardation is not due to the slow fragmentation of the intermediate radical in the absence of intermediate radical termination reactions.

3.4.1.3 The effect of the intermediate radical termination

The intermediate radicals in RAFT polymerization are expected to affect the polymerization rate, because they are able to terminate with any propagating radical or with each other, thereby leading to a loss of propagating radicals and a consequent reduction in polymerization rate. Cross termination between an intermediate radical and a propagating radical was experimentally confirmed in RAFT mediated polymerization systems (Kwak *et al.*, 2004a; Kwak *et al.*, 2002; Monteiro and de Brouwer, 2001). Taking this into account, simulations were carried out using the cross termination rate coefficient of $0.4k_t^{'}$ obtained experimentally (Kwak *et al.*, 2004a). The fragmentation rate coefficient of the intermediate radical was estimated to be 7×10^4 s^{-1} (Kwak *et al.*, 2004a).

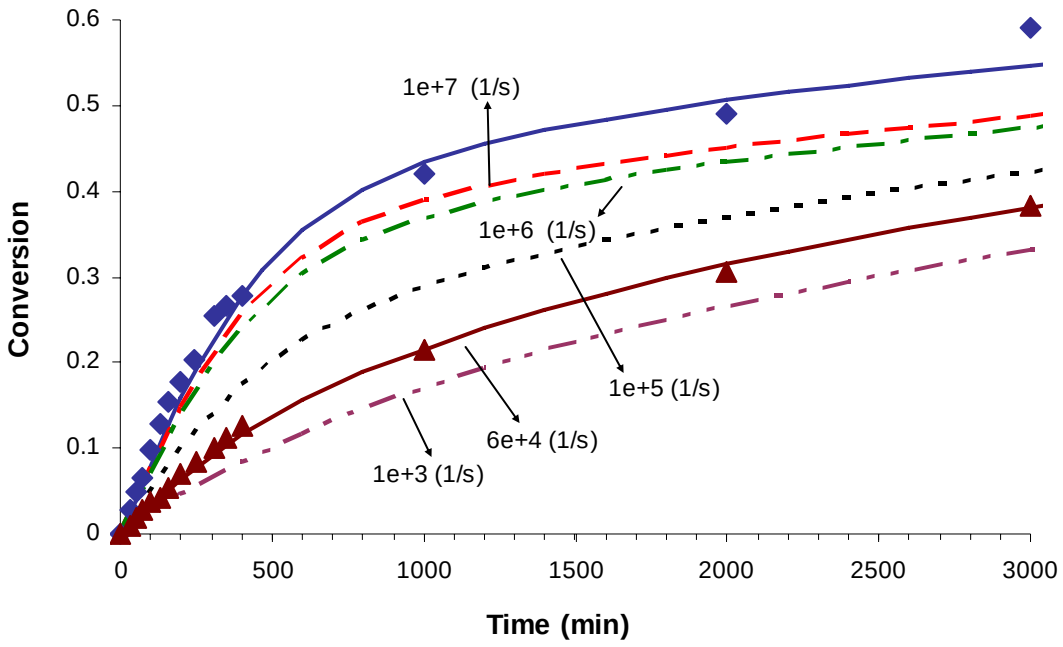

Figure 3-4: Effect of fragmentation rate on the polymerization rate in the presence of the intermediate radical cross termination. Legend: polymerization with 0.06M RAFT agent (▲); polymerization without RAFT agent (♦); model simulations (–).

In this work, a fragmentation rate coefficient of $6\times10^4 s^{-1}$ was found to provide a good agreement between simulations and experimental data in the presence of intermediate radical termination. When only cross termination between the intermediate and the propagating radicals is included, good agreement was obtained between experimental data and simulation as shown in Fig.3-4. Figure 3-5a, shows the predicted intermediate

radical concentration which is of the order of 4×10^{-8}M, and is one order of magnitude lower than the measured value.

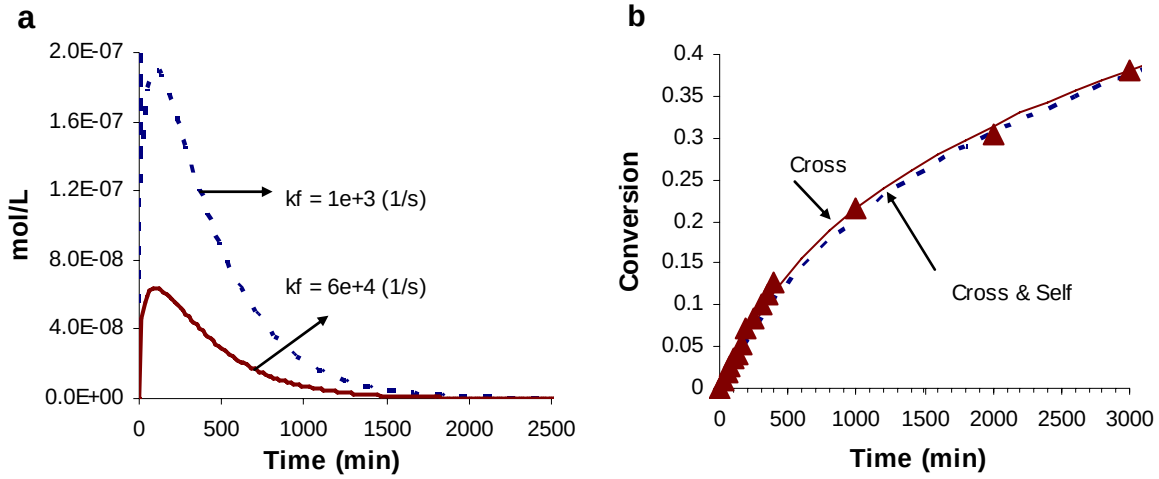

Figure 3-5: Experimental (symbols) and simulated (lines) solution polymerization of 3M styrene: (a) Intermediate radical concentration in the presence of intermediate radical termination; (b) Effect of intermediate radical cross and self terminations (dotted line) on the monomer conversion.

Further investigations were carried out by including the effect of the intermediate-intermediate self termination. A four-arm star polymer is a possible product of such a reaction. In this work, the intermediate-intermediate termination is considered as an irreversible reaction so that the termination of the intermediate radicals will result in radical loss, and hence lowering of the polymerization rate. Otherwise, its effect on the polymerization rate is negligible as the terminated intermediate radicals convert back to their originating species.

The simulation results for both cross and self terminations are presented in Fig. 3-5b. Self termination rate coefficient (k_{st}) as high as the cross termination rate coefficient was considered in these simulations. As the fragmentation rate coefficient is of the order of 10^4 s^{-1}, self termination has a negligible effect on the polymerization rate. This supports the claim that intermediate-intermediate termination is kinetically insignificant in the styrene system (Kwak *et al.*, 2004a). The prediction is based on the assumption that the intermediate-intermediate termination is an irreversible process which accounts for maximum effect on the polymerization rate. If the intermediate-intermediate termination is a reversible or even a partially reversible process then its effect on the polymerization rate would be definitely lower than its effect as an irreversible process.

Similar findings regarding the slow fragmentation and intermediate termination have been reported elsewhere in literature (Monteiro and de Brouwer, 2001).

3.4.1.4 Polymerization rate and polymerization ratio (Y)

One common characteristic of living polymerization systems is a reduction in the rate of polymerization, although the extent of this effect appears to be RAFT-agent dependent. The reasons behind the observed retardation in the solution polymerization of 3*M* styrene with 0.06*M* RAFT agent have so far been assessed. These are: the relatively slow fragmentation ($k_{frag} / k_{add} \approx 0.01$), intermediate radical terminations, and the increase in average termination rate. Among these, increasing termination rate and cross termination of the intermediate radical were found to be major contributors to rate retardation.

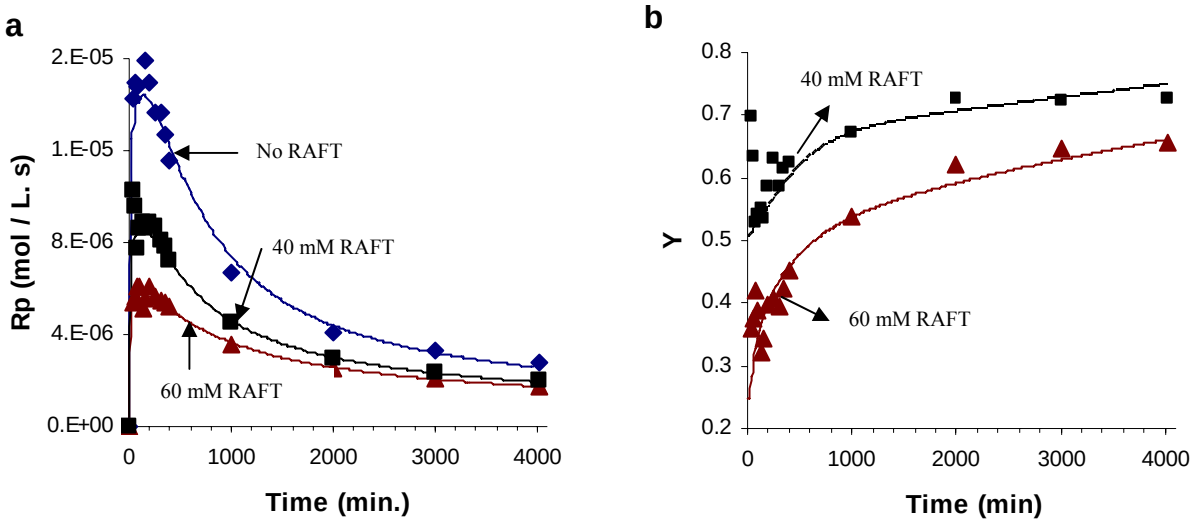

Figure 3-6: Experimental (symbols) and simulated (lines) solution polymerization of styrene: (a) Polymerization rates; (b) Retardation degree Y. Legend: polymerization with 0.06M RAFT agent (▲); polymerization with 0.04M RAFT agent(■); polymerization without RAFT agent (♦); model simulations (—).

These three factors along with the effect of RAFT agent concentration on the polymerization rate have been combined in Equation (3-23). This equation indicates that the polymerization ratio (Y) increases with decreasing RAFT agent concentration. Using Equation (3-23) along with Equations (3-21) & (3-22), the polymerization rates of 3*M* styrene with 0.06M and 0.04M RAFT agent have been simulated and validated against experimental data as shown in Fig. 3-6. In Fig. 3-6a, the experimental

polymerization rates were calculated by differentiating the monomer conversion data, while the simulated polymerization rates were obtained from Equations (3-21) and (3-22). In Fig. 3-6b, the experimental Y values were obtained by dividing the experimental polymerization rate with RAFT agent by that for polymerization without RAFT agent, and the simulated Y values were obtained from Equation (3-23). The polymerization rate with 0.06M RAFT agent is lower than that with 0.04M RAFT agent. This indicates that the rate retardation depends on the RAFT agent concentration and increases with an increase in RAFT agent concentration (Fig. 3-6a).

The polymerization ratio (Y) with 0.06M RAFT agent is lower than that with 40 m*M* RAFT agent (Fig. 3-6b). The polymerization ratio (Y) for both systems increases with time and their polymerization rates decrease later and converge to a constant value (Fig. 3-6a). This increase in Y and decrease in Rp are due to the effect of the RAFT agent on the chain-length dependent termination rate, which dissipates as the chain length of the propagating radical increases.

3.4.1.5 Pre and Core-equilibrium stages

The two stages of pre-equilibrium and core-equilibrium are shown in Fig. 3-7 where the change in the concentration of participating species in solution polymerization of 3*M* styrene with 0.06M RAFT agent is summarized. The Figure shows the full consumption of the RAFT agent and the formation of all the chains, including dormant species during pre-equilibrium stage.

The core-equilibrium stage commences once the initial RAFT agent is consumed. During this stage, the concentration of short radicals ($R^{\bullet}$) generated from RAFT agent is almost zero, and the concentration of the unsymmetrical intermediate radical is low and decreasing with time (Fig. 3-8). Very shortly after the establishment of the core-equilibrium stage, the total concentration of the intermediate radical (TAT) is equal to the concentration of the symmetrical intermediate radicals (PAP) as shown in Figure 3-8 indicating the disappearance of the other intermediate radicals such as PAR, RAP and RAR. In this stage the concentration of all the chains is constant and is equal to the concentration of the initial RAFT agent plus the concentration of the initiator (dashed curve, Fig. 3-7).

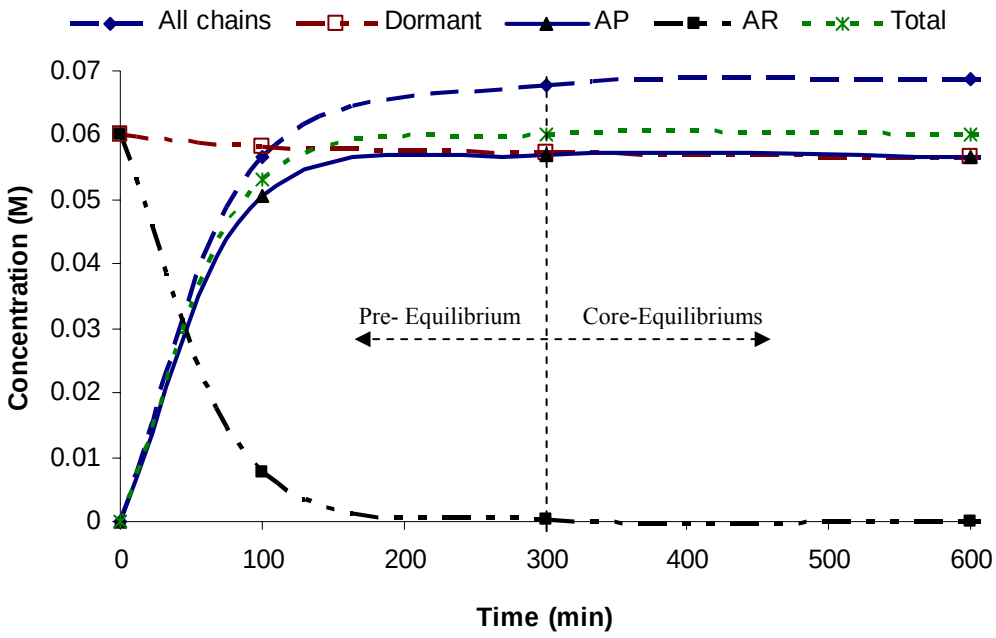

Figure 3-7: Pre and core equilibrium stages.

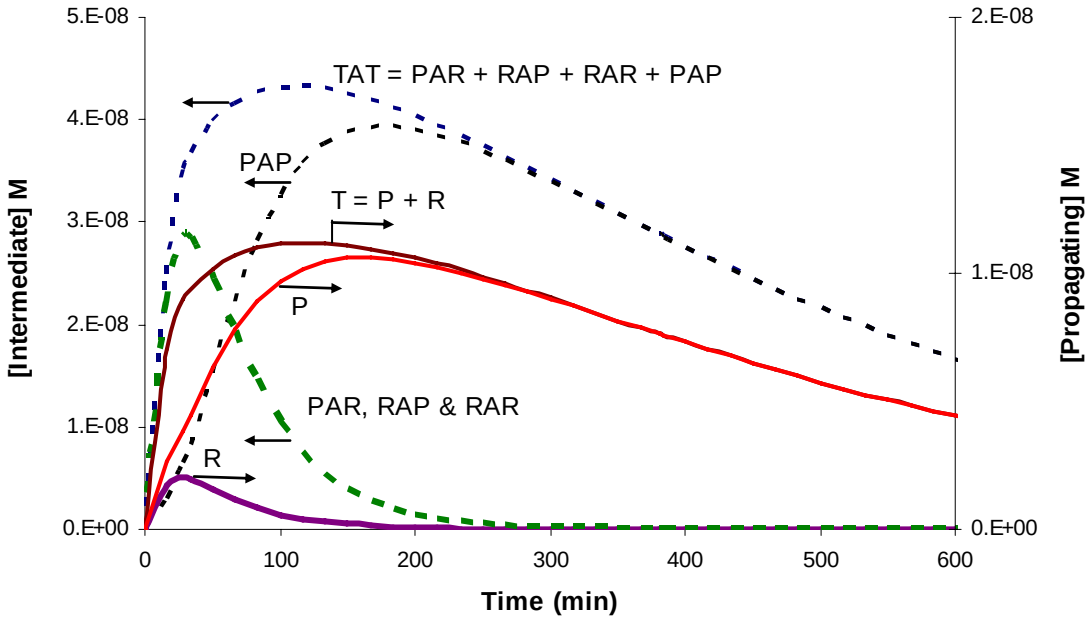

Figure 3-8: Simulated concentrations of the intermediate and propagating radicals for styrene solution polymerization with 0.06M RAFT agent.

The concentration profile of the dormant species (AR + AP) indicates that a small proportion (9.33%) of the RAFT agent is lost or destroyed through polymerization. This small amount of RAFT agent is actually distributed among the intermediate radicals and the terminated intermediate species (3-arm star dead species). The curve (Total)

indicates that the total concentration of the polymeric RAFT agent (AP), the dead polymer generated by cross termination of intermediate radical and the dead polymer produced by the intermediate-intermediate termination, is constant and equal to the initial concentration of the RAFT agent.

3.4.1.6 Molecular weight and polymer polydispersity

Despite the pronounced retardation, free radical polymerization with a high active RAFT agent (e.g. CDB) is one of the most effective synthetic routes for the production of well-defined polymers due to its very high transfer constant. Equation (3-25) indicates that to produce a high molecular weight polymer, the amount of RAFT agent should be much lower relative to the amount of monomer, while the amount of initiator should be even lower. It is worth noting that the monomer/RAFT ratio determines the maximum theoretical degree of polymerization at full conversion. If polymerization is not complete, the degree of polymerization will be simply proportional to conversion.

For the polymerization system discussed above, no data on number average molecular weight and polydispersity is available. However, two simulations were carried out for this system using the same parameters (Table 3-2). For the first simulation, the recipe in Table 3-1 was used (initiator concentration = 0.0044M, case 1), and for the second case the initiator concentration was increased by one order of magnitude (initiator concentration = 0.044M, case 2). The results are shown in Fig. 3-9; the number average molecular weight (Mn) and polydispersity index (PDI) for polymerization with low initiator concentration (solid lines, case 1), represent the system addressed in this work. A higher initiator concentration (dashed lines, case 2) was introduced in order to investigate the effect of initiator concentration on the living nature of RAFT polymerization. For case 1, the PDI decreases rapidly to 1.07 (at about 42% conversion), which indicates the formation of polymer chains of almost uniform chain length. Values of PDI below 1.1 have been reported in the literature for bulk and solution polymerization of styrene with CDB at different RAFT concentrations and monomer conversions (Barner-Kowollik *et al.*, 2001; Kwak *et al.*, 2004a). A dramatic change for the PDI is predicted as the initiator concentration increased by one order of magnitude (Fig. 3-9a, dashed line).

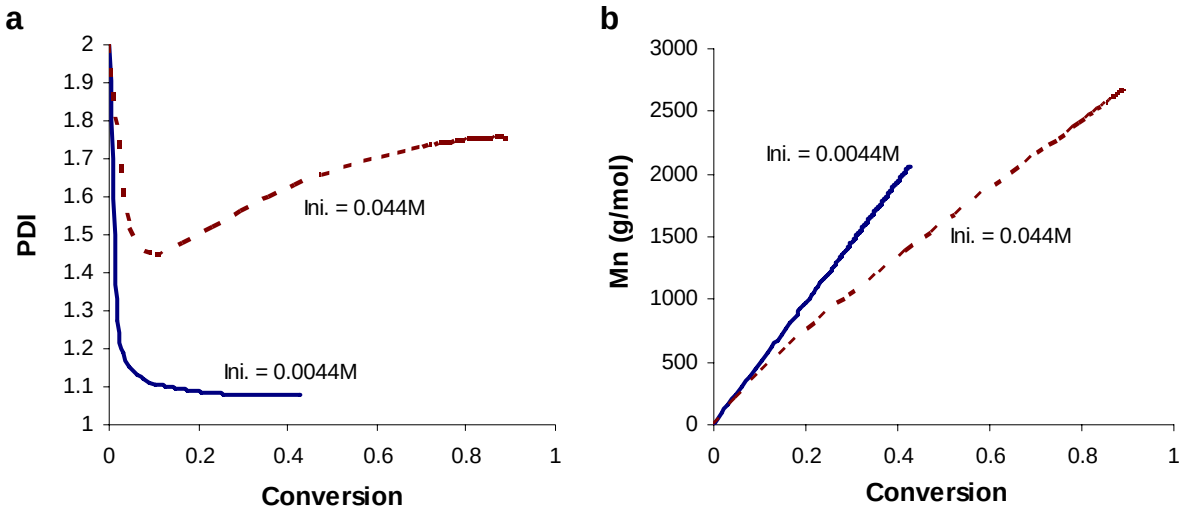

Figure 3-9: Simulated effect of initiator concentration: (a) On polymer polydispersity; (b) On number average molecular weight.

At low conversion, the PDI decreases rapidly from 2 to 1.43 and then starts to increase gradually with conversion. At the beginning of the reaction, not all of the initiator molecules have decomposed and hence the termination rate is close to that for case 1. Once all the initiator molecules have decomposed and are involved in the polymerization reaction, the termination rate is higher due to high concentration of the active radicals. Consequently, a considerable amount of dead low molecular weight material and a high number of chains are produced leading to a broad molecular weight distribution (high PDI).

The number average molecular weight (Fig. 3-9b) grows linearly with conversion, which indicates that the system exhibits living characteristics. At low conversion (x < 0.1) both profiles follow similar trends as the PDI decreases. The growth of the number average molecular weight (for case 1) follows a linear trend, reaching a maximum value of 2050 g mol^{-1} at approximately 40% conversion. Whereas (for case 2) an almost linear growth is predicted with a deviation occurred at the initial stage (x = 0.1). This deviation is due to the higher number of chains in case 2. Hence, the molecular weight tends to decrease as the termination rate increases, producing a large number of low molecular weight dead chains. In addition, the simulated number average molecular weight (Mn) profile for case 2 shows a notable curvature as a result of continuous generation of new chains by initiation, which causes an increase in the total number of polymer chains resulting in a reduction of the number average molecular weight.

Therefore, an increase in initiator concentration reduces the living nature of RAFT polymerization by means of increasing the termination rate. Thus, to preserve the living nature of RAFT polymerization, a low initiator concentration is recommended, which results in minimizing the termination frequencies, and hence minimizing the contribution of the low molecular weight dead chains to the final polydispersity.

3.4.2 Styrene solution polymerization with a low active RAFT agent

The model was also used to investigate the effect of low activity RAFT agent on the polymerization rate, molecular weight, and polydispersity for solution polymerization of 4M styrene with 0.02M RAFT agent (xanthate) in toluene at 80^{o}C. Experimental data was taken from literature (Smulders, 2002). Simulations were carried out using propagation and decomposition rate coefficients given in Table 3-2 for styrene. A low activity RAFT agent does not significantly affect the average termination rate; thus a value of about 3×10^{8} L/mol.s was used instead of the CLD termination rate coefficient.

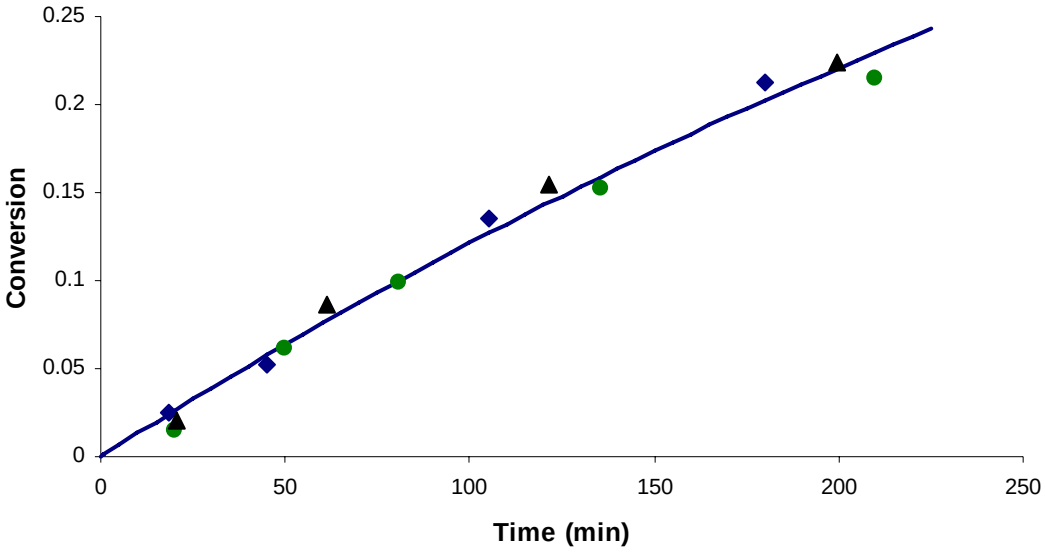

Figure 3-10: Solution polymerization of 2M styrene with 0.00M (♦), 0.01M (●) and 0.02M (▲) O-ethylxanthyl ethyl propionate as RAFT agent in toluene at 80 ^{o}C and 0.005 M AIBN.

The addition rate coefficient was estimated based on the experimentally measured transfer constant (C_{tr} = 0.7) and found to be of about 924 L/mol.s. In this system no retardation was observed when using higher concentrations of the RAFT agent, indicating that the fragmentation rate coefficient of the intermediate radical formed in

the polymerization with xanthate is likely to be higher than the addition rate. Additionally, due to the lower resonance of the ethoxide (on the xanthate) compared with the phenyl (on the CDB), the intermediate radical formed in the polymerization with xanthates is less stable and may have a fragmentation rate higher than the reported one for the intermediate radical formed in the polymerization with CDB (~$10^5 s^{-1}$) (Smulders, 2002)

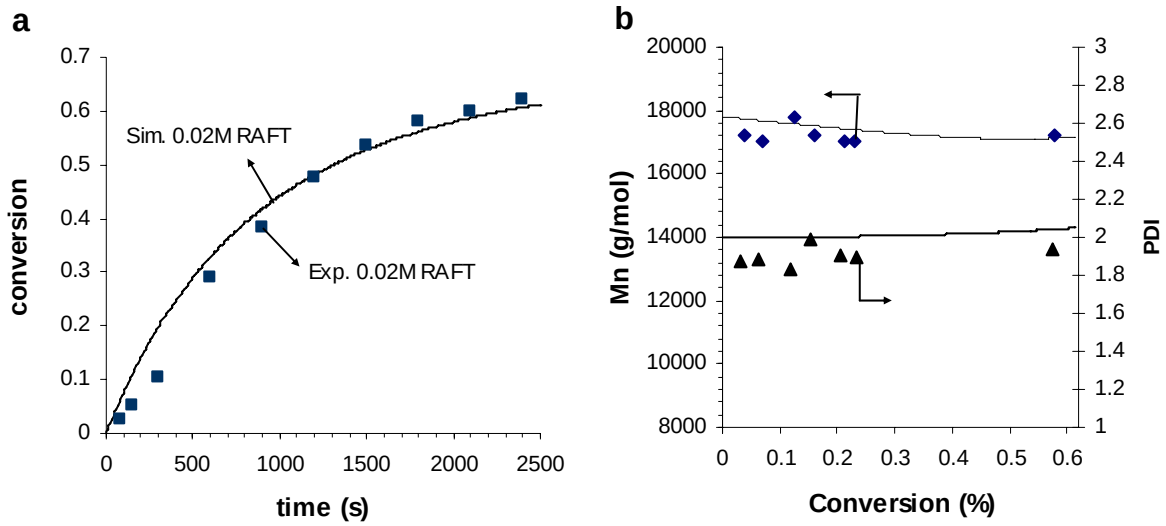

Figure 3-11: Experimental (symbols) and simulated (lines) solution polymerization of 4M styrene with 0.02M O-ethylxanthyl ethyl propionate as RAFT agent (Monomer/RAFT = 200) in toluene at 80 °C: (a) Monomer conversion; (b) Mn and PDI.

Muller equations were used to predict the number average molecular weight and the PDI using the calculated conversion data (Fig. 3-11a). The evolution of Mn with conversion (Fig. 3-11b) shows that both of Mn and PDI are relatively constant over the conversion range. The constant value of Mn over the conversion range is due to the low transfer rate of the growing radical to the RAFT agent used in this experiment.

3.4.3 Styrene bulk polymerization with a high active RAFT agent

The kinetic model was further validated in terms of conversion, polydispersity (PDI) and number average molecular weight (Mn) against the experimental data for RAFT bulk polymerization of styrene. The experimental recipe is given in Table 3-3 (Butté, 2000). Simulations were performed using a styrene propagation rate coefficient of 660

(L/mol.s) at 80°C (Buback *et al.*, 1995; Monteiro and de Brouwer, 2001), and effective decomposition rate coefficient of initiator, $fk_d = 1.1\times10^{-4}$ (s^{-1}) (Monteiro and de Brouwer, 2001). While the termination rate coefficient was calculated using Equations **(3-17), (3-18)** and **(3-19).** In this experiment the molar ratio of the monomer to the initiator was chosen large and equal to 1000 in order to reduce the rate of the termination reactions and hence reduce the contribution of the dead chains to the final polydispersity (Butté, 2000)

3.4.3.1 Estimation of the transfer constant from Mn data

The apparent initial transfer constant of the initial RAFT agent for this system is calculated using the Mayo method. For this system, Mayo equation $(Mn = (104.15 \cdot [M_o])/(C_{tr} \cdot [AR_o]))$ is valid at very low conversions, where a negligible amount of RAFT agent and monomer is consumed (Smulders, 2002). Extrapolating the number average molecular weight data (Fig. 3-12b) versus conversion to zero conversion gives a molecular weight value of about 514 g mol^{-1} at zero conversion. Based on this, the calculated transfer constant was found to be 82. The transfer rate coefficient $(k_{tr} = k_p \cdot C_{tr})$ is then equal to 5.41×10^4L/mol.s. Assuming that the intermediate radical is symmetrical $(k_{frag} \approx k_{-frag})$, the addition rate coefficient is equal to 1.08×10^5 (l $mol^{-1}s^{-1}$). This value was used in the model with the fragmentation rate coefficient as a fitting parameter.

3.4.3.2 Monomer conversion, Mn and PDI

As shown in Fig. 3-12, with a fragmentation rate coefficient of about 6×10^4 s^{-1}, the simulated conversion, Mn and PDI compare well with the corresponding experimental data. The low initiator concentration results in a low polymerization rate, hence a long polymerization time (1500 min) is required to achieve high conversion. The system exhibits living characteristics as indicated by the linear growth of the number average molecular weight and by the low final polydispersity, confirming the effectiveness of RAFT agent **1a**. Ideally, the maximum value of Mn at 80% conversion would be equal to 33328 g mol^{-1}, as Equation 3-25 suggests, and the final PDI would be close to one. This, however, is not the case because of the presence of unavoidable termination

reactions and continuous generation of new radicals by initiation, which results in a low experimental Mn value which is equal to 28200 g mol^{-1} and PDI of about 1.3.

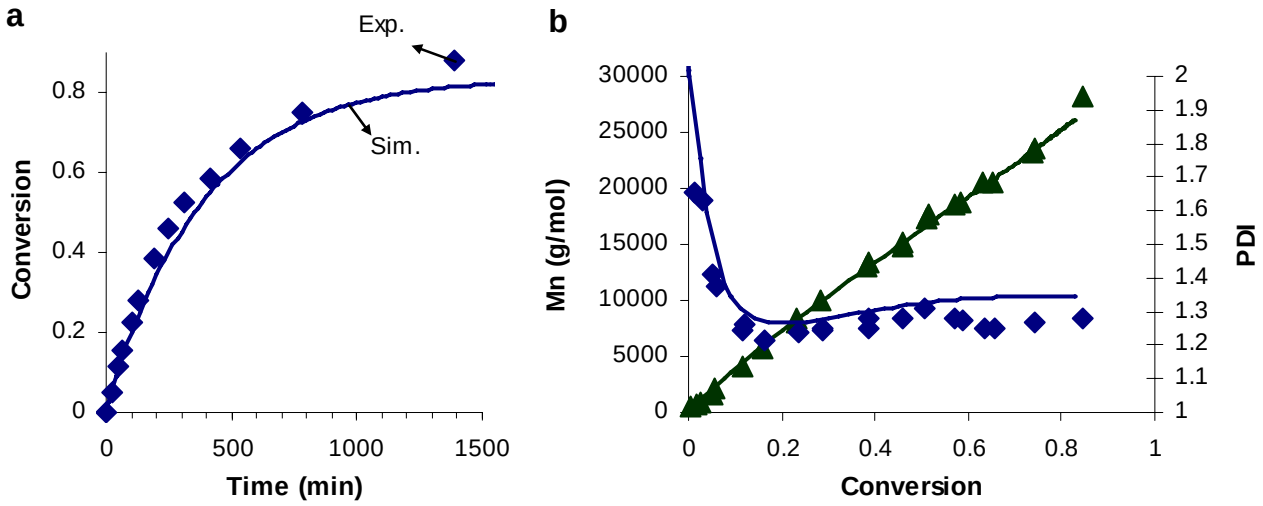

Figure 3-12: Comparison of experimental data (symbols) with model simulations (solid lines) for bulk polymerization of styrene with RAFT agent 1a at 80^0C: (a) Conversion as a function of time; (b) Molar mass and polydispersity index as a function of conversion.

To investigate the effect of initiator concentration on Mn and PDI, simulations were carried out without including the initiator contribution in order to minimize the frequency of termination reactions. The results are shown in Fig.3-13 and compared with the experimental data given in Fig. 3-12 along with the simulation results in the presence of initiator contributions.

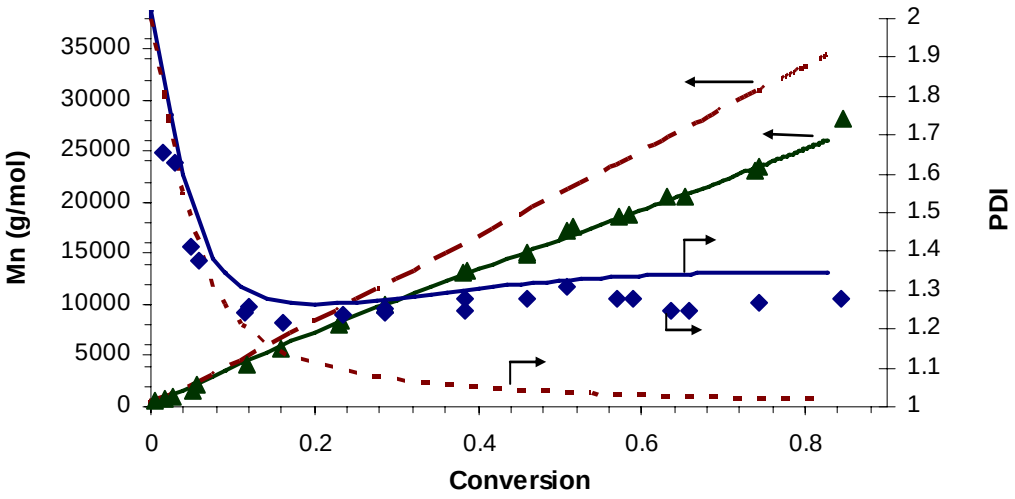

Figure 3-13: Effect of initiator concentration on Mn and PDI in bulk polymerization of styrene with RAFT agent (1a) at 80^oC.

The experimental Mn values show a curvature and deviation from the predicted ideal linear Mn profile (dashed line). Referring to Fig. 3-9b, such deviation has also been predicted for polymerization with high initiator concentrations and ascribed to the increased number of chains due to the initiator contribution. Theoretically, the final value of PDI at full conversion is 1.012 (dotted curve, Fig 3-13) when the estimated transfer constant is used ($PDI = 1 + 1/C_{tr}$), while experimentally, the final PDI value lies between 1.2 and 1.3. Again, this behaviour can be attributed to the presence of termination/initiation reactions resulting in the production of a considerable amount of dead low molecular weight chains, and hence broadening of the molecular weight distribution. These explanations are also valid for the Mn and PDI predictions presented in Figure 3-9.

3.5 Sensitivity analysis

The experimentally determined propagation rate coefficient used in this work is well documented and has been frequently used in the literature. In addition, the transfer constant was determined from the experimental data on Mn and hence it is considered to be of high certainty. However, the values of the overall fragmentation rate coefficient (K_{frag}), forward fragmentation rate coefficient (k_{frag}) and backward fragmentation rate coefficient (k_{-frag}) are not well documented and hence a sensitivity analysis on the effect of these parameters is required. In this section, the experimental recipe given in table 3-3 is selected. The aim of this analysis is to illustrate, with the example of variation of K_{frag}, k_{frag}, and k_{-frag}, how the size of these rate coefficients affects the simulated monomer conversion, Mn and PDI

3.5.1 Effect of the overall fragmentation rate on Mn and PDI

The overall fragmentation rate coefficient K_{frag} is defined to be equal to $k_{frag} + k_{-frag}$, where $k_{frag} = xK_{frag}$, $k_{-frag} = yK_{frag}$ and $x + y = 1$. The value of (x) represents the probability of the forward fragmentation (fragmentation in the desired direction) of the intermediate radical, while (y) represents the probability of the backward fragmentation of the intermediate radical. The effect of the overall fragmentation rate

of the intermediate radical on the final molecular weight, monomer conversion and final polydispersity has been investigated. As the partitioning factor of the intermediate radical between the reactants and products remains constant ($x = y \Rightarrow k_{frag} = k_{-frag}$), the evolution trends of the number average molecular weight Mn with conversion are slightly influenced by decreasing or increasing the overall fragmentation rate coefficient K_{frag} with a final value of monomer conversion being proportional to the value of K_{frag} (rate retardation) as illustrated in Fig 3-14.

A linear increase of Mn with conversion is predicted for all K_{frag} values. Because of the retardation effect, however, the final value of Mn is substantially influenced by the magnitude of the fragmentation rate K_{frag} ; i.e. the lower the value of K_{frag} the lower the value of Mn. It is worth noting that a sever retardation is predicted with a predicted conversion being equal to 40% and Mn equal to 13026g/mol. This is due to the very low fragmentation rate coefficient ($1.2s^{-1}$) of the intermediate radical which results in promoting the side reactions that the intermediate radicals undergo and eventually converting a considerable amount of the retained propagating radicals into low molecular weight dead chains (radical loss).

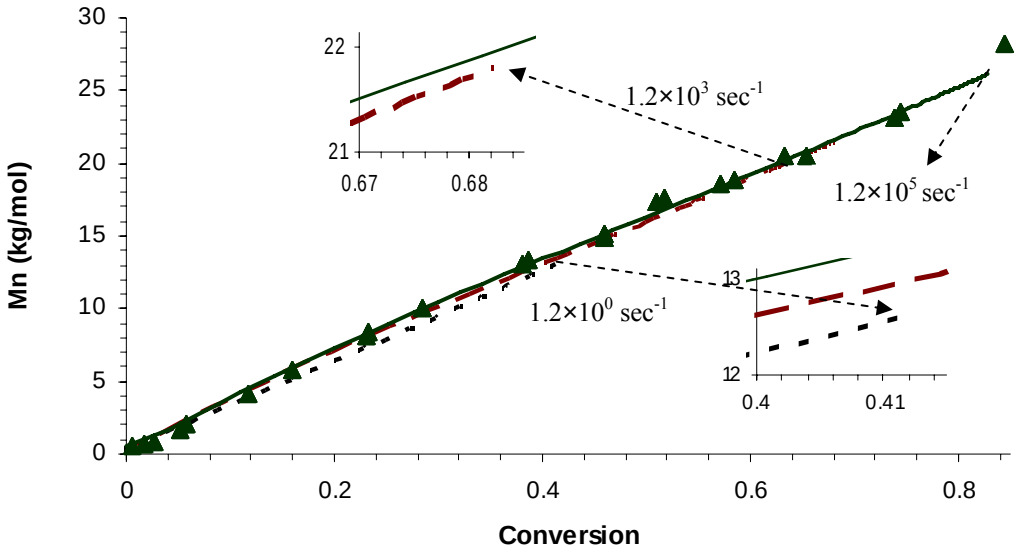

Figure 3-14: Effect of fragmentation rate coefficient on Mn. Arrows mark the final value of Mn at different overall fragmentation rate coefficient values.

In contrast, the time evolution of monomer conversion (polymerization rate) is very sensitive to the value of the overall fragmentation rate of the intermediate radical K_{frag}. Fig 3-15a, shows the effect of the overall fragmentation rate value on monomer conversion. As K_{frag} is higher than or close to the addition rate coefficient no retardation is predicted. This is because the rate at which a propagating radical adds to the RAFT agent is balanced by the rate at which it leaves the intermediate radical and hence radical concentration is not altered. A dramatic decrease in polymerization rate is predicted when K_{frag} decreases to $1.2\times10^{3}s^{-1}$ (dashed curve, Fig. 3-15a) and to $1.2s^{-1}$ (dotted curve, Fig. 3-15a). The reduced simulated polymerization rate (indicated by monomer conversion) is due to the accumulation of the intermediate radicals, which results in radicals loss via cross and self termination of the intermediate radical. A good agreement with the experimental monomer conversion is obtained when a high value of K_{frag} was used. Thus, the relatively high experimental conversions indicate that the disappearance rate of the intermediate radical is not the rate determining step and the intermediate radical does not undergo slow fragmentation.

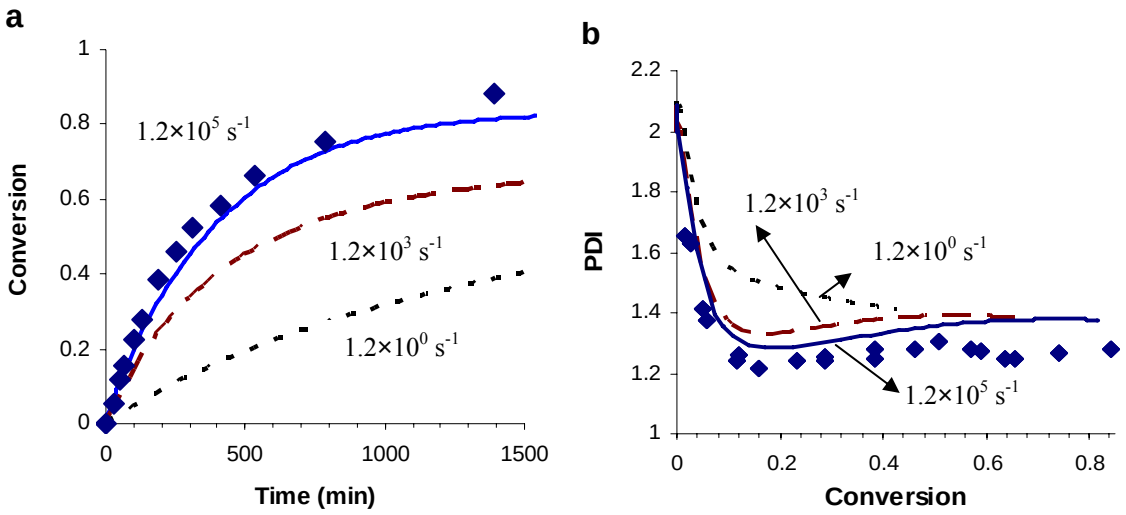

Figure 3-15: Effect of fragmentation rate coefficient; (a) On monomer conversion; (b) On polymer polydispersity.

Polymer polydispersity is more sensitive to increasing or decreasing the value of K_{frag}. Fig. 3-15b shows the predicted conversion-evolution of PDI with the best fit line being given in solid bold curve. As $k_{frag} = k_{-frag}$, the transfer constant is similar and hence the system shows living characteristics as indicated by the decreased PDI. At the beginning

of the reaction all PDI profiles drop, with deviations from the best fit curve occurring at low conversion (x~0.05) when K_{frag} equal to $1.2s^{-1}$, and at conversion of about 0.1 when K_{frag} equal to $1.3\times10^{3}s^{-1}$. This deviation is due to the formation of low molecular weight species during the reaction resulting in broadening the molecular weight distribution and hence increasing PDI. The rate of termination reactions increases with an increase in the intermediate radical concentration; thus the formation of low molecular weight species is accelerated by decreasing the overall fragmentation rate of the intermediate radical. Experimental PDI (Fig. 3-15b) agrees well with the simulation when high K_{frag} is used, suggesting that the overall fragmentation rate coefficient is close to or even higher than the addition rate coefficient.

3.5.2 Effect of the fragmentation direction on Mn and PDI

The effect of the leaving group has been presented in the previous sections based on the assumption that the forward fragmentation rate is equal to the backward fragmentation rate, in which there is no preference to which direction the intermediate radical fragmentation would take place. In the following simulations this assumption is no longer applicable. The fragmentation of the intermediate radical takes place in the desired direction (forward fragmentation), if and only if the forward fragmentation rate coefficient (k_{frag}) is higher than the backward fragmentation rate coefficient $(k_{\_frag})$.

The released radical will then add monomer until it adds again to RAFT agent or terminates with other radicals. The model can accommodate this case by increasing the forward fragmentation rate coefficient at the expense of the backward fragmentation rate coefficient and the summation of these two parameters is equal to K_{frag}. The simulated Mn and PDI as a function of conversion are shown in Fig. 3-16. It is clear from this Figure that the evolution of the number average molecular weight is not sensitive to increasing and decreasing K_{frag}, as all Mn profiles follow similar trends and overlap each other, showing living characteristics by the linear growth with conversion.

Referring to Equation 2-18a, increasing the value of the forward fragmentation rate coefficient from $6\times10^{4}s^{-1}$ to $11.95\times10^{4}s^{-1}$ and decreasing the value of the backward fragmentation rate coefficient from $6\times10^{4}s^{-1}$ to $5\times10^{2}\,s^{-1}$ results in the transfer constant

increasing from 82 to 162. Consequently, the living efficiency is increased as the intermediate radical partitions in favour of products, thereby resulting in a lower PDI (dotted curve, Fig. 3-16b). By increasing the forward fragmentation rate coefficient, the number of the converted (R) radicals into polymeric radicals increases and the fraction of the polymeric radicals increases as well. These polymeric radicals will then have an equal probability to get involved in the transfer reaction, resulting in consistent growth and hence low PDI.

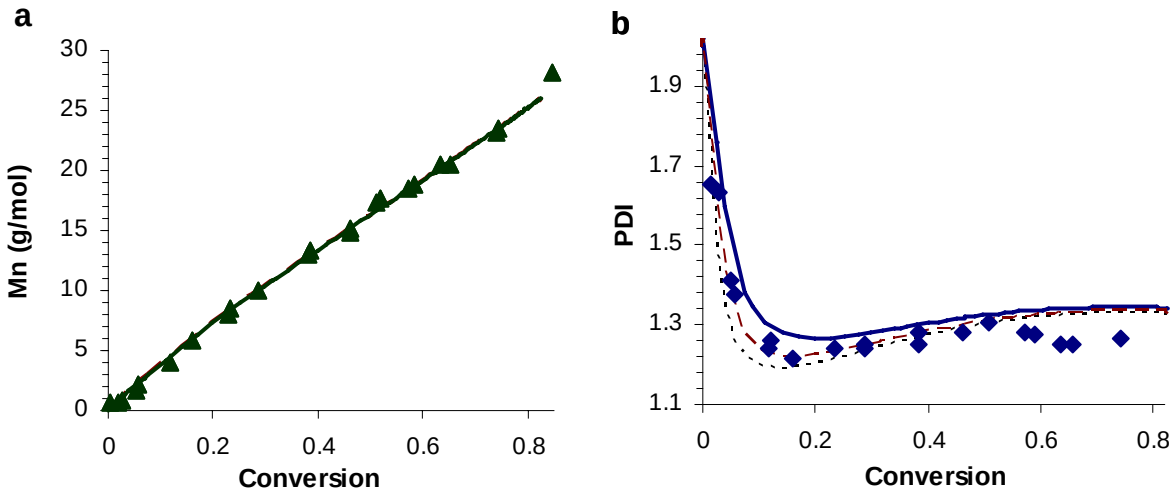

Figure 3-16: Effect of the forward fragmentation rate coefficient ($k_{frag} > k_{-frag}$); (a) On Mn; (b) On PDI. Legend: forward fragmentation (k_{frag}) = 6×10^4 s^{-1}, backward fragmentation (k_{-frag}) = 6×10^4 s^{-1} (solid curve); forward fragmentation (k_{frag}) = 9×10^4 s^{-1}, backward fragmentation (k_{-frag}) = 3×10^4 s^{-1} (dashed curve); forward fragmentation (k_{-frag}) = 11.95×10^4 s^{-1}, backward fragmentation (k_{-frag}) = 5×10^2 s^{-1} (dotted curve).

On the other hand, if the RAFT agent has a poor leaving group where the fragmentation rate of the leaving group is lower than the fragmentation rate of the newly attached polymer chain, the intermediate radical will prefer fragmentation to the direction of the reactants (backward fragmentation). In the pre-equilibrium stage, the forward fragmentation rate coefficient controls the rate at which R radicals form in the system. Thus, it is expected that the polymerization rate will be significantly decreased by decreasing k_{frag} and increasing k_{-frag}. It is clear from figure 3-17 that the production rate of R radicals in the system has a significant effect on the polymerization rate, final Mn, and final PDI (dashed line in Figures. 3-17a and 3-17b). As k_{frag} decreased to $3\times10^4 s^{-1}$ and k_{-frag} increased to $9\times10^4 s^{-1}$ (dotted curve, Fig 3-17a), the polymerization rate exhibits retardation in which the maximum predicted conversion over the whole period

of the simulation (1500 min) is ~ 41%, and is obviously lower than the predicted conversion (solid curve) when k_{frag} is equal to k_{-frag} .

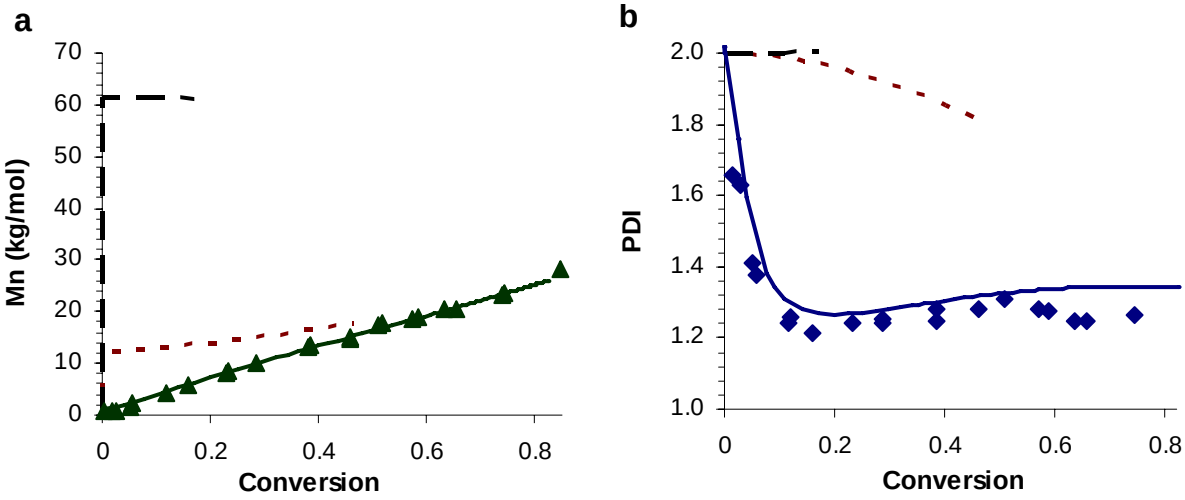

Figure 3-17: Effect of the backward fragmentation rate coefficient ($k_{frag} < k_{-frag}$) in presence of retardation effect: (a) On Mn; (b) On PDI. Legend: forward fragmentation (k_{frag}) = 6×10^4 s^{-1}, backward fragmentation (k_{-frag}) = 6×10^4 s^{-1} (solid curve); forward fragmentation (k_{frag}) = 3×10^4 s^{-1}, backward fragmentation (k_{-frag}) = 9×10^4 s^{-1} (dotted curve); forward fragmentation (k_{-frag}) = 5×10^2 s^{-1}, backward fragmentation (k_{-frag}) = 11.95×10^4 s^{-1} (dashed curve).

A further reduction in k_{frag} results in more retardation (dashed curve, Fig 3-17a). The predicted retardation in the simulated experiments is due to the fact that the concentration of R radicals decreases by decreasing k_{frag}, and the growing polymeric radical has to add more often to a RAFT agent before an effective chain transfer event takes place because in most cases the formed intermediate radical will fall back into its originating species ($k_{-frag} > k_{frag}$) . Thus, the number of the propagating polymeric radicals will be as low as the number of the initiator radicals, unless R radicals are produced.

In order to get the complete evolution of Mn and PDI with conversion the effect of decreasing k_{frag} on the polymerization rate is assumed to be negligible in the subsequent simulations. In these simulations the intermediate-intermediate termination reactions (cross and self) have been deliberately set to zero in order to omit the retardation effect. Decreasing the forward fragmentation rate coefficient k_{frag} from $6\times10^4 s^{-1}$ to $3\times10^4 s^{-1}$ results in the intermediate radical partition in favour of the reactants with a partitioning

factor (x) equal to 0.75; this factor means that 75% of the intermediate radicals will collapse into its originating species, and 25% will undergo fragmentation in the desired direction producing R radicals and polymeric RAFT agent. Accordingly, the transfer constant C_{tr} decreases from 82 to 9, resulting in PDI starting with a high value and decreasing with conversion at a slower rate (dotted curve, Fig. 3-18b).

The evolution of the number average molecular weight (Fig. 3-18a) shows the characteristics of living polymerization, in which the number average molecular weight increases linearly, but with a significant deviation from the ideal behaviour at the beginning of the reaction. Such deviation is attributed to the fact that not all of the active radicals start polymerization at the same time, since almost all of the R radicals are still retained in the RAFT agent due to the low forward fragmentation rate coefficient k_{frag} .

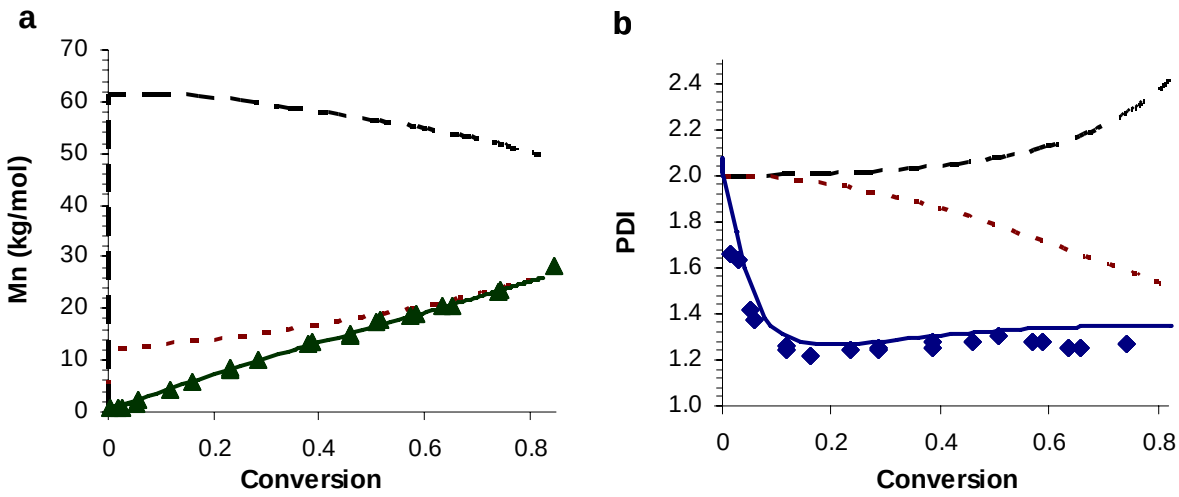

Figure 3-18: Effect of the backward fragmentation ($k_{-frag} > k_{frag}$) in the absence of retardation effect: (a) On Mn; (b) On PDI. Legend: forward fragmentation (k_{frag}) = 6×10^4 s^{-1}, backward fragmentation (k_{-frag}) = 6×10^4 s^{-1} (solid curve); forward fragmentation (k_{frag}) = 3×10^4 s^{-1}, backward fragmentation (k_{-frag}) = 9×10^4 s^{-1} (dotted curve); forward fragmentation (k_{-frag}) = 5×10^2 s^{-1}, backward fragmentation (k_{-frag}) = 11.95×10^4 s^{-1} (dashed curve).

Further reductions in the k_{frag} to $500s^{-1}$ result in reducing the transfer constant to a value of about 0.68, in which 95% of the intermediate radicals fall back into their originating species, resulting in a very high number average molecular weight at the very beginning of the reaction (dashed curve, Fig 3-18a). Consequently, as the reaction proceeds, a

decrease in the number average molecular weight is predicted due to the formation of high amounts of low molecular weight species, and leading to an increase in the polydispersity (dashed curve, Fig. 3-18b). Finally, by comparing the experimental results with our simulations, it may be concluded that the optimal overall fragmentation rate is close or even higher than the addition rate, and most of the intermediate radicals are symmetrical.

3.6 Conclusions

A mathematical model of the novel RAFT mediated free radical polymerization has been developed. It is well known that the rate at which radicals terminate with each other depends on their diffusion rates toward each other, which decrease as the radical length increases. To account for this behaviour, a chain length dependent termination model was used and integrated with the RAFT polymerization model. Careful simulations of conversion versus time have been carried out for solution polymerization of 3*M* styrene in toluene with 0.06*M* 2-phenylprop-2-yl dithiobenzoate as the RAFT agent. It has been shown that slow fragmentation of the intermediate radical can not be used alone to explain the observed retardation. Simulations indicate that the use of a RAFT agent reduces the gel effect and increases the average termination rate coefficient by reducing the molar mass distribution of the propagating radicals. Simulations also showed that reducing the gel effect is one of the main reasons behind the observed retardation, especially for the systems employing highly active RAFT agents. Good agreement between simulations and experimental data was obtained when the effect of cross termination of the intermediate radical is included in the model. In contrast, the hypothesised irreversible self termination of the intermediate radicals is kinetically insignificant, and its effect on the polymerization rate would be much lower if it is a reversible or a partially reversible process.

Simulations also showed that the number average molecular weight increases linearly with conversion for both systems (bulk and solution polymerization). Such linear growth was due to the high transfer constant of RAFT agents, where a propagating chain adds to RAFT agent quit often before undergoing further propagation. The addition of a propagating chain to a RAFT agent resulted in increasing its life-time by maintaining it as a dormant chain and hence protecting it from termination. The

polymer polydispersity index was predicted to decrease rapidly with conversion at a rate dependent on the transfer constant of the employed RAFT agent. In addition, simulations showed that the initiator concentration is a crucial factor in RAFT polymerization. High initiator concentration resulted in continuous production of small radicals, and hence reducing the living characteristics of RAFT polymerization.

Finally, by comparing experimental results with simulations, it may be concluded that the overall fragmentation rate is close to or higher than the addition rate, and the intermediate radical may prefer fragmentation in the direction of the products as illustrated by the good fit with the experimental PDI. This confirms that the R-group in RAFT agent 1a is a good leaving group.

Table 3-1: Experimental conditions for RAFT solution polymerization of styrene in toluene

AIBN	0.0044 mol/L
Mo	3 mol/L
RAFTo	0.06 mol/L, 0.04 mol/L
T	80 ^{o}C
Solvent	Toluene

Table 3-2: Parameters used for the styrene polymerization simulations

Parameter	Value	Reference
fk_d	1.1×10^{-4} s^{-1}	(Drache *et al.*, 2005)
k_p	660 dm^3/mol. s	(Buback *et al.*, 1995)
k_{pi}	$2\times k_p$ dm^3/mol. s	
k_{add}	7.96×10^{6} dm^3/mol. s	(Monteiro and de Brouwer, 2001)
$k_{frag} = k_{-frag}$	1×10^{4}-1×10^{5} s^{-1}	(Kwak *et al.*, 2004a; Wang *et al.*, 2003)
k_{ct}	0.4×<kt>	(Kwak *et al.*, 2004a)
k_{ct}	0.4×<kt>	(Kwak *et al.*, 2004a)
k_{st}	kct/1000	(Buback *et al.*, 1995)
D_{mon}	2.09×10^{-7} dm^2/s	(Griffiths *et al.*, 1998)
r	6.02×10^{-9} dm	(Russell, 1994)
P_{ij}	0.25	(Russell, 1994)

The chain length-dependent termination rate coefficient $k_t^{'}$ is calculated using Equations (3-17), (3-18) and (3-19).

Table 3-3: Experimental conditions for RAFT bulk polymerization of styrene at 80^{o}C (Butté, 2000)

AIBN	0.0087 mol/l (Mo/Io = 1000)
Mo	Bulk styrene ~ 8.7 mol/l
RAFTo	0.02175 mol/l (Mo/RAFTo = 400)
RAFT agent **(1a)**	R-group is: $-CH(CH_3)C_6H_5$ and Z-group is: Pyrrole

3.7 References

Adamy, M.; van Herk, A.M.; Destarac, M. and Monteiro, M.J., 2003. Influence of the Chemical Structure of MADIX Agents on the RAFT Polymerization of Styrene. *Macromolecules*, 36(7): 2293.

Altarawneh, I.S.; Srour, M. and Gomes, V.G., 2007. RAFT with Bulk and Solution Polymerization: An Approach to Mathematical Modelling and Validation. *Polymer-Plastics Technology and Engineering*, 46(11): 1103

Barner-Kowollik, C. *et al*., 2006. Mechanism and kinetics of dithiobenzoate-mediated RAFT polymerization. I. The current situation. *Journal of Polymer Science, Part A: Polymer Chemistry*, 44(20): 5809.

Barner-Kowollik, C.; Buback, M.; Egorov, M.; Fukuda, T.; Goto, A.; Olaj, O.F.; Russell, G.T.; Vana, P.; Yamada, B. and Zetterlund, P.B., 2005. Critically evaluated termination rate coefficients for free-radical polymerization: Experimental methods. *Progress in Polymer Science*, 30(6): 605.

Barner-Kowollik, C.; Quinn, J.F.; Morsley, D.R. and Davis, T.P., 2001. Modeling the reversible addition-fragmentation chain transfer process in cumyl dithiobenzoate-mediated styrene homopolymerizations: Assessing rate coefficients for the addition-fragmentation equilibrium. *Journal of Polymer Science, Part A: Polymer Chemistry*, 39(9): 1353.

Barner-Kowollik, C.; Vana, P.; Quinn, J.F. and Davis, T.P., 2002. Long-lived intermediates in reversible addition-fragmentation chain-transfer (RAFT) polymerization generated by g radiation. *Journal of Polymer Science, Part A: Polymer Chemistry*, 40(8): 1058.

Buback, M.; Gilbert, R.G.; Hutchinson, R.A.; Klumperman, B.; Kuchta, F.D.; Manders, B.G.; O'Driscoll, K.F.; Russell, G.T. and Schweer, J., 1995. Critically evaluated rate coefficients for free-radical polymerization, 1. Propagation rate coefficient for styrene. *Macromolecular Chemistry and Physics*, 196(10): 3267.

Buback, M.H., B.; Kuchta, F.; Russell, G. T.; Schmid, E. , 1994. Initiator efficiencies in 2,2-azoisobutyronitrile-initiated free-radical polymerizations of styrene. *Macromolecular Chemistry and Physics*, 195(6): 2117.

Butté, A., 2000. Living free radical polymerization in miniemulsion Thesis (Ph. D.) Thesis, Zurich, 2000.

Chiefari, J.; Chong, Y.K.; Ercole, F.; Krstina, J.; Jeffery, J.; Le, T.P.T.; Mayadunne, R.; Meijs, G.F.; Moad, C.L.; Moad, G.; Rizzardo, E. and Thang, S.H., 1998. Living Free-Radical Polymerization by Reversible Addition-Fragmentation Chain Transfer: The RAFT Process. *Macromolecules*, 31(16): 5559.

Chiefari, J.; Mayadunne, R.T.A.; Moad, C.L.; Moad, G.; Rizzardo, E.; Postma, A.; Skidmore, M.A. and Thang, S.H., 2003. Thiocarbonylthio Compounds (S:C(Z)S-R) in Free Radical Polymerization with Reversible Addition-Fragmentation Chain Transfer (RAFT Polymerization). Effect of the Activating Group Z. *Macromolecules*, 36(7): 2273.

Coote, M.L., 2004. Ab Initio Study of the Addition-Fragmentation Equilibrium in RAFT Polymerization: When Is Polymerization Retarded? *Macromolecules*, 37(13): 5023.

de Brouwer, H.S., M. A. J.; Klumperman, B.; Monteiro, M. J.; German, A. L. , 2000. Controlled radical copolymerization of styrene and maleic anhydride and the synthesis of novel polyolefin-based block copolymers by reversible addition-

fragmentation chain-transfer (RAFT) polymerization. *Journal of Polymer Science Part A: Polymer Chemistry*, 38(19): 3596.

Donovan, M.S.; Lowe, A.B.; Sumerlin, B.S. and McCormick, C.L., 2002. RAFT Polymerization of N,N-dimethylacrylamide Utilizing Novel Chain Transfer Agents Tailored for High Reinitiation Efficiency and Structural Control. *Macromolecules*, 35(10): 4123.

Drache, M.; Schmidt-Naake, G.; Buback, M. and Vana, P., 2005. Modeling RAFT polymerization kinetics via Monte Carlo methods: cumyl dithiobenzoate mediated methyl acrylate polymerization. *Polymer*, 46(19): 8483.

Feldermann, A.; Coote Michelle, L.; Stenzel Martina, H.; Davis Thomas, P. and Barner-Kowollik, C., 2004. Consistent experimental and theoretical evidence for long-lived intermediate radicals in living free radical polymerization. *Journal of the American Chemical Society*, 126(48): 15915.

Fukuda, T.; Yoshikawa, C.; Kwak, Y.; Goto, A. and Tsujii, Y., 2003. Mechanisms and kinetics of living radical polymerization: Absolute comparison of theory and experiment. *ACS Symposium Series*, 854(Advances in Controlled/Living Radical Polymerization): 24.

Goto, A.; Sato, K.; Fukuda, T.; Moad, G.; Rizzardo, E. and Thang, S.H., 1999. Mechanism and kinetics of RAFT (reversible addition-fragmentation chain transfer)-based controlled radical polymerization of styrene. *Polymer Preprints (American Chemical Society, Division of Polymer Chemistry)*, 40(2): 397.

Griffiths, M.C.; Strauch, J.; Monteiro, M.J. and Gilbert, R.G., 1998. Measurement of Diffusion Coefficients of Oligomeric Penetrants in Rubbery Polymer Matrixes. *Macromolecules*, 31(22): 7835.

Hawthorne, D.G.; Moad, G.; Rizzardo, E. and Thang, S.H., 1999. Living Radical Polymerization with Reversible Addition-Fragmentation Chain Transfer (RAFT): Direct ESR Observation of Intermediate Radicals. *Macromolecules*, 32(16): 5457.

Kapfenstein-Doak, H.; Barner-Kowollik, C.; Davis, T.P. and Schweer, J., 2001. A Novel Method for the Measurement of Chain Transfer to Monomer Constants in Styrene Homopolymerizations: The Pulsed Laser Rotating Reactor Assembly. *Macromolecules*, 34(9): 2822.

Kubo, K.; Goto, A.; Sato, K.; Kwak, Y. and Fukuda, T., 2005. Kinetic study on reversible addition-fragmentation chain transfer (RAFT) process for block and random copolymerizations of styrene and methyl methacrylate. *Polymer*, 46(23): 9762.

Kwak, Y.; Goto, A. and Fukuda, T., 2004a. Rate Retardation in Reversible Addition-Fragmentation Chain Transfer (RAFT) Polymerization: Further Evidence for Cross-Termination Producing 3-Arm Star Chain. *Macromolecules*, 37(4): 1219.

Kwak, Y.; Goto, A.; Komatsu, K.; Sugiura, Y. and Fukuda, T., 2004b. Characterization of Low-Mass Model 3-Arm Stars Produced in Reversible Addition-Fragmentation Chain Transfer (RAFT) Process. *Macromolecules*, 37(12): 4434.

Kwak, Y.; Goto, A.; Tsujii, Y.; Murata, Y.; Komatsu, K. and Fukuda, T., 2002. A kinetic study on the rate retardation in radical polymerization of styrene with addition-fragmentation chain transfer. *Macromolecules*, 35(8): 3026.

Luo, Y.; Wang, R.; Yang, L.; Yu, B.; Li, B. and Zhu, S., 2006. Effect of Reversible Addition-Fragmentation Transfer (RAFT) reactions on (mini)emulsion polymerization kinetics and estimate of RAFT equilibrium constant. *Macromolecules*, 39(4): 1328.

Matyjaszewski, K. and Xia, J., 2001. Atom Transfer Radical Polymerization. *Chem. Rev.*, 101(9): 2921.

Mayadunne, R.T.A.; Rizzardo, E.; Chiefari, J.; Krstina, J.; Moad, G.; Postma, A. and Thang, S.H., 2000. Living Polymers by the Use of Trithiocarbonates as Reversible Addition-Fragmentation Chain Transfer (RAFT) Agents: ABA Triblock Copolymers by Radical Polymerization in Two Steps. *Macromolecules*, 33(2): 243.

Moad, G.; Chiefari, J.; Chong, Y.K.; Krstina, J.; Mayadunne, R.T.A.; Postma, A.; Rizzardo, E. and Thang, S.H., 2000. Living free radical polymerization with reversible addition-fragmentation chain transfer (the life of RAFT). *Polymer International*, 49(9): 993.

Moad, G.; Rizzardo, E.; Solomon, D.H.; Johns, S.R. and Willing, R.I., 1984. Application of carbon-13-labeled initiators and carbon-13 NMR to the study of the kinetics and efficiency of initiation of styrene polymerization. *Makromolekulare Chemie, Rapid Communications*, 5(12): 793.

Moad, G.; Rizzardo, E. and Thang, S.H., 2005. Living radical polymerization by the RAFT process. *Australian Journal of Chemistry*, 58(6): 379.

Monteiro, M.J., 2005. Design strategies for controlling the molecular weight and rate using reversible addition-fragmentation chain transfer mediated living radical polymerization. *Journal of Polymer Science, Part A: Polymer Chemistry*, 43(15): 3189.

Monteiro, M.J. and de Brouwer, H., 2001. Intermediate radical termination as the mechanism for retardation in reversible addition-fragmentation chain transfer polymerization. *Macromolecules*, 34(3): 349.

Mueller, A.H.E.; Yan, D.; Litvinenko, G.; Zhuang, R. and Dong, H., 1995. Kinetic Analysis of Living Polymerization Processes Exhibiting Slow Equilibria. 2. Molecular Weight Distribution for Degenerative Transfer (Direct Activity Exchange between Active and Dormant Species) at Constant Monomer Concentration. *Macromolecules*, 28(22): 7335.

Perrier, S.; Barner-Kowollik, C.; Quinn, J.F.; Vana, P. and Davis, T.P., 2002. Origin of inhibition effects in the reversible addition fragmentation chain transfer (RAFT) polymerization of methyl acrylate. *Macromolecules*, 35(22): 8300.

Piton, M.C.; Gilbert, R.G.; Chapman, B.E. and Kuchel, P.W., 1993. Diffusion of oligomeric species in polymer solutions. *Macromolecules*, 26(17): 4472.

Russell, G.T., 1994. On exact and approximate methods of calculating an overall termination rate coefficient from chain length dependent termination rate coefficients. *Macromolecular Theory and Simulations*, 3(2): 439.

Russell, G.T.G., R. G.; Napper, D. H., 1993. Chain-length-dependent termination rate processes in free-radical polymerizations. 2. Modeling methodology and application to methyl methacrylate emulsion polymerizations. *Macromolecules*, 26(14): 3538.

Saricilar, S.; Knott, R.; Barner-Kowollik, C.; Davis, T.P. and Heuts, J.P.A., 2003. Reversible addition fragmentation chain transfer polymerization of 3-[tris(trimethylsilyloxy)silyl]propyl methacrylate. *Polymer*, 44(18): 5169.

Schilli, C.; Lanzendorfer, M.G. and Muller, A.H.E., 2002. Benzyl and cumyl dithiocarbamates as chain transfer agents in the RAFT polymerization of N-isopropylacrylamide. In situ FT-NIR and MALDI-TOF MS investigation. *Macromolecules*, 35(18): 6819.

Schulte, T.; Knoop, C.A. and Studer, A., 2004. Nitroxide-mediated living free-radical polymerization of styrene: A systematic study of the variation of the

alkoxyamine concentration. *Journal of Polymer Science Part a-Polymer Chemistry*, 42(13): 3342.

Smulders, W.W., 2002. Macromolecular architecture in aqueous dispersions: 'living' free-radical polymerization in emulsion. Ph.D. Thesis, Technische Universiteit Eindhoven, Eindhoven, Neth.

Smulders, W.W.; Gilbert, R.G. and Monteiro, M.J., 2003. A kinetic investigation of seeded emulsion polymerization of styrene using reversible addition-fragmentation chain transfer (RAFT) agents with a low transfer constant. *Macromolecules*, 36(12): 4309.

Solomon, D.H.; Rizzardo, E. and Cacioli, P., 1985. Free radical polymerization and the produced polymers. Eur. Pat. Appl, EP 135280

Vana, P.; Davis, T.P. and Barner-Kowollik, C., 2002a. Easy access to chain-length-dependent termination rate coefficients using RAFT polymerization. *Macromolecular Rapid Communications*, 23(16): 952.

Vana, P.; Davis, T.P. and Barner-Kowollik, C., 2002b. Kinetic analysis of reversible addition fragmentation chain transfer (RAFT) polymerizations: conditions for inhibition, retardation, and optimum living polymerization. *Macromolecular Theory and Simulations*, 11(8): 823.

Vana, P.; Quinn, J.F.; Davis, T.P. and Barner-Kowollik, C., 2002c. Recent advances in the kinetics of reversible addition fragmentation chain-transfer polymerization. *Australian Journal of Chemistry*, 55(6 & 7): 425.

Venkatesh, R.; Staal, B.B.P.; Klumperman, B. and Monteiro, M.J., 2004. Characterization of 3- and 4-Arm Stars from Reactions of Poly(butyl acrylate) RAFT and ATRP Precursors. *Macromolecules*, 37(21): 7906.

Wang, A.R.; Zhu, S.; Kwak, Y.; Goto, A.; Fukuda, T. and Monteiro, M.S., 2003. A difference of six orders of magnitude: A reply to the magnitude of the fragmentation rate coefficien. *Journal of Polymer Science, Part A: Polymer Chemistry*, 41(18): 2833.

Chapter Four

Modelling of RAFT in Emulsion Polymerization

Chapter 4

Modeling of RAFT in Emulsion Polymerization

Abstract

This Chapter outlines the development of a comprehensive dynamic model for batch and semi-batch RAFT mediated emulsion polymerisation processes to predict key polymer properties such as the molecular weight distribution (MWD), average particle size, conversion and particle size distribution (PSD). The model takes into account the complex physico-chemical phenomena occurring in the different phases, i.e. aqueous phase, monomer droplet phase, and polymer particle phase. The mathematical model includes nucleation models, reaction kinetic models that incorporate various stages of the reaction, dynamics of continuous phases, phase transfer events and reversible addition-fragmentation chain transfer events occurring in the particle phase.

By using the model to investigate the effect of the RAFT agent on the polymerization attributes, it is found that the rate of polymerization and the average size of the latex particles decrease with an increasing amount of the RAFT agent. It is also found that the molecular weight distribution can be controlled as it is strongly influenced by the presence of the RAFT based transfer agent. Model validation against experiments will be presented in the next chapters.

4.1 Introduction

Emulsion polymerization, due to its substantial technical, commercial, and environmental benefits, is the most widely used industrial process to manufacture coatings, paints, adhesives and resins. It can also be used to modify natural rubber latex to make high-value-added products. Approximately 15% of the Western worlds 10^8 tons/year of polymers is produced in emulsion polymerization processes (Gilbert, 1995). Due to its multiphase and compartmentalized nature, an emulsion polymerization

system provides the possibility of manufacturing a product with unique properties and performance characteristics. The compartmentalization effect results in a high molecular weight polymer at relatively high polymerization rate. As compared to other types of free radical polymerization such as bulk, solution and suspension polymerization, emulsion polymerization has other clear advantages. These advantages include a moderate viscosity increase for high solids polymerization, which makes the process as well as the product easy to handle. In addition, emulsion polymerization is a water-based, rather than solvent-based, system; thus there is no significant mass or heat transfer limitation, which therefore makes it an environmentally friendly.

A successful controlled/living free radical polymerization (CLFRP) requires negligible radical-radical termination. This can be achieved by reducing the initiator concentration or by adding more control agent. Such a reduction in the initiator concentration, or adding more RAFT agent, results in low polymerization rates in homogeneous systems such as bulk and solution polymerizations. Consequently, reaction times of about 24 hours or even longer were frequently reported for RAFT bulk or solution polymerizations (Barner-Kowollik *et al.*, 2001; Butté, 2000; Monteiro and de Brouwer, 2001). This problem can be overcome in principle by using emulsion polymerization, so as to take advantage of radical segregation, compartmentalization effect, to decrease terminations without significantly reducing the polymerization rate with respect to the corresponding nonliving processes (Altarawneh *et al.*, 2008; Gilbert, 1995; Gilbert *et al.*, 1999; Monteiro and De Barbeyrac, 2001; Smulders *et al.*, 2003; Van Herk and Monteiro, 2003). Since the polymerization times are of considerable importance when scaling up to an industrial process, emulsion polymerization offers great hope in this area. Therefore emulsion polymerization is an important process for the polymer industry. Furthermore, combining RAFT with emulsion polymerization has the potential to manufacture polymers in a manner such that polymer properties (MWD, PSD, PDI, polymer structure) can be controlled precisely, allowing for the synthesis of block copolymers and polymers with complex architecture.

Mathematical modelling enhances the understanding of the process and allows the process engineer to make predictions, and possibly informs how to control the part of the real world (the system) that is under investigation. Emulsion polymerization process is a complex process that requires an accurate model with efficient computation

capabilities in order to predict accurately the polymer properties, and be useful for real-time applications.

In this Chapter, a dynamic reactor model is developed for a styrene emulsion polymerisation batch/semi-batch processes in the presence of a RAFT-based transfer agent. The model is used to predict the evolution of the PSD and MWD over the entire range of monomer's conversion, and to address the effect of the RAFT-based transfer agent on the polymerization attributes.

4.2 Conventional emulsion polymerization

The first qualitative description of the kinetics of emulsion polymerization was described by Harkins (1945), followed by a widely used quantitative description by Smith and Ewart (1948). A comprehensive detailed description for emulsion polymerization based on the works of Harkins, Smith and Ewart was published by Gilbert in 1995.

Emulsion polymerization is based on a system consisting of water as the continuous phase, hydrophobic monomers, a water-soluble initiator, and an emulsifier (surfactant). All the ingredients are incorporated at the beginning of the reaction. The monomer is the main component of the polymerization, usually has a very low solubility in water and is capable of swelling its polymer. The initiator is water-soluble to avoid polymerization in the monomer droplets. The stabilizer (surfactant) is used to impart colloidal stability to the latex particles, along with forming the primary sites for nucleation and can be ionic, non-ionic or polymeric. The surfactant is a surface-active agent composed of both hydrophobic and hydrophilic segments; it adsorbs at the interface and provides stabilization by either electrostatic effect (anionic and cationic surfactant) or steric effect (non-ionic surfactant). The water-insoluble monomer droplets are stabilized with the micelle-forming surfactant (Gilbert, 1995; McLeary and Klumperman, 2006; Perrier, 2005; Zeaiter *et al.*, 2002). Since, the monomer being used in emulsion polymerization has low water solubility, it is clear that there will be three phases, referred to as the monomer phase, aqueous phase and micellar phase.

The aqueous phase is the most abundant, and initially contains the initiator, the surfactant, micelles, and small amounts of the slightly soluble monomer. The inside of the micelle, with the high concentration of the hydrophobic portions of the surfactants, provides an attraction for the hydrophobic monomer that diffuses through the water phase and swells the micelle. The number of monomer-swollen micelles is much larger than the number of monomer droplets present in the aqueous phase, resulting in the surface area of the monomer-swollen micelles is much greater than that of the monomer droplets. Thus the probability that a monomer swollen micelle captures an aqueous phase radical is far greater than that of a monomer droplets (Gilbert, 1995; Urban and Takamura, 2002). The droplets act as monomer reservoirs, and supply monomer(s) to the polymerization loci via diffusion of the monomer molecules through the aqueous phase. The water soluble initiator triggers the polymerization reaction by producing highly reactive radicals in the aqueous phase. These radicals have to propagate in the aqueous phase until they attain the critical degree of polymerization, z, at which these radicals become water insoluble, and hence increasing the probability of entering into monomer-swollen micelles or pre-existing particles. This radical is usually called 'z-mer', with a degree of polymerization equal to 3 if the monomer being polymerized is styrene (Gilbert, 1995). Radical entry initiates polymerization in monomer swollen micelles converting them into monomer swollen polymer particles and finally a dispersion of polymer particles is obtained.

Emulsion polymerization can be divided into three intervals. In interval **I** micelles and monomer droplets are present. The aqueous phase radical which has added enough aqueous phase monomer units to become surface active enters the micelle, converting it into a monomer swollen polymer particle. Therefore, the particle number increases in this stage as the micelles convert into particles and the rate of polymerization increases due to the increase in the number of the polymerization loci. At the end of interval **I** all micelles have disappeared and particle nucleation stops (Gilbert, 1995; Hawkett *et al.*, 1980). Interval **II** commences when the particle nucleation ceases and just monomer droplets and polymer particles are present in the system. The polymerization continues inside the particle with monomer migration from the emulsified monomer droplets through the aqueous phase into polymeric particles to replenish the polymerized monomer. As a result, equilibrium between the monomer migration rate and the polymerization rate is established, making the monomer concentration in the polymer

particle constant. The active radical within the particle keeps growing in size until it terminates with the entry of another radical or a transfer reaction with either monomer or transfer agent occurs. The newly formed radical generated from the transfer reaction can either propagate within the particle or exit the particle into the aqueous phase. As this process continues, the particles obviously increase in size with further adsorption of the free surfactant molecules at the particles surface in order to maintain the stability of the particles. Eventually, the monomer droplets disappear and the concentration of the free surfactant molecules decreases, resulting in interval **II** finishes at this point (Gilbert, 1995).

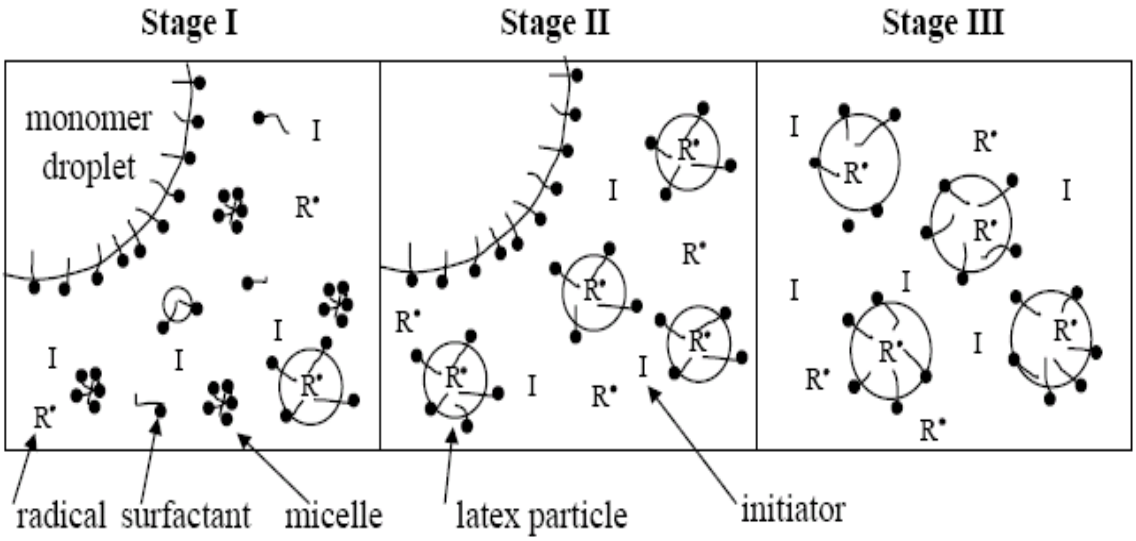

Scheme 4-1: Illustration of the classical three intervals for the emulsion polymerization process. Interval I, characterized by the presence of large monomer droplets, micelles, surfactant and aqueous phase radicals along with the initiator. Interval II, the particle formation has ceased and all micelles have been converted into polymeric particles. Interval III, all monomer droplets have disappeared (Gilbert, 1995).

In Interval **III**, only the latex particles and the aqueous phase are present. The concentration of the remaining monomer in the polymer particles decreases with an increase in conversion, viscosity and polymer volume fraction. At high conversions, propagation and termination become diffusion controlled, resulting in accelerating the polymerization rate. Moreover, exit of the small radical becomes less likely, thereby allowing the particle to have more than one active radical. Eventually, the system becomes glassy (polymer fraction in the particle is high, in order of 0.85) and the propagation rate slows down, resulting in a decrease in the rate of polymerization and polymerization comes to an end as almost all of the monomer is depleted.

4.3 RAFT emulsion polymerization

Many of the previously described principles apply in emulsion polymerization with RAFT agent. It has been argued that the compartmentalization effect in conventional emulsion polymerization is still effective in RAFT emulsion/miniemulsion polymerizations (Altarawneh *et al.*, 2008; Monteiro *et al.*, 2000a; Peklak and Butte, 2006; Smulders *et al.*, 2003). Controlled living emulsion polymerization via RAFT agent was first reported by the CSIRO group for the polymerization of butyl methacrylate, and was used also for the polymerization of styrene and MMA (Chiefari *et al.*, 1998). The results reported by the CSIRO group and others suggest that the implementation of the RAFT process in emulsion/miniemulsion systems could be problematic, as rate retardation and phase separation most likely occur (Charmot *et al.*, 2000; Monteiro *et al.*, 2001; Monteiro *et al.*, 2000a; Prescott *et al.*, 2002a; Prescott *et al.*, 2002b; Tsavalas *et al.*, 2001; Uzulina *et al.*, 2000). It has been reported in the literature that RAFT emulsion polymerization exhibits the inhibition/retardation effect (Luo *et al.*, 2006; Prescott *et al.*, 2005; Smulders *et al.*, 2003). This effect in emulsion polymerization could be more severe than in a bulk counterpart. Such retardation has been attributed to the exit of the small sized radicals ($R^{\bullet}$) that are generated from the RAFT agent or by transfer to monomer (Monteiro *et al.*, 2005).

4.3.1 Emulsion polymerization with high active RAFT agents

Studies on the application of a RAFT agent in *ab-initio* emulsion polymerization are rather limited. The first attempt to employ RAFT agent in such system was carried out by Le *et al. (1998)*, who noted that the selected RAFT agent should diffuse through the aqueous phase from monomer droplets into latex particles, and the importance of an optimum hydrophobic has been acknowledged in this work. Monteiro *et al.* (2000a), carried out seeded emulsion polymerizations of styrene in the presence of CDB and EMA RAFT agents. They observed that the polymerization rates were significantly retarded by the presence of the RAFT agent. The retardation in the polymerization with EMA RAFT agent was greater than that with CDB RAFT agent. The observed

retardations were attributed to the radical exit from the particles. In their work the effect of the leaving group (R) had been rationalized, in which the more water-soluble the leaving group (e.g. $C(CH_3)CO_2Et$, in EMA RAFT agent) the greater the extent to exit and hence the greater the retardation. Another observation the authors made was the formation of a RAFT-coloured layer above the latex consisting of low molecular weight dormant chains, swollen with monomer. As the system switches to interval **III** (no monomer droplets in the aqueous phase), the RAFT-coloured layer coalesces yielding a highly viscous coloured layer which often exhibits a loss of colloidal stability. The same observation about the formation of a RAFT-coloured layer was recorded by Moad *et al.* (2000), in miniemulsion polymerization with ionic surfactant.

Some of the essential factors for successful use of the RAFT process in emulsion polymerization were discussed by Moad *et al.* (2000), such as the selection of the RAFT agent and the polymerization conditions. They confirmed that the use of a high active RAFT agent such as cumyl dithiobenzoate (CDB) in *ab-initio* emulsion polymerization provided problems of inhomogeneous distribution of the RAFT agent and marked retardation was observed in the early stages of polymerization. The transport limitations of the RAFT agent between phases and its solubility were discussed as possible reasons behind the observed difficulties.

Indeed, a successful RAFT emulsion polymerization requires that the transfer agent distributes between the monomer droplets, aqueous phase and micelles, and must be transported from the droplets through the aqueous phase to the particles. A too hydrophilic RAFT agent (water-soluble) with a high addition rate constant would react quickly with the aqueous phase radicals to yield a dormant chain that remains water soluble, and takes some time for a z-mer to be formed and enters a micelle/particle when it attains a sufficient chain length. When an unreacted transfer agent molecule enters a particle, it remains capable of desorbing out from that particle unless it reacts with a growing radical of sufficient length to render it insoluble in the aqueous phase (Cunningham, 2002; Uzulina *et al.*, 2000). On the other hand, a hydrophobic RAFT agent (water-insoluble) will be mainly present in the monomer phase; this could allow RAFT polymerization within the droplet, thereby producing dormant chains that would be unable to transfer across the aqueous phase and resulting in a viscous, highly coloured layer as the monomer evaporates (Charmot *et al.*, 2000; Monteiro *et al.*, 2001;

Monteiro *et al.*, 2000a; Prescott *et al.*, 2002a; Prescott *et al.*, 2002b; Tsavalas *et al.*, 2001; Uzulina *et al.*, 2000). Thus, one of the most important factors for a successful RAFT mediated emulsion polymerization is to get RAFT agent at the locus of polymerization and keep it there (Prescott *et al.*, 2002a; Uzulina *et al.*, 2000). Problems such as colloidal instability can be minimized with high levels of the surfactant, while the formation of the oily red layer can be minimized by reducing the concentration of the monomer droplets in the aqueous phase by operating under semi-batch conditions.

Almost all of the observed problems were in emulsion polymerization with anionic sodium dodecyl sulfate, SDS, used as the surfactant. Replacing the anionic surfactant with a non-ionic surfactant may not be a reasonable alternative to obtain a successful RAFT emulsion polymerization, as a high amount of the non-ionic surfactant is required. Consequently, impurities in such large amounts will certainly have a significant effect on the product quality. Operating under miniemulsion conditions seems to be an ideal alternative to overcome these inherent problems, since the entire amount of the RAFT agents is concentrated in the monomer droplets which are the location of the polymerization reaction (Butte *et al.*, 2001; de Brouwer *et al.*, 2000; Lansalot *et al.*, 2002; Luo *et al.*, 2006; Simms *et al.*, 2005; Tsavalas *et al.*, 2001). However, miniemulsions produce broad particle size distributions, whereas in most applications involving nanotechnology, the PSD must be narrow in order for the particle to be useful; hence miniemulsion polymerizations are less suitable for PSD control.

A highly active water-insoluble RAFT agent (PPPDTA, C_{tr} = 6000) was utilized in seeded emulsion polymerization of styrene (Prescott *et al.*, 2002b; Prescott *et al.*, 2005; Prescott *et al.*, 2006). An organic co-solvent (acetone) was used to surmount the difficulties associated with RAFT transportation to the seed particles. The organic co-solvent facilitates the transportation of hydrophobic species (water-insoluble) in the aqueous phase in emulsion polymerization reaction. Such a technique allows the RAFT agent to be transported and resides in the pre-prepared particles before the onset of the polymerization reaction. Polymerization was started in interval **III** after removing the acetone and living polymerization characteristics were observed, leading to the production of a narrow polydispersity polymer. It is worth noting that for a high active RAFT agent, the exit process can only explain rate retardation or inhibition in the early stages of the polymerization (low conversion) as long as the small R radicals are

present. However, a reduction in rate was observed throughout the reaction (Prescott *et al.*, 2006).

A novel approach of RAFT emulsion polymerization to overcome such problems has been reported by Ferguson *et al*., (2005). The approach is based on polymerizing a water-soluble monomer such as acrylic acid (AA) in the water phase to a low degree of polymerization with a trithiocarbonate RAFT agent to form a short stabilizing macro RAFT agent. A hydrophobic monomer (BA) was then added under controlled feed conditions to form diblocks which were designed to self assemble and form rigid micelles (RAFT containing seed). The reaction conditions were chosen in such a manner as to avoid the presence of monomer droplets during the nucleation stage. Up to this point, polymerization could be continued at any desired feed rate and composition of the monomer (Ferguson *et al.*, 2005; Ferguson *et al.*, 2002a).

4.3.2 Emulsion polymerization with low active RAFT agents

So far, it would appear that using highly active RAFT agents in emulsion polymerization is unsuccessful. Therefore the following works in *ab-initio* RAFT emulsion polymerization focused on using a low active RAFT agent (such as xanthates) (Altarawneh *et al.*, 2008; Charmot *et al.*, 2000; Monteiro *et al.*, 2005; Monteiro and De Barbeyrac, 2001; Monteiro *et al.*, 2000a; Smulders *et al.*, 2003; Smulders and Monteiro, 2004). Xanthates (MADIX agents) are an important class of RAFT agents, and are currently considered as the only RAFT-based transfer agents that can be employed successfully in *ab-initio* emulsion polymerization, in which novel nanostructures can be prepared. Furthermore, since a high percentage of the polymeric chains are dormant and carry RAFT moiety, block copolymers with a controlled MWD can also be produced (Monteiro *et al.*, 2000b; Smulders and Monteiro, 2004).

Charmot *et al.* (2000) pointed out that emulsion polymerization with low active RAFT agents such as xanthates yield no rate retardation in *ab-initio* emulsion polymerization of butyl acrylate in a batch reactor, and a broad polydispersity was reported to be ~ 2.1 for styrene, and as low as 1.4 for butyl acrylate. However, when *ab-initio* emulsion polymerization with low active RAFT agent was carried out under semi-batch

conditions, the system was found to exhibit the characteristics of living polymerization in which a linear increase of molecular weight with conversion was observed.

Rate retardation was observed in styrene *ab-initio* emulsion polymerization with xanthate(Altarawneh *et al.*, 2008; Monteiro and De Barbeyrac, 2001). Such retardation is not surprising, since the employed low active RAFT agent had not been consumed completely during the polymerization, which resulted in an increased exit rate through the polymerization reaction. Depending on the RAFT agent concentration the number average molecular weight (Mn) started at a certain value and remained almost constant over the whole period of polymerization with a constant polydispersity close to 2.20. Using fluorinated xanthate with a transfer constant of 3.8 in *ab-initio* emulsion polymerization was investigated (Monteiro *et al.*, 2005). Again the polymerization rate was decreased with an increased concentration of RAFT agent. As the transfer rate of the employed RAFT agent is greater than 1, the polymerization displayed living characteristics in which a linear growth of the Mn was observed with a polydispersity commencing at ~2 and decreasing with conversion to 1.5.

Experiments conducted by Smulders *et al*. (2003) demonstrated that employing a low active xanthate RAFT-based agent (C_{tr}~0.7) results in a large effect on the kinetics of seeded emulsion polymerization of styrene. The exit rate was determined by using gama-relaxation experiments and was found to increase linearly with the RAFT concentration. As the RAFT agent used in Smulders' work is surface active, the entry rate was found to decrease with the amount of the RAFT agent, resulting in a significant retardation effect. Polydispersities close to 2 for all experiments were obtained, and the number average molecular weight was manipulated by RAFT concentration. Interestingly, the enhanced exit rate can be used to control the particle size while maintaining the predicted MWD, which allows one to control not only the MWD but also the particle size distribution (Altarawneh *et al.*, 2008; Monteiro and De Barbeyrac, 2001). The use of less reactive RAFT agents (i.e., ethyl 2-(*O*-ethylxanthyl) propionate which has a C_{tr} of about 0.68 for styrene) has proved to be quite successful in producing polymers with controlled MWDs, fast rates of polymerization, and controllable particle size distributions (Altarawneh *et al*., 2008).

4.4 The applicability of zero-one kinetics

In conventional emulsion polymerization systems following zero-one kinetics, the entry of an aqueous phase oligomeric radical into a latex particle containing one growing radical results in instantaneous termination, and thus the particles either have one or zero active radical at any time. Monteiro *et al.* (2000a) noted that RAFT mediated emulsion polymerization systems may not exhibit the expected zero-one kinetics in styrene polymerization with a high active RAFT agent (e.g. Cumyl and EMA RAFT agents). In the presence of a RAFT agent, the entering oligomeric radical (z-mer) can transfer its activity to a long radical, where the probability of termination between two long radicals is much lower than that between a short and long radical, and hence termination may not be instantaneous.

Prescott *et al*., (2005), pointed out that the z-meric-RAFT adduct (intermediate radical) is a surface active species, which remains as a dormant species on the surface of the particle until it is reactivated via a transfer reaction, thereby reproducing the active z-mer and a dormant RAFT agent. Provided that the characteristics of the newly released z-mer radical are identical to those for the first entered radical, the probability of this reactivated z-mer radical exiting from one particle and moving to another is quite significant for a living polymerization system with a high active RAFT agent. However, in the presences of a low active RAFT agent the entered oligomeric radical has a high probability (~0.999, see section 4.5.3.2) to propagate when it adsorbs into a latex particle and forms a more water-insoluble radical. Such a radical is unable to desorb out from the latex particle. Thus, it is concluded that emulsion polymerization with small particles and with a low active RAFT agent follows zero-one kinetics.

Smulders *et al*. (2003) used a zero-one system to predict the effect of employing a low active RAFT agent on the kinetics of seeded emulsion polymerization of styrene in a batch reactor. Prescott *et al*. (2006) used it to describe the inhibition period observed in the seeded emulsion polymerization of styrene with a highly active RAFT agent, when the dormant chains are quite small and radical-radical termination reactions take place with quit large rate coefficients (such conditions meet at low conversions).

Finally, it has been demonstrated by Monteiro *et al.* (2001) that a system utilizing a low active RAFT agent acts as the one employing a conventional chain transfer agent. The authors ended with the conclusion that an *ab-initio* emulsion polymerization employing low active RAFT agents fits the criteria for zero-one conditions, mainly due to the small size of the particles and the low re-initiation constant of the radical formed through transfer to styrene.

4.5 Modelling RAFT in emulsion polymerization

An understanding of various polymerization processes is gained through studies of the kinetics and mechanisms of the events which occur during the given process. The complexity of heterogeneous chemical reactions typified by emulsion polymerization makes this understanding difficult. Mathematical modelling is a powerful tool for the development of process understanding and advanced reactor technology in the polymer industry. Modelling RAFT-emulsion polymerization processes with a focus on PSD and MWD is a very challenging task due to the disturbed nature of such systems. In spite of these challenges, a comprehensive kinetic mathematical model for RAFT mediated emulsion polymerization provides a good tool to understand the relationship between process variables and product characteristics via understanding the interaction between the events that take place in the system.

4.5.1 Overview

A kinetic model for RAFT polymerization of styrene in seeded emulsion was developed by Peklak *et al*. (2006). The model consists of a set of simple population balance equations of the radical species in aqueous and particle phases. The model results were compared to experiments using cumyl dithiobenzoate in batch seeded emulsion polymerization of styrene with an organic solvent as the phase transfer agent. In terms of monomer conversion, using the transfer rate constants as fitting parameter, the agreement was good, and the model was able to describe the effect of the RAFT agent on the polymerization rate. However, the model did not provide predictions for PSD and MWD. A kinetic model of controlled living microemulsion polymerization was developed by Hermanson *et al*. (2006); the model accounted for the reaction rate,

molecular weight polydispersity and particle size (PS). The model predicted the effect of increasing RAFT agent on polymerization rate and PS at low RAFT agent concentrations (RAFT/Initiator <1) but failed to predict PS at higher concentrations. The predicted trends were qualitatively consistent with those observed experimentally. The authors reported that uncertainties in the kinetic parameters precluded accurate predictions.

In general, no comprehensive model exists for either high or low active RAFT agents in *ab-initio* or seeded emulsion polymerization. The models developed so far focus only on the inhibition and retardation phenomena associated with the use of RAFT process in batch emulsion polymerization (Liu *et al.*, 2006; Peklak and Butte, 2006; Prescott, 2003), and the effect of RAFT agent on the radical exit and entry steps (Smulders *et al.*, 2003). The predictions of PSD and MWD have not been addressed in these models.

4.5.2 Model basis

A system with zero-one kinetics was employed for RAFT-emulsion polymerization combining the effect of radical entry, exit and re-entry. Based on the RAFT mechanism discussed in Chapter 3, the conventional emulsion polymerization mechanism (Gilbert, 1995; Zeaiter *et al.*, 2002) is modified to accommodate the reversible addition-fragmentation chain transfer reaction that occurs in the aqueous and particle phases. Several assumptions must be made in order to obtain an accurate description of the events taking place in the zero-one system, these are:

- Polymerization occurs only in the latex particle and the aqueous phase radical grows to length z in order to enter a latex particle.
- Particles form through micellar nucleation (which is the dominant one) and homogenous nucleation.
- Reaction with a RAFT agent occurs in the aqueous phase as well as in the particle phase. The aqueous phase RAFT-derived radical may enter a latex particle or propagate and terminate in the aqueous phase.
- The entry of a z-mer, RAFT-derived radical and re-entry of any exited radical into a latex particle that already contains a free radical results in instantaneous

termination. As the termination between an intermediate radical and a normal radical is experimentally confirmed, entry into a particle containing an intermediate radical results in instantaneous termination.

- Due to the relatively small surface area of the monomer droplets, the amount of surfactant covering the monomer droplets is considered a negligible fraction of the total surfactant in the reactor.
- The concentration of the monomer and the RAFT agent in the monomer-swollen polymer particles, water phase and monomer droplets are in thermodynamic equilibrium.
- Propagation and transfer to dormant chain reactions occurs within the particle and in the aqueous phase following the RAFT mechanism. In addition, due to their low concentrations, addition of small radicals ($M^{\bullet}$ and $R^{\bullet}$) to the RAFT agent inside a particle is insignificant.
- The diffusion rate of the RAFT-derived radical ($R^{\bullet}$) in water phase is equal to that for the monomeric radical (styrol radical), as well as its partitioning coefficient between water and particle phases.
- The transfer rate of RAFT agent is higher than its consumption rate (Smulders, 2002), and hence transport of the RAFT agent is not the rate determining step.
- In this work, the concentration of the emulsifier is higher than the critical micellar concentration (cmc). Thus, the latex particles are assumed to be well stabilized and coagulation is neglected.
- The symmetrical intermediate radical has no preference regarding which direction the fragmentation would take place ($k_{frag} \approx k_{-frag}$) (Altarawneh *et al.*, 2007).

It has been shown experimentally (Hawkett *et al.*, 1980) and theoretically (Casey *et al.*, 1994) that the zero-one styrene emulsion polymerization model is valid for conditions such as small particle size where particles are saturated with monomer and therefore far from glass transition. Typically, polymerisation within small particles is controlled by zero-one kinetics, while large particles are controlled by pseudo-bulk kinetics. The size at which particles cross from the zero-one regime to the pseudo-bulk regime for propagational growth within particles varies between monomers and is known as the "cross-over radius". The value of cross over radius for styrene was reported in literature to be in the range 50-60 nm (Coen *et al.*, 2004; Gilbert, 1995; Thickett and Gilbert,

2007). Small particle size corresponds to lower radical entry rate, higher radical exit and higher termination rates (Gilbert, 1995). Thus, for our system, all experiments were designed to produce small latex particles with a maximum average diameter of about 100 nm.

4.5.3 Aqueous phase mechanism

The decomposition of the initiator in the water phase triggers the polymerization process by generating free radicals, which react with the aqueous phase monomer to generate oligomeric radical ($P_n^{\bullet}$), which in turn reacts with the aqueous phase RAFT agent. The fragmentation rate of the intermediate radical produced by the addition to the RAFT agent is sufficiently high (Altarawneh *et al.*, 2008; Smulders, 2002). Thus, the overall transfer reaction is considered to express the reaction with RAFT agent in the aqueous phase. The following reactions represent the different fates of the initiator derived radical in the aqueous phase:

$$I_2 \xrightarrow{k_d} 2I^{\bullet} \qquad \textbf{(4-1)}$$

$$I^{\bullet} + M \xrightarrow{k_p^i} P_1^{\bullet} \qquad \textbf{(4-2)}$$

$$I^{\bullet} + AR \xrightarrow{k_{tr}^I} I - A + R^{\bullet} \qquad \textbf{(4-3)}$$

$$I^{\bullet} + T_{aq}^{\bullet} \xrightarrow{k_{t,aq}^I} D \qquad \textbf{(4-4)}$$

where k_d is the initiator first-order dissociation rate coefficient (s^{-1}); k_p^i is the second-order propagation rate coefficient (1/mol.s); k_{tr}^I and $k_{t,aq}^I$ are the transfer rate coefficient of the initiator radical to RAFT agent and the aqueous phase termination rate coefficient, respectively; T_{aq}^* is the total aqueous phase radical concentration. Reaction 4-1 describes the production of primary free radicals and reaction 4-2 requires that at least some of the free radicals from reaction 4-1 react with monomer rapidly enough to avoid recombination reactions. Reaction (4-2) is faster than the subsequent propagation reaction, and hence predominates reactions (4-3) and (4-4) because of the high concentration of the aqueous phase monomer compared with the aqueous phase initiator and RAFT agent; as such reactions (4-3) and (4-4) are insignificant and can be ignored.

The oligomeric radical ($P_1^\bullet$) undergoes a sequence of propagation reactions in the water phase and termination as outlined below:

$$P_n^\bullet + M \xrightarrow{k_{P,aq}^i} P_{n+1}^\bullet, \quad n < z \qquad \textbf{(4-5)}$$

$$P_n^\bullet + T_{aq}^\bullet \xrightarrow{k_{t,aq}^I} D \ , \quad n < z \qquad \textbf{(4-6)}$$

Further propagation of the oligomers which escape termination and transfer enables them to reach a degree of polymerization at which the oligomer becomes surface-active. This degree of polymerization was estimated, based on free energies of hydration, to be ~3 for styrene (Gilbert, 1995). The theoretically derived value of 'z' is in excellent agreement with experiment (Thickett and Gilbert, 2007). A z-mer radical that escapes termination, addition to RAFT agent and entry into a pre-existing particle or a micelle, undergoes further propagation to attain a higher degree of polymerization, j_{crit}, at which the charged initiator fragment becomes unable to solubilise the growing hydrophobic polymer chain.

$$P_{j_{crit}}^\bullet \longrightarrow new\ particle \qquad \textbf{(4-7)}$$

Under these circumstances the formation of a particle by homogenous nucleation, precipitation of a j-mer in the aqueous phase, becomes important. The homogenous and micellar nucleation mechanisms are pictorially depicted in Scheme 4-3.

4.5.3.1 Radical entry into particles

The entry model proposed by Maxwell *et al.*(1992) is now widely accepted as the mechanism for describing the aqueous phase events that lead to entry. This model has been shown to agree with a wide range of data and has been successfully used to account for the entry efficiency in emulsion polymerization, the homogenous nucleation of new particles, and the formation of core-shell particles (Coen *et al.*, 1998; Ferguson *et al.*, 2002b; Gilbert, 1995; Maxwell *et al.*, 1991; Prescott *et al.*, 2006). The model assumes that the free radical formed in the aqueous phase irreversibly enters a latex particle only when it adds a sufficient number of monomer units to attain a critical degree of polymerization 'z'. The entry of the initiator derived oligomer with a degree

of polymerization equal or higher than z into a micelle or a particle is given in the following reactions :

$$P_n^{\bullet} + micelle \xrightarrow{k_{e,micelle}^{i}} new\ particle,\ z \le n \le j_{crit} - 1 \quad \textbf{(4-8)}$$

$$P_n^{\bullet} + Particle \xrightarrow{k_e^i} entry,\ z \le n \le j_{crit} - 1 \quad \textbf{(4-9)}$$

In the aqueous and particle phases, addition of the propagating radical $Pn^{\bullet}$ ($n < j_{crit-1}$, in the aqueous phase) to the thiocarbonylthio reagent (compound 1, Scheme 4-2) followed by forward fragmentation of the intermediate radical (compound 2), gives rise to a polymeric RAFT agent (compound 3) and a new reinitiating radical $R^{\bullet}$ (Scheme 4-2). Similar to the initiator fragment, a reaction of the re-initiating radical $R^{\bullet}$ with monomer forms a new propagating radical $Pm^{\bullet}$ ($m < j_{crit-1}$) which can add to the polymeric RAFT agent 3 resulting in a symmetrical intermediate radical 4. For simplicity, the addition-fragmentation reaction occurring in the aqueous phase can be simplified by considering the overall transfer reaction without including the intermediate radical; the simplified reaction is valid because of the high fragmentation rate compared with the addition rate:

$$P_n^{\bullet} + AR \xrightarrow{k_{tr,aq}^{AR}} P_i - A + R^{\bullet},\ \ n < z \quad \textbf{(4-10)}$$

In emulsion polymerization in the presence of a RAFT agent as a chain transfer agent, reaction (4-10) must be taken into account. In this work, the leaving-group radical, RAFT-derived radical $R^{\bullet}$, can enter a micelle or a pre-existing particle, assuming it is not extremely water soluble and has enough surface activity to enter either a micelle or a particle (Altarawneh *et al.*, 2008; Smulders *et al.*, 2003). It is assumed that the RAFT-derived radical has the same fate as the initiator derived radical in the aqueous phase; thus it follows the same behaviour in terms of propagation, entry and termination, and this may be described as:

$$R^{\bullet} + micelle \xrightarrow{k_{e,micelle}^{R}} new\ particle \quad \textbf{(4-11)}$$

$$R^{\bullet} + Particle \xrightarrow{k_e^R} entry \quad \textbf{(4-12)}$$

$$R^{\bullet} + T_{aq}^{\bullet} \xrightarrow{k_t^{aq}} D \quad \textbf{(4-13)}$$

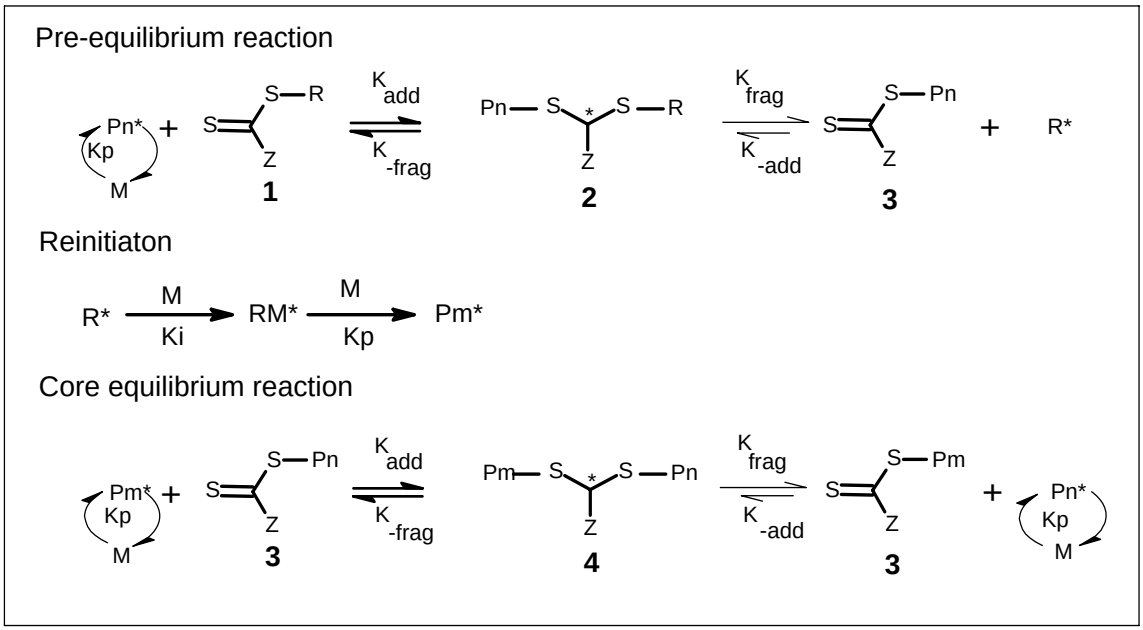

Scheme 4-2: RAFT mechanism.

There are two different treatments for zero-one systems; one is to discriminate between particles containing zero or one radicals, while the other one, consists in further dividing particles having one radical into different categories in which each category represents particles with a specific type of radical. In RAFT mediated emulsion polymerization these one-radical-particles can be:

- *Particles having one initiator-derived polymeric radical, which would not readily diffuse out of the particle due to its size.*
- *Particles having one small radical generated by the fragmentation of the intermediate RAFT radical or by transfer to monomer, which presumably can readily exit.*
- *Particles having one intermediate radical generated by the addition to the RAFT agent, these kinds of particles can be further divided into four types depending on the nature of the added radical and RAFT agent:*
    - *Particles having PAR type intermediate radical generated from the addition of z-mer to the initial RAFT agent AR.*
    - *Particles having RAR type intermediate radical generated from the addition of $R^{\bullet}$ to the initial RAFT agent AR.*
    - *Particles having PAP type intermediate radical generated from the addition of z-mer to the polymeric RAFT agent AP.*

- *Particles having RAP type intermediate radical generated from the addition of $R^{\bullet}$ to the polymeric RAFT agent AP.*

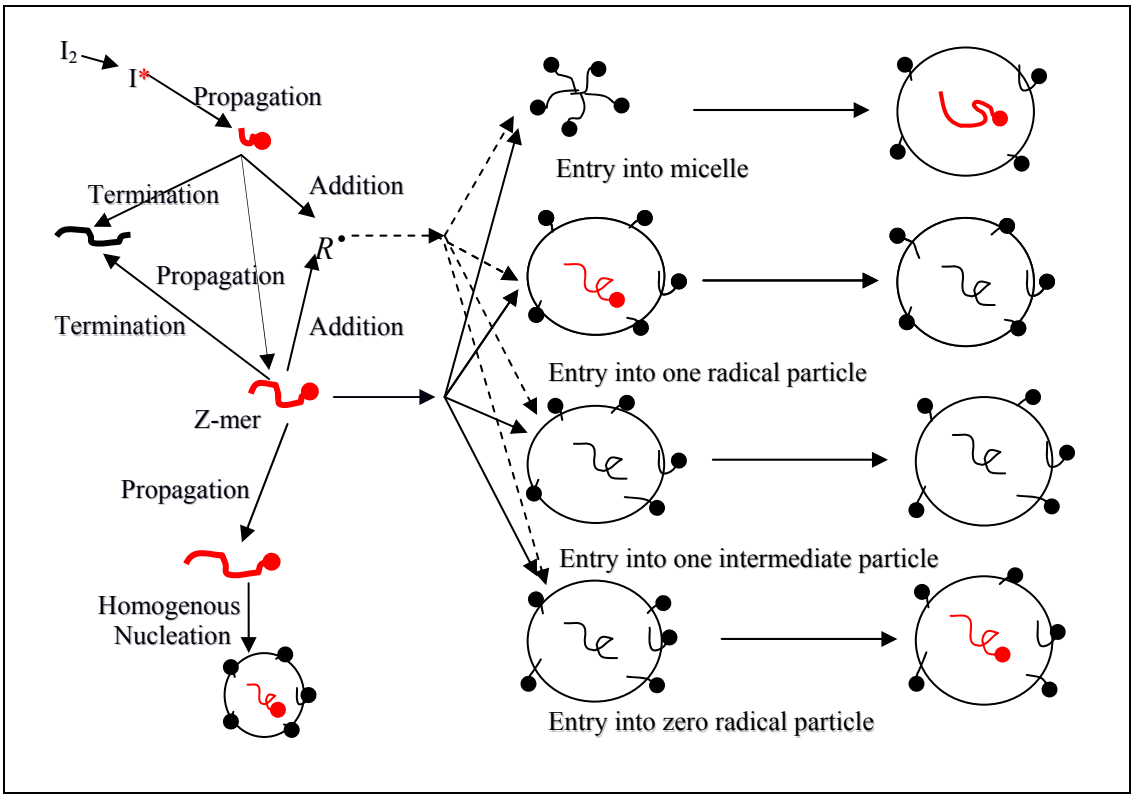

Scheme 4-3: A schematic representation of the modified kinetic events that are expected to occur in RAFT-Emulsion polymerization system.

As the termination of the intermediate radical was experimentally confirmed (Kwak *et al.*, 2004; Monteiro and de Brouwer, 2001), entry into such kinds of particles results in instantaneous termination and produces particles with zero radical. Scheme 4-3 illustrates the aqueous phase mechanism along with the formation of different types of particles. Once particles are formed in significant amounts, entry of new radicals produced in the aqueous phase into pre-existing particles becomes the main entry mode and completely dominates the alternative fate of forming new particles.

4.5.3.2 Radicals exit from particles

The propagating polymeric radical inside the particle may undergo a radical transfer reaction with a monomer molecule producing the monomeric radical ($M^{\bullet}$), and with

the RAFT agent producing a RAFT-derived radical ($R^{\bullet}$) (Smulders, 2002). If it escapes termination, the produced radicals may propagate inside the particle and convert into less water-soluble radicals that can not exit the particle. However, these radicals (($R^{\bullet}$) and ($M^{\bullet}$)) may also diffuse through the interior of the latex particle to the particle surface where they can exit the particle, and such exited radicals are denoted as $E^{\bullet}$ (Zeaiter *et al.*, 2002). Once the desorbed monomeric radical or RAFT-derived radical $R^{\bullet}$ meets the surface of a particle that contains a radical or not, it immediately penetrates the particle due to its high lipophilic nature. The adsorption-desorbtion process is reversible, as illustrated below:

$$E^{*} + \text{Particle} \underset{k_{dE}}{\overset{k_{e\,E}}{\rightleftharpoons}} \text{Particle-}E^{*}$$

Recently, Prescott *et al.* (2005), proposed that the "RAFT induced exit" mechanism has a significant effect in the polymerization rate when a high active RAFT agent is used in emulsion polymerization. Such a mechanism describes the exit of a z-mer from a particle resulting in reducing the average number of radicals per particle and hence reducing the polymerization rate. According to this mechanism, a z-mer radical converts to a z-meric RAFT adduct (intermediate radical) after entry. Upon fragmentation, the released z-mer radical may not propagate inside the particle, and since it is still at the particle surface it may exit the particle.

Obviously, there are two possible events that the entered z-mer may undergo, these are: (i) entry followed by an immediate propagation inside the particle with a probability given by: $P(prop) = C_p^M / (C_p^M + C_{tr} C_p^{AR})$ and (ii) entry followed by an immediate addition to the RAFT agent (deactivation) with a probability given by: $P(add) = C_{tr} C_p^{AR} / (C_p^M + C_{tr} C_p^{AR})$. In these two equations, C_p^M , C_p^{AR} are the concentrations of monomer and RAFT agent in the particle, respectively. Under the conditions that there is no transfer limitation of the RAFT agent through the aqueous phase to the particles, the assumption that the molar ratio of RAFT/monomer in the particle is equal to that in the monomer droplets is valid. Thus, the RAFT agent concentration 'C_p^{AR}' can be calculated from the RAFT/monomer molar ratio and the saturated concentration of monomer in the particles during interval II.

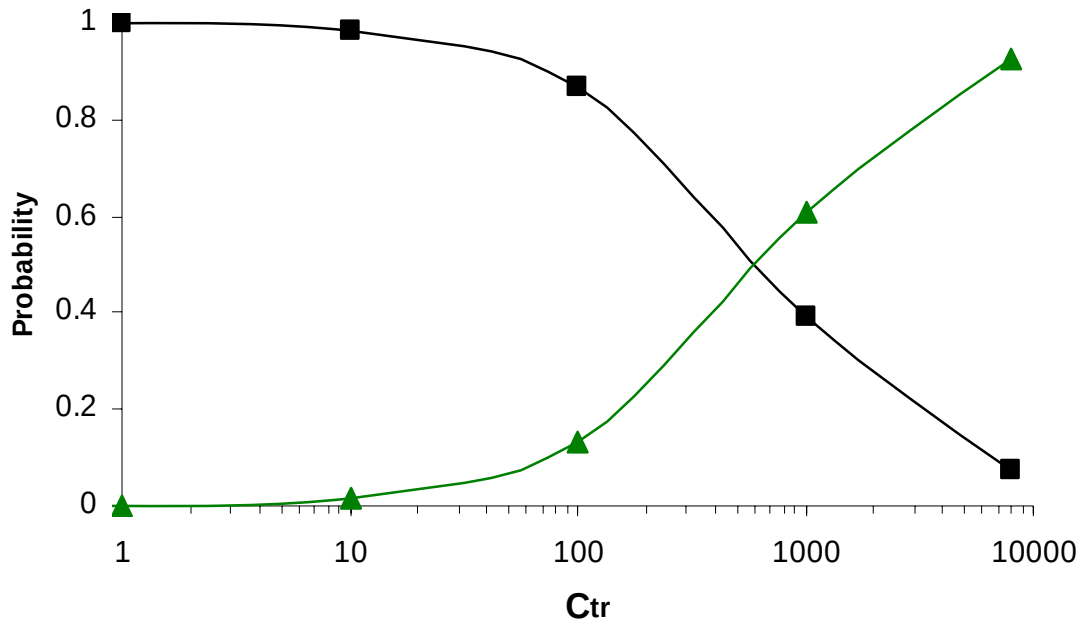

Figure 4-1: Probabilities of the entered z-mer propagates (■) with monomer or forms the intermediate radical via addition to RAFT agent (▲).

By using these equations our preliminary probability calculations, shown in figure 4-1, suggest that a low active RAFT agent with a transfer constant lower than 10 has a high probability (~0.99) to propagate when it adsorbs into a latex particle and form a (z +1)-mer and becomes more water-insoluble and unable to desorb out from the latex particle. Therefore, this exit mechanism is excluded from the kinetic model since the RAFT agent being used in this study is a low active one with a transfer constant close to one.

4.5.3.3 Species concentration

Having described the mechanism of the aqueous and particle phases for both RAFT and initiator-derived radicals, a mass balance of the various aqueous species leads to the following set of rate equations:

$$\frac{d[I]}{dt} = -k_d[I] \qquad \textbf{(4-14)}$$

$$\frac{d[I^\bullet]}{dt} = 2fk_d[I] - k^1_{p,aq}[I^\bullet]C^M_w \qquad \textbf{(4-15)}$$

$$\frac{d[P_1^\bullet]}{dt} = k_{p,aq}^1[I^\bullet]C_w^M - k_{p,aq}^1[P_1^\bullet]C_w^M - k_{tr,aq}^{AR}[P_1^\bullet]C_w^{AR} - k_{t,aq}[P_1^\bullet][T_{aq}^\bullet] \quad \textbf{(4-16)}$$

For $n < z$ **then**

$$\frac{d[P_n^\bullet]}{dt} = k_{p,aq}^{n-1}[P_{n-1}^\bullet]C_w^M - k_{p,aq}^n[P_n^\bullet]C_w^M - k_{tr,aq}^{AR}[P_n^\bullet]C_w^{AR} - k_{t,aq}[P_n^\bullet][T_{aq}^\bullet] \quad \textbf{(4-17)}$$

For $n = z,..., j_{crit} - 1$ **then**

$$\begin{aligned}\frac{d[P_n^\bullet]}{dt} &= k_{p,aq}^{n-1}[P_{n-1}^\bullet]C_w^M - k_{p,aq}^n[P_n^\bullet]C_w^M - k_{tr,aq}^{AR}[P_n^\bullet]C_w^{AR} - k_{t,aq}[P_n^\bullet][T_{aq}^\bullet] \\ &\quad - k_e^i[P_n^\bullet]\frac{N_{tot}}{N_A} - k_{e,micelle}^i C_{micelle}[P_n^\bullet]\end{aligned} \quad \textbf{(4-18)}$$

$$\frac{d[P_{j_{crit}}^\bullet]}{dt} = k_{p,aq}^{j_{crit}-1}[P_{j_{crit}-1}^\bullet]C_w^M - k_{t,aq}[P_{j_{crit}}^\bullet][T_{aq}^\bullet] \quad \textbf{(4-19)}$$

$$\begin{aligned}\frac{d[E^\bullet]}{dt} &= \sum_{n=1}^{j_{crit}-1} k_{tr}^{AR}[P_n^\bullet]C_w^{AR} - k_e^E[E^\bullet]\frac{N_{tot}}{N_A} - k_{e,micelle}^R C_{micelle}[E^\bullet] \\ &\quad + k_d^E\frac{N_1^R}{N_A} - k_{t,aq}[E^\bullet][T_{aq}^\bullet]\end{aligned} \quad \textbf{(4-20)}$$

$$[T_{aq}^\bullet] = E^\bullet + \sum_{i=1}^{z-1}[P_n^\bullet] \quad \textbf{(4-21)}$$

In these equations, C_w^M, C_w^{AR} and $C_{micelle}$ are the monomer, RAFT agent and micellar concentrations in the water phase, respectively; N_{tot}, N_1^P, N_1^R are the total number concentration of latex particles, particles with one polymeric radical and particles with one RAFT-derived radical per litre of aqueous phase, respectively; N_A is the Avogadro's number; $P_n^\bullet$ is the concentration of the oligomeric initiator-derived radical; $k_e^i, k_{e,micelle}^i, k_e^R, k_{e,micelle}^R$ are the second order entry rate coefficients of the initiator and RAFT-derived radicals into a particle and a micelle respectively; k_d^E is the rate coefficient for desorption of monomeric and RAFT radicals $(E^\bullet)$ into the water phase; $k_{tr,aq}^{AR}$ is the transfer rate coefficient of the aqueous phase radicals to RAFT agent. The concentration of the aqueous phase radicals T_{aq}^* is given by the summation of the exited radical and aqueous phase oligomeric radical. The aqueous phase propagation and termination rate coefficients are characterized by: $k_{p,aq}^i$ and $k_{t,aq}$, respectively. The

monomer and AR concentrations are calculated using their partitioning coefficients. Equation (4-15) describes the rate of initiator-derived radical production proceeding with a decomposition rate coefficient (k_d); this parameter is a temperature dependent parameter which can be given for persulfate in terms of Arrhenius equation as the following (Gilbert, 1995)

$$k_d = 8 \times 10^{15} e^{-135/RT} \quad \textbf{(4-22)}$$

The latex particles and slightly soluble monomer droplets are dispersed in the aqueous phase and stabilized by the adsorption of surfactant molecules onto their surface. The adsorbed surfactant is in equilibrium with the surfactant amount in the dispersed phases and in the aqueous phase. The micelle concentration ($C_{micelle}$) can be determined by the rate of surfactant consumption (Coen *et al.*, 1998; Enzo, 1993; Zeaiter *et al.*, 2002) and using the maximising function which gives:

$$C_{micelle} = \text{Maximum} \left[0, \frac{[S_{added}] - [S_{ads}] - [cmc]}{n_{agg}} \right] \quad \textbf{(4-23)}$$

$$S_{ads} = \frac{4 \pi r_s^2 N_{tot}}{N_A a_s} \quad \textbf{(4-24)}$$

where *cmc* is the critical micellar concentration; n_{agg} is the mean aggregation number for the surfactant; S_{tot} is the total concentration of the added surfactant; S_{ads} represents the amount of surfactant per unit volume adsorbed onto the polymer surface; a_s is the area occupied by an adsorbed surfactant molecule. From equation 4-23 it may be concluded that micellar nucleation (particle formation via micelles) stops when the surfactant concentration falls below its critical value (cmc).

4.5.4 Particle size distribution

Population balance equations are conveniently expressed in terms of unswollen volume (V). The equations can also be expressed in terms of unswollen radius (r), and the two distribution functions are related by $n(V) = n(r)/4\pi r^2$, where, radius and volume

distributions are denoted by $n(r)$ and $n(V)$, respectively. The simplest version of a zero-one model for RAFT free systems accounts only for the number of particles with one radical and without any radicals. Differently from this approach, in the presence of RAFT agent the particles are distinguished in this work upon the type of radical that they contain. In RAFT mediated emulsion polymerization, following zero-one kinetics, seven types of particles can be identified, including:

1. Particles containing a single polymeric radical (n_1^P), generated by the entry of an initiator derived radical ($P_n^\bullet$) with a degree of polymerization equal to or greater than 3 into a zero radical particle (n_0), propagation of a small radical within an (n_1^R), and by fragmentation of the intermediate radical within (n_1^{PAR}), (n_1^{PAP}) and (n_1^{RAP}) type particles. Particles containing such polymeric radical are consumed by entry of any radical from the aqueous phase into this type of particles resulting in instantaneous termination, by transfer to monomer and by exchange with RAFT agent. Propagation within these kinds of particles does not change their identity:

$$\begin{aligned}\frac{\partial n_1^P(V,t)}{\partial t} &= \delta(V-V_o)\left[k_{p,aq}^{J_{crit}-1}C_w^M[P_{J_{crit}-1}^\bullet]+\sum_{i=1}^{J_{crit}-1}k_{e,micelle}^i C_{micelle}[P_n^\bullet]\right]\\ &+k_p^R C_p^M n_1^R - k_{add}C_P^{AR}n_1^P - k_{add}C_P^{AP}n_1^P + k_{-frag}^{PAR}\cdot n_1^{PAR} + k_{frag}^{RAP}\cdot n_1^{RAP}\\ &+k_{frag}^{PAP}\cdot n_1^{PAP} + k_{-frag}^{PAP}\cdot n_1^{PAP} - k_{tr}^M C_p^M n_1^P + \rho_i n_0 - \rho n_1^P - \frac{\partial(Kn_1^P)}{\partial V}\\ &+\left(\int_0^\infty B(V,V-V')\left[n_0(V')n_1^P(V-V')+n_1^P(V')n_0(V-V')\right]dV'\right.\\ &\left.-n_1^P(V)\int_0^\infty B(V,V')\left[n_0(V')+n_1^P(V')\right]dV'\right)\end{aligned} \quad \textbf{(4-25)}$$

2. Particles containing no free radicals (n_0) generated by entry of a radical into (n_1^R) and (n_1^P) type particles. They are also formed when monomeric and RAFT derived radicals exit an (n_1^R) type particle. The population of (n_0) decreases when oligomeric ($P_n^\bullet$) and small exited ($E^\bullet$) radicals enter an existing (n_0) type particle :

$$\frac{\partial n_0(V,t)}{\partial t} = \rho \cdot (n_1^P + n_1^{PAR} + n_1^{PAP} + n_1^{RAR} + n_1^{RAP} + n_1^R - n_0) + k_{dE} \cdot n_1^R + \int_0^\infty B(V, V - V')\left[n_0(V')n_0(V - V') + n_1^P(V')n_1^P(V - V')\right]dV' - n_1^P(V)\int_0^\infty B(V, V')\left[n_0(V';) + n_1^P(V')\right]dV' \quad \textbf{(4-26)}$$

3. Particles containing a monomeric or a RAFT-derived radical (n_1^R) generated by entry of a small radical (monomeric or RAFT derived radical) into (n_0) type particle, transfer reaction to RAFT agent or to monomer within (n_1^R) and (n_1^P) type particles and by the fragmentation of the intermediate radical in (n_1^{PAR}), (n_1^{RAR}) and (n_1^{RAP}) type particles. The population of (n_1^R) decreases by propagation, entry of any radical into such type of particle, exit, transfer to monomer, and by exchange with RAFT agent :

$$\frac{\partial n_1^R(V,t)}{\partial t} = k_{e,micelle}^R\, C_{micelle}\,[E] + k_{eE}[E]n_0 - \rho n_1^R - k_{dE}\, n_1^R - k_p^R C_p^M n_1^R - k_{add}\, C_P^{AR} n_1^R - k_{add}\, C_P^{AP} n_1^R + k_{-frag}^{RAP} \cdot n_1^{RAP} + k_{frag}^{PAR} \cdot n_1^{PAR} + k_{frag}^{RAR} \cdot n_1^{RAR} + k_{-frag}^{RAR} \cdot n_1^{RAR} + k_{tr}^M C_p^M n_1^P \quad \textbf{(4-27)}$$

4. Particles containing an intermediate radical (n_1^{PAR}), generated from the addition of a polymeric radical to the RAFT agent (AR):

$$\frac{\partial n_1^{PAR}(V,t)}{\partial t} = k_{add} C_p^{AR} n_1^P - (k_{frag} + k_{-frag}) n_1^{PAR} - \rho n_1^{PAR} \quad \textbf{(4-28)}$$

5. Particles containing an intermediate radical (n_1^{PAP}) generated from the addition of a polymeric radical to the polymeric RAFT agent (AP)

$$\frac{\partial n_1^{PAP}(V,t)}{\partial t} = k_{add} C_p^{AP} n_1^P - (k_{frag} + k_{-frag}) n_1^{PAP} - \rho n_1^{PAP} \quad \textbf{(4-29)}$$

6. Particles containing an intermediate radical (n_1^{RAR}) generated from the addition of a small radical to the RAFT agent (AR).

$$\frac{\partial n_1^{RAR}(V,t)}{\partial t} = k_{add} C_p^{AR} n_1^R - (k_{frag} + k_{-frag}) n_1^{RAR} - \rho n_1^{RAR} \quad \textbf{(4-30)}$$

7. Particles containing an intermediate radical generated from the addition of a small radical to the polymeric RAFT agent (AP) (n_1^{RAP}).

$$\frac{\partial n_1^{RAP}(V,t)}{\partial t} = k_{add} C_p^{AP} n_1^R - (k_{frag} + k_{-frag}) n_1^{RAP} - \rho n_1^{RAP} \quad \textbf{(4-31)}$$

The cross termination between an intermediate and propagating radical was experimentally confirmed (Monteiro and de Brouwer, 2001), and hence particles containing an intermediate radical are consumed by entry of an aqueous phase radical. These coupled partial integro-differential equations describe the evolution of latex particles in RAFT-emulsion polymerization as a function of particle volume and polymerization time, where K is the propagational growth rate for particle containing a single free radical and is given by: $k_p M_w^M C_p(V) / N_A d_p$, where $C_p(V)$ is the monomer concentration in the particle as a function of particle size. Growth significantly affects n_1^P type particles only, as radicals propagate without changing particle identity. The last two terms in equations (4-25) and (4-26) account for coagulation, and were neglected since the surfactant concentration used in the experiments is higher than the critical micellar concentration to ensure a negligible occurrence of coagulation.

Equation (4-25) accounts for particle formation by both micellar and homogenous mechanisms, through the terms involving $k_{e,micelle}^i C_{micelle}[P_n^\bullet]$ for micellar nucleation via radical entry into a micelle to form a precursor particle and $k_{p,aq}^{J_{crit}-1} C_w^M [P_{J_{crit}-1}^\bullet]$ for homogenous nucleation. The Dirac delta function $\delta(V - V_o)$ in the expression for n_1^p denotes that nucleation of particles occurs only at a minimum size. In estimating the particle size distribution, we accounted for the swollen and unswollen (absence of monomer) particle sizes. The swollen (r_s) and unswollen (r) radii are related by mass conversion (assuming ideal mixing of monomer and polymer) as follows:

$$\frac{r_s}{r} = \left[\frac{d_m}{d_m - C_p^M M_w^M} \right]^{1/3} \quad \textbf{(4-32)}$$

The total number of particles in the system is calculated from:

$$\begin{aligned} n(V,t) = n_0(V,t) + n_1^P(V,t) + n_1^R(V,t) + n_1^{PAR}(V,t) \\ + n_1^{PAP}(V,t) + n_1^{RAP}(V,t) + n_1^{PAP}(V,t) \end{aligned} \quad \textbf{(4-33)}$$

The total number of particles with an intermediate radical in the system is given by:

$$n_1^{Int}(V,t) = n_1^{PAR}(V,t) + n_1^{PAP}(V,t) + n_1^{RAR}(V,t) + n_1^{PAR}(V,t) \quad \textbf{(4-34)}$$

The average number of radicals per particle, $\bar{n}$, is given by:

$$\bar{n}(V,t) = \frac{n_1^P(V,t) + n_1^R(V,t)}{n(V,t)} \quad \textbf{(4-35)}$$

The average number of intermediate radicals per particle, $\overline{n_{Int}}$, by:

$$\overline{n_{Int}}(V,t) = \frac{n_1^{Int}(V,t)}{n(V,t)} \quad \textbf{(4-36)}$$

The above set of coupled-partial deferential equations describes the volume-based distribution for the latex particles in RAFT-mediated emulsion polymerization. It is often convenient to represent the distribution by one or more parameters. Such parameters can include the number average radius, defined as:

$$< r >= \frac{\sum_{i=1}^{G} n(i) r(i)}{\sum_{i=1}^{G} n(i)} \quad \textbf{(4-37)}$$

This parameter gives an indication of the location of the distribution. The polydispersity index PSPI indicates the spread of the distribution and is estimated as the ratio of the mean squared radius to the mean radius squared

$$PSPI = < r^2 > / < r >^2 \quad \textbf{(4-38)}$$

where the mean squared radius is given by:

$$< r^2 >= \frac{\sum_{i=1}^{G} n(i) r(i)^2}{\sum_{i=1}^{G} n(i)} \quad \textbf{(4-39)}$$

If all particles are identical, the mean squared radius and the mean radius squared will be equal. This corresponds to a polydispersity index of 1, and the distribution is said to be monodispersed. As the distribution widens, the larger particles will more heavily influence the numerator (due to the r^2 term), and hence the index will increase.

4.5.5 Concentrations of monomer and RAFT agent

During intervals I and II of batch emulsion polymerization, monomer is partitioned over monomer droplets, aqueous phase and polymer particle. In the polymer particles, the polymerized monomer is replenished by monomer that is transferred through the aqueous phase, from monomer droplets, into the particle phase. In interval III there are no monomer droplets and almost all of the remaining monomer is located in the polymer particles. In semi-batch emulsion polymerization, monomer is fed into the reactor in which only the newly fed monomer droplets are present in the aqueous phase. Due to the continuous transfer of monomer into the particles, the life time of these droplets is short (Van Herk, 2005). Under most circumstances, the rate of mass transfer of monomer between the different phases of the system is sufficient for thermodynamic equilibrium of monomer between phases to be achieved (Gilbert, 1995).

Experimental results have shown that, for styrene emulsion polymerization, the monomer mass transfer is high enough to bring about a rapid thermodynamic equilibrium (Mendoza *et al.*, 2000). Thus, for monomer with low solubility in water, under thermodynamic equilibrium, the model with constant partitioning coefficients (equilibrium equations) in combination with the overall mass balances and

polymerization rate can be used to calculate monomer concentration (Altarawneh *et al.*, 2008; Gugliotta *et al.*, 1995; Mendoza *et al.*, 2000; Salazar *et al.*, 1998; Zeaiter *et al.*, 2002). Experimental data (from this work, i.e. Chapters 5 and 6) show that for this system, RAFT agent mass transfer is not subjected to diffusional limitation, similar conclusion was reported in the literature (Smulders *et al.*, 2003) in which the consumption rate of RAFT agent was found to be lower than its transportation rate from the droplets through the aqueous phase to the particles. Hence the mass transfer of the RAFT agent is not the rate determining step, and any consumed amount of RAFT agent in the particle is readily replenished. Three phases coexist in emulsion polymerization, these are: water (w), monomer droplets (d) and polymer particles (p). The monomer and AR partition coefficients were calculated from saturation data of the monomer and RAFT in water and in the polymer particle. Saturation data for both monomer and RAFT agent used in this work are available in literature (Gilbert, 1995; Smulders *et al.*, 2003; Zeaiter *et al.*, 2002). The partitioning coefficients (Γ) of the monomer and RAFT agent between these phases at equilibrium are given as follows:

$$\Gamma^i_{wp} = C^i_{w,sat} / C^i_{p,sat} \quad \textbf{(4-40a)}$$

$$\Gamma^i_{dp} = d_i \Gamma^i_{wp} / M^i_w C^i_{w\_sat} \quad \textbf{(4-40b)}$$

$$\Gamma^i_{dw} = \Gamma^i_{dp} / \Gamma^i_{wp} \quad \textbf{(4-40c)}$$

The volumes of droplet (V_d), water (V_w) and particle (V_p) phases are given as follows:

$$V_d = \frac{(N_m M^M_w + N_{AR} M^{AR}_w - C^M_w M^M_w V_w - C^{AR}_w M^{AR}_w V_w - C^M_p M^M_w V_p - C^{AR}_p M^{AR}_w V_p)}{d_m} \quad \textbf{(4-41)}$$

$$V_w = \frac{V_{wo}}{1 - ((M^M_w C^M_w / d_m) + (M^{AR}_w C^{AR}_w / d_{AR}))} \quad \textbf{(4-42)}$$

$$\frac{dV_p}{dt} = \frac{M^M_w R^M_p V_r}{d_p} \quad \textbf{(4-43)}$$

The total reaction volume (V_r) is described by:

$$\frac{dV_r}{dt} = M_w^M R_p^M V_r (\frac{1}{d_p} - \frac{1}{d_m}) + M_w^{AR} R_p^{AR} V_r (\frac{1}{d_p} - \frac{1}{d_{AR}}) + \frac{F_m M_w^M}{d_m} + \frac{F_{AR} M_w^{AR}}{d_{AR}} \quad \textbf{(4-44)}$$

where F_m and F_{AR} are the monomer and RAFT agent flow rates, respectively. The polymerization rate (R_p^M) and the consumption rate of the RAFT agent (R_p^{AR}) are given as follows:

$$R_p^M = k_p C_p^M C_p^{Rad} \quad \textbf{(4-45)}$$

$$R_p^{AR} = k_{add} C_p^{AR} C_p^{Rad} - k_{-frag}^{PAR} C_p^{PAR} - k_{frag}^{RAP} C_p^{RAP} - (k_{frag}^{RAR} + k_{-frag}^{RAR}) C_p^{RAR} \quad \textbf{(4-46)}$$

In these equations, C_p^{Rad} is the concentration of all radicals inside the particle and is given by:

$$C_p^{Rad} = \bar{n}(N_{tot} / N_A)(V_w / V_r) \quad \textbf{(4-47)}$$

where C_p^{RAR}, C_p^{RAP} and C_p^{PAR} are the concentrations of the intermediate radicals RAR, RAP and PAR in the particle, respectively. Inside the particle, each addition of a propagating radical to the RAFT agent (AR) results in a new radical and polymeric RAFT agent (AP). Hence the production rate of the polymeric RAFT agent (AP) is equal to the consumption rate of the RAFT agent (AR). Mass balances for the monomer and the RAFT agent in three phases are given by:

$$\frac{dN_m}{dt} = F_m - R_p^M V_r \quad \textbf{(4-48)}$$

$$\frac{dN_{AR}}{dt} = F_{AR} - R_p^{AR} V_r \quad \textbf{(4-49)}$$

$$\frac{dN_{AP}}{dt} = R_p^{AR} V_r \quad \textbf{(4-50)}$$

In the absence of monomer droplets, the concentrations of monomer and RAFT agents in the particles and aqueous phases are given by:

$$C_p^M = \left(\frac{N_m}{V_p + \Gamma_{wp}^M V_w + \Gamma_{dp}^M V_d} \right), \quad V_d = 0 \tag{4-51a}$$

$$C_w^M = C_p^M \Gamma_{wp}^M, \quad V_d = 0 \tag{4-51b}$$

$$C_p^{AR} = \left(\frac{N_{AR}}{V_p + \Gamma_{wp}^{AR} V_w + \Gamma_{dp}^{AR} V_d} \right), \quad V_d = 0 \tag{4-52a}$$

$$C_w^{AR} = C_p^{AR} \Gamma_{wp}^{AR}, \quad V_d = 0 \tag{4-52b}$$

$$C_p^{AP} = \left(\frac{N_{AP}}{V_p} \right) \tag{4-53}$$

Equation (4-53) accounts for the concentration of the dormant polymeric chains in the particle (C_p^{AP}), where (N_{Ap}) is the moles of the dormant polymeric RAFT agent and equal to the reacted number of moles of the initial AR.

In the presence of monomer droplets and under the equilibrium conditions there will be continuous replenishment of the reacted monomer and RAFT agent, hence the concentrations of monomer and RAFT agent in the aqueous and particles phases are approximated by the following equations:

$$C_p^M = C_{p,sat}^M, C_w^M = C_{w,sat}^M, \quad V_d > 0 \tag{4-54}$$

$$C_p^{AR} = \gamma_o C_{p,sat}^M, C_w^{AR} = \gamma_o C_{w,sat}^M, \quad V_d > 0 \tag{4-55}$$

Monomer and AR conversions are calculated as:

$$x_{mon} = 1 - \frac{N_m}{N_{m,total}} \tag{4-56}$$

$$x_{AR} = 1 - \frac{N_{AR}}{N_{AR,total}} \tag{4-57}$$

where $N_{m,total}$, $N_{AR,total}$ are the total amount of monomer and RAFT agent fed into the reactor, respectively, and are given by:

$$\frac{dN_{m,total}}{dt} = F_m \,, \quad N_{m,total}(t=0) = N_{mo} \tag{4.-58}$$

$$\frac{dN_{AR,total}}{dt} = F_{AR} \,, \quad N_{AR,total}(t=0) = N_{ARo} \tag{4-59}$$

4.5.6 Molecular weight distribution

The evolution of the molecular weight distribution (MWD) contains the record of the kinetic events that control polymer formation during the polymerization. The number molecular weight distribution is the number of non growing (dead) chains with a given molecular weight. The population of dead chains is controlled by the number of living chains, the rate at which chains grow, and by the kinetic events that stop the growth of the living chains. These evens are: entry, re-entry, exit and transfer reactions facilitated by the transfer agent. The instantaneous number MWD is defined as $P(M)$, such that $P(M)dM$ is the number of polymer chains with molecular weight in the range of M to $M + dM$ and the cumulative one is denoted by $\overline{P}(M)$. The instantaneous MWD can be calculated over the range of conversion using (Clay and G., 1995):

$$\frac{\partial \overline{P}(M)}{\partial t} = P(M) = \bar{n}(k_{tr}^{M} C_p^{M} + \rho_{avg} + k_{tr}^{AR} C_p^{AR}) \exp\left(- \frac{(k_{tr}^{M} C_p^{M} + \rho_{avg} + k_{tr}^{AR} C_p^{AR})}{k_p C_p^{M}} \frac{M}{M_w^{M}} \right) \tag{4-60}$$

The number and weight average molecular weights are given by the first and the second moments of the distribution:

$$Mn = \frac{\sum M \cdot P(M)}{\sum P(M)} \approx \left[\frac{k_p C_p^{M}}{k_{tr}^{AR} C_p^{AR} + k_{tr}^{M} C_p^{M} + \rho_{avg}} \right] \tag{4-61}$$

$$Mw = \frac{\sum M^2 \cdot P(M)}{\sum P(M)} \tag{4-62}$$

The molecular weight polydispersity index is the ratio of the weight average to the number average molecular weights and is given by:

$$PDI = Mw / Mn \tag{4-63}$$

As postulated by Monteiro *et al*. (2001), a low active RAFT agent with a transfer constant close to one reacts about once during polymerization, and acts as a conventional chain transfer agent. Thus, the approximation of equation (4-61) is valid for emulsion polymerization with a low active RAFT agent and follows zero-one kinetics. Additionally, the Muller equations (Mueller *et al.*, 1995), obtained via the method of moments, can be used to predict the number average molecular weight (Mn) and weight average molecular weight (Mw) of the polymer produced by RAFT process in bulk and solution polymerizations. Assuming negligible bimolecular termination, Mn and Mw are given by:

$$Mn = \frac{\gamma_o \cdot x_{mon}}{(1-(1-\alpha)(1-x_{mon})^{C_{tr}}) + +2f(I_o - I)} M_w^M \qquad \textbf{(4-64)}$$

where γ_o is the initial ratio of monomer to RAFT agent concentration. The molecular weight polydispersity index is given by:

$$\frac{Mw}{Mn} = \frac{1}{\gamma_o x_{mon}} + \frac{1}{x_{mon}}\left[2 + \frac{C_{tr}-1}{\alpha - C_{tr}}(2 - x_{mon})\right] - \frac{2\alpha(1-\alpha)}{({C_{tr}}^2 - \alpha^2)x_{mon}^2}\left[1-(1-x_{mon})^{1+C_{tr}/\alpha}\right] \qquad \textbf{(4-65)}$$

The assumption used in these expressions is that the ratio of the growing radicals to the RAFT agent (α) is negligible. Monteiro *et al*. (2001), pointed out that equation (4-64) is valid for the three intervals if the transportation rate of the low active RAFT agent from droplets to the particles is equal to or higher than its consumption rate. Else, these equations can not be used to approximate the evolution of the Mn, Mw and PDI over the polymerization time, or conversion range for emulsion polymerization.

4.5.7 Kinetic parameters

4.5.7.1 Entry and exit rate coefficients

The entry of a radical derived directly from an initiator is assumed to occur only for radicals of degree of polymerization ‘ z ’ or greater, while entry and re-entry of R^* and an exited radical does not require a similar degree of polymerization (Smulders, 2002).

The entry process of z-mer to the particle and to the micelle, and hence their rate coefficients 'k_e^i' and '$k_{e,micelle}^i$', are considered to be diffusion-controlled (Altarawneh *et al.*, 2008; Coen *et al.*, 1998; Gilbert, 1995; Thickett and Gilbert, 2006; Zeaiter *et al.*, 2002). An exponent of ½ characterizes the chain length-dependent diffusion coefficient of the entered radical. The entry coefficients for the $z-mer$ and R^* are calculated using the Smoluchowski diffusion expression as follows:

- Rate coefficient of z-mer entry into particle and micelle:

$$\left.\begin{aligned} k_e^i(V) &= 0.0 \\ k_{e,micelle}^i(V) &= 0.0 \end{aligned}\right\} for \quad i < z \qquad \textbf{(4-66)}$$

$$\left.\begin{aligned} k_e^i(V) &= 4\pi\varepsilon r_s N_A \frac{D_w}{i^{1/2}} \\ k_{e,micelle}^i(V) &= 4\pi r_{micelle} N_A \frac{D_w}{i^{1/2}} \end{aligned}\right\} for \quad i \geq z$$

- Rate coefficient of R-radical entry into particle and micelle:

$$\begin{aligned} k_e^R(V) &= 4\pi r_s N_A D_R \\ k_{e,micelle}^R(V) &= 4\pi r_{micelle} \end{aligned} \qquad \textbf{(4-67)}$$

where D_R is the diffusion rate coefficient of the $R^\bullet$ radical in the water phase; D_w is the diffusion rate coefficient for a monomeric radical in the water phase; $r_{micelle}$, r_s are the radii of micelles and latex particles swollen with the monomer, respectively. In this work it is assumed that the diffusion rate of the RAFT radical in the water phase is close to that for the monomeric radical. As the RAFT-derived radical is surface active and not extremely water-soluble, it is assumed that the exited radicals re-enter without propagating, i.e., their degree of polymerization is one (Casey *et al.*, 1994). The re-entry rate coefficient for exited small radical (E^*) is defined in a similar manner as follows:

$$k_e^M(V) = k_e^R(V) = k_e^E(V) = 4\pi r_s N_A D_w \qquad \textbf{(4-68)}$$

The rate coefficient for desorption of small radicals (E^*) is a function of radical diffusion both in water and inside the particle, the aqueous and particle concentrations

of the desorbed radical and the particle volume. For monomeric radicals this is given as follows (Maxwell *et al.*, 1991; Nomura *et al.*, 1982; Ugelstad and Hansen, 1976):

$$k_{dE}(V) = \frac{3D_w D_{mon}}{(qD_{mon} + D_w)r_s^2} \quad \textbf{(4-69)}$$

where q is the partitioning coefficient of the exited monomeric species and equal to C_P/C_w; D_{mon} is the diffusion rate coefficient for the monomer inside the particle, and is given by the following experimentally determined expressions (Zeaiter *et al.*, 2002):

$$\begin{aligned} D_{mon} &= 10^{\,0.417\,\Phi - 29.51\,\Phi + 53.14\,\Phi^2 - 36.03\,\Phi^3}, \qquad \Phi < 0.8 \\ D_{mon} &= 9 * 10^{-8} \exp(-19.16\,\Phi), \qquad \Phi \geq 0.8 \end{aligned} \quad \textbf{(4-70)}$$

where Φ is the polymer volume fraction inside the particle and is estimated as a function of time from the monomer concentration inside the particle:

$$\Phi = 1 - (C_p^M M_o / d_m) \quad \textbf{(4-71)}$$

At high Φ the particle becomes glassy, resulting in a reduced entry rate of z-mer into such a particle. To account for this change in the particle state an empirical equation for the entry efficiency, $\varepsilon = (1-\Phi)^{C_{p,sat}^M}$, was used (Zeaiter *et al.*, 2002).

4.5.7.2 Propagation and termination rate coefficients

The most accurate propagation rate coefficient values at different reaction temperatures were obtained from a single pulsed laser polymerization technique in conjunction with ESR and MWD data (Buback *et al*., 1995). This technique has been recently recognized as the most accurate one by IUPAC. The technique involves the exposure of a system containing monomer and photo-initiator to laser pulses, each of which generates a burst of short radicals which then proceeds to initiate polymerization. Some (but by no means all) chains photo-initiated by one laser pulse are terminated "instantly" by short radicals formed from the subsequent one. If one can identify '$\overline{DP}$' the average degree of polymerization of the chains so terminated at low conversion, the value of k_{po} can then

be found from a knowledge of the monomer concentration $[M]$, and the time between pulses t_p:

$$\overline{DP} = k_p[M]t_p \quad \textbf{(4-72)}$$

Monomer concentration can be measured from the monomer conversion data or by GC technique and $\overline{DP}$ can be obtained from MWD data. Using this technique, Gilbert and Buback (1995) measured the propagation rate coefficient of styrene as a function of reaction temperature and is best fitted by:

$$k_{po} = 10^{7.63} \exp(-32500 / RT) \quad \textbf{(4-73)}$$

At high monomer conversions, the viscosity inside the particle increases sharply and propagation and termination rates become diffusion controlled. At this stage, the zero-one kinetics no longer holds. To account for these dramatic changes, the propagation rate coefficient can be expressed as follows (Gilbert, 1995; Zeaiter *et al.*, 2002):

$$k_p = 1/(1/k_{po} + 1/k_{diff}) \quad \textbf{(4-74)}$$

where k_{po} is the propagation rate coefficient at low conversions, while k_{diff} is the diffusion controlled rate coefficient and is given by:

$$k_{diff} = 4\pi\sigma N_A(D_{mon} + D_{rd}) \quad \textbf{(4-75)}$$

$$D_{rd} = k_p C_p \alpha^2 / 6 \quad \textbf{(4-76)}$$

Similarly, and by using ESR to measure radical concentration the termination rate coefficient was measured for the same system, and is best fitted by:

$$k_{t,aq} = k_{to} = 1.703 \times 10^9 \exp(-23400 / RT) \quad \textbf{(4-77)}$$

Small radicals inside the particle moves faster than the polymeric chain, and hence the propagation rate coefficient of these radicals is higher than that for the polymeric chains. To account for the effect of radical mobility inside the particle the propagation rate of a small radical is taken to be four times higher than that for a polymeric radical (Gilbert, 1995).

4.5.7.3 Transfer rate coefficient

The overall transfer rate coefficient (k_{tr}^{AR}) can be represented as a composite of the addition-fragmentation rate coefficients. From the pre or core-equilibrium reactions (Scheme 4-2), the backward (k_{-tr}^{AR}) and forward (k_{tr}^{AR}) transfer rate coefficients can be calculated and as:

$$k_{tr}^{AR} = k_{add} \frac{k_{frag}}{k_{frag} + k_{-frag}} \quad \textbf{(4-78a)}$$

$$k_{-tr}^{AR} = k_{-add} \frac{k_{-frag}}{k_{frag} + k_{-frag}} \quad \textbf{(4-78b)}$$

The transfer constant is defined as the ratio of the transfer rate coefficient (k_{tr}^{AR}) and the propagation rate coefficient (k_p):

$$C_{tr} = \frac{k_{tr}^{AR}}{k_p} \quad \textbf{(4-79)}$$

The transfer rate coefficient of a growing radical to RAFT agent was also experimentally determined by using the Mayo method (Adamy *et al.*, 2003; Smulders, 2002). This method is, so far, the most common and accepted technique for determining the transfer constant. The method is based on performing a series of experiments at low conversions, in which the RAFT agent to monomer ratio is varied, and the relation between these variables is given in the Mayo equation:

$$\frac{1}{\overline{DP}} = C_{tr}^{M} + C_{tr} \frac{[AR]}{[M]} \quad \textbf{(4-80)}$$

where C_{tr}^{M}, is the transfer constant to monomer. At low conversion the amount of the consumed monomer is negligible and hence transfer to monomer can be neglected from equation (4-80), $(1/\overline{DP})$ can be plotted versus $([AR]/[M])$ and the slope of this plot is equal to C_{tr}. Using this method the transfer constant to RAFT agent as a function of temperature is given by:

$$C_{tr} = k_{tr}^{AR} / k_p = 1.414 \exp(-1870/RT) \quad \textbf{(4-81)}$$

O-ethylxanthyl ethyl propionate was used as a RAFT agent in this work. This RAFT agent has a transfer rate constant equal to 0.7 (Adamy *et al.*, 2003; Smulders *et al.*, 2003). In the pre-equilibrium stage, larger chains are most likely to be released resulting in shifting the equilibrium toward the starting materials. To accommodate this event in the model, the backward fragmentation rate coefficient of the intermediate radical of type PAR is assumed to be higher than the forward fragmentation rate coefficient and its optimal value was determined from the experimental data obtained in this work. In addition, as the concentration of small radicals generated from the fragmentation of the intermediate radical is relatively negligible, the backward addition is assumed to be insignificant.

4.5.8 Numerical solution methods

To convert the evolution equations (Eq.4-25 to Eq.4-31) into a set of coupled ordinary differential equations for each particle size, the population balance equations (PBEs) were discretised with respect to radius, r(i). Computationally, discretising the population balance equations (PBEs) by radius is efficient, since the particle radius increases much more slowly than the particle volume. A number of discrete groups of particles, G, was used in the model, in which each group has a constant radius and one ordinary differential equation describes the particle population in that group. Discretization allows for the integro-differential components of the equations to be expressed as finite differences approximation in equally spaced radius increments (Δr). In the dynamic model, the Dirac delta function $\delta(V - V_o)$, used to describe the process of particle formation, becomes $1/\Delta r$ (Gilbert, 1995). The differential growth term can be approximated by one of the finite difference methods, these are:

1- centered finite difference:

$$\frac{\partial(Kn_1^P)}{\partial V} = \frac{-K}{8\pi\Delta r}\left(\frac{n_1^P(r_{i+1})}{r_{i+1}^2} - \frac{n_1^P(r_{i-1})}{r_{i-1}^2}\right) \quad \textbf{(4-82)}$$

2- forward finite difference:

$$\frac{\partial(Kn_1^P)}{\partial V} = \frac{-K}{4\pi\Delta r}\left(\frac{n_1^P(r_{i+1})}{r_{i+1}^2} - \frac{n_1^P(r_i)}{r_i^2}\right) \quad \textbf{(4-83)}$$

3- backward finite difference:

$$\frac{\partial(Kn_1^P)}{\partial V} = \frac{-K}{4\pi\Delta r}\left(\frac{n_1^P(r_i)}{r_i^2} - \frac{n_1^P(r_{i-1})}{r_{i-1}^2}\right) \quad \textbf{(4-84)}$$

When using the centered finite difference method, Zeaiter (2002) noticed an oscillatory response of the total particle number. Notice that the forward approximation relies on populations *'i'* and *'i+1'* and the backward relies on populations *'i-1'* and *'i'*. The '4', in the forward and backward approximations replace the '8' in the denominator of the centered difference approximation as the interval has been halved in size. It was found that the forward finite difference approximation produced an unstable particle number. The backward approximation, on the other hand, eliminated the oscillation and predicted a more stable PSD. Consequently, the backward finite difference approximation was adopted for the discretisation of the PBEs in this work.

4.6 Model simulation results

Some of the simulation results from the model developed throughout this Chapter are shown in this section. It is important to note that the model is solely based on the real kinetics of the system. This means that all the results obtained by the simulation should reasonably explain the reality of the process. This will be clearly seen from the results showing the true evidence of the agreement with the kinetics.

The key polymer properties are validated against the experimental results in the next Chapter. This section is devoted to show the results obtained by the model are obeying the kinetics. The Simulation conditions are given in Table 4-1. Figure 4-2 illustrates the effect of the RAFT agent concentration on the monomer conversion (Fig. 4-2a), polymerization rate (Fig. 4-2b) and monomer concentration in the particle phase (Fig. 4-2c), respectively.

Table 4-1: Recipe used to simulate emulsion polymerization with RAFT agent

	Water (g)	Initiator (KPS in g)	Surfactant (SDS)	Monomer (M in g)	RAFT (AR in g)	Mo/ARo
Sim 1	520	0.2	2.5 cmc	80	0.0	-
Sim 2	520	0.2	2.5 cmc	80	1.7	200
Sim 3	520	0.2	2.5 cmc	80	1.7	100
Sim 4	520	0.2	2.5 cmc	80	6.8	25
Sim 5	520	0.2	2.0 cmc	80	1.7	100
Sim 6	520	0.2	1.5 cmc	80	1.7	100

Increasing the RAFT agent concentration results in low monomer conversion and polymerization rate as compared with the simulation without the RAFT agent. The point at which the polymerization rate and the monomer concentration start to drop characterizes the end of interval II. This point corresponds to the first inflection point in the conversion time profile. After this point the monomer concentration in the particle decreases as the monomer droplets in the aqueous phase are no longer present. It is quite clear that in the presence of RAFT agent the lifetime of interval II is longer. That is the higher the concentration of the RAFT agent the longer the lifetime of interval II. In general, the presence of the RAFT agent results in slowing down the polymerization rate. This phenomenon is known as rate retardation and is an inherent characteristic of RAFT polymerization.

As discussed in chapter 3, intermediate radical termination and slow fragmentation of the intermediate radical were used to explain the retarded polymerization rate in RAFT solution and bulk polymerizations. With the intermediate radical termination being the most likely reason behind the observed retardation, slow fragmentation was excluded, as experimental data suggest fast fragmentation of the intermediate radical. However, the intermediate radical termination mechanism, used to explain the observed retardation in RAFT solution and/or bulk polymerizations, is not significant in the compartmentalized RAFT emulsion polymerization that obeys zero-one kinetics since each particle contains only one radical.

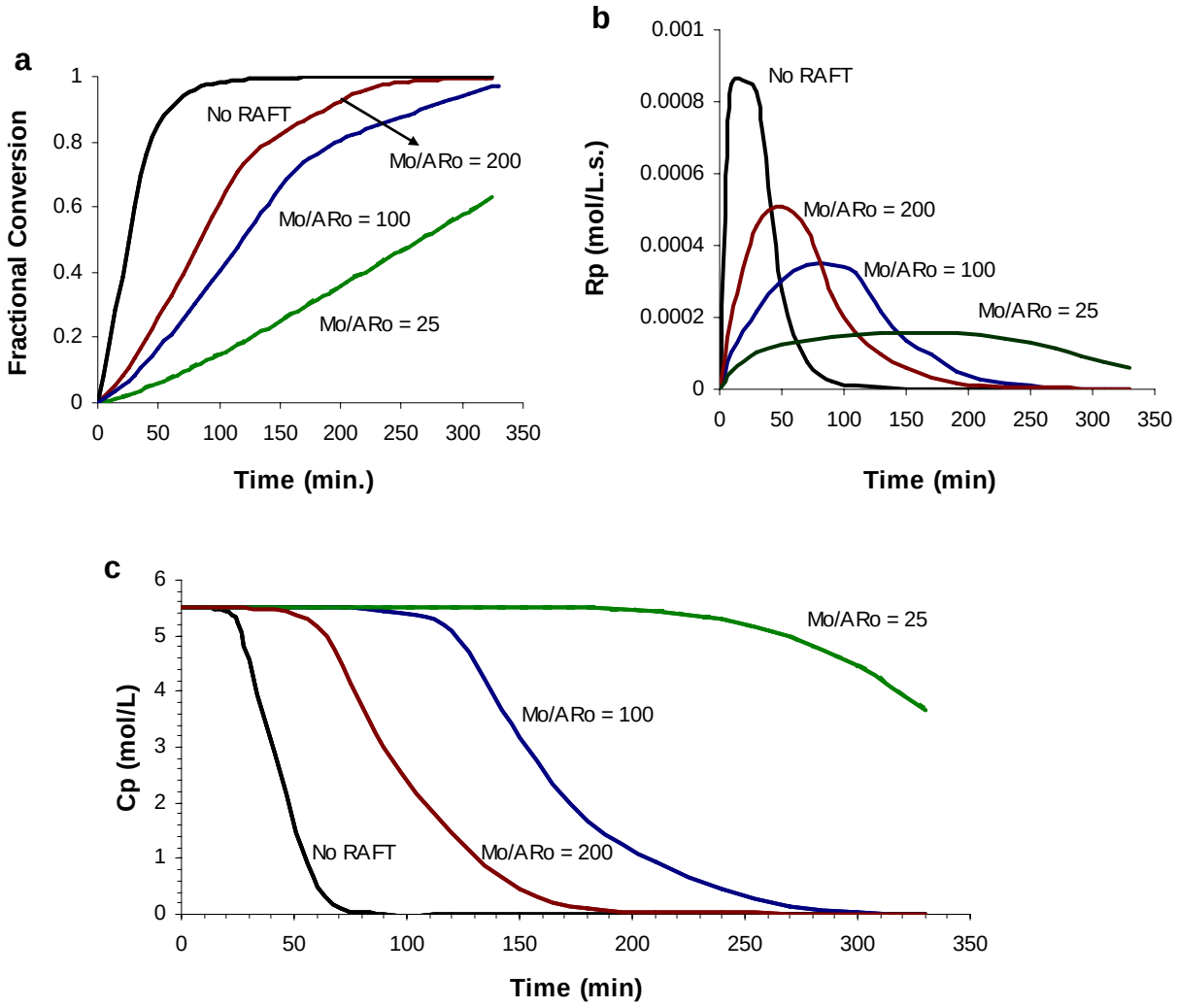

Figure 4-2: Model simulations: (a) Monomer conversion; (b) Polymerization rate; (c) Monomer concentration in the particle phase.

The RAFT agent used in this work has an experimentally measured addition rate coefficient of about 10^3 L/mol.s (Adamy *et al.*, 2003). In RAFT emulsion polymerization, each particle contains only one radical. This one radical is either present as a normal radical capable of propagating, and hence consume monomer, or as an intermediate radical. The intermediate radical does not consume monomer which may lead to a reduction in the polymerization rate, if the lifetime of such a radical is quite longer. No retardation was observed when a low active RAFT agent, similar to the one used in this work, was used in solution and bulk polymerizations (Adamy *et al.*, 2003) indicating fast fragmentation of the intermediate radical with a fragmentation rate coefficient of about 10^4 s^{-1}. The lifetimes of the propagating and intermediate radicals in

the particle are given by: $\tau_p = 1/(k_{add} C_p^{AR})$ and $\tau_{Int} = 1/(2k_{frag})$, where τ_p, τ_{Int} are the lifetime of the normal propagating and intermediate radicals, respectively.

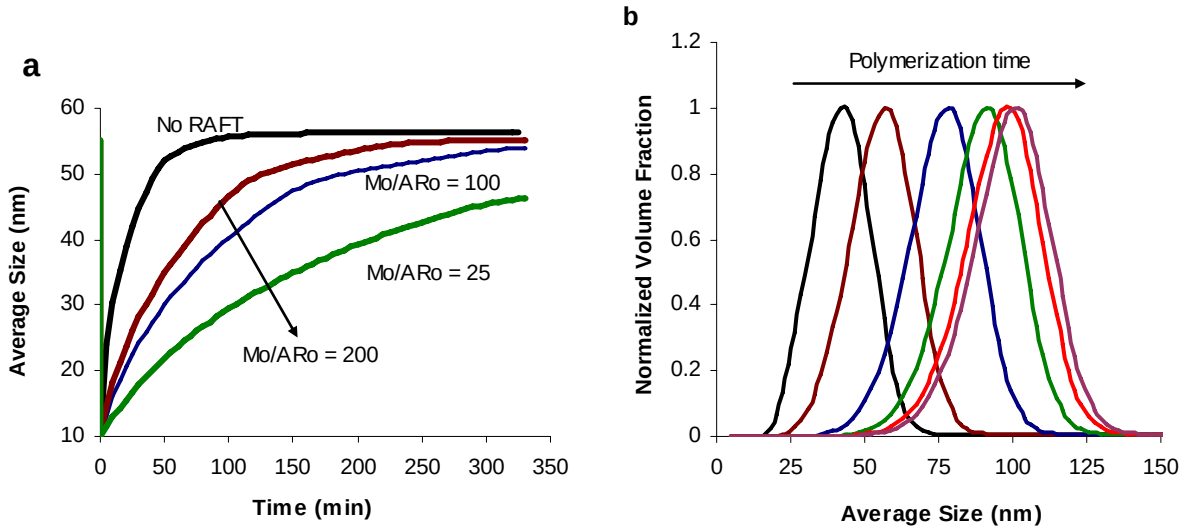

Figure 4-3: Model simulations: (a) Average size; (b) particle size distribution.

Typical calculations using the above mentioned addition and fragmentation rate coefficients and dormant chains concentration suggest a lifetime of the propagating radical of 1.97×10^{-2} s, and a lifetime of 1×10^{-4} s^{-1} for an intermediate radical. This means that the fraction of time that a radical is present as a propagating radical in this system is 99%, indicating that the intermediate radical has almost no contribution to the predicted retardation. The low active RAFT agent used in this work has a transfer constant of about 0.7. Thus the used RAFT agent reacts slowly throughout the polymerization reaction. This means that there will be a continuous production of a RAFT-derived small radical that is capable of exiting from the particle and hence reducing the polymerization rate.

In Figure 4-3, the adherent to zero-one kinetics is clearly observed. As can be seen in Figure 4-3a, the average radius of the particle size is 40-55 nm, which means an instantaneous termination takes place, when a radical meets another radical. The predicted decrease in the particle size in the presence of a RAFT agent is due to the retardation in the polymerization rate. However, at longer polymerization times the polymerization rate in the presence of a low concentration of the RAFT agent (Mo/ARo = 200) recovers, resulting in monomer conversion approaching that for the

polymerization without the RAFT agent (Fig. 4-2a) and the average particle size as well (Fig.4-3a). In Figure 4-3b, it can be seen that the distribution is shifted to the right, giving a higher average of particle size, as polymerization proceeds and more monomer is consumed. The distributions get close to each other at longer polymerization times as the amount of the remaining monomer decreases. It should be noted that the area under the distribution is almost constant, reflecting the constant number of particles that were formed.

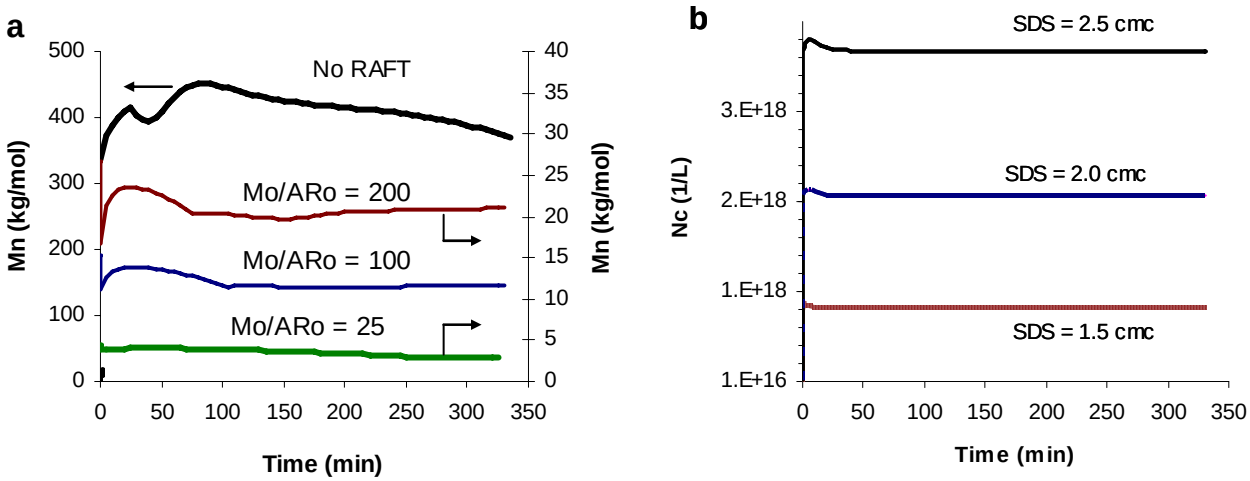

Figure 4-4: Model simulations: (a) Number average molecular weight at different RAFT agent amounts; (b) Particles number at different surfactant amounts.

Figure 4-4a shows the time evolution of the number average molecular weight (Mn) for a range of monomer to RAFT ratios. It is quite clear that Mn decreased with increasing the concentration of RAFT agent and is proportional to the initial molar ratio of monomer to RAFT. This ratio determines the maximum theoretical Mn at full conversion. As the RAFT agent used in this work has a low transfer constant, the number average molecular weight increases instantly to a certain value at the very beginning of the reaction and remains almost constant throughout the polymerization reaction.

Comparing Mn in the presence of RAFT agent with that without RAFT agent, it may be concluded that Mn decreases by almost two orders of magnitude. A further decrease in Mn is predicted when the concentration of RAFT agent is further increased. This indicates that the use of RAFT agent results in a controlled molecular weight. It is

observed from Figure 4-4b, that the number of particles increases very rapidly on the initiation of the reaction. The number of particles produced then tends to come to a constant value, unless new particles are formed due to a secondary nucleation that could be due to micellar nucleation or homogeneous nucleation. It is also predicted that the total number of particle strongly depends on the concentration of surfactant, in which it decreased by two orders of magnitude when the emulsifier concentration decreased from 2.5 cmc (1.3g) to 1.5 cmc (0.8g) where cmc is equal to 0.003M.

4.7 Conclusions

Particle size (PSD) and molecular weight (MWD) distributions represent the complete kinetic history of a polymerization process and constitute a unique tool for analyzing RAFT emulsion polymerization systems. In addition these two characteristics determine the product properties and hence product quality.

In this chapter the fundamental kinetics were used to predict the MWD and PSD of the produced polymer in RAFT emulsion polymerization. A detailed mechanistic dynamic model was developed for a RAFT-styrene emulsion polymerization reactor to predict theoretically the evolution of the product MWD and PSD. A system with zero-one kinetics was employed for RAFT-emulsion polymerization. The model describes the numerous elementary chemical and physical mechanisms which operate simultaneously in both the organic particle phase and the aqueous continuous phase. The reactor mass balances, which comprise differential equations, were developed to describe the system transients for batch operation. Furthermore, the model comprises a set of rigorously developed population balance equations that accounts for the effect of the repeatedly occurring addition fragmentation reactions.

The complex model equations comprising sets of integro-partial differential and nonlinear algebraic equations were solved using an efficient finite difference scheme using strong computer simulation software with high efficient capabilities to be used for real time application. The model was simulated and numerically solved in gPROMS package. The simulation results were demonstrated to reflect the applicability of the

mathematical model developed. In the next Chapter, the model will be validated against the experimental results under different operating conditions.

4.8 References

Adamy, M.; Van Herk, A.M.; Destarac, M. and Monteiro, M.J., 2003. Influence of the chemical structure of MADIX agents on the RAFT polymerization of styrene. *Macromolecules*, 36(7): 2293.

Altarawneh, I.S.; Gomes, V.G. and Srour, M.S., 2008. The Influence of Xanthate-Based Transfer Agents on Styrene Emulsion Polymerization: Mathematical Modeling and Model Validation. *Macromolecular Reaction Engineering*, 2(1): 58.

Altarawneh, I.S.; Srour, M. and Gomes, V.G., 2007. RAFT with Bulk and Solution Polymerization: An Approach to Mathematical Modelling and Validation. *Polymer-Plastics Technology and Engineering*, 46(11): 1103

Barner-Kowollik, C.; Quinn, J.F.; Morsley, D.R. and Davis, T.P., 2001. Modeling the reversible addition-fragmentation chain transfer process in cumyl dithiobenzoate-mediated styrene homopolymerizations: Assessing rate coefficients for the addition-fragmentation equilibrium. *Journal of Polymer Science, Part A: Polymer Chemistry*, 39(9): 1353.

Buback, M.; Gilbert, R.G.; Hutchinson, R.A.; Klumperman, B.; Kuchta, F.D.; Manders, B.G.; O'Driscoll, K.F.; Russell, G.T. and Schweer, J., 1995. Critically evaluated rate coefficients for free-radical polymerization, 1. Propagation rate coefficient for styrene. *Macromolecular Chemistry and Physics*, 196(10): 3267.

Butté, A., 2000. Living free radical polymerization in miniemulsion Thesis (Ph. D.) Thesis, Zurich, 2000.

Butte, A.; Storti, G. and Morbidelli, M., 2001. Miniemulsion living free radical polymerization by RAFT. *Macromolecules*, 34(17): 5885.

Casey, B.S.; Morrison, B.R.; Maxwell, I.A.; Gilbert, R.G. and Napper, D.H., 1994. Free radical exit in emulsion polymerization. I. Theoretical model. *J. Polym. Sci., Part A: Polym. Chem.*, 32(4): 605.

Charmot, D.; Corpart, P.; Adam, H.; Zard, S.Z.; Biadatti, T. and Bouhadir, G., 2000. Controlled radical polymerization in dispersed media. *Macromolecular Symposia*, 150(Polymers in Dispersed Media): 23.

Chiefari, J.; Chong, Y.K.; Ercole, F.; Krstina, J.; Jeffery, J.; Le, T.P.T.; Mayadunne, R.; Meijs, G.F.; Moad, C.L.; Moad, G.; Rizzardo, E. and Thang, S.H., 1998. Living Free-Radical Polymerization by Reversible Addition-Fragmentation Chain Transfer: The RAFT Process. *Macromolecules*, 31(16): 5559.

Clay, P.A. and G., G.R., 1995. Molecular Weight Distributions in Free-Radical Polymerizations. 1. Model Development and Implications for Data Interpretation. *Macromolecules*, 28(2): 552.

Coen, E.M.; Gilbert, R.G.; Morrison, B.R.; Leube, H. and Peach, S., 1998. Modelling particle size distributions and secondary particle formation in emulsion polymerisation *Polymer*, 39(26): 7099.

Coen, E.M.; Peach, S.; Morrison, B.R. and Gilbert, R.G., 2004. First-principles calculation of particle formation in emulsion polymerization: pseudo-bulk systems. *Polymer*, 45(11): 3595.

Cunningham, M.F., 2002. Living/controlled radical polymerizations in dispersed phase systems. *Progress in Polymer Science (Oxford)*, 27(6): 1039.

de Brouwer, H.; Tsavalas, J.G.; Schork, F.J. and Monteiro, M.J., 2000. Living radical polymerization in miniemulsion using reversible addition-fragmentation chain transfer. *Macromolecules*, 33(25): 9239.

Enzo, G., 1993. Nucleation mechanisms and particle size distributions of polymer colloids. *AIChE Journal*, 39(7): 1210.

Ferguson, C.J.; Hughes, R.J.; Nguyen, D.; Pham, B.T.T.; Gilbert, R.G.; Serelis, A.K.; Such, C.H. and Hawkett, B.S., 2005. Ab initio emulsion polymerization by RAFT-controlled self-assembly. *Macromolecules*, 38(6): 2191.

Ferguson, C.J.; Hughes, R.J.; Pham, B.T.T.; Hawkett, B.S.; Gilbert, R.G.; Serelis, A.K. and Such, C.H., 2002a. Effective ab initio emulsion polymerization under RAFT control. *Macromolecules*, 35(25): 9243.

Ferguson, C.J.; Russell, G.T. and Gilbert, R.G., 2002b. Modelling secondary particle formation in emulsion polymerisation: application to making core-shell morphologies. *Polymer*, 43(17): 4557.

Gilbert, R.G., 1995. Emulsion polymerization: a mechanistic approach. Academic Press, London.

Gilbert, R.G.; Anstey, J.F.; Subramaniam, N. and Monteiro, M.J., 1999. Emulsion polymerization as a novel tool in controlled free-radical polymerization. *Book of Abstracts, 218th ACS National Meeting, New Orleans, Aug. 22-26*: POLY.

Gugliotta, L.M.; Arzamendi, G. and Asua, J.M., 1995. Choice of monomer partition model in mathematical modeling of emulsion copolymerization systems. *Journal of Applied Polymer Science*, 55(7): 1017.

Harkins, W.D., 1945. A general theory of the reaction loci in emulsion polymerization. *Journal of Physical Chemistry*, 13(9): 381.

Hawkett, B.S.; Napper, D.H. and Gilbert, R.G., 1980. Seeded emulsion polymerization of styrene. *Journal of the Chemical Society, Faraday Transactions 1: Physical Chemistry in Condensed Phases*, 76(6): 1323.

Hermanson, K.D.; Liu , S. and Kaler, E.W., 2006. Kinetic modeling of controlled living microemulsion polymerizations that use reversible addition-fragmentation chain transfer. *Journal of Polymer Science Part A: Polymer Chemistry*, 44(20): 6055.

Kwak, Y.; Goto, A.; Komatsu, K.; Sugiura, Y. and Fukuda, T., 2004. Characterization of Low-Mass Model 3-Arm Stars Produced in Reversible Addition-Fragmentation Chain Transfer (RAFT) Process. *Macromolecules*, 37(12): 4434.

Lansalot, M.; Davis, T.P. and Heuts, J.P.A., 2002. RAFT miniemulsion polymerization: Influence of the structure of the RAFT agent. *Macromolecules*, 35(20): 7582.

Le, T.P.; Moad, G.; Rizzardo, E. and Thang, S.H., 1998. Polymerization with living characteristics with controlled dispersity. PCT Int. Appl, WO 9801478.

Liu, S.; Hermanson, K.D. and Kaler, E.W., 2006. Reversible Addition-Fragmentation Chain Transfer Polymerization in Microemulsion. *Macromolecules*, 39(13): 4345.

Luo, Y.; Wang, R.; Yang, L.; Yu, B.; Li, B. and Zhu, S., 2006. Effect of Reversible Addition-Fragmentation Transfer (RAFT) reactions on (mini)emulsion polymerization kinetics and estimate of RAFT equilibrium constant. *Macromolecules*, 39(4): 1328.

Maxwell, I.A.; Morrison, B.R.; Gilbert, R.G.; Sangster, D.F. and Napper, D.H., 1992. Free radical entry in emulsion polymerizations. *Makromolekulare Chemie, Macromolecular Symposia*, 53(Polym. 91: Int. Symp. Polym. Mater.--Prep., Charact. Prop., 1991): 233.

Maxwell, I.A.; Morrison, B.R.; Napper, D.H. and Gilbert, R.G., 1991. Entry of free radicals into latex particles in emulsion polymerization. *Macromolecules*, 24(7): 1629.

McLeary, J.B. and Klumperman, B., 2006. RAFT mediated polymerisation in heterogeneous media. *Soft Matter*, 2(1): 45.

Mendoza, J.; De La Cal, J.C. and Asua, J.M., 2000. Kinetics of the styrene emulsion polymerization using n-dodecyl mercaptan as chain-transfer agent. *Journal of Polymer Science Part A: Polymer Chemistry*, 38(24): 4490.

Moad, G.; Chiefari, J.; Chong, Y.K.; Krstina, J.; Mayadunne, R.T.A.; Postma, A.; Rizzardo, E. and Thang, S.H., 2000. Living free radical polymerization with reversible addition-fragmentation chain transfer (the life of RAFT). *Polymer International*, 49(9): 993.

Monteiro, M.J.; Adamy, M.M.; Leeuwen, B.J.; van Herk, A.M. and Destarac, M., 2005. A "living" radical ab initio emulsion polymerization of styrene using a fluorinated xanthate agent. *Macromolecules*, 38(5): 1538.

Monteiro, M.J.; Bussels, R. and Wilkinson, T.S., 2001. Emulsion polymerization of methyl methacrylate in the presence of novel addition-fragmentation chain-transfer reactive surfactant (transurf). *Journal of Polymer Science, Part A: Polymer Chemistry*, 39(16): 2813.

Monteiro, M.J. and De Barbeyrac, J., 2001. Free-radical polymerization of styrene in emulsion using a reversible addition - Fragmentation chain transfer agent with a low transfer constant: Effect on rate, particle size, and molecular weight. *Macromolecules*, 34(13): 4416.

Monteiro, M.J. and de Brouwer, H., 2001. Intermediate radical termination as the mechanism for retardation in reversible addition-fragmentation chain transfer polymerization. *Macromolecules*, 34(3): 349.

Monteiro, M.J.; Hodgson, M. and De Brouwer, H., 2000a. Influence of RAFT on the rates and molecular weight distributions of styrene in seeded emulsion polymerizations. *Journal of Polymer Science, Part A: Polymer Chemistry*, 38(21): 3864.

Monteiro, M.J.; Sjoberg, M.; Van der Vlist, J. and Gottgens, C.M., 2000b. Synthesis of butyl acrylate-styrene block copolymers in emulsion by reversible addition-fragmentation chain transfer: effect of surfactant migration upon film formation. *Journal of Polymer Science, Part A: Polymer Chemistry*, 38(23): 4206.

Mueller, A.H.E.; Yan, D.; Litvinenko, G.; Zhuang, R. and Dong, H., 1995. Kinetic Analysis of \"Living\" Polymerization Processes Exhibiting Slow Equilibria. 2. Molecular Weight Distribution for Degenerative Transfer (Direct Activity Exchange between Active and \"Dormant\" Species) at Constant Monomer Concentration. *Macromolecules*, 28(22): 7335.

Nomura, M.; Yamamoto, K.; Horie, I.; Fujita, K. and Harada, M., 1982. Kinetics of emulsion copolymerization. II. Effect of free radical desorption on the rate of emulsion copolymerization of styrene and methyl methacrylate. *Journal of Applied Polymer Science*, 27(7): 2483.

Peklak, A.D. and Butte, A., 2006. Kinetic model of reversible addition fragmentation chain transfer polymerization of styrene in seeded emulsion. *Journal of Polymer Science, Part A: Polymer Chemistry*, 44(20): 6114.

Perrier, S.T., P., 2005. Macromolecular design via reversible addition-fragmentation chain transfer (RAFT)/xanthates (MADIX) polymerization. *Journal of Polymer Science Part A: Polymer Chemistry*, 43(22): 5347.

Prescott, S.W., 2003. Chain-length dependence in living/controlled free-radical polymerizations: Physical manifestation and Monte Carlo simulation of reversible transfer agents. *Macromolecules*, 36(25): 9608.

Prescott, S.W.; Ballard, M.J.; Rizzardo, E. and Gilbert, R.G., 2002a. RAFT in emulsion polymerization: What makes it different? *Australian Journal of Chemistry*, 55(6-7 SPEC): 415.

Prescott, S.W.; Ballard, M.J.; Rizzardo, E. and Gilbert, R.G., 2002b. Successful use of RAFT techniques in seeded emulsion polymerization of styrene: Living character, RAFT agent transport, and rate of polymerization. *Macromolecules*, 35(14): 5417.

Prescott, S.W.; Ballard, M.J.; Rizzardo, E. and Gilbert, R.G., 2005. Radical Loss in RAFT-mediated emulsion polymerizations. *Macromolecules*, 38(11): 4901.

Prescott, S.W.; Ballard, M.J.; Rizzardo, E. and Gilbert, R.G., 2006. Rate optimization in controlled radical emulsion polymerization using RAFT. *Macromolecular Theory and Simulations*, 15(1): 70.

Salazar, A.; Gugliotta, L.M.; Vega, J.R. and Meira, G.R., 1998. Molecular Weight Control in a Starved Emulsion Polymerization of Styrene. *Ind. Eng. Chem. Res.*, 37(9): 3582.

Simms, R.W.; Davis, T.P. and Cunningham, M.F., 2005. Xanthate-mediated living radical polymerization of vinyl acetate in miniemulsion. *Macromolecular Rapid Communications*, 26(8): 592.

Smith, W.V. and Ewart, R.H., 1948. Kinetics of emulsion polymerization *Journal of Physical Chemistry*, 16(6): 592.

Smulders, W.W., 2002. Macromolecular architecture in aqueous dispersions: 'living' free-radical polymerization in emulsion. Ph.D. Thesis, Technische Universiteit Eindhoven, Eindhoven, Neth.

Smulders, W.W.; Gilbert, R.G. and Monteiro, M.J., 2003. A kinetic investigation of seeded emulsion polymerization of styrene using reversible addition-fragmentation chain transfer (RAFT) agents with a low transfer constant. *Macromolecules*, 36(12): 4309.

Smulders, W.W. and Monteiro, M.J., 2004. Seeded emulsion polymerization of block copolymer core-shell nanoparticles with controlled particle size and molecular weight distribution using xanthate-based RAFT polymerization. *Macromolecules*, 37(12): 4474.

Thickett, S.C. and Gilbert, R.G., 2006. Rate-controlling events for radical exit in electrosterically stabilized emulsion polymerization systems. *Macromolecules*, 39(6): 2081.

Thickett, S.C. and Gilbert, R.G., 2007. Emulsion polymerization: State of the art in kinetics and mechanisms. *Polymer*, 48(24): 6965.

Tsavalas, J.G.; Schork, F.J.; De Brouwer, H. and Monteiro, M.J., 2001. Living radical polymerization by reversible addition-fragmentation chain transfer in ionically stabilized miniemulsions. *Macromolecules*, 34(12): 3938.

Ugelstad, J. and Hansen, F.K., 1976. Kinetics and mechanism of emulsion polymerization. *Rubber Chemistry and Technology*, 49(3): 536.

Urban, D. and Takamura, K., 2002. Polymer dispersions and their industrial applications. Wiley-VCH, Weinheim.

Uzulina, I.; Kanagasabapathy, S. and Claverie, J., 2000. Reversible addition fragmentation transfer (RAFT) polymerization in emulsion. *Macromolecular Symposia*, 150(Polymers in Dispersed Media): 33.

Van Herk, A.M., 2005. Chemistry and technology of emulsion polymerisation. Blackwell Pub., Ames, Iowa.

Van Herk, A.M. and Monteiro, M.J., 2003. Heterogeneous Systems. In: T.P.D. Krzysztof Matyjaszewski (Editor), Handbook of Radical Polymerization.

Zeaiter, J., 2002. A framework for advanced/intelligent operation of emulsion polymerisation reactors. Ph.D. Thesis, Dept. of Chemical Engineering, University of Sydney, Sydney.

Zeaiter, J.; Romagnoli, J.A.; Barton, G.W.; Gomes, V.G.; Hawkett, B.S. and Gilbert, R.G., 2002. Operation of semi-batch emulsion polymerisation reactors: Modelling, validation and effect of operating conditions. *Chemical Engineering Science*, 57(15): 2955.

Chapter Five

Experimental Setup and Model Validation

Chapter 5
Experimental Setup and Model Validation

Abstract

In this Chapter the design and installation of an automated emulsion polymerization reactor facility is explained first. A description of the facility in terms of the major components of which it is comprised is addressed in detail. The materials comprising the experimental work are specified. The experimental design strategy with the objective of systematically investigating the effects of the different manipulated variables under consideration on the emulsion polymerization outcomes is explained. Next, the experimental validation of the model predictions for the styrene RAFT emulsion polymerization system is studied. The effects of the xanthate transfer agent (AR), surfactant (SDS), initiator (SPS) and temperature are investigated. The polymerization rate (Rp), the number average molecular weight (Mn), and the particle size (r) decreased with increasing AR. Rp increased with increase in SDS and SPS, while an increase in temperature led to a decrease in Mn, an increase in Rp, and an increase in r. The observed retardation in rate was attributed to the exit and re-entry of small radicals. It is found that the model is capable of accurately predicting monomer conversion, molecular weight and particle size distributions of the polymer. This tool is suitable for advanced model-based control of polymerization reactors to obtain desired polymer products.

5.1 Introduction

Simulation studies presented in Chapter 4 indicated that the reaction conditions and the presence of a RAFT agent have a significant effect on the polymerization attributes. The preliminary studies suggested that the presence of a RAFT agent resulted in reducing the polymerization rate and particle size while keeping the molar mass under control with a predetermined value proportional to the initial molar ratio of monomer to RAFT agent. In order to test the validity of the kinetic model developed in Chapter 4, experiments were carried out to characterize the effect of reaction conditions, and most

importantly the effect of the RAFT agent concentration, on the polymerization rate, particle size and molecular weight distributions. Styrene was chosen as a case study due to the fact that the kinetic parameters for such system are well defined and the reaction mechanisms are well understood. Furthermore, styrene is considered to be the most environmentally friendly among all other monomers.

5.2 Experimental setup

5.2.1 Polymerization reactor

Batch and semi-batch RAFT emulsion polymerization experiments were carried out in a 1L stirred tank reactor. The reactor system, from Pdc Machines Inc., (Schemes 5-1 and 5-2) comprises the reactor container, a supporting aluminum stand and an agitation assembly. The reactor vessel consists of a 1-litre glass cylinder with a jacket for heating and cooling held together between two steel plates.

The bottom plate is equipped with an outlet valve for drainage, while the top plate is fitted with multiple process connection ports: sample tube, temperature sensors, cooling coil, gas lines, and a rupture disc assembly. The reactor is equipped with a magnetically driven agitator with a six-pitched blade impeller, which was designed to provide adequate mixing inside the reactor (scheme 5-3). The covering is placed on the reactor such that the stirrer rod passes through the central opening of the lid.

The stirrer rod fits into the chuck of the motor. The clearance of the impeller from the bottom was always taken as one half of the vessel diameter. An agitation speed of 350 RPM was found to guarantee proper mixing, and was used in all experimental polymerizations. The impeller is driven by a 90-volt permanent magnet DC motor (from LESSON Electric Corporation), capable of speeds of 0-1750 RPM with the use of an associated motor speed controller (KBIC$^{(R)}$ from KB Electronics, INC.) that manipulates the motor's torque, and a digital tachometer that monitors the rotation speed.

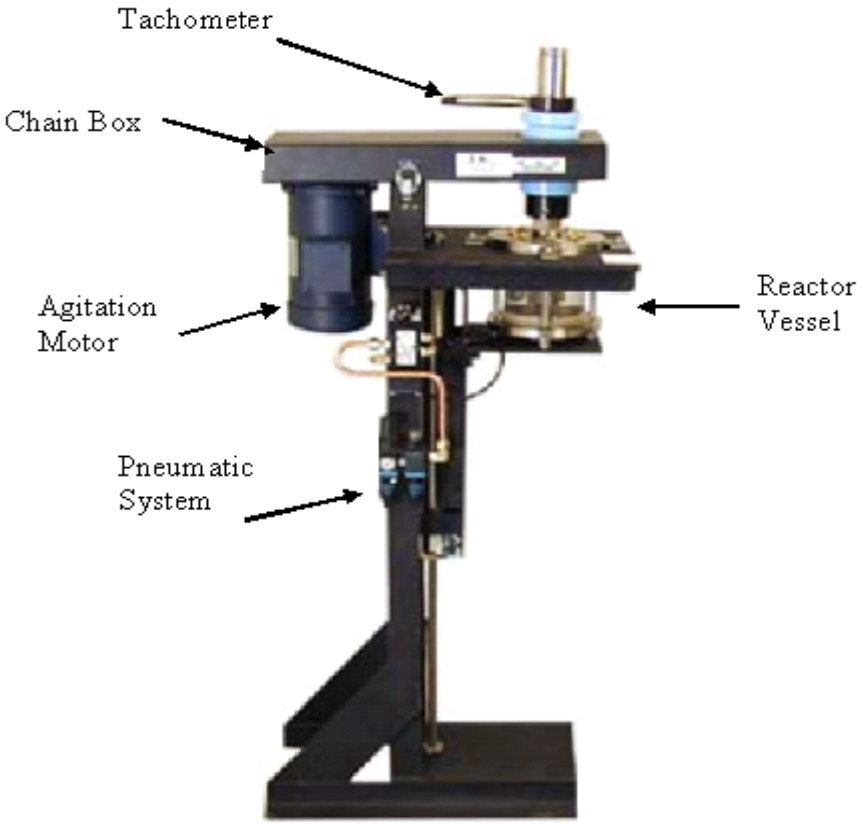

Scheme 5-1: Side-view schematic of the reactor system.

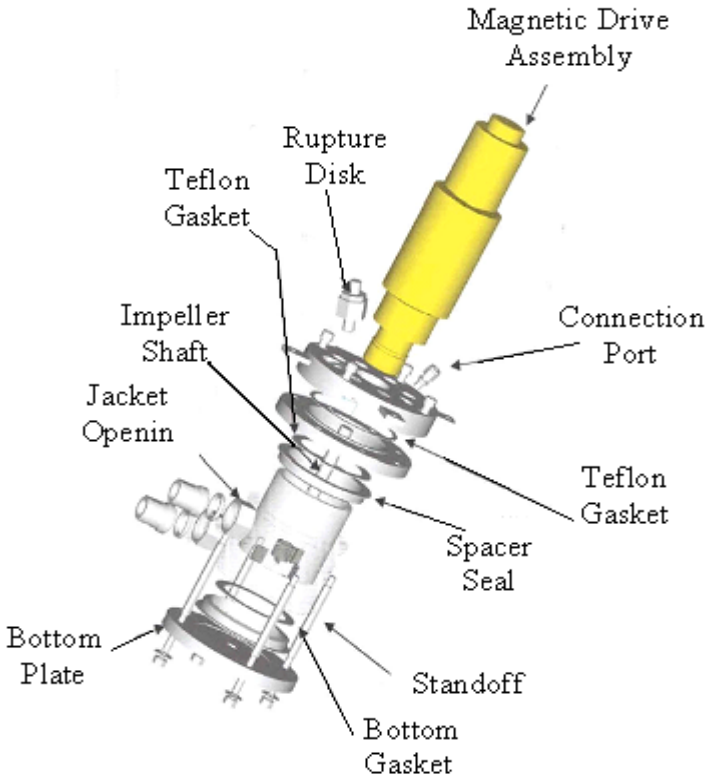

Scheme 5-2: Schematics of the reactor vessel.

The maximum operating pressure and temperature of the reactor are 6 bar and 200 ^{o}C respectively. The reactor vessel has a pneumatic actuation system that can be used to lower the vessel for cleaning and maintenance purposes. A temperature controlled circulator (Julabo) provided heating/cooling flows through the external reactor jacket was used to maintain the reaction temperature at the desired level.

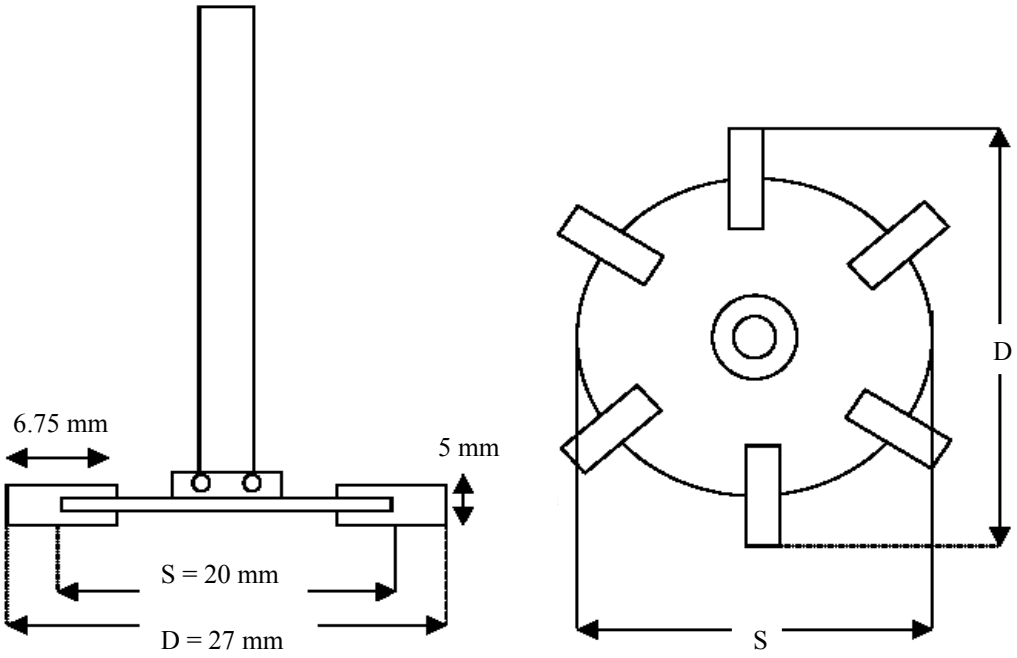

Scheme 5-3: Illustration of the six-blade impeller used inside the polymerization reactor.

Nitrogen is used for blanketing against oxygen which acts as an inhibitor during polymerization reaction. Thus it is a practice to keep the polymerization under a nitrogen layer with a very slight positive pressure. Excess nitrogen is highly undesirable as it cools down the reaction media and can lead to a pressure build up which may cause a disk rupture, or, in the worst case, a vessel rupture. In order to rectify these problems a pressure regulator was installed on the nitrogen supply line along with a dreschell bottle so as to control and monitor the nitrogen flow entering the reactor. A fume hood was designed to cover the whole polymerization plant.

5.2.2 Heating and cooling system

The reaction temperature plays a significant role in many kinetic events in the emulsion polymerization process. It affects propagation, transfer, and termination rates, and hence

alters the polymerization attributes such as the polymerization rate, PSD and MWD. Thus, controlling the reaction temperature is an essential task that helps in controlling the polymerization reaction. A temperature sensor (Pt-100) is installed inside the reactor to continuously monitor the reaction temperature. In addition, there are two other temperature sensors (Pt-100) located on the inlet and outlet of the jacket. The Refrigerating and Heating Circulator (Julabo) provides a constant high water flow rate of 40 L/min through the reactor jacket. The circulator is equipped with a PID controller built in it for temperature control. The heating circulator can be operated manually or remotely via a computer and is equipped with a PID controller within the Control Builder Software (Honywell) for internal and external temperature control.

5.3 RAFT-emulsion polymerization

5.3.1 Materials

Styrene monomer, purification columns, initiator (sodium persulfate, KPS), and surfactant (sodium dodecyl sulfate, SDS) were obtained from Sigma-Aldrich. Styrene was purified by passing it through an inhibitor-removal column; the purification procedure was repeated twice to ensure high purity. All other chemicals were used as received. Water to a Milli-Q-standard was used, while dissolved oxygen was removed by bubbling high purity nitrogen through the mixture of the RAFT agent and the monomer for about one hour.

5.3.2 RAFT agent synthesis

The RAFT agent **(O-ethylxanthyl ethyl propionate, Scheme 5-4)** was synthesized in our laboratory according to established procedures (Smulders *et al.*, 2003). **O-ethylxanthyl ethyl propionate** was synthesized by adding 101.4g of Potassium ethyl xanthogenate (Fluka) to a mixture of 102g ethyl 2-bromopropionate (Aldrich) dissolved in 1L of ethanol at 0°C under a nitrogen atmosphere. The mixture was immersed in ice bath and stirred for 6 hours in the absence of light. 1L of water was added, and the product was extracted using a 1:2 mixture of diethyl ether and pentane. The solvent was removed and the remaining ethyl 2-bromopropionate distilled off under vacuum.

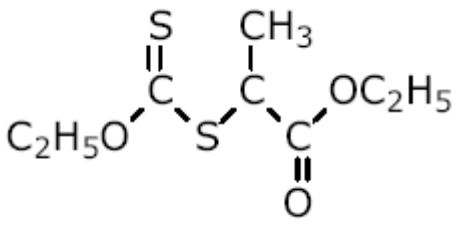

Scheme 5-4: RAFT agent structure.

5.3.3 Experimental procedure

Ab-initio batch emulsion polymerizations with O-ethylxanthyl ethyl propionate were carried out in a 1L laboratory reactor (described above) at an agitation speed of 350 rpm. The polymerizations were performed using 520g water and 80g styrene, with varying amounts of initiator, surfactant and RAFT agent at different reaction temperatures. A temperature controlled circulator (Julabo) provided heating/cooling flows through the external reactor jacket was used to maintain the reaction temperature at the desired level. The emulsifier was dissolved in distilled water and loaded into the reactor.

The mixture of the RAFT agent and monomer was added to the reactor and agitated with water and surfactant under a slight nitrogen pressure. Once the reactor was sealed, nitrogen was passed through the reactor and bubbled through the reaction medium. The flow rate was set such that the nitrogen bubbled very slowly through the oil in the dreschell bottle, ensuring a slightly positive pressure was maintained in the vessel. The preheated solution of initiator and buffer in water (at the reaction temperature) was then added to trigger the polymerization reaction. Samples were taken periodically to monitor conversion, molecular weight and particle size distributions. The procedure was repeated for a number of RAFT agent, surfactant and initiator concentrations and reactor temperatures. The typical procedural details are given in Table 5-1.

5.4 Sample characterization

5.4.1 Monomer conversion

Monomer conversion is a key indicator of the product property and composition, and is defined as the ratio of the polymer mass formed in the reactor to the total monomer fed until time *t* (Equation 5-1). Monomer conversion was determined gravimetrically. Small latex samples (approximately 5-10ml) were taken from the reactor and transferred directly into a dry, clean 20ml vial, where the reaction was short-stopped by the addition of hydroquinone. The sample portion used to measure monomer conversion was weighed in a dry clean aluminum cup. The free liquid was evaporated on a steambath and the resulting product was dried in an oven at 80°C, until a constant weight was obtained. For *ab-initio* emulsion polymerizations, the conversion (x) was calculated according to the following equation

$$x = \frac{(A/B) - C}{D} \qquad \textbf{(5-1)}$$

where D is weight fraction of monomer in the reactor; A is weight of dried sample; B is weight of sample; and C is the initial solid fraction.

5.4.2 Molecular weight distribution

Size exclusion chromatography (SEC), also known as gel permeation chromatography (GPC), is one of the most reliable and accurate methods for the determination of number and weight average molecular weights and molecular weight distribution (MWD) of polymers. The instrument uses the principle of hydrodynamic fractionation, in which macromolecules (polymer chains) are separated according to their size (hydrodynamic volume). The chromatography process starts with continuous flow at a rate of 1ml/min of the mobile phase through the system. A dilute polymer solution containing a broad molecular weight distribution of polymer chains is allowed to pass through a column packed with finely divided solid particles (porous material) such as polystyrene gel, glass beads, and silica gel. The larger molecules travel faster through the porous packing than the smaller molecules, which are slowed while entering various pores. The macromolecular chains are detected by polymer-sensitive detectors, such as

a refractive index detector. A refractive index detector (RI) is an essential component in multi-detector systems, as it is used to measure the concentration of each eluted fraction of the polymer solution after the separation process. It responds directly to the difference between the refractive indices of the pure solvent and the solution. The output, the solution concentration versus time, is then analysed and reported using a computer with appropriate software.

The task of GPC data interpretation is to convert the detector response (the solution concentration) versus elution time profile obtained from the chromatogram into a molecular weight distribution using a calibration curve. To calibrate the instrument, a standard with a known absolute molecular weight (gathered by using an absolute technique such as viscometry) is generally used. In this work, MWD analyses were carried out using a high temperature chromatography system (PL-GPC 120) with a PLgel guard 5μm 50×7.5mm column connected in series with two PLgel (Mixed-C 10μm 300×7.5mm) columns (PL, Polymer Laboratories). The samples were prepared by dissolving 0.05g of dry latex in 1g of tetrahydrofuran (THF), producing a concentration of 5% wt/wt. Samples were allowed to dissolve for at least twelve hours to ensure complete dissolution. The samples were then analysed at 40^{o}C and at a THF flow rate of 1ml/min. Calibration was carried out using narrow-distribution polystyrene standards (with molecular weight from 580 to 7.1×10^{6} g/mol). A PL Data stream unit was used for data acquisition. The data obtained from the RI detector was processed using Cirrus^{TM} GPC software.

5.4.3 Particle size distribution

The particle size distribution can have a fundamental effect on the physical properties of dispersions that are common polymer products. The measurement of just the average particle size may not be sufficient. For example, the presence of different size populations resulting in a multimodal distribution could have a strong influence on the final properties, and may need to be controlled. To validate model predictions and quantify the effects of changes in process variables, an efficient way of measuring the particle size distribution has to be provided. There are numerous techniques for sizing emulsions, most of which rely on the movement of suspended particles in response to a

variety of forces. However, the fact that the latex particles prepared by emulsion polymerisation can have diameters considerably less than the wavelength of visible light limits the techniques available. Furthermore, many of the techniques currently available suffer from high cost, complexity of instrumentation, and slow processing time.

Non-fractionation techniques, including those revolving around radiation scattering and absorption, provide rapid determination of the average size or estimating the size distribution of highly disperse samples. However, they are less suited for the analysis of multi-modal samples or samples with broad particle size distributions due to the low resolution of the method. Fractionation techniques, including packed column HDC, offer advantages over non-fractionation techniques for particle sizing and the method produces information about the average particle size and the distribution of particle size.

In this work, particle size measurements were performed using the PL-PSDA instruments. The PL-PSDA particle size distribution analyser is an integrated, automated system for the rapid determination of particle size distribution of colloidal dispersions. It operates on the principle of packed column hydrodynamic chromatography (HDC) to separate particles in the interstitial void spaces created by the solid spherical packing material. PL-PSDA measures complex particle size distributions with high precision and accuracy, and is independent of particle chemistry, making it ideal for narrow distribution, multi-modal or polydisperse samples. The automated features and user friendly software combine to deliver remarkable ease of operation which, together with the high resolution of the technique, makes it suitable for both quality control and research applications. (Polymer_Laboratories, operating manual for PL PSDA, 2003).

The latex samples were diluted with CHDF eluent to approximately 1-2% solids. A proprietary eluent was continuously pumped through the system at a constant flow rate. The sample under investigation and a small molecule marker solution are introduced into the system via a two position, electrically actuated valve, such that the eluent flow is not interrupted. The sample components are separated by an HDC mechanism in a 'cartridge', and their concentration is measured by a UV detector as polystyrene latex can absorb light in the ultraviolet region. The ultra violet (UV) detector response is used

to calculate the concentration of particles of different sizes present in the sample. The subsequent computation of particle size distribution simply requires a calibration procedure employing latex particle size standards. The system was calibrated using a series of particle size standards with sizes ranging from 20 nm to 2 μm. The PL-PSDA is simple to operate with an analysis time of the order of ten minutes. The results are independent of the particle density or the sample nature. However, extensive calibration and sample dilution are required.

5.5 Results and discussions

Prediction of the kinetics of controlled free radical polymerization is by far more straight-forward for homogeneous systems than for heterogeneous ones like emulsion polymerization. This is mainly due to the multiplicity of the reaction loci in an emulsion polymerization system. To overcome this complexity, a mathematical model accounting for the different kinetic events that occur in a RAFT-emulsion polymerization was developed in Chapter 4. The model is capable of predicting the effect of the reaction conditions on the polymerization rate, MWD and PSD. Model simulations, presented in Chapter 4, suggest that the presence of a transfer agent could have a significant effect on the polymerization outcomes.

To test the effect of the reaction conditions and hence validate the model, the experiments were designed to explore the effect of varying the concentrations of the RAFT agent, the surfactant, and the initiator, along with varying the reaction temperature on the polymerization rate, MWD and PSD in batch *ab initio* emulsion polymerization of styrene. The experimental reaction conditions are given in Table 5-1. The general parameters used in modelling styrene emulsion polymerization with **O-ethylxanthyl ethyl propionate** are given in Table 5-2.

5.5.1 Effect of reaction conditions on polymerization rate

With the kinetic parameters (Table 5-2) the model was validated using experimental data obtained in our laboratory. Figures 5-1 to 5-6 show that the experimental results for the overall conversion and RAFT concentration are in good agreement with the model simulations. Figure 5-1 presents the evolution of monomer conversion in runs IS.1-IS.5,

in which the amount of the RAFT agent was varied from 0 to 8.5 wt % (0 to 6.8g) relative to monomer amounts with constant initiator and surfactant concentrations at 70°C.

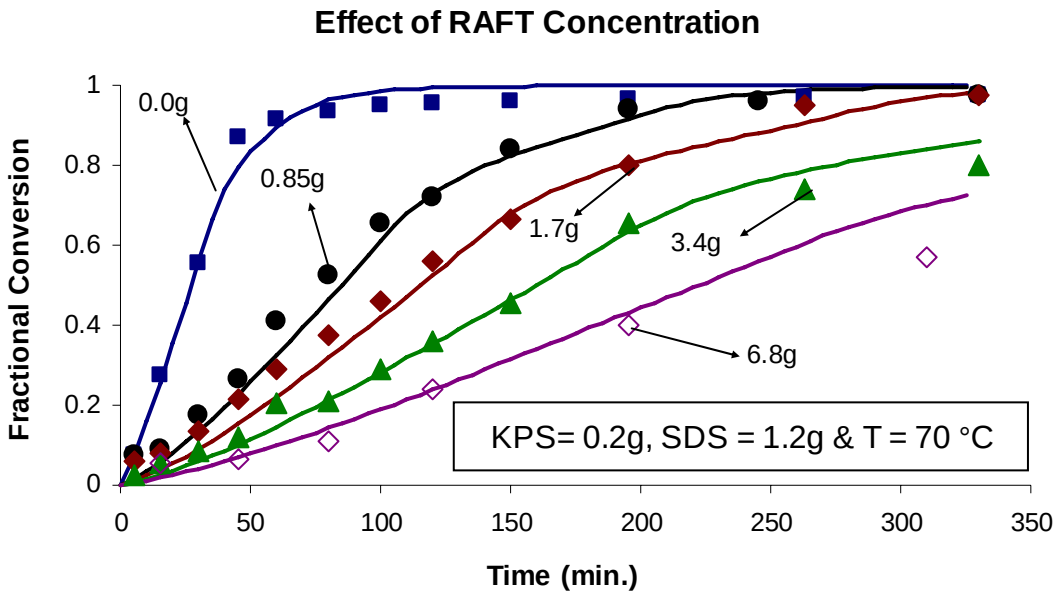

Figure 5-1: Effect of RAFT agent concentration on monomer conversion for polymerization at 70^{0}C with high concentration of surfactant (1.2 g). Legend: Run IS.1 (■); Run IS.2 (●); Run IS.3 (♦); Run IS.4 (▲); Run IS. 5 (◊); model predictions (—).

The RAFT agent had a marked effect on reducing the polymerization proportion to the amount of RAFT agent employed. This indicates that a significant amount of the small radicals ($R^{\bullet}$) generated by chain transfer to AR were not able to reinitiate polymerization. The ability of such small radicals to reinitiate polymerization inside the particles depends mainly on the time that they can stay inside the particles or as part of the intermediate radicals formed by the addition to the RAFT agent. Since no retardation has been observed in bulk and solution polymerization of styrene with the same RAFT agent (Adamy *et al.*, 2003), the latter may have no effect on the polymerization rate as the fragmentation rate of the intermediate radical is sufficiently high. Thus, it is concluded that the observed retardation is due to the exit of small radicals from particles resulting in reduction in the average number of radicals per particle. The first inflection point in any conversion profile represents the point at which the polymerization switched from interval II to interval III.

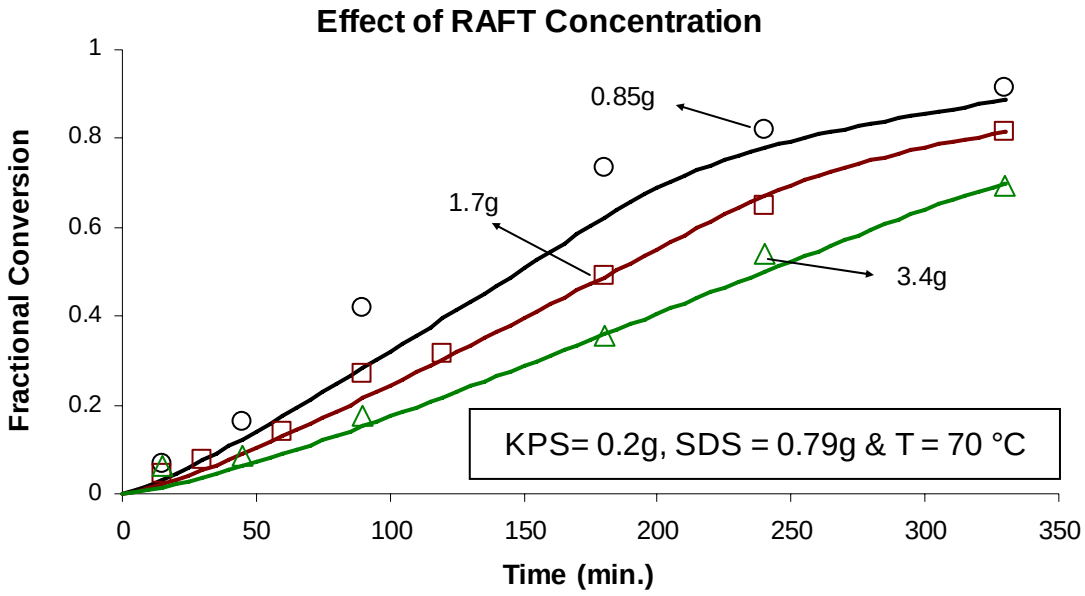

Figure 5-2: Effect of RAFT agent concentration on monomer conversion for polymerization at 70^0C with low concentration of surfactant (0.79 g). Legend: Run IS.8 (○); Run IS.9 (□); Run IS.10 (Δ); model predictions (—).

After this point the droplet phase no longer exists, and hence there is no extra monomer to replenish the polymerized monomer in the particles. Thus, monomer concentration decreases, resulting in lowering the rate at which monomer is consumed. On the other hand, the second inflection point represents the point after which there is no more RAFT agent present in the system (Fig. 5-6). It is quite clear that after this point monomer conversion for runs IS.2 and IS.3 reaches unity as the exit effect no longer exists.

As illustrated in Figure 5-2, similar observations were successfully predicted by the model and validated against experimental data when the surfactant concentration was reduced to 0.79g while keeping the rest of the reaction conditions unchanged. The amount of surfactant was varied in order to investigate the effect of the emulsifier concentration on the polymerization rate, molecular weight and particle size distributions. Figure 5-3 shows the effect of the reduced surfactant concentration at constant amounts of the initiator (0.2g), the RAFT agent (1.7g), and reaction temperature (70^oC). It is not surprising that the polymerization rate decreased with the decreased surfactant concentration.

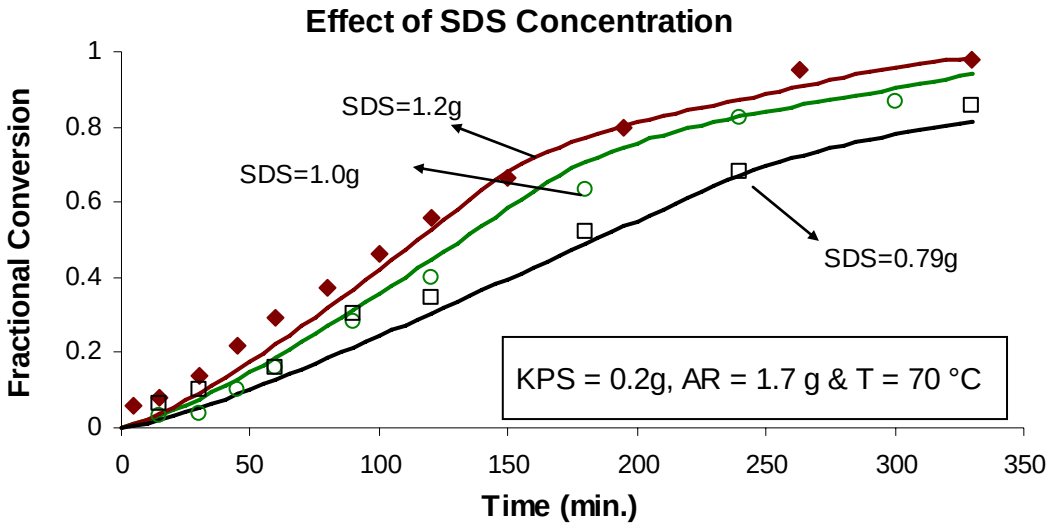

Figure 5-3: Effect of SDS concentration on monomer conversion. Legend: Run IS.3 (♦); Run IS.9 (□); Run IS.12 (○); model predictions (—).

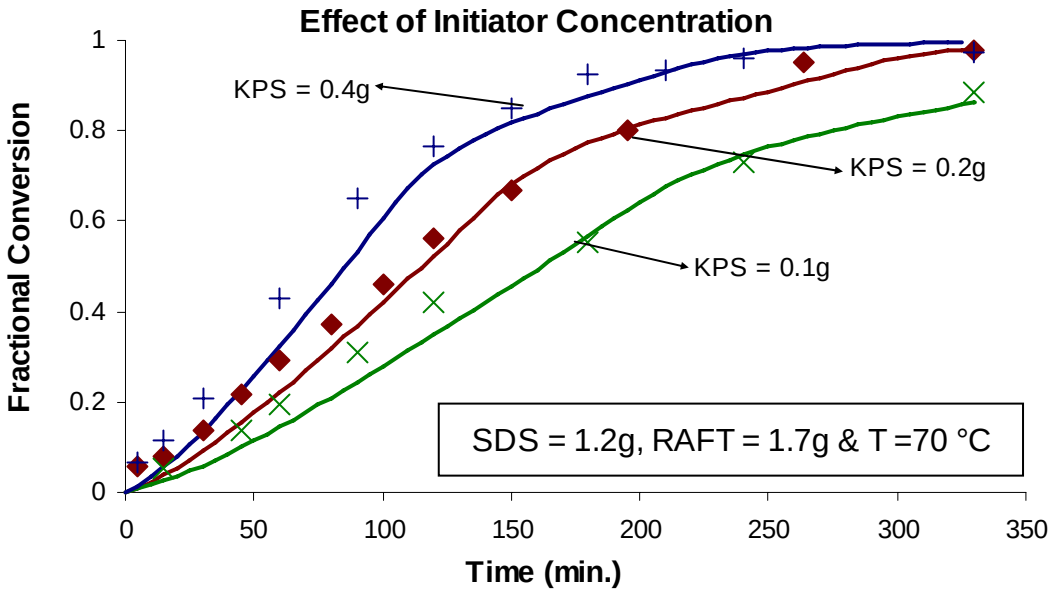

Figure 5-4: Effect of initiator concentration on monomer conversion. Legend: Run IS.3 (♦); Run IS.6 (×); Run IS.7 (+); model predictions (—).

As the micellar nucleation is the prevailing mechanism for particle formation, the number of polymeric particles is then strongly dependent on the surfactant concentration (see Figure 5-16b). Consequently, reducing surfactant concentration results in reducing the total number of polymerization loci, thereby leading to a reduction in the polymerization rate. Increasing the initiator concentration (Figure 5-4)

results in a high polymerization rate due to the increased number of the primary radicals generated from the initiator.

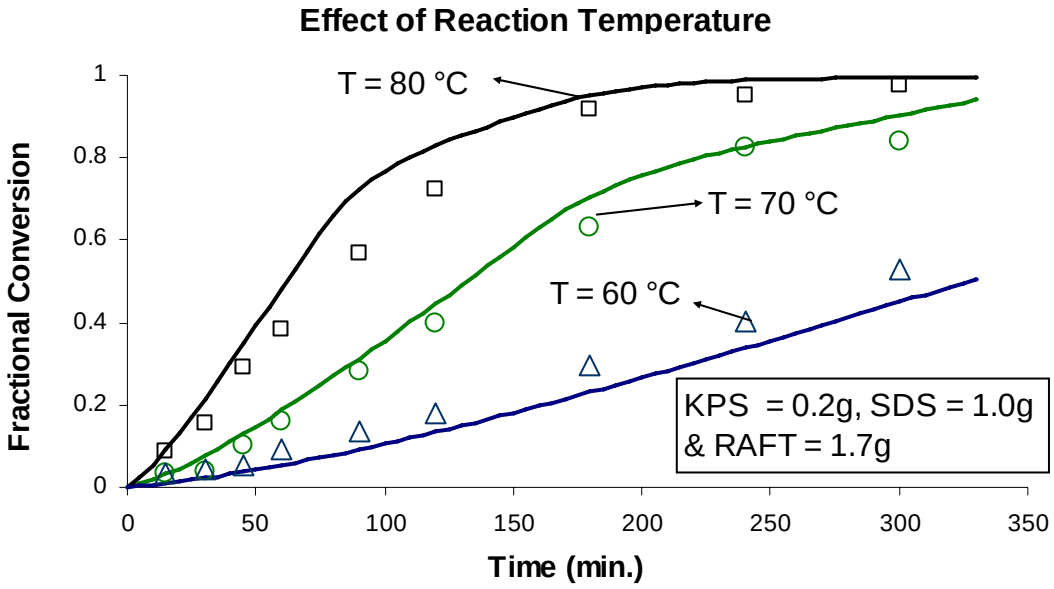

Figure 5-5: Effect of reaction temperature on monomer conversion. Legend: Run IS.11 (□); Run IS.12 (○); Run IS.13 (Δ); model predictions (—).

Figure 5-5 represents the overall conversion as functions of reaction time and reaction temperature with constant RAFT agent and initiator concentrations. The polymerization rate was markedly improved by increasing the reaction temperature. This is expected because reaction rate constants are temperature dependent by an exponential function according to Arrhenius law and can be explained by the fact that higher temperatures generally cause an increase in the rate of propagation.

The moles of the RAFT agent remaining in the reactor can be calculated as a function of time from experimental data (for Mn) and monomer conversion using equation (4-64), and is given in Figure 5-6 for runs IS.2-IS.5. The RAFT agent used in this work has a low transfer constant (C_{tr}~0.7) and is consumed gradually during the reaction. Thus, there is a continuous production of small radicals that exit from the particle. Consequently, the amount of these radicals increases with increasing the RAFT agent concentration, resulting in an increase in the exit rate and hence in the retardation effect. In run IS.2, the remaining amount of the RAFT agents approaches zero after almost 250 minutes from the beginning of the reaction.

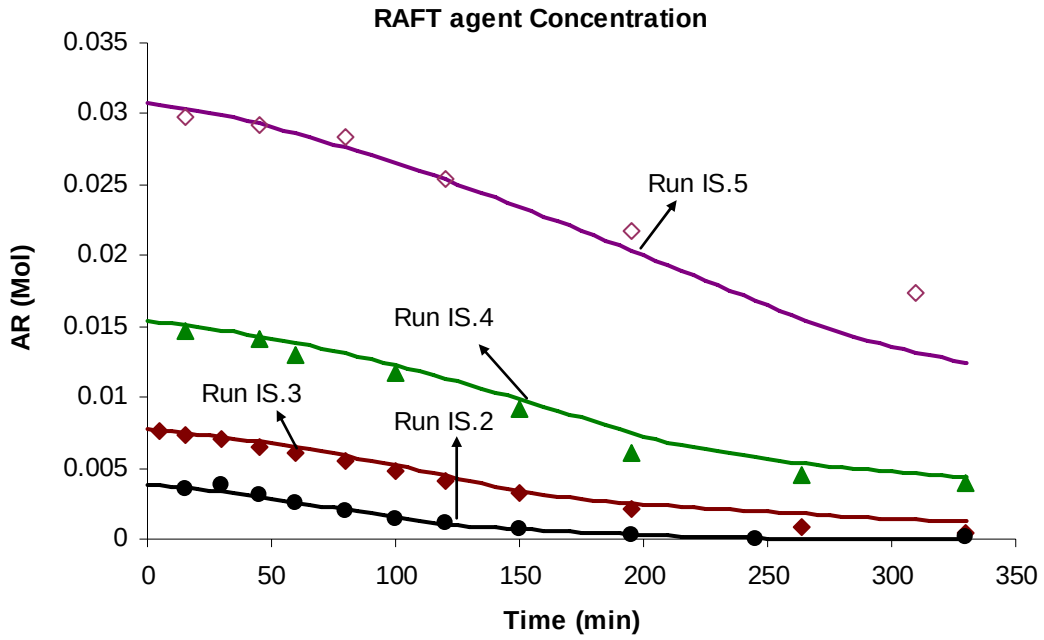

Figure 5-6: Decay in RAFT (AR in moles) concentration as a function of time. Legend: Run IS.2 (●); Run IS.3 (♦); Run IS.4 (▲); Run IS.5 (◊); model predictions (—).

After this point there are no more small radicals that can exit from the particle, hence the second inflection point in the conversion time profile occurs and the monomer conversion reaches unity

5.5.2 Effect of reaction conditions on molecular weight

For polymerization with a highly active RAFT agent, the addition of the propagating radical to the active $(C=S)$ double bound is fast, compared to its addition to monomer $(k_{add}C_p^{AR} >> k_pC_p^M)$. Hence, the radicals will exchange rapidly among the chains. Consequently, the system will show living polymerization characteristics in which the Mn increases linearly with conversion, thereby providing a narrow MWD. However, such linear growth is not expected for polymerization with a low active RAFT agent. Figure 5-7 shows Mn obtained from runs IS.2 to IS.5, while Figure 5-8 shows their corresponding polydispersities. Symbols in both figures represent experimental data, while solid lines and dotted lines represent model simulations as predicted by equation (4-61) and (4-64), respectively.

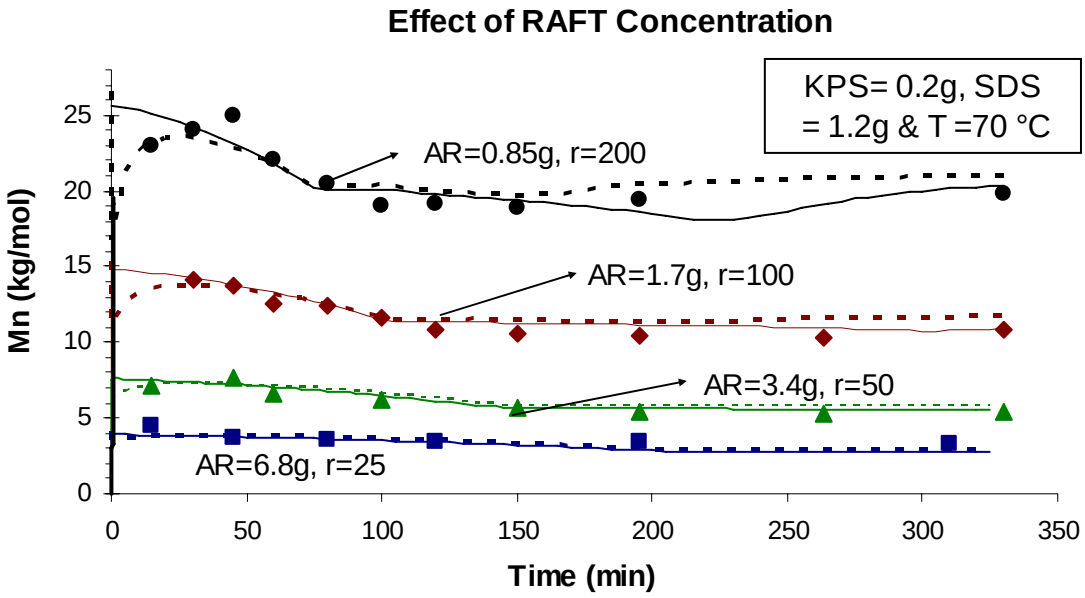

Figure 5-7: Effect of AR concentration on the number average molecular weight. Legend: Run IS.2 (●); Run IS.3 (♦); Run IS.4 (▲); Run IS.5 (■); model predictions (solid and dotted lines).

At the early stages, the Mn decreases with time, until it attains a constant value at a later stage. The decrease in Mn with increased concentration of the RAFT agent is mainly due to the increased number of chains provided by the RAFT agent. Equation 4-64 was able to predict such behaviour and good agreement with experiment was obtained as shown in figure 5-7 (solid lines). Further, equation 4-61 (dotted lines) also provides reasonable predictions with additional kinetic information of all chain stopping events included in the equation. The polydispersities for these products are similar, ranging between 2.17 to 2.25 (Figure 5-8).

In an experiment without the RAFT agent (not shown), the Mn values were within 0.3×10^6 and 0.5×10^6 with a polydispersity of about 3.5. It was expected that the Mn would be equal to the ratio of the monomer to the RAFT agent multiplied by the monomer molecular weight. However, experimental data show that the Mn at the beginning of the reaction is higher than the theoretical value. The high Mn observed at the beginning of polymerization is due to the low concentration of RAFT agent in the particles. This may be due to slow transfer of RAFT agent into the particles phase. At longer times, the monomer/RAFT ratio reaches a constant value of Mo/RAFTo.

The solubility of the RAFT agent used in this work is 0.002M at 50°C which is about half that for the monomer. Considering that the diffusion rate coefficient for the monomer and the RAFT agent in the water phase are comparable in magnitude, one can conclude that the monomer transfer rate into particles is higher. On the other hand, the transfer rate of AR from the monomer droplets through the aqueous phase into the particles is higher than its consumption rate (Smulders, 2002). Thus, it is expected that AR will accumulate in a particle as long as the monomer droplet phase (which contains AR) is present, resulting in a decrease of Mn with time.

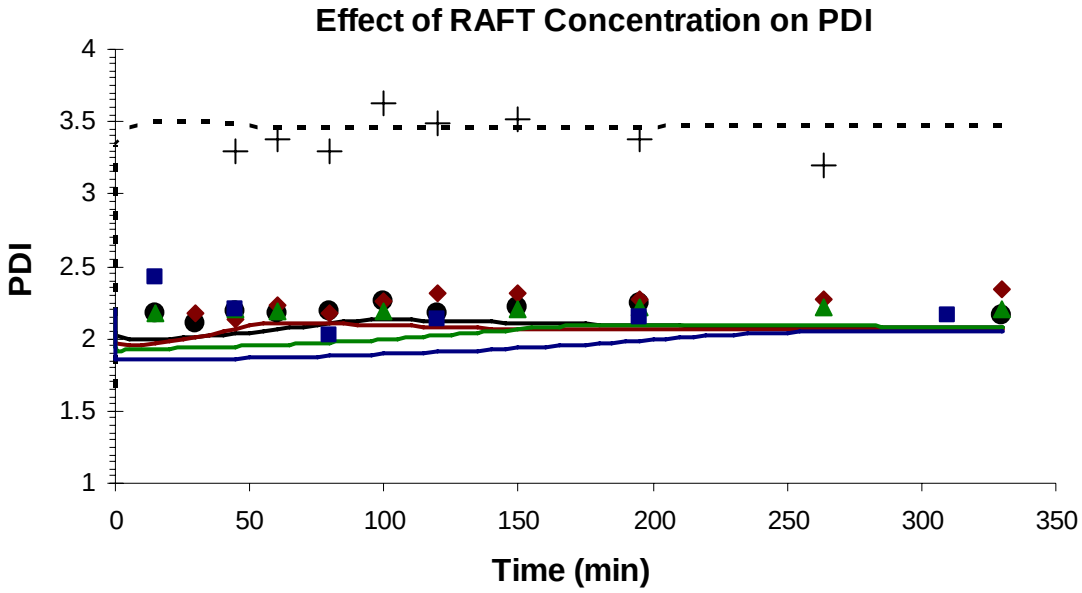

Figure 5-8: Molar mass polydispersity with time at 70°C. Legend: Run IS.1 (+); Run IS.2 (●); Run IS.3 (♦); Run IS.4 (▲); Run IS.5 (■); model predictions (solid and dotted lines).

The maximum AR concentration in a particle is equal to the initial ratio of RAFT to monomer multiplied by the saturated concentration of monomer in the particle (supporting information in (Monteiro *et al.*, 2005)) . Once the system attains this value, the number of polymeric chains in the particle reaches constant value, and hence the Mn becomes constant. Simulations presented in figure 5-7 (dotted lines, predicted by equation 4-61) show that, at the very beginning, Mn increases and after going through a maximum, decreases. The entry of the aqueous phase radicals (termination) into polymeric particles could be the reason behind this increase in Mn. At the same time,

the number of the active radicals generated from AR increases as more RAFT agent transports into particles.

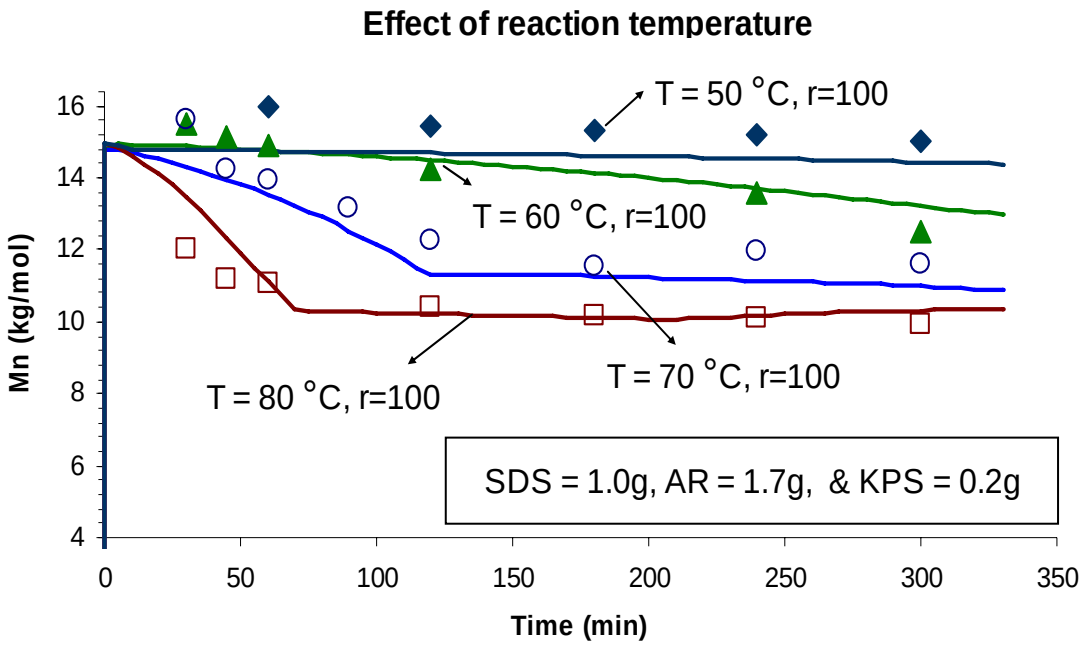

Figure 5-9: Effect of reaction temperature on number average molecular weight. Legend: Run IS.11 (□); Run IS.12 (○); Run IS.13 (▲); Run IS.14 (♦); model predictions (—).

During the early stages of polymerization, the amount of the terminated radicals by entry is then balanced by the amount of those produced from the RAFT agent. At this point, the Mn reaches its maximum value. Then, the Mn decreases because of the increased number of RAFT radicals. Once the AR attains its maximum concentration in the particles, the number of RAFT radicals becomes constant, resulting in a constant Mn. In addition, experimental data obtained from run IS.2, where a small amount of AR was used (Figure 5-7), show a slight increase in Mn during interval III where almost the entire RAFT agent was consumed (Figure 5-6, run IS.2). Such an increase in Mn could be due to a decrease in the number of active chains inside the particles. In general, it can be seen that a desired polymer with a predetermined molecular weight can be produced by manipulating the initial amount of the RAFT agent. The investigation on the effect of the initiator showed that when the initial initiator amount increased from 0.1g to 0.2g, the Mn decreased by about 10% at the end of the reaction, and the same trend was observed when the initiator amount was increased to 0.4g. Not surprisingly, the decreased Mn is due to an increase in the concentration of the aqueous phase radicals

and hence an increased entry rate. Such an increase in the entry rate results in increasing the number of the active polymeric chains in the polymer particles, and reduces Mn.

Due to its effect on the reaction rate, reaction temperature had a marked effect on Mn, in which high Mn was obtained at lower reaction temperatures (Fig. 5-9). In Equation 4-61, the ratio of the rate of chain propagation to the rate of chain termination quantifies the lifetime of a radical in terms of the number of propagation steps in which it participates (these events are also temperature dependent through the Arrhenius relation). The dependence of the chain length on the rate constants is dictated by the relative values of the activation energies for the various events. Thus the chain length decreases with increasing temperatures because the dominant factor is the much greater rate of production of radicals (and hence entry) and transfer. During polymerization, this ratio changes subject to many other events; for instance, at high conversions, termination becomes diffusion-controlled. This event leads to a greater rate of polymerization because a severe decrease in termination brings about an increase in the concentration of radicals, hence an increase in the chain length. In a similar fashion, propagation and transfer are expected to become diffusion-controlled later than termination, but only when the system becomes glassy. Thus the glass transition temperature of the polymer formed has a decisive effect on the polymerization at very high conversions.

The effect of reducing surfactant concentration on the number average molecular weight is almost negligible. Reducing the surfactant concentration had a significant effect on the polymerization rate due to reducing the number of the polymerization loci. It was expected that reducing surfactant concentration would result in increasing Mn, presumably because of a decrease of the RAFT concentration in the polymer particles and hence low numbers of polymeric chains. However, our experimental results do not support this argument. The reason behind the negligible effect of reducing the surfactant concentration may be due to the increased size of the particles. In which, by increasing the particle radius the probability of exit decreases as $k_{dM} \alpha \ (1/r_s^2)$, and the probability for the entry rate increases. Thus, the change in these two events may sustain the polymeric chains in the particles. As equations 4-61 and 4-64 agree with the experimental data, they validate the assumption that the partitioning coefficient of the

RAFT agent between water and polymer phases is close to that for the monomer and hence a rapid thermodynamic equilibrium is achieved.

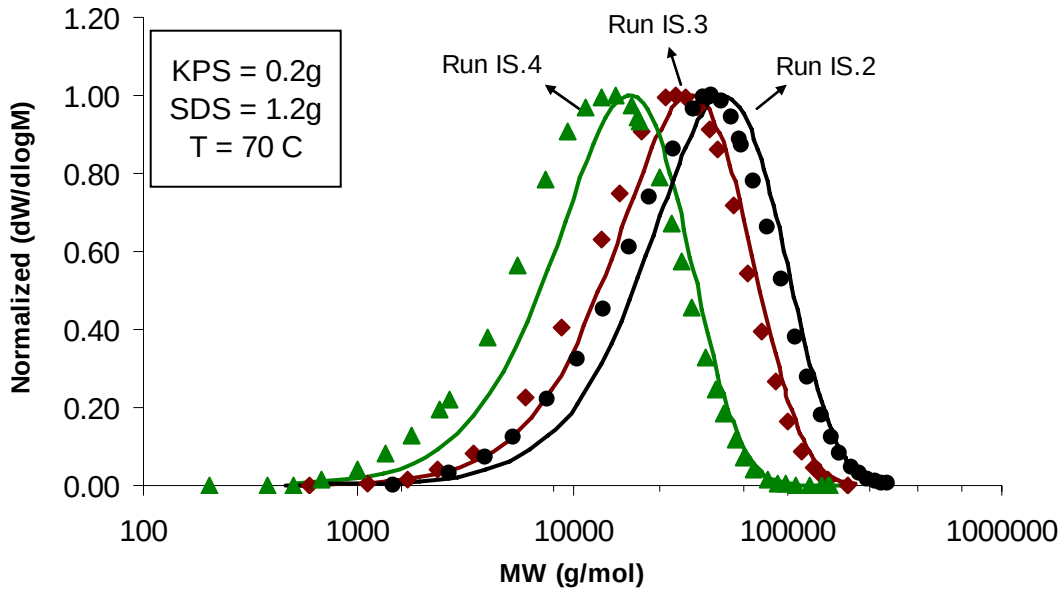

Figure 5-10: Effect of AR concentration on the MWD, samples were taken at the end of the polymerization. Legend: Run IS.2 (●); Run IS.3 (♦); Run IS.4 (▲); Run IS.5 (■); model predictions (–).

The MWDs measured by GPC were compared to the simulated results, for runs IS.2, IS.3 and IS.4, with the two distributions having similar characteristics as shown in Figure 5-10. It is very clear from Figure 5-10 that increasing AR concentration resulted in shifting the distribution to the left confirming the effect of increasing RAFT agent concentration on reducing the number average molecular weight Mn.

Due to its low transfer constant, the evolution of Mn (Figures 5-7 and 5-9) remains almost constant over the period of polymerization (conversion range) and no linear growth of Mn with conversion was observed. On the basis of this, one may argue that xanthates act as conventional irreversible chain transfer agents and they are not able to induce living characteristics on the polymerization. If the polymer chains are alive, they would continue to propagate with monomer and grow in length resulting in an increase in the Mn. This would have resulted in the distribution curves shifting to the right. Experimental data (Figure 5-11) obtained from semi-batch emulsion polymerization of styrene with O-ethylxanthyl ethyl propionate indicate that a high proportion of the

previously prepared polystyrene-xanthate chains act as a macro-RAFT agent which enable addition of more monomer when a subsequent batch of monomer is added.

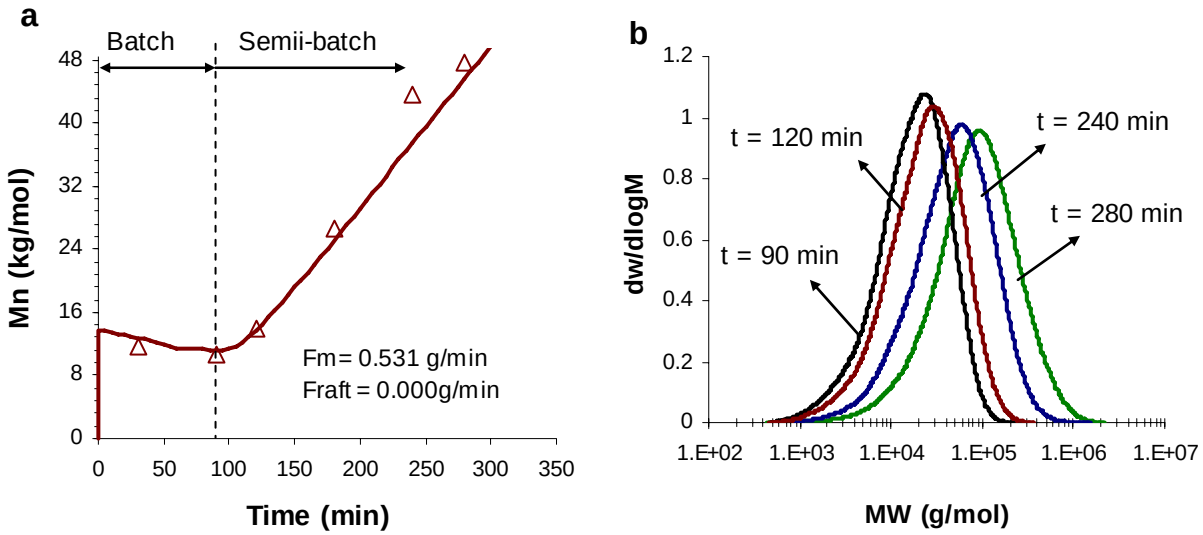

Figure 5-11: Experimental (symbols) and simulated (lines) MWD: (a) Number average molecular weight for batch and semi-batch emulsion polymerization; (b) Experimental MWD and molar chain extension with semi-batch emulsion polymerization of styrene with monomer flow rate = 0.531g/min.

Therefore, chain extension was successfully achieved, confirming that the previously prepared polymeric chains were able to regain radical activity and hence demonstrate the living nature of the polymer in the presence of a low active RAFT agent. In the event the previously prepared chains did not possess the living nature, the newly added monomers would have polymerized separately, resulting in high and uncontrolled molecular weight polydispersity or an increase in the MWD modality. The unimodal molecular weight distribution for the extended polystyrene-xanthate chains (Figure 5-11b) provides a confirmation that the previously prepared polystyrene-xanthate chains were involved in the second stage polymerization with the added monomer.

5.5.3 Effect of reaction conditions on particle size

In conventional free radical emulsion polymerization, particle size is affected mostly by surfactant concentration, while molecular weight distribution is affected mostly by the initiator concentration and temperature. While, in xanthate emulsion polymerization particle size is affected by AR, the initiator concentration, and reaction temperature.

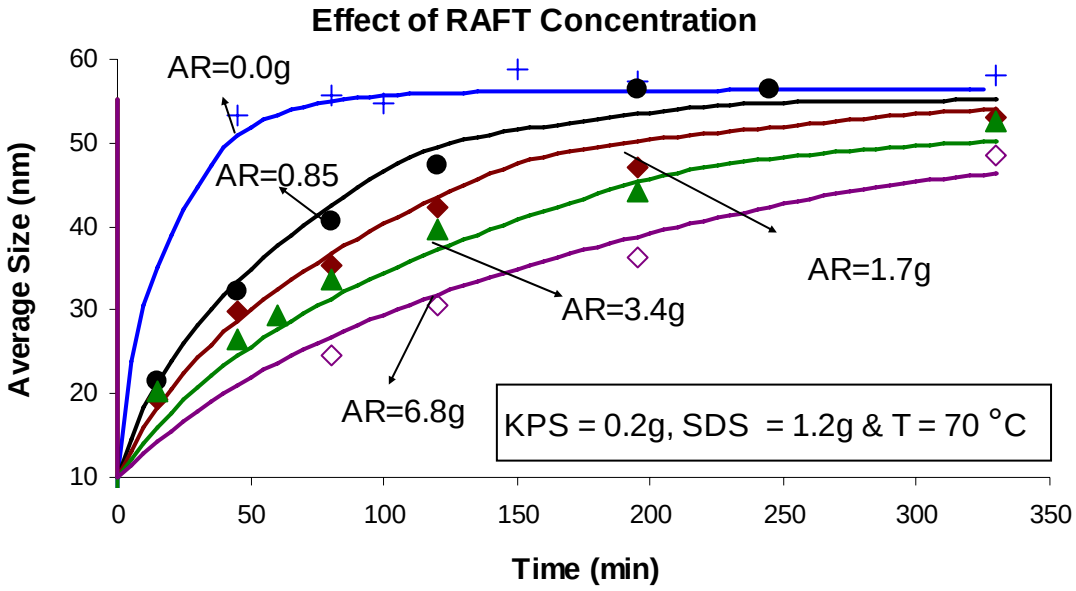

Figure 5-12: Effect of AR concentration on average particle diameter. Legend: Run IS.1 (+); Run IS.2 (●); Run IS.3 (♦); Run IS.4 (▲); Run IS.5 (◊); model predictions (—).

As illustrated in Figure 5-12, different particle sizes were obtained at 70^{o}C by varying AR concentration, while keeping the surfactant and initiator concentrations constant. Regarding the reduced particle size, as the concentration of RAFT agent increases, the concentration of the RAFT radicals increases. These radicals are able to exit from the particles resulting in the cessation of the process of particle growth, and hence a reduction in the average particle size.

The exited radical may enter an untouched micelle and form a new particle, thus causing an increase in the number of particles (Table 5-2). As the size of this newly formed particle is still small, it may enter into a large particle with no radical and promotes its growth in size. The process of exit and re-entry repeats itself as long as the source of these small radicals (unreacted RAFT agent) is present in the system. Therefore, in the presence of the RAFT agent there is a mixture of particles with differing sizes at the end of the reaction, resulting in a broadening of the particle size distribution (as illustrated in figures 5-15a and 5-15b).

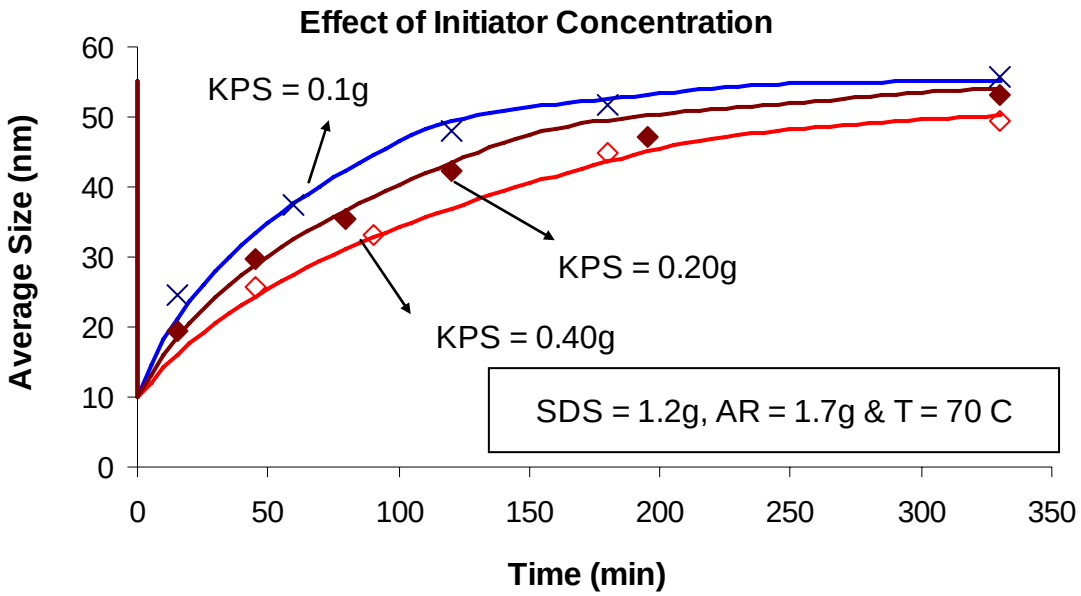

Figure 5-13: Effect of initiator concentration on average particle diameter. Legend: Run IS.3 (♦); Run IS.6 (×); Run IS.7 (◊); model predictions (—).

By keeping the AR and surfactant concentrations constant, the increased initiator concentration causes a decrease in the average particle size (Figure 5-13). An initiator-derived radical enters a particle when it attains the critical degree of polymerization in the aqueous phase. Such a radical is water insoluble and is not capable of exiting from the particle.

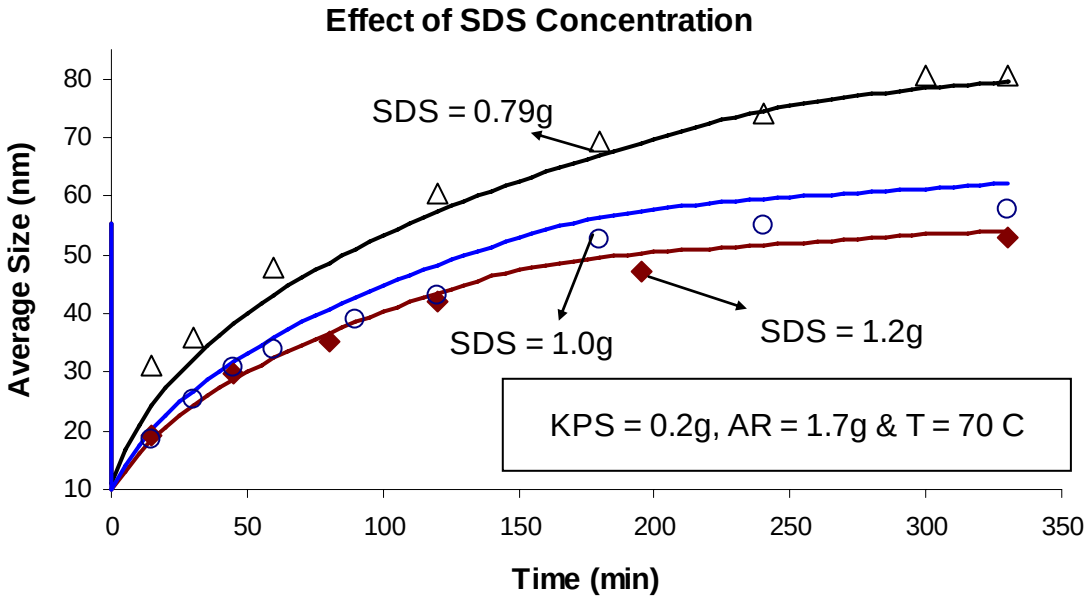

Figure 5-14: Effect of surfactant concentration on average particle diameter. Legend: Run IS.3 (♦); Run IS.9 (Δ); Run IS.12 (○); model predictions (—).

In combination with the increased polymerization rate, an increase in initiator concentration results in an increase in the number of initiator-derived radicals in the aqueous phase. This in turn results in a higher initial micellar nucleation and nucleation rate leading to an increase in the total number of particles (Table 5-1). As a result monomer conversion is increased (Figure 5-4) and average particle size decreased (figure 5-13). If the fragmentation of the intermediate radical in the particle resulted in an initiator derived radical no exit would occur and the propagation reaction would start resulting in an increase in the particle size.

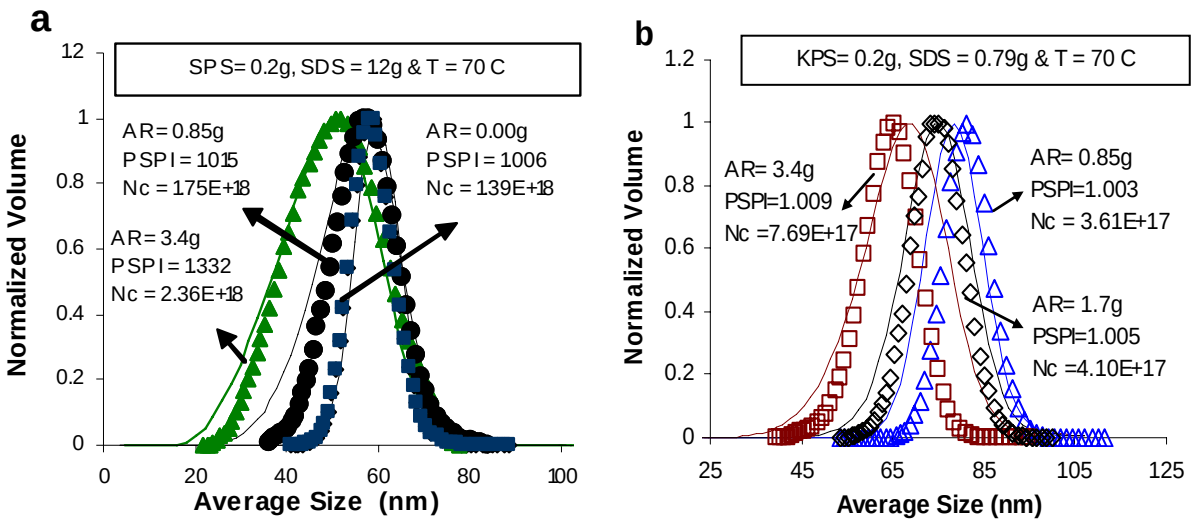

Figure 5-15: Experimental and Simulated PSD: (a) Effect of variable AR and high SDS concentration on particle size distribution; (b) Effect of variable AR and low SDS concentration on particle size distribution. All samples were taken at the end of polymerization. Legend: Run IS.1 (■); Run IS.2 (●); Run IS.4 (▲); Run IS.8 (∆); Run IS.9 (◊); Run IS.10 (□); model predictions (—).

Figure 5-14 shows that increasing surfactant concentration from 0.79g to 1.2g resulted in a dramatic decrease in the average particle size. A high surfactant concentration results in a large number of particles, and a small number of radicals per particle as shown in figure 5-16b Thus, each particle receives small number of radicals resulting in a particle with a low probability to grow in size. In figure 5-16a, the distribution is shifted to the right, giving a higher average particle size. The continuous increase in the particle size is due to the continuous particle growth driven by propagation reactions. At longer reaction times, the distributions approach each other, indicating that the polymerization rate at this stage is decreasing as a result of monomer depletion. On estimating the area under the curves, we conclude that the distributions presented in

Figure 5-16a have approximately the same area, indicating that a constant number of particles were formed.

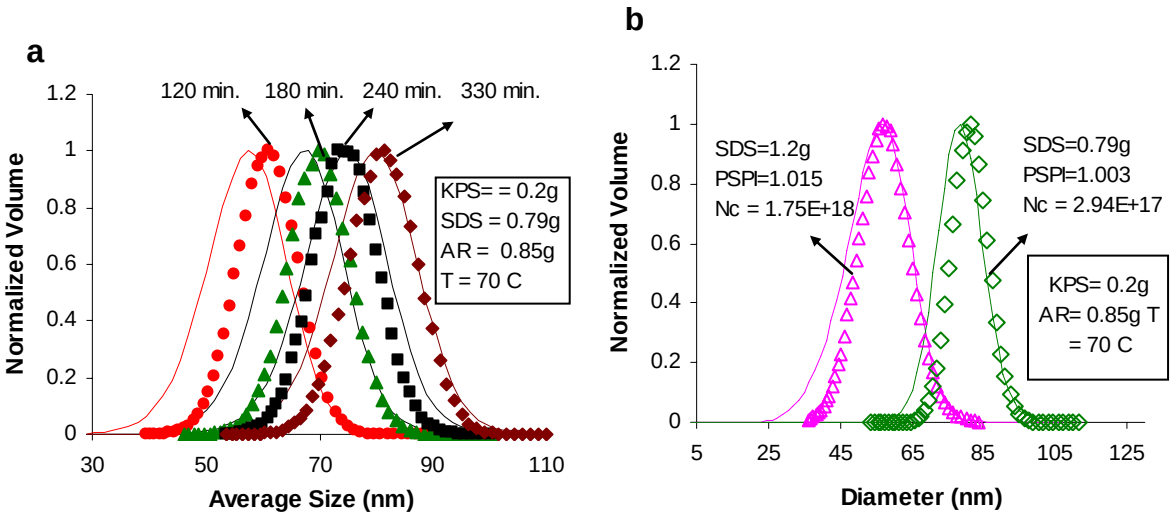

Figure 5-16: Experimental and Simulated PSD: (a) Effect of reaction time on particle size distribution. (b) Effect of surfactant concentration on particle size distribution. In figure (b) all samples were taken at the end of polymerization. Legend: Run IS.2 (Δ); Run IS.8 (◊); model predictions (—).

In Figures 5-15a, 5-15b and 5-16b, the polydispersity index, PSPI, indicates the spread of the distribution and is estimated as the ratio of the mean squared radius to the mean radius squared ($PSPI =< r^2 > / < r >^2$) and the number average radius was computed from:

$$< r >= \frac{\sum_{i=1}^{G} n(i) r(i)}{\sum_{i=1}^{G} n(i)}$$

So far it has been established that the PSD model predictions are in reasonable accord with experimental data. Consequently, the model can be used to study accurately the effect of operating conditions on the polymer properties. This information can then be used to conduct optimization studies and determine the optimal trajectories that produce polymer latex with specified properties.

5.6 Kinetic parameters and sensitivity analysis

Kinetic parameters such as the propagation rate coefficient (Buback *et al.*, 1995), the aqueous phase termination rate coefficient (Gilbert, 1995), the transfer rate coefficient

to monomer (Gilbert, 1995), and the addition rate coefficient of the RAFT agent (Adamy *et al.*, 2003; Smulders *et al.*, 2003) are known with precision and are not suitable as fitting parameters. The addition rate coefficient, k_{add}, controls the bimolecular reaction between the propagating free radicals and the initial or polymeric RAFT agents, while the forward and backward fragmentation rate coefficients (k_{frag} and k_{-frag}, respectively) control the disappearance rate of the intermediate radical. These rate coefficients determine the equilibrium. In typical RAFT process recipes, monomer concentration is usually two orders of magnitude greater than that for the RAFT agent. Thus, the probability that a small radical may propagate with a monomer is much greater than that for the addition to a RAFT agent (see Chapter 3). Therefore, addition of small radicals to a RAFT agent is assumed to be kinetically insignificant and the inverse transfer reaction is neglected (see Chapter 3).

Once the initial RAFT compound is consumed, the carbon-centered intermediate radical (species 4 in Scheme 4-2) produced is attached with two polymeric chains (P_n^* and P_m^*) of approximately the same length. As such, the two attached polymeric radicals can produce a radical with identical stability, and hence the symmetrical intermediate radical has no preference regarding which direction the fragmentation would take place ($k_{frag} \approx k_{-frag}$). The chain length of the two attached polymeric radicals to both sides of the intermediate radical may not be exactly similar. This may have no effect on the fragmentation direction, unless one of the two polymeric radicals is extremely short; in such a case, the larger chains are most likely to be released resulting in shifting the equilibrium toward the starting materials (Heuts *et al.*, 1999).

A severe retardation in the solution polymerization of styrene was observed with a high active RAFT agent (e.g. 2-phenylprop-2-yl dithiobenzoate (CDB)) (Monteiro and De Barbeyrac, 2001). Such retardation was attributed to the termination of the intermediate radicals with propagating radicals. For this particular RAFT agent, values of the order of 1×10^4 s^{-1} for the overall fragmentation rate have been reported (Kwak *et al.*, 2002; Monteiro and de Brouwer, 2001). In contrast, no retardation was observed in solution polymerization of styrene with O-ethylxanthyl ethyl propionate (Adamy *et al.*, 2003; Altarawneh *et al.*, 2007), indicating that the intermediate radical has no effect on the

polymerization rate and may have a fragmentation rate coefficient equal to or greater than the addition rate coefficient.

Due to the lower resonance of the ethoxide (on the xanthate) compared to the phenyl (on the CDB), the intermediate radical in the polymerization with xanthates may have a fragmentation rate coefficient higher than 1×10^4 s^{-1}. Work carried out by Heuts *et al.* (1999), revealed that larger chains attached to the intermediate radicals (unsymmetrical radicals) have a greater tendency to break, which suggests that the equilibrium is even shifted toward the starting materials. Based on this finding, the best descriptions of the experimental data were obtained with the optimum values for the backward and forward fragmentation rate coefficients of the unsymmetrical intermediate radicals and these are given in Table 5-2.

In a series of simulations, the sensitivity of the individual rate coefficients (especially the backward and forward fragmentation rate coefficients of the unsymmetrical intermediate radical PAR) toward an adequate description of the experimental data and the full MWD was tested. Significant variations in the coefficients were tested and have been reported elsewhere (Altarawneh *et al.*, 2007). Nevertheless, our model sensitivity will be tested against the variation of the overall fragmentation rate coefficient of the intermediate radicals (PAP, RAR, PAR), the forward and backward fragmentation rate coefficients (fragmentation direction) of the unsymmetrical intermediate radicals and how the size of these rate coefficients influences the simulated Mn, monomer conversion, and particle size as functions of time.

Initially, for a fixed concentration of RAFT agent, we varied k_{frag}^{PAR} and k_{-frag}^{PAR}, and investigated their influence on conversion, particle size and molecular weight evolution with time. It is noted that the summation of these two fragmentation rate coefficients is equal to the overall disappearance rate coefficient of the intermediate radical PAR ($k_{frag} = xk_{frag}^{PAR} + yk_{-frag}^{PAR}$, where $x + y = 1$). The experimental/simulation conditions given in Table 5-1 for run IS.3 were selected.

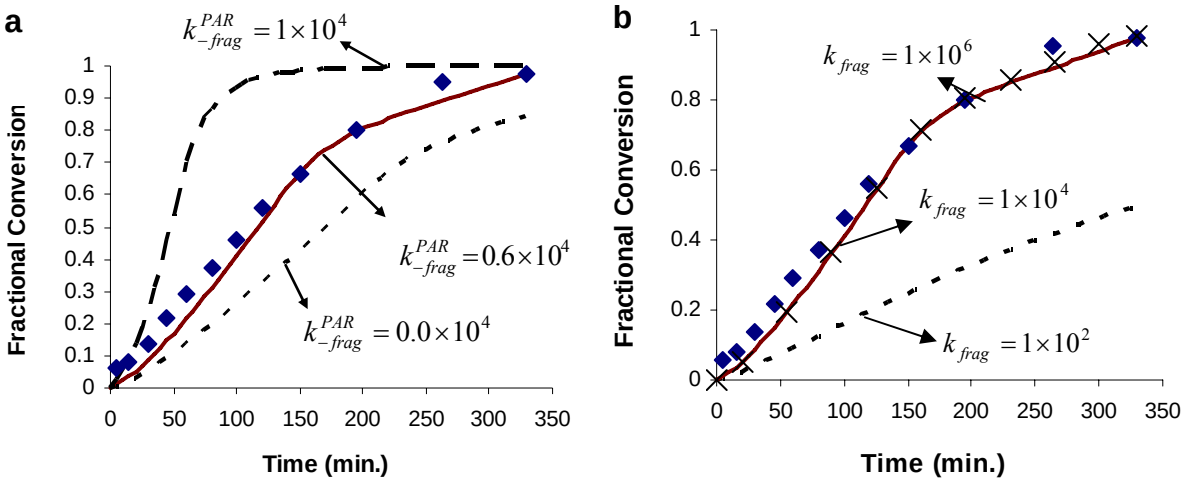

Figure 5-17: Simulated emulsion polymerization of styrene: (a) Effect of change in fragmentation direction on monomer conversion with overall fragmentation rate coefficient k_{frag} =1×10^4 s^{-1}; (b) Effect of overall fragmentation rate coefficient on monomer conversion with k_{-frag}^{PAR} =0.6×10^4 s^{-1}and k_{frag}^{PAR} =0.4×10^4 s^{-1}. Experimental data: marker symbols; model predictions (—).

Figure 5-17a clearly shows that the increase or decrease in the backward fragmentation rate coefficient of the intermediate radical PAR results in a substantial deviation from the experimental data and optimal predictions (bold line). The dashed line in Figure 5-17a represents the simulated monomer conversion for the case that the intermediate radical completely collapses toward the starting material (k_{-frag}^{PAR} = 1×10^4 s^{-1} and k_{frag}^{PAR} = 0 s^{-1}), thereby producing a polymeric radical that is incapable of exiting the particle. The system, under this condition, behaves similar to a RAFT-free system, indicated by high conversion (dashed line, Figure 5-17a), large particle size (dashed line, figure 5-18a) and high Mn (dashed line, Figure 5-19a). The simulated molecular weight (figure 5-19a) is close to that obtained experimentally for the RAFT-free system.

A corresponding variation of the forward fragmentation rate coefficient was carried out, and the results are shown in Figures 5-17a, 5-18a and 5-19a (dotted lines). For these simulations we set the backward fragmentation rate coefficient to zero (k_{-frag}^{PAR} = 0 s^{-1}and k_{frag}^{PAR} = 1×10^4 s^{-1}). Under these conditions, the intermediate radical undergoes a complete forward fragmentation, producing a macro RAFT agent (AP) and a small radical (R$^{\bullet}$) that is capable of exiting a particle and resulting in more retardation. It is not surprising that the particle size decreases by increasing the forward fragmentation

rate coefficient; this is mainly due to the increase in the exit rate in which the average number of the propagating radicals per particle is low.

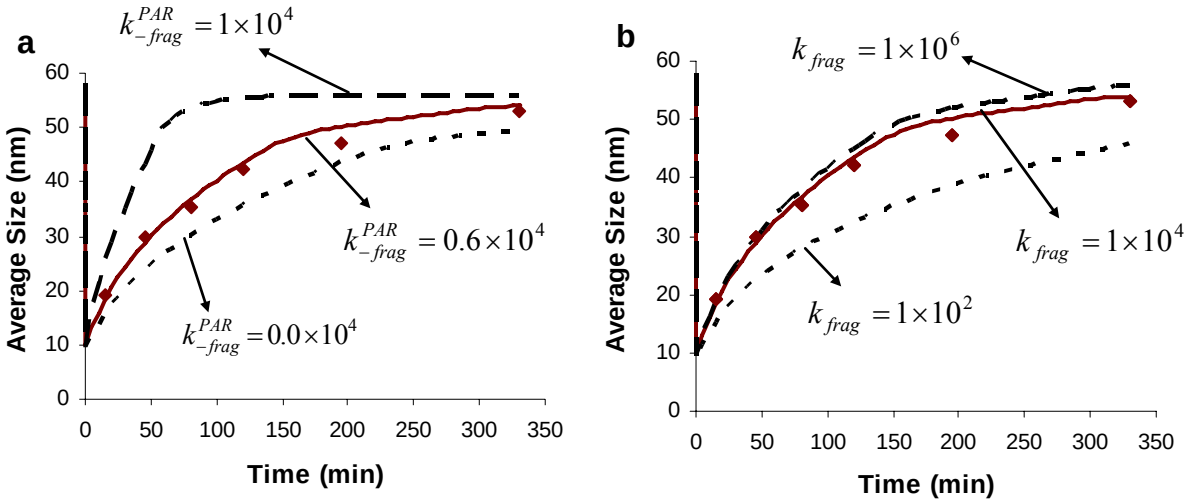

Figure 5-18: Simulated emulsion polymerization of styrene: (a) Effect of change in fragmentation direction on particle size with overall fragmentation rate coefficient k_{frag} =1×10^4 s^{-1}; (b) Effect of overall fragmentation rate coefficient on particle size with k_{-frag}^{PAR} = 0.6×10^4 s^{-1} and k_{frag}^{PAR} = 0.4×10^4 s^{-1}. Experimental data: marker symbols; model predictions (—).

The effect of increasing the forward fragmentation rate coefficient has a slight effect on the Mn as demonstrated by the dotted line in Figure 5-19a. Figure 5-17b shows the effect of the variation of *the overall fragmentation rate coefficient* (k_{frag}) by a factor of 100 to demonstrate how sensitive the conversion–time relation is to a change in (k_{frag}). Figures 5-17b, 5-18b and 5-19b clearly indicate that increasing (k_{frag}) has no effect on monomer conversion, particle size and number average molecular weight for all (k_{frag}) values higher than the addition rate coefficient. The decrease of the monomer conversion and particle size is due to the long retention time of the propagating radicals in the intermediate radical. Figures 5-17b and 5-18b show that the evolutions of the monomer conversion and particle size are very sensitive to decreasing the overall fragmentation rate coefficients for all values lower than the addition rate coefficient. In contrast, no changes in monomer conversion and particle size were predicted for all values higher than the addition rate. Figure 5-19b shows that the time evolution of Mn is not sensitive to either an increase or decrease in the overall fragmentation rate coefficient, indicating that for $(k_{frag} > 0)$ successful transfer reactions occur.

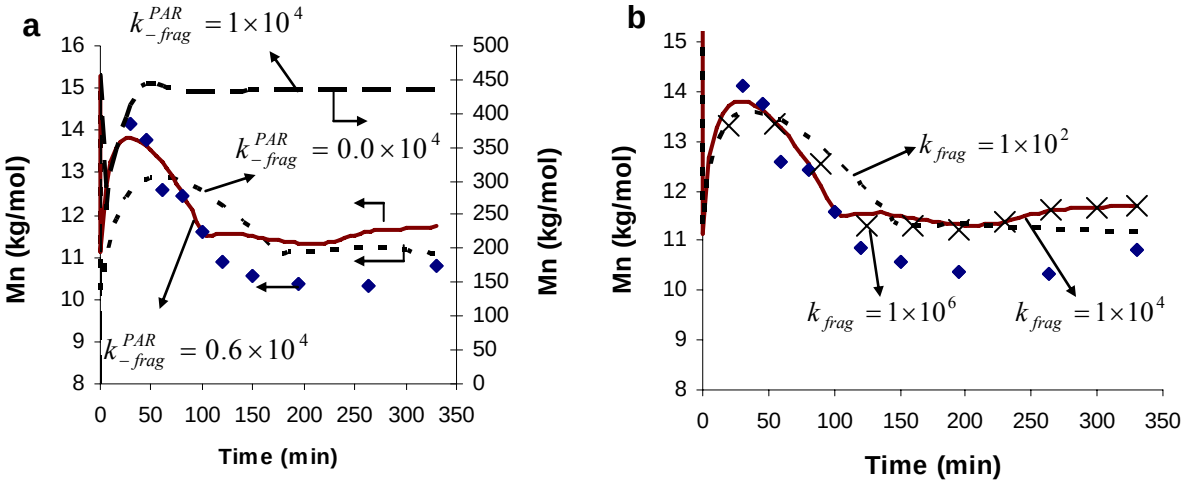

Figure 5-19: Simulated emulsion polymerization of styrene: (a) Effect of change in fragmentation direction on Mn with overall fragmentation rate coefficient k_{frag} =1×10^4 s^{-1}; (b) Effect of overall fragmentation rate coefficient on Mn with k_{-frag}^{PAR} = 0.6×10^4 s^{-1}and k_{frag}^{PAR} = 0.4×10^4 s^{-1}. Experimental data: marker symbols; model predictions (—).

It can be thus inferred that, from a consideration of the Mn alone, the value of the forward (k_{frag}^{PAR}) and backward (k_{-frag}^{PAR}) fragmentation rate coefficients cannot be derived; that is, only a careful analysis of the Mn, monomer conversion, and particle size evolution with time in parallel can yield reliable rate coefficients. The second important confirmation of the value of the fragmentation rate coefficients is from an assessment of their sensitivity toward a change in experimental conditions. In our work, this validation was achieved by a variation of the RAFT agent, initiator and surfactant concentrations.

5.7 Conclusions

A mathematical model based on zero-one kinetics for *ab initio* polymerization of styrene was developed to account for the presence of a xanthate-based transfer agent (RAFT agent). The model was designed for low active RAFT agents, such as xanthates, as they can be directly implemented in emulsion polymerization. The model accounts for the effect of the RAFT agent on the polymerization rate, number average molecular weight, weight average molecular weight, molecular weight distribution, polydispersity

index, particle average radius, and particle size distribution. The validation of the high-order mathematical model developed in Chapter 4 was carried out in an automated reactor facility, over a wide range of operating conditions. A detailed description of the design and installation of the different components in the facility was presented first. Then, the experimental model validation was carefully conducted for the emulsion polymerization of styrene in batch operating mode.

The model was validated against experimental data obtained in our laboratory in terms of polymerization rate, molecular weight distribution and particle size distribution. O-ethylxanthyl ethyl propionate was used as a xanthate based transfer agent (RAFT agent, AR) in the *ab initio* emulsion polymerization of styrene. The polymerizations were carried out using variable amounts of AR agent, surfactant (SDS) and initiator (KPS) at different reaction temperatures (Table 5-1). The polymerization rate was found to be retarded by increasing the concentration of AR; the observed retardation was attributed to small radicals exiting from the polymeric particles.

The number average molecular weight decreased with an increase in RAFT agent in such a manner that it could be controlled by manipulating the initial amount of the RAFT agent. Increasing the initiator concentration had a small effect on the number average molecular weight, while the polymerization rate was significantly improved. The surfactant concentration had insignificant effects on the MWD with an increase in polymerization rate with surfactant concentration. The model was able to accurately predict the effects of the RAFT agent, the emulsifier, and the initiator with respect to the key polymer properties.

From the experimental observations and theoretical predictions, it became clear that the model is capable of adequately predicting important polymer attributes such as the PSD, MWD and conversion, over a wide range of reactor operating conditions. No adjustable parameters were used in the model equations, as they were obtained from the available literature for styrene/polystyrene polymerization system. The investigation showed that a variety of outcomes could be obtained by varying the operating conditions. The model will be used in Chapter 6 to investigate RAFT emulsion polymerization when operating under semi-batch conditions. Additionally it will be used for the purpose of optimizing

the process and developing optimal trajectories to produce a polymer with specific PSD and MWD characteristics.

Table 5-1: RAFT-emulsion polymerization experimental results

Run No.	SDS (g)	KPS (g)	AR (g)	T (^oC)	Conversion		Mn $\times 10^{-3}$ (g/mol)		Avg. D (nm)		Nc$\times 10^{-18}$
					Exp.	Sim.	Exp	Sim.	Exp.	Sim.	
IS. 1	1.2	0.2	0.0	70	0.97	0.99	421	369	58.1	56.3	1.39
IS. 2	1.2	0.2	0.85	70	0.96	0.97	19.8	21.0	56.4	55.1	1.75
IS. 3	1.2	0.2	1.70	70	0.95	0.91	10.8	11.7	53.1	52.6	1.90
IS. 4	1.2	0.2	3.40	70	0.79	0.85	5.40	5.79	52.7	50.2	2.36
IS. 5	1.2	0.2	6.80	70	0.56	0.70	3.31	2.92	48.6	46.3	3.17
IS. 6	1.2	0.1	1.7	70	0.91	0.86	11.6	11.3	55.7	54.9	1.70
IS. 7	1.2	0.4	1.7	70	0.97	0.99	9.58	10.1	49.3	50.2	2.09
IS. 8	0.79	0.2	0.85	70	0.91	0.88	-	-	80.6	78.8	0.361
IS. 9	0.79	0.2	1.7	70	0.85	0.81	10.3	11.2	74.2	74.8	0.410
IS. 10	0.79	0.2	3.4	70	0.72	0.69	5.17	5.63	69.2	75.9	0.769
IS. 11	1.0	0.2	1.70	80	0.99	0.95	9.90	10.3	70.3	65.0	-
IS. 12	1.0	0.2	1.70	70	0.86	0.90	11.6	10.8	57.6	62.2	-
IS. 13	1.0	0.2	1.70	60	0.44	0.41	12.5	12.9	41.1	46.3	-
IS. 14	1.0	0.2	1.70	50	0.16	0.11	15.0	13.7	32.3	28.5	-

***The number of particles per unit volume was calculated from the conversion and average diameter data for all samples taken at the end of the reaction.**

Table 5-2: Parameters used for simulating RAFT-styrene emulsion polymerization

Parameter	value	ref
a_s	42×10^{-18}	(Gilbert, 1995)
C_{tr}	$1.414\exp(-1870/RT)$	(Adamy *et al.*, 2003; Smulders, 2002)
cmc	0.003	(Gilbert, 1995)
$C^{AR}_{w\_sat}$	0.002 at 50 ^{o}C	(Smulders *et al.*, 2003)
$C^{M}_{p\_sat}$	*5.5*	(Gilbert, 1995)
$C^{M}_{w\_sat}$	$e^{(-1.514-1259/T)}$	(Gilbert, 1995)
d_p	*1050.1-0.621T*	(Gilbert, 1995)
d_m	923.6-0.887T	(Zeaiter *et al.*, 2002)
d_{RAFT}	1.12	This work
D_w	1.55×10^{-7}	(Gilbert, 1995)

j_{crit}	5	(Coen *et al.*, 1998; Gilbert, 1995)
k_{tr}	$k_p 10^{-0.658} e^{(-23400/RT)}$	(Gilbert, 1995)
$k_{t,aq} = k_{to}$	6.8×10^7	(Gilbert, 1995; Zeaiter *et al.*, 2002)
k_{po}	$1.259 \times 10^7 e^{(-29000 / RT)}$	(Gilbert, 1995; Zeaiter *et al.*, 2002)
k_d	$8 \times 10^{15}\ e^{(-13500 / RT)}$	(Gilbert, 1995; Zeaiter *et al.*, 2002)
k_{frag}	$>10^4$	(Altarawneh *et al.*, 2008)
k_{frag}^{PAP}	$0.5 \times k_{frag}$	(Altarawneh *et al.*, 2008)
k_{-frag}^{PAP}	k_{frag}^{PAP}	(Altarawneh *et al.*, 2008; Smulders, 2002)
k_{frag}^{RAP}	$0.6 \times k_{frag}$	(Altarawneh *et al.*, 2008)
k_{-frag}^{RAP}	$0.4 \times k_{frag}$	(Altarawneh *et al.*, 2008)
k_{frag}^{RAR}	$k_{-frag}^{RAR} = k_{frag}^{PAP}$	(Altarawneh *et al.*, 2008; Smulders, 2002)
k_{frag}^{PAR}	$0.4 \times k_{frag}$	(Altarawneh *et al.*, 2008)
k_{-frag}^{PAR}	$0.6 \times k_{frag}$	(Altarawneh *et al.*, 2008)
K_{wp}^{M}	$C_{w\_sat}^{M} / C_{p\_sat}^{M}$	(Zeaiter *et al.*, 2002)
K_{wp}^{AR}	K_{wp}^{M}	assumed
k_{add}	$2k_p C_{tr}$	(Moad *et al.*, 2003; Smulders *et al.*, 2003)
$k_{p,aq}^{1}$	$4k_p$	(Gilbert, 1995; Prescott *et al.*, 2006)
$k_{p,aq}^{2}$	$2k_p$	(Zeaiter *et al.*, 2002)
$k_{p,aq}^{3}$	k_p	(Zeaiter *et al.*, 2002)
$k_{p,aq}^{4}$	$k_{p,aq}^{3}$	(Zeaiter *et al.*, 2002)
k_p^R	$4k_p$	(Altarawneh *et al.*, 2008; Prescott *et al.*, 2006)
n_{agg}	60	(Gilbert, 1995; Zeaiter *et al.*, 2002)
z	3	(Coen *et al.*, 1998; Gilbert, 1995)
σ	6.02×10^{-9}	(Zeaiter *et al.*, 2002)
α	7.4×10^{-9}	(Zeaiter *et al.*, 2002)

5.8 References

Adamy, M.; Van Herk, A.M.; Destarac, M. and Monteiro, M.J., 2003. Influence of the chemical structure of MADIX agents on the RAFT polymerization of styrene. *Macromolecules*, 36(7): 2293.

Altarawneh, I.S.; Gomes, V.G. and Srour, M.S., 2008. The Influence of Xanthate-Based Transfer Agents on Styrene Emulsion Polymerization: Mathematical Modeling and Model Validation. *Macromolecular Reaction Engineering*, 2(1): 58.

Altarawneh, I.S.; Srour, M. and Gomes, V.G., 2007. RAFT with Bulk and Solution Polymerization: An Approach to Mathematical Modelling and Validation. *Polymer-Plastics Technology and Engineering*, 46: 1.

Buback, M.; Gilbert, R.G.; Hutchinson, R.A.; Klumperman, B.; Kuchta, F.D.; Manders, B.G.; O'Driscoll, K.F.; Russell, G.T. and Schweer, J., 1995. Critically evaluated rate coefficients for free-radical polymerization, 1. Propagation rate coefficient for styrene. *Macromolecular Chemistry and Physics*, 196(10): 3267.

Coen, E.M.; Gilbert, R.G.; Morrison, B.R.; Leube, H. and Peach, S., 1998. Modelling particle size distributions and secondary particle formation in emulsion polymerisation *Polymer*, 39(26): 7099.

Gilbert, R.G., 1995. Emulsion polymerization: a mechanistic approach. Academic Press, London.

Heuts, J.P.A.; Davis, T.P. and Russell, G.T., 1999. *Macromolecules*, 32: 6019.

Kwak, Y.; Goto, A.; Tsujii, Y.; Murata, Y.; Komatsu, K. and Fukuda, T., 2002. A kinetic study on the rate retardation in radical polymerization of styrene with addition-fragmentation chain transfer. *Macromolecules*, 35(8): 3026.

Moad, G.; Mayadunne, R.T.A.; Rizzardo, E.; Skidmore, M. and Thang, S.H., 2003. Kinetics and mechanism of RAFT polymerization. *ACS Symposium Series*, 854(Advances in Controlled/Living Radical Polymerization): 520.

Monteiro, M.J.; Adamy, M.M.; Leeuwen, B.J.; van Herk, A.M. and Destarac, M., 2005. A "living" radical ab initio emulsion polymerization of styrene using a fluorinated xanthate agent. *Macromolecules*, 38(5): 1538.

Monteiro, M.J. and De Barbeyrac, J., 2001. Free-radical polymerization of styrene in emulsion using a reversible addition - Fragmentation chain transfer agent with a low transfer constant: Effect on rate, particle size, and molecular weight. *Macromolecules*, 34(13): 4416.

Monteiro, M.J. and de Brouwer, H., 2001. Intermediate radical termination as the mechanism for retardation in reversible addition-fragmentation chain transfer polymerization. *Macromolecules*, 34(3): 349.

Prescott, S.W.; Ballard, M.J.; Rizzardo, E. and Gilbert, R.G., 2006. Rate optimization in controlled radical emulsion polymerization using RAFT. *Macromolecular Theory and Simulations*, 15(1): 70.

Smulders, W.W., 2002. Macromolecular architecture in aqueous dispersions: 'living' free-radical polymerization in emulsion. Ph.D. Thesis, Technische Universiteit Eindhoven, Eindhoven, Neth.

Smulders, W.W.; Gilbert, R.G. and Monteiro, M.J., 2003. A kinetic investigation of seeded emulsion polymerization of styrene using reversible addition-fragmentation chain transfer (RAFT) agents with a low transfer constant. *Macromolecules*, 36(12): 4309.

Zeaiter, J.; Romagnoli, J.A.; Barton, G.W.; Gomes, V.G.; Hawkett, B.S. and Gilbert, R.G., 2002. Operation of semi-batch emulsion polymerisation reactors: Modelling, validation and effect of operating conditions. *Chemical Engineering Science*, 57(15): 2955.

Chapter Six

Polymer Chain Extension

Chapter 6
Polymer Chain Extension

Abstract

In this Chapter semi-batch emulsion polymerization of styrene with O-ethylxanthyl ethyl propionate is investigated using the previously developed model. First, a short review on the application of RAFT process in emulsion polymerization is presented. Then the experimental approach used in this Chapter is discussed. The effects of the transfer agent (AR), surfactant, initiator and temperature were investigated. Monomer conversion, MWD and PSD were found to be strongly affected by the monomer feed rate. The polymerization rate (Rp), number average molecular weight (Mn) and particle size (<r>) decreased with increasing AR. With increases in surfactant and initiator concentrations Rp was found to increase, while in the batch pre-period an increase in temperature led to an increase in Rp as well as decrease in both Mn and <r>.

In semi-batch mode, Mn and <r> increased with an increase in the monomer flow rate. By feeding the RAFT agent along with the monomer ($F_M/F_{AR} = N_{Mo}/N_{ARo} = 100$), Mn attained a constant value proportional to monomer/RAFT molar ratio. The observed retardation in polymerization and growth rates is due to the exit and re-entry of small radicals. It has been found that living polymerization can be attained by operating under semi-batch conditions. Thus, chain extension was successfully achieved in semi-batch mode. The simulations compared well with our experimental data and the model was able to accurately predict monomer conversion, Mn, MWD and PSD of polymer products. Our simulations and experimental results show that the monomer feed rate is suitable for controlling the PSD, and the initial concentration and the feed rate of AR are suitable for controlling the MWD and PSD.

6.1 Introduction

Emulsion polymerization is one the most versatile processes for manufacturing synthetic polymers, with products ranging from elastomeric lattices for coatings, bulk

plastics, paints, adhesives to resins. The quality of the polymer latex strongly depends on the process operation; hence, tailor made polymers are most often produced in a semi batch manner. Due to their flexibility in product design and process control, semi-batch emulsion polymerization processes are being used widely for the production of many varieties of commercial commodities, as well as for high value-added products. The process is preferred due to its substantial technical, commercial, and environmental benefits. The process enables control of polymer molecular weight (MWD) and particle size (PSD) distributions, which strongly affect product mechanical, rheological, thermal and chemical properties. Although early studies on solution, bulk and even batch emulsion polymerizations were not overly promising, semi-batch emulsion polymerization offers significant benefits to living polymerization systems. It offers faster polymerization rate while maintaining good temperature control, negligible change of viscosity with conversion, and various environmental advantages. Further, this technique offers more control variables (higher degree of freedom) to be manipulated throughout the reaction. Hence, it guarantees a good control over polymer molecular weight, polymerization rate and particle size distribution via the manipulation of, for example, monomer feed rate.

MWD is commonly controlled using chain transfer agents such as mercaptans (Gugliotta *et al.*, 2001; Mendoza *et al.*, 2000) or living free radical polymerization (Matyjaszewski and Xia, 2001; Moad *et al.*, 2005; Schulte *et al.*, 2004), while PSD is controlled by surfactants and optimal process conditions (Gilbert, 1995; Zeaiter *et al.*, 2002). Despite its successful application with solution and bulk techniques, RAFT polymerization suffers serious problems in emulsions, and hence RAFT emulsion polymerization is yet to be established. Lack of colloidal stability, phase separation, rate retardation, and poor molecular weight control especially when a high active RAFT agent (with Ctr>>1) is used have been reported (Charmot *et al.*, 2000; Chiefari *et al.*, 1998; Monteiro and De Barbeyrac, 2001; Monteiro *et al.*, 2000; Prescott *et al.*, 2002a; Prescott *et al.*, 2002b). A successful RAFT LFRP in emulsion requires that the transfer agent distributes itself between the monomer droplets, the aqueous phase, and micelles, and be transported from the droplets through the aqueous phase to the particles. Difficulties in transporting RAFT agent into polymer particles were overcome by the use of low active RAFT agents such as xanthates (Altarawneh *et al.*, 2008; Charmot *et al.*, 2000; Monteiro and De Barbeyrac, 2001; Smulders *et al.*, 2003), or by special

interventions, e.g., the use of cyclodextrins (Apostolovic *et al.*, 2006), the use of an organic co-solvent (Prescott *et al.*, 2002b) and the use of water soluble monomers to produce short stabilizing RAFT agents (Ferguson *et al.*, 2005). Moad *et al*. (2000) overcame the problem of phase separation (layer formation) by using a semi-batch process, where all the RAFT agent with surfactant (sodium dodecyl sulfate, SDS) and water soluble initiator (potassium persulfate, KPS), in the presence of small amount of the monomer, was polymerized at 80^{o}C for 40 min, after which the monomer was fed in slowly. By adopting this approach, polymerization during the feeding stage occurred in the absence of monomer droplets, resulting in good control over the MWD.

Xanthates were used in *ab initio* emulsion polymerization to synthesize novel nanostructures with a predetermined molecular weight (Altarawneh *et al.*, 2008; Charmot *et al.*, 2000; Monteiro and De Barbeyrac, 2001; Smulders *et al.*, 2003). Since most of the polymeric chains carry the RAFT moiety, block copolymers can be produced (Smulders and Monteiro, 2004). In the work of Smulders *et al*. (2003), a surprising reduction in the entry rate coefficient was observed when O-ethylxanthyl ethyl propionate was used in seeded emulsion polymerization of styrene. The author attributed this to surface activity of the used xanthate RAFT agent molecules, in which they reside near the surface of the particle. Since the entered z-mers are also surface active species, they will have a high probability of transfer to the RAFT agent, resulting in possible exit instead of propagation into the interior of the particle. Hence, exit of the radical resulting from the transfer reaction between a z-mer and the RAFT agent at the surface will result in a decrease in the effective rate of entry.

Most kinetic studies have focused on batch heterogeneous polymerizations with different kinds of RAFT agents (Hermanson *et al.*, 2006; Luo *et al.*, 2006; Peklak and Butte, 2006; Prescott, 2003; Prescott *et al.*, 2006; Smulders *et al.*, 2003). These studies helped explain the different competing mechanisms involved, and led to a number of mathematical models with varying degrees of complexity capable of predicting the key product attributes. Unfortunately, comprehensive kinetic models accounting for the application of the RAFT based transfer agents in batch and/or semi-batch emulsion polymerization is lacking, and the differences between batch and semi-batch RAFT emulsion are still largely unexplored in literature.

Modelling of RAFT emulsion polymerization to accurately predict polymer architectural properties (MWD and PSD) is of great practical significance as it is crucial in design, scale-up, and developing desirable new products for the market. It is reasonable that living polymerization could be approached with a low active RAFT agent if the rate of transfer over the rate of propagation is increased via controlled feed rate of monomer (Smulders *et al.*, 2003). Thus, this work aims to address the application of low active RAFT based transfer agent (xanthate) in semi-batch emulsion polymerization of styrene with controlled monomer feed. For precise control of product properties and process understanding, a dynamic reactor model for RAFT emulsion polymerization combining conventional emulsion polymerization kinetics (Coen *et al.*, 1998; Gilbert, 1995; Zeaiter *et al.*, 2002) with RAFT process kinetics (Altarawneh *et al.*, 2007; Hermanson *et al.*, 2006; Moad *et al.*, 2005; Peklak and Butte, 2006; Smulders *et al.*, 2003) was developed (presented in Chapter 4) and published elsewhere (Altarawneh *et al.*, 2008).

6.2 Experimental

6.2.1 Materials

The RAFT agent **(O-ethylxanthyl ethyl propionate)** was synthesized in our laboratory according to the procedure described in Section 5-3-2 Chapter 5. Milli-Q-standard water was used, and dissolved oxygen was removed by bubbling high purity nitrogen through the mixture of the RAFT agent and monomer for one hour. Styrene monomer, initiator (potassium persulfate), purification columns, and the surfactant (sodium dodecyl sulfate) were obtained from Sigma-Aldrich (USA). Styrene was purified by passing through an inhibitor-removal column. The purification was repeated twice to ensure high purity. All other chemicals were used as received.

6.2.2 Polystyrene chain extension with polystyrene

Ab initio semi-batch emulsion polymerizations were carried out under slight nitrogen pressure in a 1L laboratory reactor equipped with a magnetically driven agitator with a pitched blade impeller operated at 350 rpm. Experiments were conducted with 520g

water, 17.8g styrene (M_o = 0.17mol), 0.377g RAFT agent (AR_o = 0.0017mol) and with varying amounts of initiator and surfactant at 70^{o}C and 80^{o}C. The remaining monomer was added to the reactor via a metering pump at variable flow rates. A temperature controlled circulator (Julabo, USA) provided heating/cooling flows through the external reactor jacket was used to maintain reaction temperatures at desired levels. The preheated solution of initiator and buffer in water (at the reaction temperature) was added to trigger the reaction. In the first stage, all the RAFT agent with surfactant (SDS) and water soluble initiator (KPS), in the presence of the monomer (17%), was polymerized for 90 min (batch pre-period) under a slight nitrogen pressure. Thereafter, the monomer was fed continuously into the reactor. Samples were taken periodically to monitor conversion, MWD and PSD. Our procedural details are given in Table 6-1

6.2.3 Analytical techniques

Monomer conversion was gravimetrically determined off-line with samples from the reactor. The dried polymer was dissolved in tetrahydrofuran (THF, Fluka) to a concentration of 1mM. Analyses were carried out using a high temperature chromatography system (PL-GPC 120) with a PLgel guard 5µm 50×7.5mm column connected in series with two PLgel (Mixed-C 10µm 300×7.5mm) columns (PL, Polymer Laboratories) at 40^{o}C. THF was used as the eluent at a flow rate of 1ml/min. Calibration was carried out using narrow-distribution polystyrene standards (with molecular weights 580 to 7.1×10^6 g/mol). A PL Data stream unit was used for data acquisition and the data were processed using Cirrus^{TM} GPC software. The PSD and average particle size were measured using Polymer Laboratory Particle Size Distribution Analysis (PL-PSDA Model PL-DG2). It uses the principle of packed column hydrodynamic chromatography (HDC) to separate particles in the interstitial void space created by the solid spherical column packing material. The particles eluting from the column are detected using a UV detector.

6.3 Results and discussions

6.3.1 Monomer conversion

Monomer conversion, defined as the mass ratio of the polymer produced to the total amount of monomer added till time t, is a key factor in determining product properties. Monomer conversion was estimated based on gravimetric measurement of the sample solid content:

$$X = \frac{(\text{Weight of dried sample / weight of sample}) - \text{Solid fraction}}{\text{Weight of the monomer fraction in the reactor}}$$

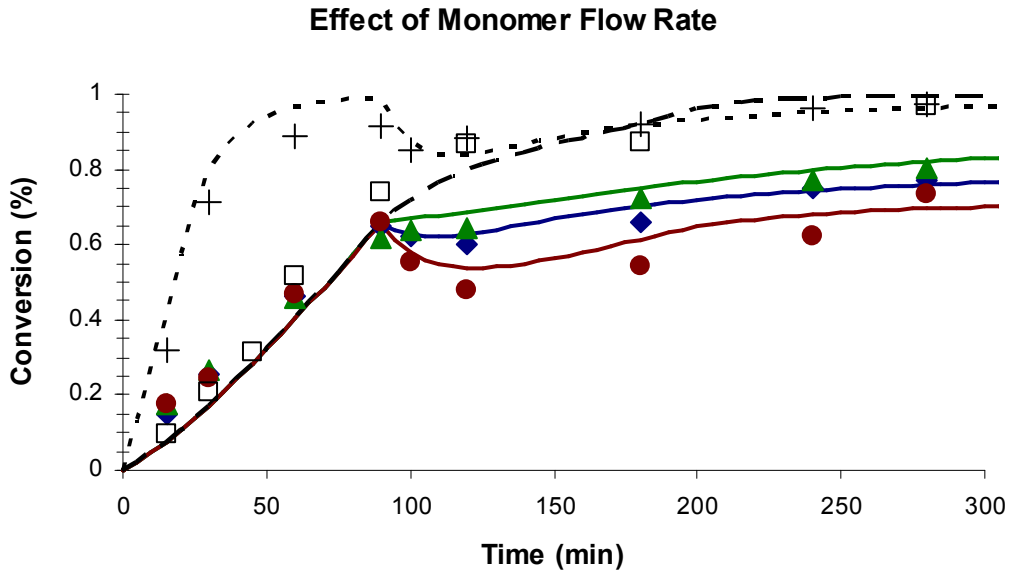

Figure 6-1: Effect of monomer flow rate (F_M) on the overall monomer conversion for polymerization at 70°C. Legend: Run IT.1 (+); Run IT.2 (□); Run IT.3 (▲); Run IT.4 (♦); Run IT.5 (●); and model simulations (–).

In the dynamic model, monomer and AR conversions are calculated using equations 4.56 and 4.57. Model predictions were compared with experiments for semi-batch emulsion polymerization. Figure 6-1 illustrates monomer conversion as a function of time at variable monomer feed rates, while Fig. 6-2 presents the impact of feeding the RAFT agent along with the monomer. In the absence of AR (dotted curve in Fig. 6-1), a high monomer conversion of about 91% was achieved (Run IT.1) at the end of the batch pre-period. At this stage, the total amount of monomer available for polymerization in the system is low (Fig. 6-3a). Hence polymer volume fraction is high

($\Phi = 1 - (C_P M_w^M / d_m)$) resulting in glassy particles; under these conditions secondary nucleation is expected unless the free surfactant concentration is higher than cmc.

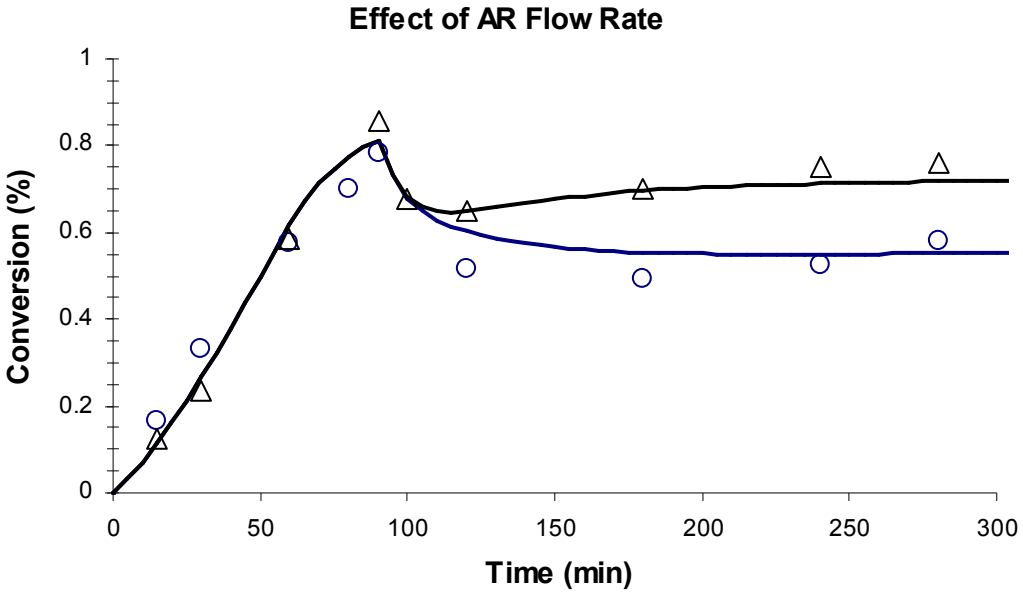

Figure 6-2: Effect of RAFT agent flow rate (F_{AR}) on monomer conversion. Legend: Run IT.7 (Δ); Run IT.8 (○); and model simulations (–).

Shortly after the initiating monomer feed, a sudden decrease in monomer conversion was observed. The sudden drop in monomer conversion is due to the accumulation of monomer in the system (Fig. 6-3a) which results in an increase in monomer concentration inside the particles. Compared with the control experiment (Run IT.1), introducing AR during the batch pre-period resulted in a dramatic decrease in polymerization rate as shown in Fig. 6-1 (Runs IT.2, IT.3, IT.4 and IT.5). In the batch experiment (Run IT.2, dashed curve in Fig. 6-1), as monomer feed rate (F_M) is zero, monomer conversion continues to increase until it approaches that for the control experiment.

The observed retardation indicates that a significant amount of small radicals ($R^\bullet$) generated by chain transfer to AR were unable to reinitiate polymerization. The ability of such small radicals to reinitiate polymerization inside particles depends mainly on the time they reside in the particles. Thus, the observed retardation is due to the exit of small radicals from particles resulting in reduction in average number of radicals per particle. In the presence of AR, a significant impact of feeding more monomer on the

polymerization rate was observed (Runs IT.3, IT.4 and IT.5 in Fig. 6-1) in which the final monomer conversions are below the batch values. In these experiments, the observed retardation during the batch pre-period is mainly due to the exit of small radicals formed by exchange with AR and by transfer to monomer.

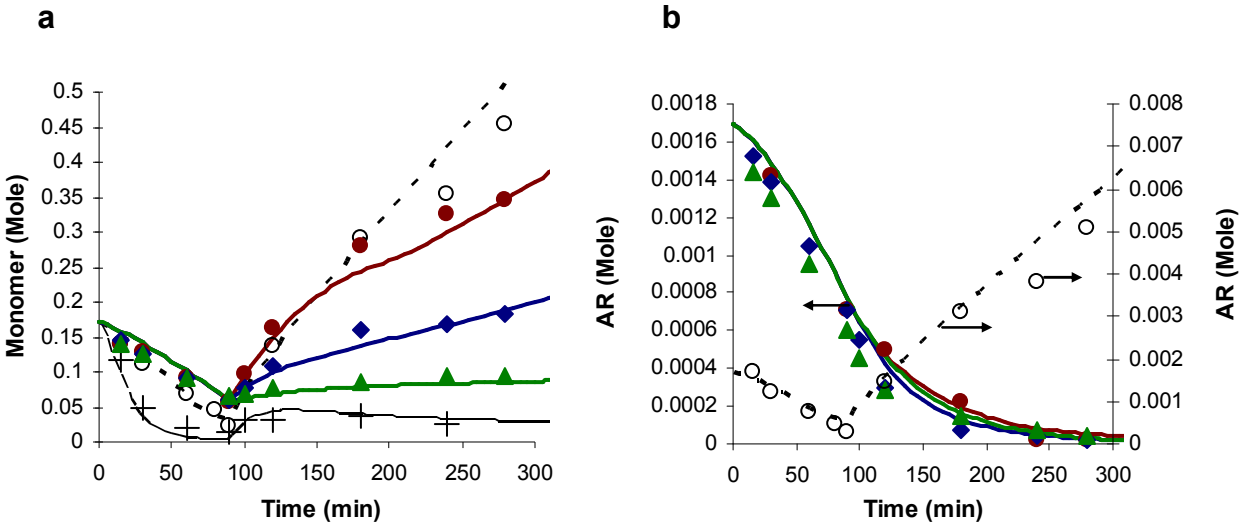

Figure 6-3: Experimental (symbols) and simulated (lines) semi-batch emulsion polymerization of styrene: (a) Total number of monomer moles in the reaction vessel; (b) Total number of RAFT agent moles in the reaction vessel. Legend: Run IT.1 (+); Run IT.3 (▲); Run IT.4 (♦); Run IT.5 (●); Run IT.8 (○); and model simulations (–).

As the conversion reduction is proportional to monomer flow rate, the effect is due to monomer accumulation in the system. At the beginning of the monomer feed period, AR concentration is low and since F_{AR} is zero, the concentration of AR continues to decrease (Fig 6-3b), resulting in low concentration of the small radicals produced. Thus, the differences in monomer conversions between the batch and semi-batch runs is mainly due to monomer feed (monomer accumulation) with exit of small radicals having a small effect on reduced monomer conversion during the feed period. This conclusion is further supported by the simulation and experimental results presented in Fig. 6-2, which shows the effect of adding AR (Run IT.8) along with monomer ($F_M/F_{AR} = N_{Mo}/N_{ARo} = 100$) on monomer conversion. In this Figure, the difference between Run IT.7 and Run IT.8 is that in Run IT.7, F_{AR} was zero and in Run IT.8, F_{AR} was equal to $F_M/100$. For Run IT.7, monomer conversion drops on initiating monomer feed, from 83% to 61% and then increases to about 75% at the end of polymerization. On the other hand, monomer conversion in Run IT.8 drops from 86% to 56% and then continues to decrease to 51%, after which monomer conversion starts to level off at 61%. Due to the

RAFT feed, the total amount of AR increased (Run IT.8, Fig 6-3b), resulting in the production of a greater number of small radicals ($R^{\bullet}$) capable of exiting from the particles and hence inducing further reduction in polymerization rate. Thus, the drop in monomer conversion in Runs IT.3, IT.4, IT.5 and IT.7 is mainly due to monomer accumulation in the system with radical exit having a minor effect, while the decrease in monomer conversion in Run IT.8 is due to both monomer accumulation and radical exit.

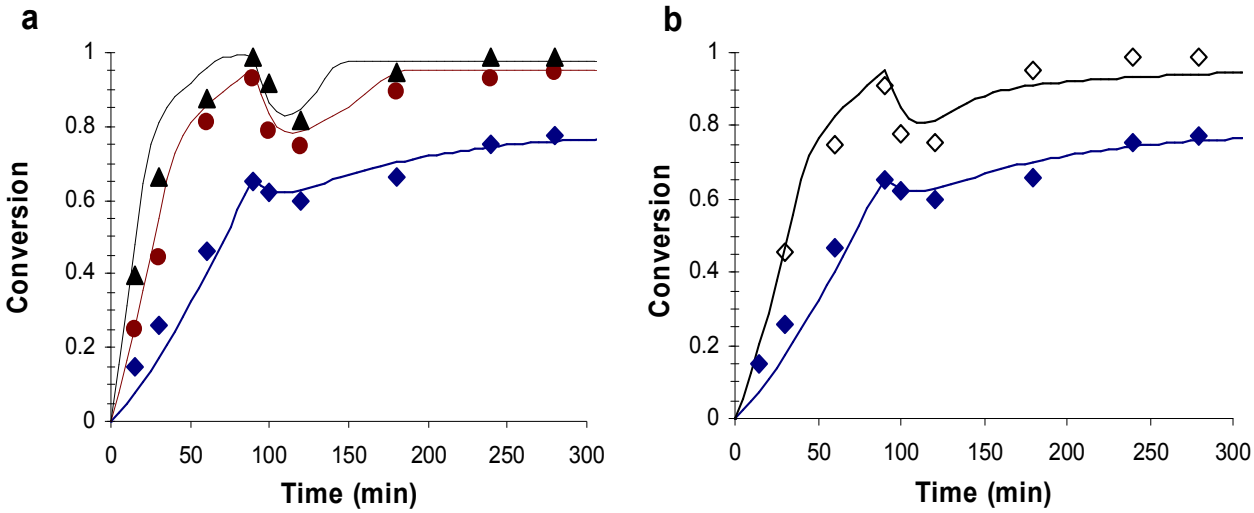

Figure 6-4: Experimental (symbols) and simulated (lines) semi-batch emulsion polymerization of styrene: (a) Effect of surfactant concentration on the overall monomer conversion at 70°C; (b) Effect of reaction temperature on monomer conversion. Legend: Run IT.4 (♦); Run IT.9 (●); Run IT.10 (▲); Run IT.11 (◊); and model simulations (–).

The amount of surfactant (SDS) was varied in order to investigate the effect of emulsifier concentration on polymerization rate, MWD and PSD. Figure 6-4a shows the effect of increased surfactant concentration at constant initiator (0.2g), RAFT (0.375g), monomer flow ($F_M = 3.37\times10^{-3}$mol/min) and reaction temperature (70°C). As expected, monomer conversion increased with increasing surfactant concentration. Since micellar nucleation is the prevailing mechanism for particle formation, the number of polymeric particles is strongly dependent on surfactant concentration. Consequently, increasing the surfactant concentration resulted in increasing the total number of polymerization loci, thereby leading to an increase in the polymerization rate. As expected, the polymerization rate was markedly improved by increasing the reaction temperature (Fig. 6-4b). This is because of the increased number of particles and an increase in the propagation rate.

6.3.2 Polymer molecular weight

The evolution of MWD records the kinetic events that control polymer formation during polymerization. The Mueller equations, obtained via the method of moments, were used to predict the number average (Mn) and weight average molecular weight (Mw) of the polymer produced by the RAFT process. Mn is given by:

$$Mn = M_w^{AR} + \frac{M_o \cdot x_{mon}}{AR_o(1-(1-\alpha)(1-x_{AR})) + 2f(I_o - I)} M_w^M \qquad \textbf{(6-1)}$$

where M_o, AR_o and I_o are the initial amounts of monomer, RAFT agent, and initiator in moles, respectively; I is the undecomposed amount of initiator in moles; M_w^M and M_w^{AR} are monomer and AR molecular weights, respectively; x_{AR} is the RAFT agent conversion which is equal to $x_{mon}^{1/C_{tr}}$ in the batch experiment. The instantaneous Mn is approximated by the rate of propagation over the rate of chain stoppage events:

$$Mn = \left[\frac{k_p C_p^M}{k_{tr}^{AR} C_p^{AR} + k_{tr}^M C_p^M + \rho_{avg}} \right] M_w^M \qquad \textbf{(6-2)}$$

These equations are valid for the three intervals if the transportation rate of the RAFT agent from droplets to the particles is equal to or higher than its consumption rate (Altarawneh *et al.*, 2008; Monteiro *et al.*, 2000), that is, the mass transfer resistance to AR is negligible. For control of Mn, using a RAFT agent (e.g., xanthate), most of the accumulated polymer is produced by the transfer reaction to the AR; thus, the global AR concentration significantly affects the polymerization rate (Altarawneh *et al.*, 2008). Hence, the instantaneously produced polymer presents as a Schulz-Flory MWD with a polydispersity index equal to $1+1/C_{tr}$ (Fig. 6-5b) and M_n given by equation (6.1). The chromatograms of Run (IT. 5) were compared (see Fig. 6-5a) with simulated chromatograms based on Schulz-Flory distributions estimated from predicted Mn; a good agreement was obtained.

Fig. 6-5b shows that a higher monomer feed rate results in higher polydispersities. This is because at higher monomer feed rates, monomer droplets are present in the aqueous

phase and monomer concentration is relatively high, resulting in the propagating chain adding large number of monomer units prior to radical activity transfer. Additionally, the relatively high monomer concentration enhances the occurrence of side reactions and termination in the aqueous phase. These lead to the formation of low molecular weight species and broadening of the MWD.

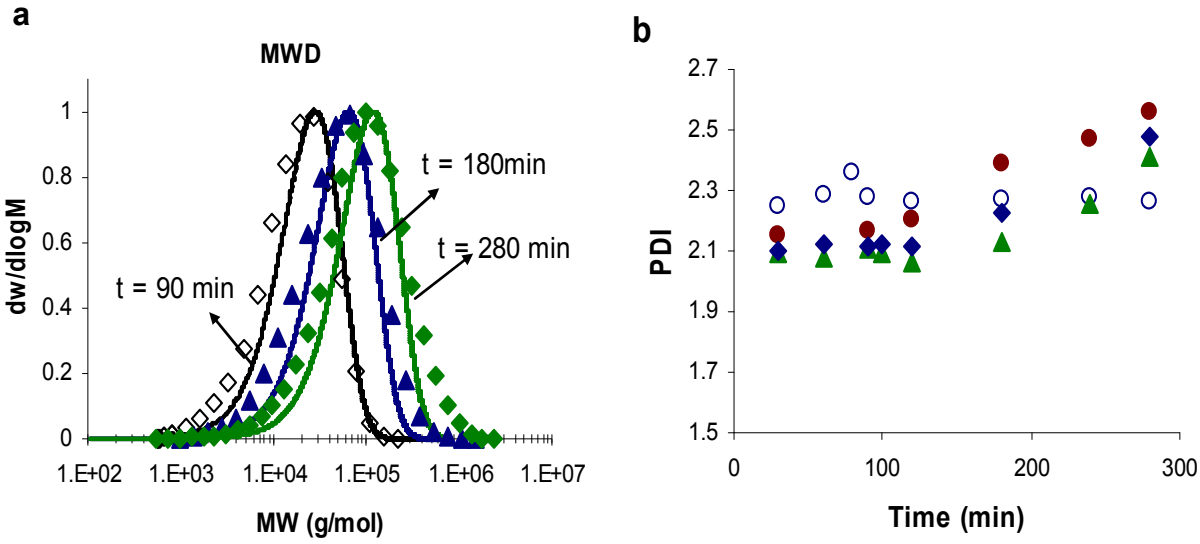

Figure 6-5: Experimental (symbols) and simulated (lines) semi-batch emulsion polymerization of styrene: (a) Experimental MWD and molar chain extension with monomer flow rate = 0.531g/min (Run IT.5). (b) Polymer polydispersity obtained from Runs IT.3, IT.4, IT.5 and IT.8 at 70°C and variable monomer flow rates. Legend: Run IT.3 (▲); Run IT.4 (♦); Run IT.5 (●); Run IT.8 (○); and model simulations (–).

For batch polymerization with AR (C_{tr} = 1), the ratio of the consumption rates of monomer to AR remains constant throughout the reaction, and hence Mn is also constant. In this work, Mn shows a slight decrease with time (Run IT.2, Fig. 6-6a) indicating that the transfer constant of the AR used in this work is lower than 1. As shown in Fig. 6-6b an almost constant Mn can still be obtained if the reaction is carried out under a starved addition of monomer-AR mixture with a molar feed rate ratio during the feeding stage equal to the initial molar ratio of monomer to AR during the batch stage (F_M / F_{AR} = N_{Mo} / N_{ARo}). The Mn values, obtained from (Run IT.8) where AR was fed along with monomer into the reactor, are close to those obtained from the batch experiment (Run IT.2).

In conventional emulsion polymerization without a transfer agent, Mn for polymers produced is unaffected by changes in monomer flow rate (Zeaiter *et al.*, 2002). An

increase in temperature results in a decrease in Mn due to an increase in initiation, transfer to monomer and termination rates relative to the propagation rate (Zeaiter *et al.*, 2002). In the presence of AR, the impact of the monomer flow rate on Mn is illustrated in Fig. 6-6a. Runs IT.3, IT.4 and IT.5 were designed to address the effect of increasing monomer flow rate on monomer conversion (Fig. 6-1), number average molecular weight Mn (Fig. 6-6) and PSD (Fig. 6-9). The M_n values are close to each other during the batch stage and show a slight decrease with time. For the batch experiment (Run IT.2, Fig. 6-6a), all monomer, AR, surfactant and initiator were loaded into the reactor at the beginning of the polymerization. Thus, monomer to AR molar ratio is constant and hence Mn evolution follows a slight continuously decreasing trend.

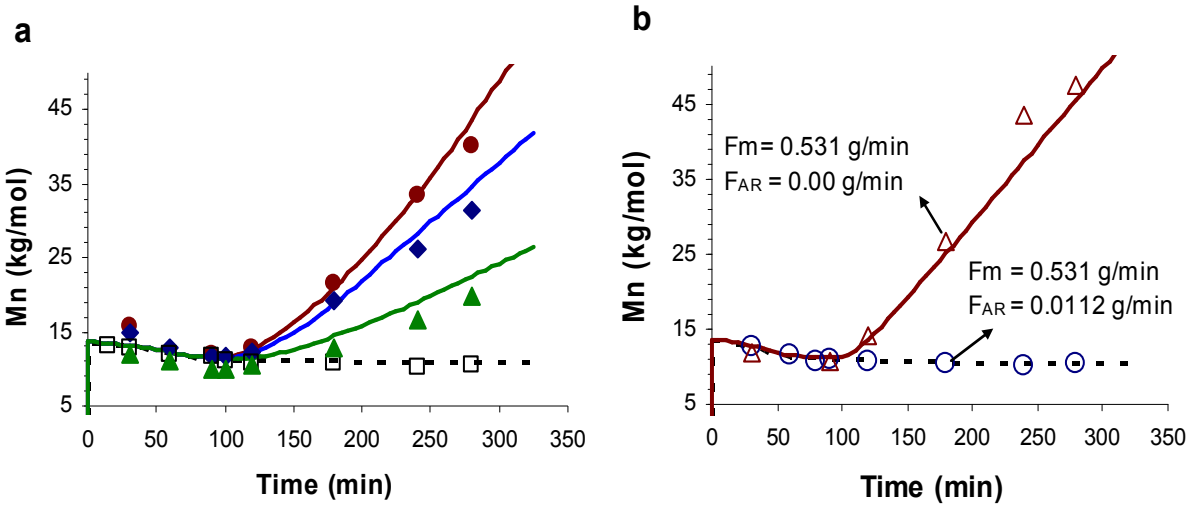

Figure 6-6: Experimental (symbols) and simulated (lines) semi-batch emulsion polymerization of styrene: (a) Effect of monomer flow rate (F_M) on the number average molecular weight at 70 °C; and, (b) Effect of RAFT agent flow rate (F_{AR}) on the number average molecular weight. Legend: Run IT.2 (□); Run IT.3 (▲); Run IT.4 (♦); Run IT.5 (●); Run IT.7 (Δ); Run IT.8 (○); and model simulations (–).

The latexes produced from the batch pre-period were used as the seeds and styrene was slowly added to the reactor during the second stage. During the period of monomer feed at the second stage, Mn increases with time due to the increase in monomer-AR molar ratio in the particle, whereas the higher the flow rate the higher the increase in M_n. That is, the amount of the RAFT end capped polymeric chains remained almost constant while the amount of the reacted monomer increased. Increasing SDS from 1g to 2g resulted in remarkable increases in Mn, and with a further increase to 3g, resulted in negligible changes in Mn, indicating that the increase in Mn is proportional to monomer conversion (Fig. 6-7a).

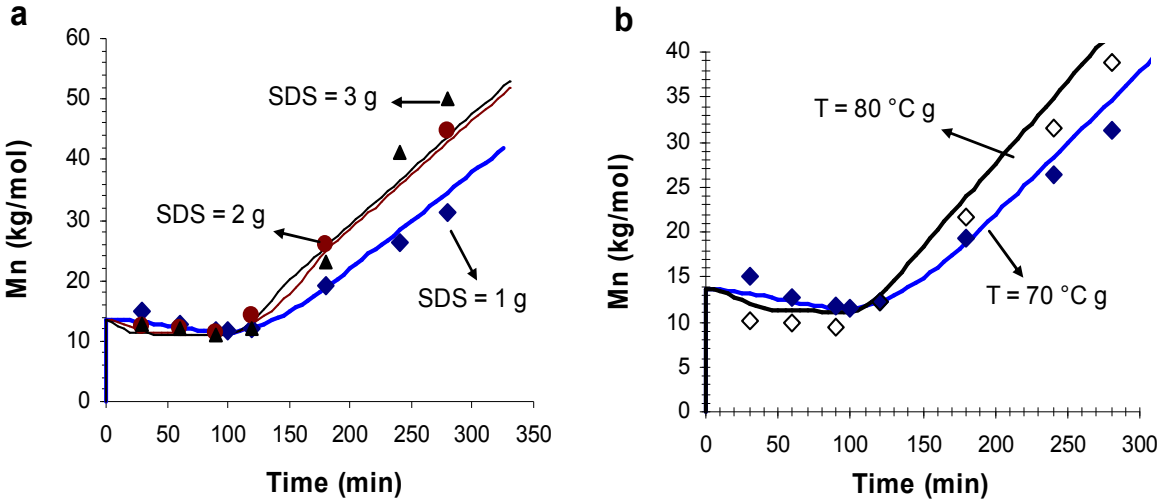

Figure 6-7: Experimental (symbols) and simulated (lines) semi-batch emulsion polymerization of styrene: (a) Effect of surfactant concentration on the number average molecular weight at 70 ^{o}C; and, (b) Effect of reaction temperature on the number average molecular weight. Legend: Run IT.4 (♦); Run IT.9 (●); Run IT.10 (▲); Run IT.11 (◊); and model simulations (–).

As shown by Gugliotta *et al*. (2001), CTA accumulates in the aqueous phase when it does not attain thermodynamic equilibrium as quickly as the monomer, resulting in the molar ratio of monomer to CTA in particles becomes greater than its initial value. This results in an increase in Mn which eventually levels off. In this work, Mn values in Run IT.8 are almost constant. Thus, we conclude that the transport rate of AR (CTA) from the aqueous phase to the particles is fast enough with negligible mass-transfer resistance to enable rapid thermodynamic partitioning and to maintain the initial molar ratio of monomer to AR at the same level during the reaction. Based on this, the constant partitioning coefficient model used in this work to calculate AR concentration is valid. The effect of surfactant concentration and reaction temperature on Mn is demonstrated in Fig. 6-7a and Fig. 6-7b, respectively.

As the temperature was increased from 70 to 80^{o}C, Mn decreased during the batch stage and increased during the monomer feed stage. This indicates that Mn is controlled by the relative rates of propagation and chain transfer. Under similar monomer flow rates, the increase in Mn during monomer feed stage at the higher temperature is due to increases in propagation rate resulting in greater monomer conversion. During the batch stage, the increased number of chains due to increased transfer reaction rate resulted in decrease in Mn.

Due to its low transfer coefficient; the evolution of Mn (Run IT.2 in Fig. 6-6a, and Run IT.8 in Fig 6-6b,) remains almost constant over the period of polymerization with no linear growth. This may lead one to surmise that xanthates act as conventional irreversible chain transfer agents and are not able to induce living characteristics. In contrast, experimental data from semi-batch styrene emulsion polymerization with O-ethylxanthyl ethyl propionate (Runs IT.3, IT.4 and IT.5 in Fig. 6-6a; Run IT.7 in Fig. 6-6b, and Runs IT.9, IT.10, IT.11 in Fig. 6-7a and 6-7b) indicate that a high proportion of the previously prepared polystyrene-xanthate chains (prepared in the batch stage) act as macro-RAFT agents which enable chain extension when a subsequent batch of the monomer is added.

The successful chain extension confirms that the previously prepared polymeric chains were able to regain radical activity, and hence demonstrates the living nature of the polymer in the presence of xanthates. In case of the previously prepared chains did not possess the living nature, the newly added monomers would have polymerized separately, resulting in high and uncontrolled polydispersity or an increase in MWD modality. The unimodal MWD for the extended polystyrene-xanthate chains (Fig. 6-5a, obtained from Run IT.5) provides confirmation that the previously prepared polystyrene-xanthate chains were involved in the second stage polymerization with the newly added monomer. In terms of MWD, feeding the AR along with monomer shows no difference in comparison with the batch experiment. Therefore, MWD control may require only the intermediate monomer addition, or the independent and simultaneous addition of monomer and AR.

To further investigate the living nature of the pre-prepared polystyrene-RAFT macro RAFT agent, the number average molecular weight is represented against the conversion of the added monomer during the semi-batch period. Monomer conversion was calculated based on the total amount of the added monomer throughout the reaction. The dormant polystyrene-xanthate produced during the batch period was considered as macro-polymeric RAFT agent with an initial molecular weight of about 10kg/mol. As shown in Figure 6-8, with the continuous addition of styrene the number average molecular weight of the initial polystyrene-xanthate species increased linearly with conversion, with little deviation from the theoretical prediction (dotted line).

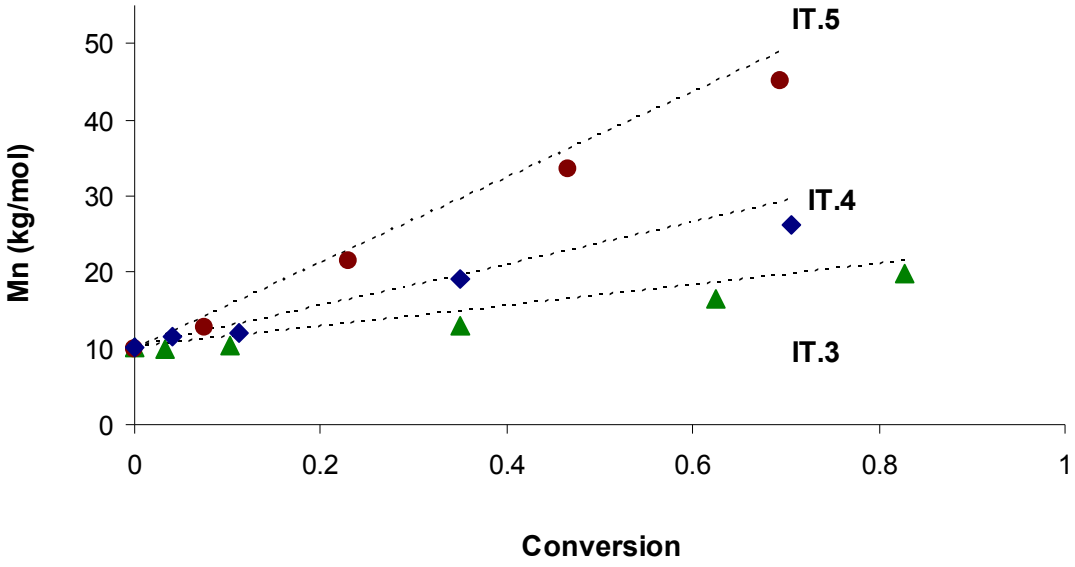

Figure 6-8: Plot of the number average molecular weight as a function of conversion of polystyrene produced via semi-batch emulsion polymerization of styrene in polystyrene-RAFT seed latex. Legend: Run IT.3 (▲); Run IT.4 (♦); Run IT.5 (●); theoretical prediction (···).

The fact that the molecular weights at very low conversions were close to theoretical suggests that the rate of the transfer reaction of the polystyrene-xanthate macro RAFT agent with styrene is indeed high enough to ensure that the polystyrene-xanthate macro-RAFT agent is incorporated into the growing chains sufficiently early in the reaction. That is, monomer concentration is kept low which results in significantly reducing the rate of propagation reaction, while the rate of transfer reaction is unaltered. In contrast, no linear growth of Mn was observed in batch experiments; this suggests the significant difference between batch and semi-batch emulsion polymerizations in which living or possibly semi-living polymerization is approached when operating under semi-batch conditions.

6.3.3 Particle size

In estimating the particle size distribution, we accounted for the swollen and unswollen (absence of monomer) particle sizes. The swollen (r_s) and unswollen (r) radii are related by mass conversion (assuming ideal mixing of monomer and polymer) as follows:

$$\frac{r_s}{r} = \left[\frac{d_m}{d_m - C_p^M M_0} \right]^{1/3} \qquad \textbf{(6-3)}$$

where d_M is the density of monomer

The predicted and experimentally measured particle sizes show a dramatic decrease with increasing RAFT agent from 0g (Run IT.12 in Fig. 6-9a, batch experiment without RAFT) to 0.375g (Run IT.2 in Fig 6-9a, batch experiment with RAFT). To investigate the effects of interim monomer addition on PSD, both Runs IT.2 and IT.12 were repeated and the results are shown in Fig. 6-9a (Run IT.1, semi-batch experiment without RAFT, and Run IT.4, semi-batch experiment with RAFT). During the batch pre-period, experimental conditions are similar to those for batch experiments; hence, the measured particle sizes are close to each other.

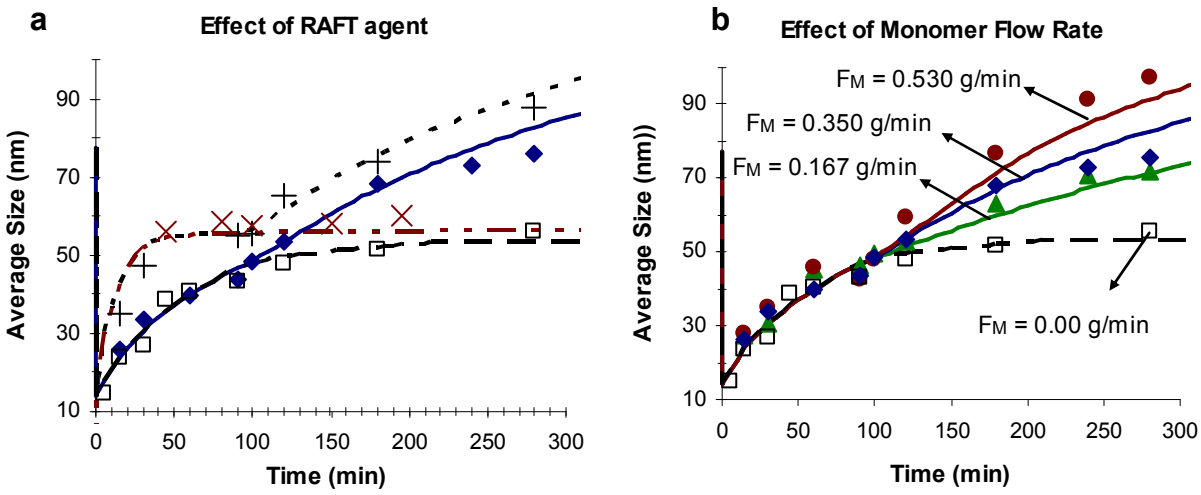

Figure 6-9: Experimental (symbols) and simulated (lines) semi-batch emulsion polymerization of styrene: (a) Effect of AR on average particle size (PS) at 70 °C; (b) Effect of variable monomer feed rates on (PS) Legend: Run IT.1 (+); Run IT.2 (□); Run IT.3 (▲); Run IT.4 (♦); Run IT.5 (●); Run IT.12 (×); and model simulations (–).

In the batch experiment without AR (Run IT.12 in Fig. 6-9a), the growth rate of the particle is higher due to the absence of rate retardation. Once all monomers have reacted, the maximum value of particle size is attained in a short period (50 min), after which it levels off. For the batch experiment with AR (Run IT.2), particle size increases slowly due to the effect of rate retardation. Thus it takes significantly longer (280 min) to attain the same size as in Run IT.12. An increase in particle size was observed

immediately after the initiation of monomer feed in both semi-batch experiments with and without AR (Run IT.4 and Run IT.1, respectively).

As shown in Fig. 6-9b, variable particle sizes were obtained using the same recipe but with different monomer feed rates. The propagational growth rate is defined as: $K = k_p M_w^M C_p(V) / N_A d_p$, and shows that particle growth is strongly affected by monomer concentration. At high feed rateas, the process resembles interval II as seen in the batch Run (i.e., the presence of monomer droplets in aqueous phase). Monomer concentration inside polymer particles increases with an increase in feed rate, eventually reaching saturation. The propagational growth rate equation indicates that particle growth rate, which depends strongly on monomer concentration, is relatively high under these conditions. Consequently, polymer volume fraction ($\Phi = 1 - (C_P M_w^M / d_m)$ inside the particles is less than 0.80 (typically ~0.46) and larger particles are obtained. As the reaction progresses, monomer concentration inside the particles becomes less than its saturation value (<5.5 M) resulting in Φ exceeding the limiting value of 0.80. Thereby, the particles become glassy, the viscosity inside the particle increases dramatically, and the system enters a diffusion controlled regime, resulting in the suppression of propagation growth rate and hence the particle size growth. This is observed with Runs IT.3 and IT.4 (Fig. 6-9b), where monomer feed rates are lower and monomer conversions are higher compared with Run IT.5.

Fig. 6-10b shows the relationship between monomer flow rate and average growth rate of particles. During the batch pre-period, the experimental conditions for Runs IT.3, IT.4 and IT.5 are similar, resulting in almost similar average growth rates of particles, and hence all particle sizes during this period are almost similar. In Fig. 6-10b, the initial particle size was taken to be the one at the end of the batch pre-period so as to address the impact of monomer addition on PSD.

It was observed that increasing monomer feed rate resulted in a larger particle growth rate (Run 5, Fig. 6-10b). For a lower monomer feed rate (Run IT.4, Fig. 6-10b), the particle growth rate is lower and approaches a steady state after 150 min of monomer feeding. In conclusion, the higher the monomer feed rate, the larger the particle size and the slower the particle growth rate approaches a steady state. Moreover, we note that at constant surfactant concentration, the particle size is roughly proportional to monomer

conversion in Runs IT.2, IT.3, IT.4 and IT.5. Thus, the retardation in particle growth rate compared with RAFT-free experiments (Runs IT.1 and IT.12) is most likely due to radical exit.

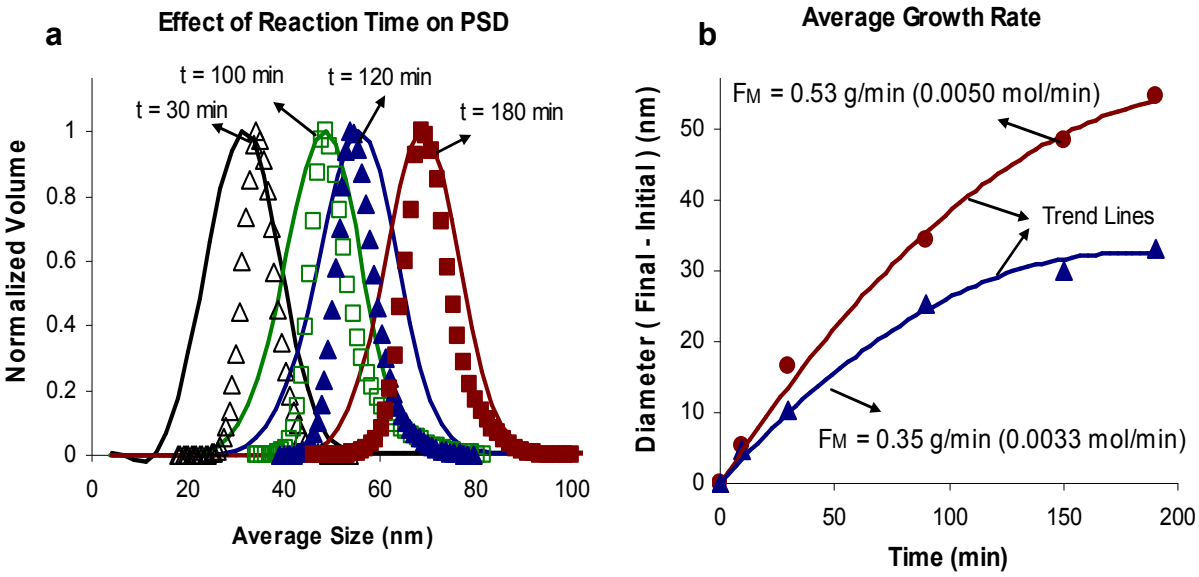

Figure 6-10: Experimental (symbols) and simulated (lines) semi-batch emulsion polymerization of styrene: (a) PSD at moderate monomer feed rate (Run IT.4), samples were taken at different reaction times; (b) Experimental average growth rate of the polymer particles at different monomer feed rates. Legend: Run IT.4 (♦); Run IT.5 (●); and model simulations (—).

As shown in Fig. 6-10a, the PSDs obtained from Run IT.4 (moderate monomer feed rate) at different reaction times are narrow and the PSD for each sample is represented by one normal (Gaussian) peak, indicating the absence of secondary nucleation (new nucleated particles with small size). Propagation of the aqueous phase radical to j_{crit} degree occurs with particles swollen with monomer. This phenomenon is often termed homogeneous nucleation (Gilbert, 1995). The absence of secondary nucleation indicates that homogeneous nucleation is insignificant, and almost all of the aqueous phase radicals (exited and initiator derived radicals) are efficiently captured by the pre-existing particles (particles formed via micellar nucleation).

Runs IT.4, IT.9 and IT.10, were designed to investigate the effect of the surfactant (SDS) concentration on monomer conversion, MWD and PSD. This parameter plays a crucial role in the nucleation process of nonliving systems, and thus, on the number of

particles formed. This is confirmed also in the work of Altarawneh *et al*. (2008) for the batch emulsion polymerization of styrene with xanthate-based living transfer agent.

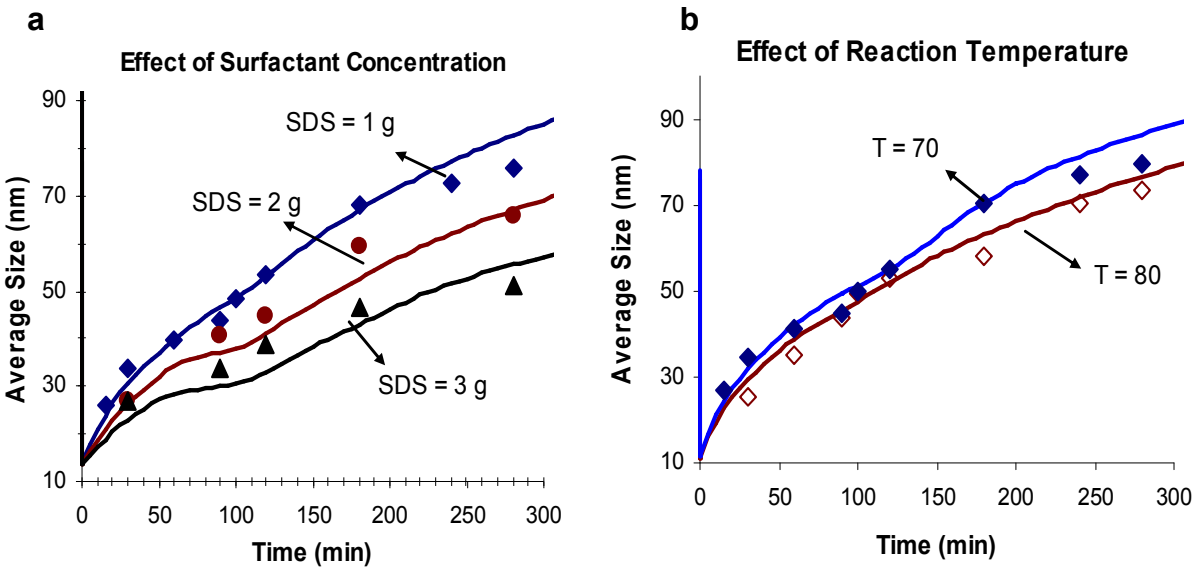

Figure 6-11: Experimental (symbols) and simulated (lines) semi-batch emulsion polymerization of styrene: (a) Effect of SDS concentration on the average particle size (PS) at 70 ^{o}C; and, (b) Effect of reaction temperature on (PS) Legend: Run IT.4 (♦); Run IT.9 (●); Run IT.10 (▲); Run IT.11 (◊); and model simulations (–).

It is observed that the final average particle size decreases as SDS concentration increases (Fig. 6-11a). We note that the concentration of initiator and AR in Runs IT.4, IT.9 and IT.10 are similar and the changes in the PSDs are entirely due to changes in SDS concentration. A high surfactant concentration results in a large number of particles and a small number of radicals per particle. Thus, with an increased SDS, each particle receives a small number of radicals resulting in a particle with a low probability to grow in size. During the monomer feed period (reaction time: from 90 to 300 min), the continuous increase in the particle size is due to the monomer addition which sustains monomer concentration inside the particle. Consequently, the process of particle growth driven by propagation reactions is enhanced. Similarly, Fig. 6-11b shows that an increase in reaction temperature results in a smaller average particle size due to an increase in the oligomeric radical concentration in the aqueous phase and increase in the nucleation rate. Consequently, the total number of particles increases at the expense of size.

6.4 Conclusions

A mathematical model was developed to describe the *ab initio* emulsion polymerization of styrene with O-ethylxanthyl ethyl propionate as the RAFT agent (AR). The model accounts for the effects of RAFT agent on the polymerization rate, number average molecular weight, weight average molecular weight, molecular weight distribution, polydispersity index, particle average radius and particle size distribution. The model was validated against experimental data obtained in our laboratory. The reactions were carried out using variable amounts of AR agent, surfactant (SDS) and initiator (KPS) at different reaction temperatures. The polymerization rate was found to be retarded by increasing AR concentration. The observed retardation was attributed to small radicals exiting from the polymeric particles.

The decline in conversion, observed to be proportional to monomer flow rate, was due to monomer accumulation in the particles when there is no RAFT feed. Further, monomer conversion was reduced due to the added effect of radical exit when the RAFT agent was fed into the reactor along with the monomer. An increase in surfactant concentration resulted in an increase in the total number of polymerization loci, leading to an increase in the polymerization rate. The polymerization rate was markedly improved by increasing the reaction temperature; this is due to an increase in the propagation rate. We investigated the effect of monomer and AR on Mn. During the batch period, Mn values were close to each other because the reaction conditions were similar. During the monomer feed period, Mn increased due to the increase in monomer/AR molar ratio in the particle. When the RAFT agent was fed along with the monomer, no change in Mn was observed, indicating that a rapid thermodynamic partitioning was achieved. The living nature of the process was confirmed by the unimodal MWD for the extended polystyrene-xanthate chains.

Monomer feed rate was found to have a profound effect on the growth of the particles, as the particle size increased with monomer feed rate. Typical particle size for uncontrolled radical emulsion polymerization range from 50 to 200nm. Polymerizations carried out with AR have been shown to provide emulsions with smaller particle sizes under similar conditions of surfactant and monomer concentrations. These indicate that controlling MWD and PSD is feasible by manipulating the surfactant and RAFT

concentrations, reaction temperature and most importantly the interim monomer and AR flow control in semi-batch, either independently or simultaneously. Our model accurately predicts the effects of the RAFT agent, surfactant and initiator on the measured polymer properties.

Table 6-1: RAFT-semi-batch styrene emulsion polymerization procedures

Run No.	Water (g)	M_o (g)	AR_o (g)	SDS (g)	KPS (g)	F_M (g/min)	F_{AR} (g/min)	T (^oC)
IT.1	520	17.8	0.00	1	0.20	0.350	0	70
IT.2	520	17.8	0.377	1	0.20	0.00	0	70
IT.3	520	17.8	0.377	1	0.20	0.167	0	70
IT.4	520	17.8	0.377	1	0.20	0.350	0	70
IT.5	520	17.8	0.377	1	0.20	0.531	0	70
IT.6	520	17.8	0.377	1	0.35	0.531	0	70
IT.7	520	17.8	0.377	1	0.50	0.531	0	70
IT.8	520	17.8	0.377	1	0.50	0.531	0.0112	70
IT.9	520	17.8	0.377	2	0.20	0.350	0	70
IT.10	520	17.8	0.377	3	0.20	0.350	0	70
IT.11	520	17.8	0.377	1	0.20	0.350	0	80
IT.12	520	17.8	0.00	1	0.20	0.00	0	70

6.5 References

Altarawneh, I.S.; Gomes, V.G. and Srour, M.S., 2008. The Influence of Xanthate-Based Transfer Agents on Styrene Emulsion Polymerization: Mathematical Modeling and Model Validation. *Macromolecular Reaction Engineering*, 2(1): 58.

Altarawneh, I.S.; Srour, M. and Gomes, V.G., 2007. RAFT with Bulk and Solution Polymerization: An Approach to Mathematical Modelling and Validation. *Polymer-Plastics Technology and Engineering*, 46(11): 1103

Apostolovic, B.; Quattrini, F.; Butte, A.; Storti, G. and Morbidelli, M., 2006. Ab initio emulsion polymerization by RAFT (reversible addition-fragmentation chain transfer) through the addition of cyclodextrins. *Helvetica Chimica Acta*, 89(8): 1641.

Charmot, D.; Corpart, P.; Adam, H.; Zard, S.Z.; Biadatti, T. and Bouhadir, G., 2000. Controlled radical polymerization in dispersed media. *Macromolecular Symposia*, 150(Polymers in Dispersed Media): 23.

Chiefari, J.; Chong, Y.K.; Ercole, F.; Krstina, J.; Jeffery, J.; Le, T.P.T.; Mayadunne, R.; Meijs, G.F.; Moad, C.L.; Moad, G.; Rizzardo, E. and Thang, S.H., 1998. Living Free-Radical Polymerization by Reversible Addition-Fragmentation Chain Transfer: The RAFT Process. *Macromolecules*, 31(16): 5559.

Coen, E.M.; Gilbert, R.G.; Morrison, B.R.; Leube, H. and Peach, S., 1998. Modelling particle size distributions and secondary particle formation in emulsion polymerisation *Polymer*, 39(26): 7099.

Ferguson, C.J.; Hughes, R.J.; Nguyen, D.; Pham, B.T.T.; Gilbert, R.G.; Serelis, A.K.; Such, C.H. and Hawkett, B.S., 2005. Ab initio emulsion polymerization by RAFT-controlled self-assembly. *Macromolecules*, 38(6): 2191.

Gilbert, R.G., 1995. Emulsion polymerization: a mechanistic approach. Academic Press, London.

Gugliotta, L.M.; Salazar, A.; Vega, J.R. and Meira, G.R., 2001. Emulsion polymerization of styrene. Use of n-nonyl mercaptan for molecular weight control. *Polymer*, 42(7): 2719.

Hermanson, K.D.; Liu , S. and Kaler, E.W., 2006. Kinetic modeling of controlled living microemulsion polymerizations that use reversible addition-fragmentation chain transfer. *Journal of Polymer Science Part A: Polymer Chemistry*, 44(20): 6055.

Luo, Y.; Wang, R.; Yang, L.; Yu, B.; Li, B. and Zhu, S., 2006. Effect of Reversible Addition-Fragmentation Transfer (RAFT) reactions on (mini)emulsion polymerization kinetics and estimate of RAFT equilibrium constant. *Macromolecules*, 39(4): 1328.

Matyjaszewski, K. and Xia, J., 2001. Atom Transfer Radical Polymerization. *Chem. Rev.*, 101(9): 2921.

Mendoza, J.; De La Cal, J.C. and Asua, J.M., 2000. Kinetics of the styrene emulsion polymerization using n-dodecyl mercaptan as chain-transfer agent. *Journal of Polymer Science Part A: Polymer Chemistry*, 38(24): 4490.

Moad, G.; Chiefari, J.; Chong, Y.K.; Krstina, J.; Mayadunne, R.T.A.; Postma, A.; Rizzardo, E. and Thang, S.H., 2000. Living free radical polymerization with reversible addition-fragmentation chain transfer (the life of RAFT). *Polymer International*, 49(9): 993.

Moad, G.; Rizzardo, E. and Thang, S.H., 2005. Living radical polymerization by the RAFT process. *Australian Journal of Chemistry*, 58(6): 379.

Monteiro, M.J. and De Barbeyrac, J., 2001. Free-radical polymerization of styrene in emulsion using a reversible addition - Fragmentation chain transfer agent with a low transfer constant: Effect on rate, particle size, and molecular weight. *Macromolecules*, 34(13): 4416.

Monteiro, M.J.; Hodgson, M. and De Brouwer, H., 2000. Influence of RAFT on the rates and molecular weight distributions of styrene in seeded emulsion

polymerizations. *Journal of Polymer Science, Part A: Polymer Chemistry*, 38(21): 3864.

Peklak, A.D. and Butte, A., 2006. Kinetic model of reversible addition fragmentation chain transfer polymerization of styrene in seeded emulsion. *Journal of Polymer Science, Part A: Polymer Chemistry*, 44(20): 6114.

Prescott, S.W., 2003. Chain-length dependence in living/controlled free-radical polymerizations: Physical manifestation and Monte Carlo simulation of reversible transfer agents. *Macromolecules*, 36(25): 9608.

Prescott, S.W.; Ballard, M.J.; Rizzardo, E. and Gilbert, R.G., 2002a. RAFT in emulsion polymerization: What makes it different? *Australian Journal of Chemistry*, 55(6-7 SPEC): 415.

Prescott, S.W.; Ballard, M.J.; Rizzardo, E. and Gilbert, R.G., 2002b. Successful use of RAFT techniques in seeded emulsion polymerization of styrene: Living character, RAFT agent transport, and rate of polymerization. *Macromolecules*, 35(14): 5417.

Prescott, S.W.; Ballard, M.J.; Rizzardo, E. and Gilbert, R.G., 2006. Rate optimization in controlled radical emulsion polymerization using RAFT. *Macromolecular Theory and Simulations*, 15(1): 70.

Schulte, T.; Knoop, C.A. and Studer, A., 2004. Nitroxide-mediated living free-radical polymerization of styrene: A systematic study of the variation of the alkoxyamine concentration. *Journal of Polymer Science Part a-Polymer Chemistry*, 42(13): 3342.

Smulders, W.W.; Gilbert, R.G. and Monteiro, M.J., 2003. A kinetic investigation of seeded emulsion polymerization of styrene using reversible addition-fragmentation chain transfer (RAFT) agents with a low transfer constant. *Macromolecules*, 36(12): 4309.

Smulders, W.W. and Monteiro, M.J., 2004. Seeded emulsion polymerization of block copolymer core-shell nanoparticles with controlled particle size and molecular weight distribution using xanthate-based RAFT polymerization. *Macromolecules*, 37(12): 4474.

Zeaiter, J.; Romagnoli, J.A.; Barton, G.W.; Gomes, V.G.; Hawkett, B.S. and Gilbert, R.G., 2002. Operation of semi-batch emulsion polymerisation reactors: Modelling, validation and effect of operating conditions. *Chemical Engineering Science*, 57(15): 2955.

Chapter Seven

Calorimetry and Process Optimization

Chapter 7
Calorimetry and Process Optimization

Abstract

In this Chapter, a model for the online energy balance of the RAFT mediated polymerization reactor has been developed with particular attention being paid to the evolution of polymerization rate and molecular weight. The rate of polymerization, which is proportional to the heat of reaction, was estimated and integrated to obtain the overall monomer conversion. The calorimetric model was validated offline for batch and semi-batch emulsion polymerization of styrene with and without RAFT agent. The number average molecular weight, measured by a SEC (GPC) with multiple detections, compared well with those estimated from the calorimetric model. We found that semi-batch emulsion polymerization could be used to approach living polymerization with a RAFT agent having a low chain transfer coefficient.

The dynamic optimisation of emulsion polymerization in the presence of low active RAFT agent is presented in this Chapter. The implementation of a dynamic process optimisation is described. The different problem formulations and solution techniques in gPROMS are discussed. Application of the offline dynamic optimisation to the emulsion polymerization process of styrene is investigated for the PSD, MWD and monomer conversion. The optimal profiles obtained are then validated experimentally.

7.1 Introduction

Many problems encountered in industrial polymerization processes are associated with inherent complexities in polymerization kinetics and mechanisms. Moreover, many of the process variables that affect product quality indices are difficult (if not impossible) to measure online, or can be measured at low sampling frequencies with time delays, making product quality monitoring and control difficult. The control of MWD, which is critical for manipulating the end-use properties of the produced polymer, suffers from these aspects. Furthermore, the offline measurements of polymer MWD and PSD are

expensive, and time consuming. This often leads to challenges in safety, productivity, and quality control. Due to the compartmentalization in emulsion polymerization, the MWD is usually unobservable from available online measurements. However, under certain conditions, the MWD of emulsion polymers is not affected by the compartmentalization of the system. A typical example is when a chain-transfer agent (e.g., RAFT agent) is used and the kinetic chain length is controlled by the molar ratio of monomer to chain transfer agent when transfer to the CTA dominates (Vicente *et al.*, 2001).

Online monitoring of emulsion polymerization reactors is necessary to implement closed-loop control strategies aimed at producing polymer latex with the required microstructure. Sensors for the monitoring of several properties (e.g., conversion, polymer composition, molecular weights, particle size, etc.) have been developed and assessed in polymerization reactors. However, not all of the reported techniques are accurate or robust enough to be implemented in industrial environments. Consequently, most of the control strategies developed in the last two decades have been open loop, based on mathematical models of the process or on extensive experimental work (Arzamendi and Asua, 1989; Arzamendi and Asua, 1991; Broadhead *et al.*, 1985; Gugliotta *et al.*, 1995a; Hamielec *et al.*, 1987). On the other hand, few closed-loop strategies using on-line measurements have been reported in the literature (de Buruaga *et al.*, 1997; Dimitratos *et al.*, 1994; Leiza *et al.*, 1993).

Emulsion polymerization kinetics studies are usually carried out using gravimetry, dilatometry, and gas chromatography (GC). In gravimetry and GC analyses, it is necessary to take special care in handling the samples. Dilatometry cannot be used in many circumstances such as for obtaining accurate rate data while one or more components are being fed into the system. These techniques are limited in accuracy, and in the number of data points that can be obtained in one run. The major problems that restrict the development of accurate online sensors for emulsion polymerizations were discussed in the work of Asua (2004). Online sensors, such as GC and densimetry require a sampling device or an auxiliary recirculating loop. This can present certain difficulties, such as coagulation in the circulating loop, sensitivity to polymer viscosity, coagulation of polymer particles in the device, and extensive calibration in-situ (Asua, 2004; Guinot *et al.*, 2000; Kiparissides and Morris, 1996). Moreover, these techniques

are usually carried out offline, resulting in a considerable measurement delay that is undesirable for any form of real time control.

To overcome the above mentioned problems, various online soft-sensor methods have been developed for the estimation of key process variables (Kim and Choi, 1991). These methods involve either detailed or simple kinetic models. For heterogeneous emulsion polymerizations, the mechanisms of the reactions are complex, the underlying kinetic and thermodynamic equations, the extent of mixing, and other process parameters, make it difficult to develop a robust model. However, some accurate models for conventional emulsion polymerization (Coen *et al.*, 1998; Gilbert, 1995; Zeaiter *et al.*, 2002b) and for RAFT emulsion polymerization (Altarawneh *et al.*, 2008) have been developed. These models are well validated for a wide range of reaction conditions and hence they can serve as a soft sensor, which can provide online accurate predictions that can be used for process optimization and control purposes.

In addition, based on overall material and energy balances, calorimetric analysis can be used to determine the conversion from temperature measurements alone, which are readily available for most processes (Asua, 2004; Schuler and Schmidt, 1992; Srour *et al.*, 2008; Vicente *et al.*, 2001; Zeaiter *et al.*, 2002a). Since most polymerization reactions are very exothermic, online reaction calorimetry is an appropriate technique for online measurement of polymerization rate (de Buruaga *et al.*, 1997; Gugliotta *et al.*, 1995a; Isabel Sáenz de Buruaga, 1997; Srour *et al.*, 2008; Varela De La Rosa, 1999; Zeaiter *et al.*, 2002a).

7.2 Reaction calorimetry

Reaction calorimetry provides an alternative technique with the advantage of continuous monitoring of the heat of reaction in a stirred tank reactor. Since the calorimetric technique can measure the heat released in a polymerization reaction, which is proportional to the rate of polymerization, then, it is possible to obtain the rate of reaction as a continuous record. This information can give an immediate insight into the course of a chemical process, and constitutes a direct method of obtaining rates of polymerization through temperature measurements. With the calorimetric technique, the rate of polymerization is determined with a high degree of resolution, and the

conversion-time information can then be obtained by integrating the polymerization rate data. This method is a promising candidate for industrial implementation of conversion monitoring and control. However, determining monomer conversion from temperature readings for different polymerization processes, such as batch, semi-batch or continuous modes of operation, requires a thorough understanding of the heat transfer mechanisms occurring within the system (Asua, 2004).

McKenna *et al.* (1996), investigated the joint use of calorimetry with densimetry and gravimetry for the purpose of online monitoring. Through a detailed sensitivity analysis, the authors concluded that calorimetry is easily adapted to polymerization reactors, and could provide, along with infrequent gravimetric measurement updates, a good estimate of monomer conversion. An online calorimetry to estimate monomer conversion and copolymer composition in emulsion polymerization was used by de Buruaga *et al.* (1997). In the work of Vicente *et al.* (2001), the molecular weight distribution (MWD) of linear polymers was controlled based on online reaction calorimetry. A method to estimate the MWD from reaction calorimetry when chain transfer to a chain-transfer agent is the main termination event was developed and its robustness assessed by simulations.

Leswin (2005) investigated the process of particle formation in RAFT-mediated emulsion polymerization using reaction calorimetry. This online monitoring technique provided detailed information about the onset of the nucleation period in the semi-batch process for both the styrene and n-butyl acrylate reactions. By measuring the heat flow during controlled feed *ab initio* emulsion polymerization in the presence of amphipathic RAFT agents, particle formation by self-assembly of these species was observed. It was pointed out that for the n-butyl acrylate system the more surface active initial macro-RAFT agent always led to earlier commencement of nucleation. For styrene no such trend was observed.

This Chapter concentrates on the development of a detailed calorimetric model as an open-loop observer for inferring monomer conversion and polymer molecular weight based on online measurements of the reaction temperature in a batch and semi-batch laboratory reactor for homopolymer production of (polystyrene) via RAFT emulsion polymerization. The significant advantage of this work over existing calorimetric

monitoring schemes is that the use of RAFT based transfer agent controls polymer molecular weight and facilitates the inferential online measurement of polymer molecular weight. In addition, the present calorimetric development includes an adaptive strategy to estimate the overall heat transfer coefficient and key evaporation/condensation parameters.

7.3 Calorimetric model

The calorimetric model aims to determine the thermal energy profiles dynamically from temperature measurements. This method provides an inexpensive and rapid method for industrial control of product quality for efficient processing and control of process attributes. The model measures the instantaneous heat evolved during a reaction as a function of time. Performing an energy balance around the system, the heat of reaction is calculated by measuring the reaction and jacket temperatures, and other reactor parameters such as the overall heat transfer coefficient (U), the heat transfer area and the evaporation/condensation parameters.

The propagation step of a free radical polymerization occurs via converting the double bond into two single bonds. The energy gained by converting the double bond into two single bonds is high with a typical value of about -69900 J/mol for styrene (Zeaiter *et al.*, 2002a). The heat of polymerization is considered to be equal to that associated with the propagation step (ΔH_P = -69900 J/mol), since the vast majority (by number) of the reactions taking place in a free-radical polymerization comprises propagation, typically orders of magnitude more than termination, initiation and transfer to monomer. In the presence of RAFT agent in the investigated systems, a number of transfer reactions to RAFT agent (addition and fragmentation reactions) are taking place. However, this may not result in any net heat effects; since with every addition step a similar bond is broken by fragmentation (see RAFT mechanism in Chapters 3 and 4). As was shown in Chapters 3 and 5, the fragmentation rate coefficient is sufficiently high, thus the addition fragmentation reactions can be simplified by the overall transfer reaction with a negligible net heat effect. The jacket inlet and outlet temperatures are very close to each other ($T_{j,in} \approx T_{j,out}$) resulting in the dynamic of the external jacket system not being significant and can be neglected. This assumption is valid only when the water flow rate in the jacket is high, since a high water flow rate ensures a negligible difference

between jacket inlet and outlet temperatures. Under these conditions, the jacket temperature is considered an input variable and heat flow calorimetry is applied (Gesthuisen *et al.*, 2005; Srour *et al.*, 2008; Zeaiter *et al.*, 2002a). In addition it is assumed that the jacket is completely filled and to model the semi-batch reactor the outflows are simply set to zero.

7.3.1 Reactor mass balance

The amounts of monomer and RAFT agent can be inferred using an open-loop observer. This observer is based on the mole balances for monomer and RAFT agent in the reactor:

$$\frac{dN_m}{dt} = F_{m,in} - R_p^M V = F_{m,in} - k_p C_p^M \frac{\bar{n} N_c}{N_A} V; \quad N_m(0) = N_{m,o} \tag{7-1}$$

$$\frac{dN_{AR}}{dt} = F_{AR,in} - R_p^{AR} V = F_{AR,in} - k_{tr}^{AR} C_p^{AR} \frac{\bar{n} N_c}{N_A} V; \quad N_{AR}(0) = N_{AR,o} \tag{7-2}$$

where N_m , N_{AR} are the number of moles of monomer and AR in the reactor, respectively; $F_{m,in}$, $F_{AR,in}$ are the monomer and AR feedrates, respectively; R_P^M is the polymerization rate; R_P^{AR} is the RAFT agent consumption rate; C_p^M ,C_p^{AR} are the concentrations of monomer and AR in the particle phase, respectively; $\bar{n}$, N_c and N_A are the average number of radicals per particle, the total number of particles and the Avogadro's number, respectively.

It has been shown in the previous Chapters that the transport rate of RAFT agent from the aqueous phase to the particles is fast enough with negligible mass-transfer resistance to enable rapid thermodynamic partitioning and to maintain the initial molar ratio of monomer to AR at the same level during the reaction. Thus, the concentration of RAFT agent (AR) in the particle phase can be calculated by:

$$C_p^{AR} = C_p^M / r \tag{7-3}$$

where r is the initial molar ratio of monomer to AR. The transfer rate coefficient k_{tr}^{AR} is given by: $k_{tr}^{AR} = C_{tr} k_p$ where C_{tr} is the transfer constant which is equal to 0.7 for the RAFT agent used in this work. Substituting equation (7-3) into equation (7-2) gives:

$$\frac{dN_{AR}}{dt} = F_{AR,in} - C_{tr} R_p^M \frac{N_{AR}}{N_m} V = ; \quad N_{AR}(0) = N_{AR,o} \tag{7-4}$$

The volume of the reactor contents, V , can be determined by:

$$\frac{dV}{dt} = \frac{N_m M_w^M}{\rho_m} + \frac{N_{AR} M_w^{AR}}{\rho_{AR}} + \frac{N_p M_w^M}{\rho_p} + V_{wo} \tag{7-5}$$

where ρ_m , ρ_{AR} and ρ_p are the monomer, AR and polymer densities respectively; M_w^M and M_w^{AR} are the molecular weight of monomer and AR respectively; V_{wo} is the volume of water used in the polymerization.

7.3.2 Reactor energy balance

Reaction calorimetry is based on the monitoring of the heat generation rate due to polymerization reaction which is mainly driven by the propagation reactions. These measurements demand the combination of the dynamic heat balances for both the reactor and the jacket with temperature and flow rate measurements. The dynamic heat balances for the stirred tank reactor and the external jacket, where both the reactor and the jacket are assumed to be perfectly mixed, can be written as follows:

$$\frac{d(Mq_P T_r)}{dt} = \sum_i F_{i,in} M_w^i q_P^i (T_i - T_r) + Q_f + Q_r - Q_{loss} + Q_{stir} \tag{7-6}$$

$$m_j q_p^w \frac{d(T_{j,out})}{dt} = W_c q_p^w (T_{j,in} - T_{j,out}) - Q_f - Q_{loss} \tag{7-7}$$

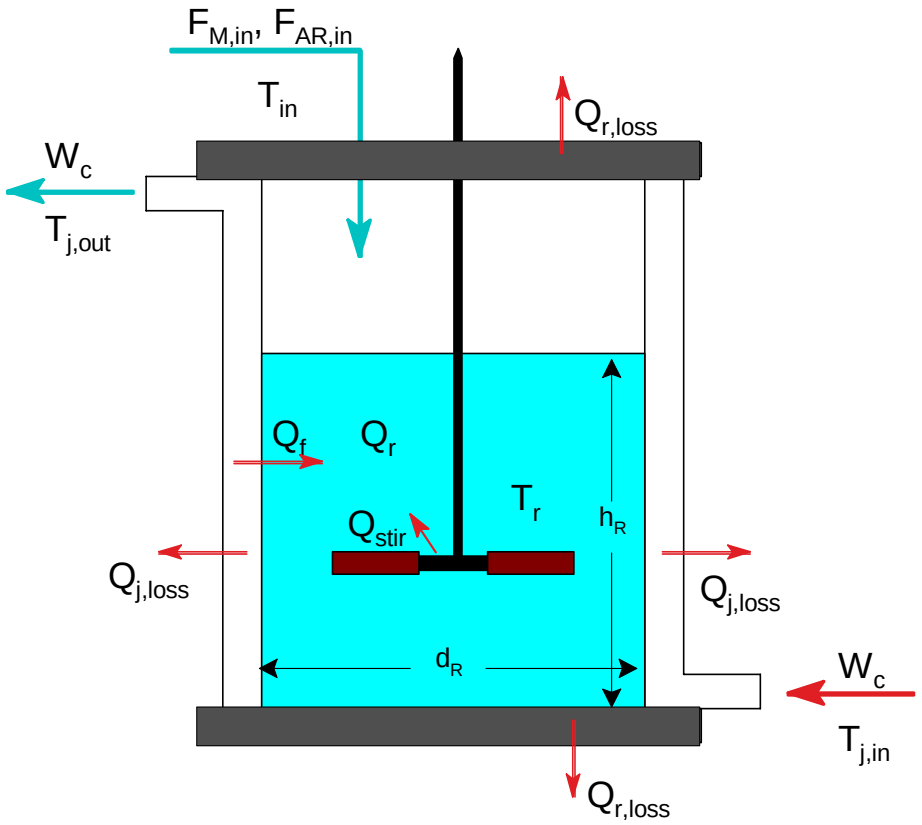

Scheme 7-1: Mass and energy balances components in a semi-batch.

In equation (7-6), the first term on the left-hand side is the heat accumulation in the reaction mass. The first term on the right-hand side member is the heat input due to the feeds; Q_f is the heat flow through the reactor wall; Q_{loss} is the heat loss to the surroundings; Q_r is the heat of reaction; and Q_{stir} is the energy input due to the stirrer. M and m_j are the masses of the reactor and jacket contents respectively, while q_p, q_p^w and q_p^i are the heat capacities of the reactor contents, water and feeds (i) respectively; T_i is the temperature of the added monomer and RAFT agent, which is equal to the ambient temperature; W_c is the mass flow rate of water through the jacket; T_r is the reactor temperature; $T_{j,in}, T_{j,out}$ are the jacket input and out temperatures, respectively. The water flow rate through the jacket is high and the jacket inlet and outlet temperatures are close to each other; under such conditions equation (7-7) is reduced to an algebraic equation with Q_f and Q_{loss} as the only unknowns. Thus, equation (7-6) becomes the only dynamic equation describing the dynamic thermal

behaviour of the reactor contents. However, this equation has three time dependent parameters that need to be determined.

It should be noted that changes in both the mass of the reactor contents and its specific heat were incorporated for the case of semi-batch operation. The energy terms involved in the energy balance equations are presented schematically in Scheme 7-1. The heat of reaction can be estimated from the other terms, if these can be calculated with sufficient accuracy and is given by.

$$\begin{aligned} Q_r &= R_p V \Delta H_p \\ &= \frac{d(Mq_P T_r)}{dt} - \sum_i F_{i,in} M_w^i q_P^i (T_i - T_r) - Q_f + Q_{loss} - Q_{stir} \end{aligned} \quad \textbf{(7-8)}$$

where ΔH_p is the heat of polymerization (reaction enthalpy) and is equal to -69900 J/mol for styrene polymerization (Zeaiter *et al.*, 2002a). For some cases, when operating under semi-batch mode, both the RAFT agent and monomer are fed as a mixture into the reactor. Typically, the fraction of RAFT agent in the feed mixture is much lower than monomer fraction; hence the heat effect of RAFT agent is not significant and can be neglected from equation (7-8). The heat flux across the reactor wall is given by:

$$Q_f = UA(T_{j,out} - T_r) \quad \textbf{(7-9)}$$

The rate of heat flow through the jacket depends on *UA*, which is the product of the overall heat transfer coefficient (*U*) and the heat-transfer surface area (*A*). The heat transfer surface area is given by:

$$A = A_B + \pi d_R h_R \quad \textbf{(7-10)}$$

where A_B is the base area of the reactor; d_R is the reactor diameter and h_R is the height of the reaction mixture in the reactor and is given by:

$$\frac{dh_R}{dt} = \frac{1}{A_B}\frac{dV}{dt}; \quad h_R(0) = h_{Ro}, \quad V(0) = V_{wo} \quad \textbf{(7-11)}$$

The overall heat transfer coefficient, *U*, was calculated from data taken during the initial heating stage, when the reactor contents were being heated to the operation temperature. During this stage, there is no polymerization reaction occurring since all the ingredient were charged into the reactor except the small quantity of initiator and no monomer is fed (i.e., batch mode operation).

The heat of stirring Q_{stir} is defined by:

$$Q_{stir} = K\rho N^3 d^5 \tag{7-12}$$

where *K* is the power number constant; *N* is the stirrer speed; *d* is the impeller diameter and ρ is the density of the latex calculated from:

$$\rho = \frac{N_m M_w^M + N_{AR} M_w^{AR} + N_p M_w^M + V_{wo}\rho_w}{(N_m M_w^M / \rho_m) + (N_{AR} M_w^{AR} / \rho_{AR}) + (N_p M_w^M / \rho_p) + V_{wo}} \tag{7-13}$$

Heating due to stirring was found to be negligible as it was estimated at about 0.5 W. Hence it was not included in further calculations (Zeaiter *et al.*, 2002a). Estimating of the heat removal through losses to the surroundings, along with the heat evolved during any evaporation/condensation processes is complex since heat loss is a function of both the reactor temperature, *Tr*, and the ambient temperature, *Tamb*. Heat loss is defined using the following empirical formula:

$$Q_{loss} = \alpha(T_r - T_{amb})^\beta \tag{7-14}$$

where α and β are constants and can be estimated by filling the reactor with a non-reacting mixture and solving Eq. (7-6) in the steady state while maintaining the reactor temperature constant. Under these conditions Eq. (7-6) becomes:

$$\alpha(T_r - T_{amb})^\beta = UA(T_{j,out} - T_r) - Mq_P \frac{dT_r}{dt} \tag{7-15}$$

7.4 Determination of U

The processes contributing to heat transfer in a polymerization reactor are the heat of reaction, thermal losses and heat of evaporation/condensation. Ignoring any of these factors will give a poor estimate of the reaction rate. An elegant way to circumvent this problem is by isolating each event and analyzing them separately. Firstly, the initial heat transfer coefficient, U_o, can be determined during the early stages of the heating process (i.e., at low operating temperatures). With all ingredients (except the small quantity of initiator) charged into the reactor, with thermal insulation on the reactor top and bottom surfaces and with no addition of feed, the effects of evaporation/condensation and heat losses from the reaction medium are kept at a minimum. Equation (7-6) with rearrangement becomes:

$$\tau \frac{dT_r}{dt} + T_r = T_{j,out}\,; \quad \tau = \frac{Mq_P}{U_o A} \tag{7-16}$$

where τ is the process time constant. Having M and q_p known U_o can then be determined from an estimate of τ at low temperature. Under low temperature conditions the jacket outlet temperature is close to the ambient temperature (isothermal conditions). Hence heat loss from the jacket to the surrounding is insignificant. For a step change in the jacket temperature (5-10 ^{o}C), τ can be obtained from the system dynamic response by using the following equation (Zeaiter *et al.*, 2002a):

$$\tau = 1.5(t_{0.632} - t_{0.283}) \tag{7-17}$$

where $t_{0.283}$ and $t_{0.632}$ are the times required by the system to reach 28.3% and 63.2% of the full response (steady state) respectively. The exact determination of such terms is a key aspect in reaction calorimetry with Q_f being the most important one. The overall heat transfer coefficient, UA, may still change during the course of polymerization. However, for the experimental conditions in this work, the volume percentage of the monomer was relatively low and the agitation speed was kept high resulting in reducing the polymer build up on the inner side of the reactor and hence UA could be assumed approximately constant.

7.5 Data acquisition and parameter estimation

The differential equations are discretised with respect to time. A link known as dynamic data exchange (DDE) is used to connect to the data acquisition software. A program written in Microsoft Excel and Microsoft Visual Basic is then used to employ the calorimetric calculations from online temperature and monomer feedrate readings. In the heating process, α and β are determined by least-squares method (Zeaiter *et al.*, 2002a). Rearranging the discretised version of Eq. (7-15) gives:

$$\ln\alpha + \beta \ln(T_r(t) - T_{amb}) = \ln\left[UA(t)(T_{j,out}(t) - T_r(t)) - M(t)q_P \frac{T_r(t) - T_r(t-1)}{\Delta t} \right] \qquad \textbf{(7-16)}$$

Equation (7-16) has a form of a straight line equation ($y = mx + c$), where

$y(t) = \ln\left[UA(t)(T_{j,out}(t) - T_r(t)) - M(t)q_P \frac{T_r(t) - T_r(t-1)}{\Delta t} \right]$, $x(t) = \ln(T_r(t) - T_{amb})$ and $c = \ln\alpha$.

Using least-squares method, the slope of the line, β, is:

$$\beta = \frac{\sum x_i y_i - \frac{\sum x_i - \sum y_i}{n}}{\sum x_i^2 - \frac{(\sum x_i)^2}{n}} \qquad \textbf{(7-17)}$$

where x_i and y_i are individual pairs of data for $\ln(T_r(t) - T_{amb})$ and $\ln\left[UA(t)(T_{j,out}(t) - T_r(t)) - M(t)q_P \frac{T_r(t) - T_r(t-1)}{\Delta t} \right]$; n is the number of pairs of data used in preparing the calibration curve, and $\bar{x}$ and $\bar{y}$ are the average values for the variable, and are given by:

$$\bar{x} = \frac{\sum x_i}{n}, \quad \bar{y} = \frac{\sum y_i}{n}$$

The intercept $\ln\alpha$ is given by: $\ln\alpha = \bar{y} + \beta\bar{x}$.

The low solids contents (~24% max.) and the high agitation rate (350 RPM) are assumed to ensure a constant heat transfer coefficient throughout the reaction phase.

Therefore, it is reasonable to assume that U is equal to U_o. During polymerization the heat losses and heat of evaporation/condensation also depend on the reactor contents, conversion and sample withdrawals. Hence the energy balance has to be adjusted to guarantee accurate estimation during reaction. In order to improve the estimation of the energy balance, the off-line gravimetric data were used to correct for uncertain parameter values. The basic procedure calculates, via optimisation, an improved value of the parameters (i.e. $\alpha\ (t)$ and $\beta\ (t)$) once new off-line gravimetric information becomes available.

7.6 Process optimization

Process optimization can have significant strategic impact on polymer plant operability and economics. The demand for polymer products having predetermined properties requires the control of microscopic characteristics during the reaction as post-treatments are expensive and not efficient in many respects. Despite its relative complexity, batch and semi-batch emulsion polymerizations are the methods of choice whenever specifications on conversion, particle size or molecular weight distribution are stringent. Since the MWD is influenced strongly by the polymerization reactor operation conditions, the production of a high quality polymer requires optimal operation of the reactor.

The objective of this work is to maximize the process productivity in a semi-batch emulsion polymerization reactor. The process variables that affect the process reactivity are the reaction temperature, the concentrations of monomer, initiator, surfactant and RAFT agent. The reaction temperature is one of the process operating conditions that affects the decomposition rate of the initiator and the propagation rate of monomer. Optimizing the process productivity can therefore be done by controlling both the reactor temperature and the concentration of monomer.

Three basic components are required to optimize an industrial process. First, the process or a mathematical model of the process must be available, and the process variables which can be manipulated and controlled must be known. Secondly, an economic model of the process is required. This is an equation that represents the profit made from the sale of products and costs associated with their production, such as raw materials,

operating costs, fixed costs, taxes, etc. Finally, an optimization procedure must be selected which locates the values of the independent variables of the process to produce the maximum profit or minimum cost as measured by the economic model. Also, the constraints in materials, process equipment, manpower, etc. must be satisfied as specified in the process mode.

The validated mathematical model that was used for optimization purposes to calculate the optimal trajectories is based on the detailed dynamic model presented in our previous work (Altarawneh *et al.*, 2008). This model was able to predict conversions, particle size and molecular weights in agreement with experimental results, demonstrating that it was accurate enough to represent the relationship between the operating conditions, kinetics, and final product properties. The mathematical equations that describe the model are presented in Chapter 4.

The continuous dynamic system is described by the following system of differential/algebraic equations:

$$\frac{dx}{dt} = f(x,u) \qquad \textbf{(7-18)}$$

$$x = g(x,u) \qquad \textbf{(7-19)}$$

where x is a state vector and u is the control variable vector to be optimized:

$$u(t) = [T, F_m, AR_o, I_o]. \qquad \textbf{(7-20)}$$

Any problem investigated in an optimization study will have as its objective the improvement of the system. The objective function is formulated in a quantitative form and subsequently subjected to a maximization or minimization. This is represented in mathematical form as follow:

$$\underset{x(i)}{Max} \quad j(x_1, x_2, ...x_n), \quad i = 1,2,....,n \qquad \textbf{(7-21)}$$

It is important to note that the maximisation problem is equivalent to the minimisation problem if the sign of the objective function is reversed. Here $j(x_1, x_2, ..., x_n)$ is a shorthand notation to denote some functional relationship between the adjustable parameters (x_1, x_2, ..., x_n) and the objective J. It is a measure of the difference between the required performance and the actual performance obtained. It should be fairly obvious that, by defining an input to the system the resulting output can be found. If this is not the case, we can not control the system, or in other words, optimise it. The vector of manipulated inputs (x_1, x_2, ..., x_n), are chosen to have the greatest influence on the objective function. These variables must be successively adjusted, during optimization, to obtain the desired maximum or minimum. Each set of adjustments to these variables is termed iteration, and in general a number of iterations is required before an optimum is obtained. In the iterative algorithm a first estimate of the decision variables must be supplied as a starting point.

The optimization problem often has more than one objective to be maximized or minimized. The problem then is formulated as a multi-objective optimization case. Such a problem is dealt with by placing some objectives in the form of constraints which is called ε-constraint method (Choi and Butala, 1991). With the ε-constraint method only one of the objectives (mainly the primary one) is expressed in the cost function while the other objectives take the form of inequality constraints:

$$\underset{x(i)}{Max} \quad j(x_1, x_2, ...x_n), \quad i = 1,2,....,n$$

Subject to,

$$j_i(x_1, x_{2,}, ..., x_n) < \varepsilon_i, \quad i = 1,2,...,n$$

The optimisation problem includes some equality and inequality constraints to the desired degree of precision. Some constraints are added to the manipulated variables, where a practical solution can be obtained. There are several types of constraints, i.e. algebraic equality constraints, algebraic inequality constraints and differential equality constraints.

7.6.1 Optimization scheme

Experiments were carried out in order to validate the optimization results obtained from the dynamic model. The first experiment (Opt.1) was designed to maximize monomer conversion via manipulating monomer feed rate over six time intervals. It is worth noting that maximizing monomer conversion is equivalent to minimizing average particle size, minimizing polymer molecular weight and minimizing the total amount of the added monomer. The second experiment (Opt.2) was designed to maximise polymer molecular weight.

Monomer conversion is defined in equation (7-27). The objective function for maximizing monomer conversion by adjusting monomer flow rate as a function of time is given by:

$$Max \quad J = [x_{mon}(N_m, t)]; \quad \forall \quad N_m \in \quad \Re; \quad t \quad \in \quad [0, t_f] \qquad \textbf{(7-22)}$$

The number average molecular weight is defined in equation (7-30). The objective function for maximizing polymer molecular weight by adjusting monomer flow rate as a function of time was defined as:

$$Max \quad J = [Mn(N_m, t)]; \quad \forall \quad N_m \in \quad \Re; \quad t \quad \in \quad [0, t_f] \qquad \textbf{(7-23)}$$

For operational reasons, the monomer feedrate was specified with the following upper and lower bounds:

$$F_m \in \quad [5 \times 10^{-5} mol / \min, \quad 8.07 \times 10^{-3} mol / \min]$$

Since this is a semi-batch process with monomer continually fed to the reactor, the maximization of equation (7-22) requires a reduction in monomer flow rate in order to ensure the absence of monomer droplets. Reducing monomer flow rate would result in reducing production rate, particle size and molecular weight. Thus, equation (7-22) must be subject to additional constraints to account for the total amount of monomer in the recipe $(N_{m,total})$ in order to guarantee maximum production rate, desired particle size and molecular weight. These constraints were defined as follows:

$$for \quad Opt.1$$
$$N_{m,total} \geq 0.4mol; \quad 5400s \leq t_{final} \leq 19800s; \quad 1 \leq PSPI \leq 1.04$$
$$23kg/mol \leq M_n \leq 28kg/mol; \quad 60nm \leq P_d \leq 100nm$$

$$for \quad Opt.2$$
$$N_{m,total} \geq 1.1mol \quad ; \quad 5400s \leq t_{final} \leq 19800s; \quad 0.85 \leq X_{mon} \leq 1$$
$$1 \leq PSPI \leq 1.04; \quad 90nm \leq P_d \leq 100nm$$

where *PSPI* is the particle size polydispersity index and P_d is the average particle diameter.

The batch pre-period is excluded from the optimization and the initial conditions for this period are outlined below:

$$\text{Initiator}: I_o = 7.4 \times 10^{-4} mol$$
$$\text{RAFT}: AR_o = 0.00169mol$$
$$\text{Monomer}: M_o = 0.170mol$$
$$\text{Surfactant}: S_o = 0.0034mol$$
$$\text{Volume}: V_o = 0.6L$$
$$\text{Temperature}: T = 70^o C$$

An initial time of 5400 seconds is specified for the first stage of the polymerization which is for seeding stage; this stage was excluded from the optimization. Six bounded time intervals (of initially equal duration of 2450s) were specified during the semi-batch period for the manipulated variable, F_m. The overall horizon was bounded between 5400 and 20000 seconds.

7.6.2 Implementation of the optimization scheme

The dynamic optimization problem is set-up in gPROMS using a dynamic model and a separate optimization file. This file includes information on the time horizon, objective function, form of the control variables and any constraints that need to be imposed on the process. The optimization is performed by IDP procedure (iterative dynamic programming) through gPROMS. The algorithm used in gPROMS employs the control parameterization approach coupled with a multi-step backward-difference method for

the integration of the set of differential algebraic equations (Vassiliadis *et al.*, 1993; Vassiliadis *et al.*, 1994). The time horizon, over which the process is optimized, is partitioned into a pre-defined number of stages. The duration of each stage is divided into a number of control intervals and the continuity of the differential variables is enforced at the boundaries through simple junction conditions. The detailed operating procedures of the dynamic optimisation processes within gPROMS are presented in gPROMS user guide (PSE, 2004)

The CVP_SS, a standard mathematical solver for optimisation in gPROMS, is implemented to solve the model based optimisation problem in this work. CVP_SS can solve optimisation problems with both discrete and continuous decision variables. For dynamic optimisation problems, CVP_SS is based on a control vector parameterisation (CVP) approach which assumes that the time-varying control variables are piecewise constant (or piecewise linear) functions of time over a specified number of control intervals. The precise values of the controls over each interval, as well as the duration of the latter, are generally determined by the optimisation algorithm.

The solver implements standard DASOLV and SRQPD codes. The DASOLV code is to find the solution of the underlying differential equation (DAE) problem and the computation of its sensitivities. While SRQPD solver employs a sequential quadratic programming (SQP) method for the solution of the nonlinear programming (NLP) problem. Both solvers have their own algorithmic parameters described in the manual of gPROMS (PSE, 2004). The solution of this problem required 148 line-search evaluations of the objective function and the constraints. The solution converged after 105 iterations and the overall computation took approximately six hours on a Pentium IV 400 MHz PC.

7.7 Results and discussions

7.7.1 Calorimetry results

Batch and semi-batch RAFT emulsion polymerizations of styrene were carried out in a jacketed 1L stainless steel reactor equipped with an agitation speed controller and three

RTD sensors. All reactions were conducted as described in Chapter 5 for batch RAFT emulsion polymerizations and in Chapter 6 for semi-batch RAFT emulsion polymerizations. Reactor dimensions are given in Table 7-1.

Table 7-1: Reactor dimensions and operating conditions.

Reactor height	0.18 m
Reactor diameter	0.085 m
Jacket height	0.13 m
Jacket volume	350 ml
Water flow rate through jacket	20 l/min
Agitation speed	350 rpm

A computer-controlled system was used for data recording and manipulation. The temperature within the reactor, inlet and outlet of the jacket and also monomer feed rate, which corresponded to the electronic balance and time, are all recorded in a database system. The recorded monomer flow rate, jacket inlet, jacket outlet, ambient and reaction temperatures were used in the calorimetric model to measure polymerization rate, monomer conversion and polymer molecular weight.

The polymerization reactions are known to be exothermic and are, therefore, usually monitored by calorimetry. The reactor and jacket temperatures are measured online. The unknown terms in the heat balance (the heat transfer coefficient U and the heat loss coefficients: α and β) can be estimated as previously described. The value of 85 $W/m^2.K$ for the overall heat transfer coefficient was estimated at low operating temperatures during the early stages of the heating process. The optimal and corrected values of the heat loss coefficients, α and β, were estimated at 1.18×10^{-3} and 2.238 respectively. These parameters were found to be constant during the reaction. Therefore, these coefficients were identified before the reaction and the obtained values were introduced into the heat balance to estimate the heat produced by the reaction.

7.7.1.1 Polymerization rate and monomer conversion

The overall heat of polymerization is equal to the heat generated from the polymerization process in the aqueous and the particle phases. The polymerization

reaction is highly occurred in the particle phase. In this model the polymerization reaction in aqueous phase is also included in the calculations even though it can be neglected since the temperature readings are for the whole reactor contents and not only for the polymer particles. The rate of polymerization is estimated from the heat of reaction and is given by:

$$R_p^M = \frac{Q_r}{V\Delta H} \tag{7-24}$$

By substituting equation (7-24) in equations (7-1) and (7-4), the amounts of the unreacted monomer and RAFT agent can be expressed as a function of heat released by polymerization. Hence, equations (7-1) and (7-4) can be rewritten as:

$$\frac{dN_m}{dt} = F_{m,in} - \frac{Q_r}{\Delta H} \tag{7-25}$$

$$\frac{dN_{AR}}{dt} = F_{AR,in} - \frac{C_{tr}}{r}\frac{Q_r}{\Delta H}; \quad r = \frac{N_m}{N_{AR}} \tag{7-26}$$

The instantaneous monomer conversion, x_{mon}, is calculated as follows:

$$x_{mon} = 1 - \frac{N_m}{N_{m,T}} \tag{7-27}$$

where $N_{m,T}$ is the total amount of monomer added during the reaction and is related to monomer flow rate F_m by:

$$\frac{dN_{m,T}}{dt} = F_m; \quad N_{m,T}(0) = N_{mo} \tag{7-28}$$

In batch mode, F_m is equal to zero and $N_{m,T}$ is equal to the total amount of monomer (moles) charged initially into the reactor.

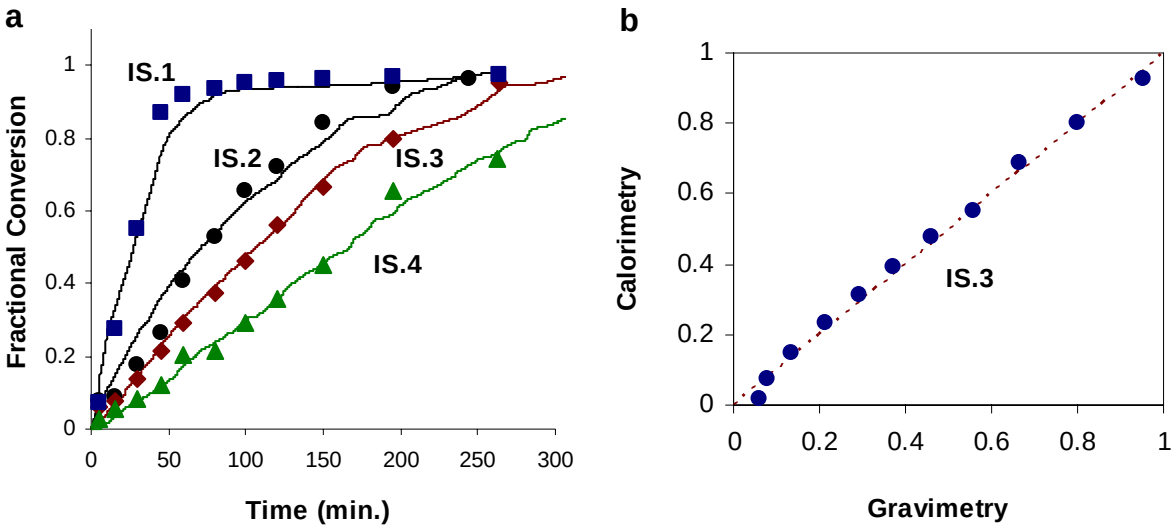

Figure 7-1: Semi-batch emulsion polymerization of styrene: (a) Comparison of the overall conversions measured by gravimetry and calorimetry; (b) Comparison of the overall conversions measured by gravimetry and calorimetry for batch emulsion polymerization of styrene. Legend: Run IS.1 (■); Run IS.2 (●); Run IS.3 (♦); Run IS.4 (▲); Calorimetry (—) and 45° scattering line (---).

By comparing the overall monomer conversion measured by the calorimetric model with those measured by gravimetry, the accuracy of the calorimetric model is confirmed as shown in Figure 7-1. Figure 7-1b presents the comparison of the overall conversion measured by the gravimetric method and calorimetry model (gravimetry is the reference technique). It can be seen that the conversion data obtained by calorimetry and gravimetry are close to each other as their distribution lie on the 45° scattering line.

In Figure 7-2, the effect of increasing the initial concentration of AR on the polymerization rate is demonstrated by comparing three batch emulsion polymerizations of styrene with different AR concentrations with the polymerization without RAFT agent. As can be seen from Figure 7-2 increasing AR concentration resulted in decreasing the heat of reaction curves (polymerization rate) as expected due to the retardation effect. Independent of the AR concentration, the rate maxima for the polymerization with AR were all reached in the 34%-40% conversion range, as can be seen by comparing Figure 7-1a with Figure 7-2.

One of the most important observations from these curves is the unclear presence of a constant rate period expected for Interval II. However, the duration of the period of the maximum polymerization rate is relatively short for the polymerization without AR and

increases with an increase in AR concentration. After this period, the rate of polymerization decreased after almost 61% conversion as a result of the disappearance of the monomer droplets and the reduction in the monomer concentration in the polymer particles.

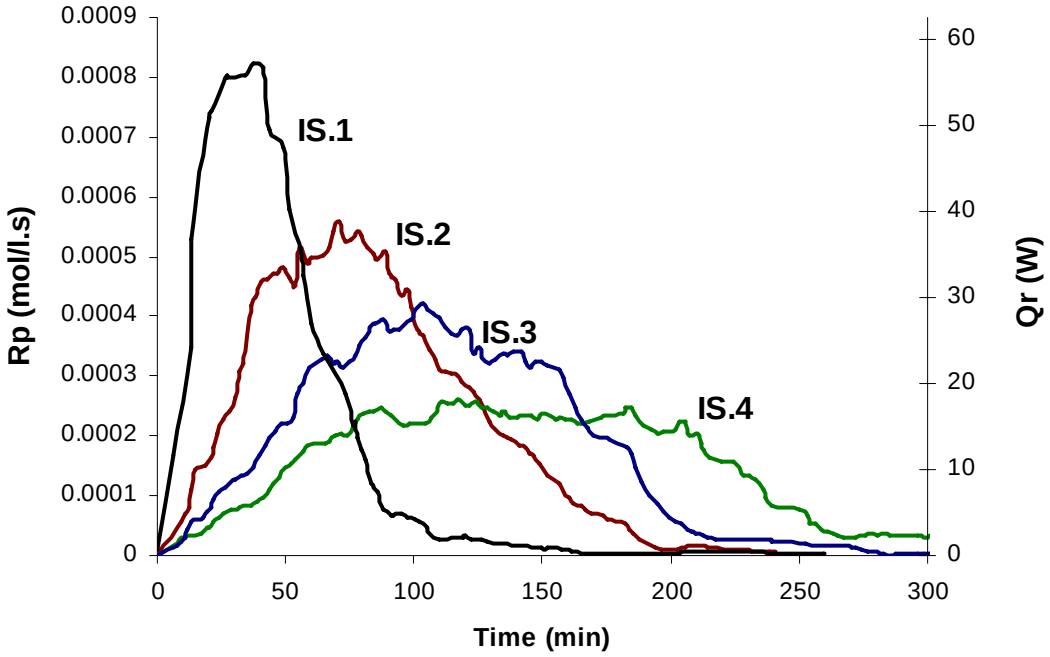

Figure 7-2: Effect of RAFT agent concentration on the polymerization rate.

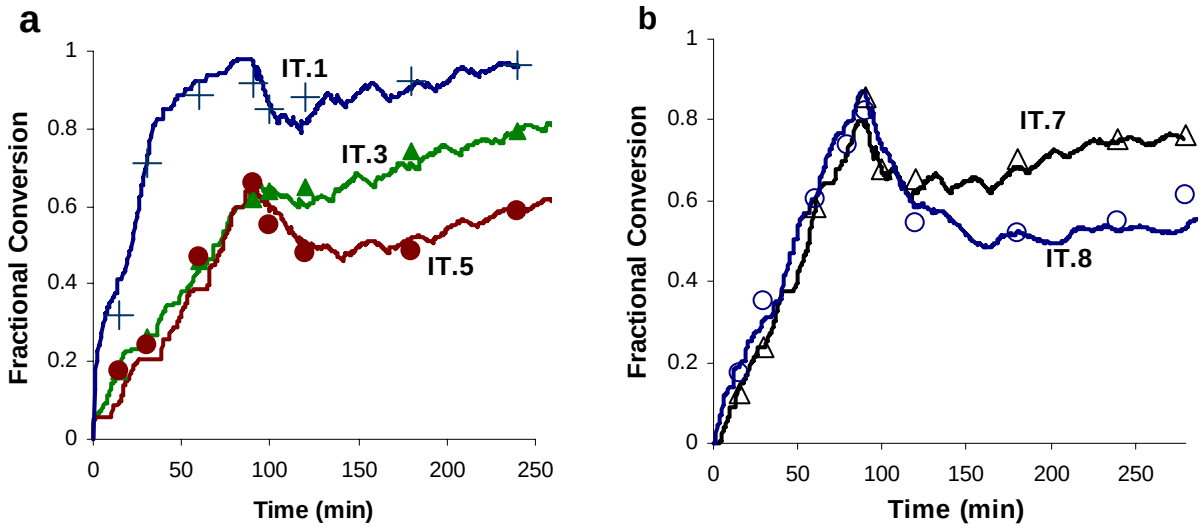

Figure 7-3: Semi-batch emulsion polymerization of styrene: (a) Effect of monomer flow rate and RAFT agent concentration; (b) effect of RAFT agent flow rate on the overall monomer conversion, gravimetric measurements (symbols), dynamic simulation (dotted curve) and calorimetry (solid curves).

For semi-batch polymerization with and without AR, (see Figure 7-3), the overall monomer conversion obtained from the calorimetric model compares well with the overall conversions predicted by the dynamic model and with the overall conversion measured by gravimetry. This is another indication that the calorimetric model is of high accuracy, and is suitable for use as an online soft sensor. During the batch period, reactions IT.3, IT.4 and IT.5 were carried out under similar conditions. Thus the data summarised in Figures 7-3 and 7-4 (IT.3, IT.4, IT.5, IT.7 and IT.8) show experimentally the reproducibility of the calorimetric model employed.

Figure 7-4a, presents a comparison of the polymerization rate between the batch and semi-batch emulsion polymerization of styrene without RAFT agent. It is clear that the batch run shows a larger exotherm, and this is due to the higher monomer content in this recipe. A rapid increase in the polymerization rate (IS.1) is initially observed due to particle nucleation taking place during the particle formation stage (Interval I). It is obvious that the first change in the polymerization rate occurs between 40-50% conversions where the polymerization rate attains its maxima. Afterwards the reaction rate reaches a short steady state period marking the start of the growth stage (interval II). At this short stage, particle nucleation ceases and the polymerizing particles are continually replenished with monomer diffusing from the monomer droplets. The number of particles and the monomer concentration inside the particles thus remain constant. Thereafter, the reaction rate decreases monotonically (due to the consumption of monomer droplets in the aqueous phase) and the exotherm “decays” with time as the concentration of monomer decreases and reaches very low values at high monomer conversion.

In the semi-batch experiment without RAFT agent (IT.1, Fig. 7-4a), the exotherm is consequently smaller, and lasts for a shorter period of time. The polymerization rate increases rapidly at the beginning of the reaction and reaches its maximum limit which is proportional to the amount of the initial charge of monomer. After this point the polymerization rate drops to a very low value which indicates that almost all of the initial charge of monomer is polymerized and a high conversion of 98% was obtained at the end of the batch pre-period (90 min).

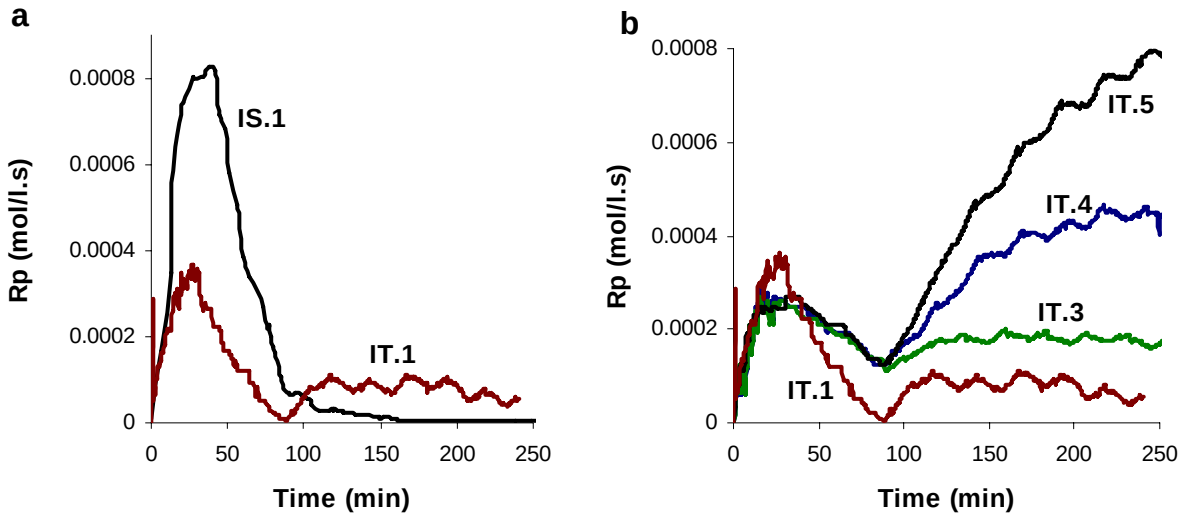

Figure 7-4: Emulsion polymerization of styrene: (a) Effect of reaction mode on the polymerization rate; (b) Effect of monomer flow rate on the polymerization rate.

As the monomer is added, unreacted monomers concentration increases in the aqueous phase, which induces an increase of monomer concentration inside the particles. Hence, additional monomer becomes available for the polymerization and resulting in the reaction rate increases and becomes in equilibrium with the monomer feedrate. Under similar conditions and in the presence of AR (IT.3, Fig. 7-4b), the increase in the polymerization rate during the batch pre-period is retarded and the drop in the polymerization rate during the semi-batch period was observed to be slower. The main reason behind the observed retardation was, intensely, investigated in Chapters 5 and 6. The effect of monomer feed rate on the polymerization rate is presented in Figure 7-4b. It should be noted that a high monomer feed rate resulted in a high reaction rate. This is because the monomer concentration in the particles increases with an increase in feedrate, thus leading to an increase in the reaction rate.

The accuracy of the calorimetric analysis was investigated by plotting monomer conversion versus time along with the results obtained by gravimetry, as shown in Figures 7-1 and 7-3. The accuracy of gravimetry is ensured by the cessation of reaction in the presence of oxygen (inhibitor) outside the reactor. Good agreement between the calorimetric measurements and the offline gravimetric results was obtained. Hence, the calorimetric model can be used as a "soft-sensor" having a 3%-5% prediction error, which is acceptable for most on-line monitoring and control purposes.

7.7.1.2 Polymer molecular weight

In emulsion polymerization systems where the compartmentalization plays a significant role, the number molecular weight distribution is the number of non growing (dead) chains with a given molecular weight. The population of dead chains is controlled by the number of living chains, the rate at which chains grow, and by the kinetic events that stop the growing of the living chains. These evens are: entry, transfer reactions facilitated by the transfer agent and transfer to monomer. It has been demonstrated, in Chapters 5 and 6, that the transfer to RAFT agent is the dominant transfer reaction occurring in RAFT emulsion polymerization. The rate of kinetic events that stop the growing of the living chains is given by:

$$R_t = k_{tr}^{AR} C_p^{AR} + k_{tr}^{M} C_p^{M} + \rho_{avg} \qquad \textbf{(7-29)}$$

where the first term in the right-hand side member accounts for the termination by chain transfer to AR, the second for the termination by chain transfer to the monomer, and the third for bimolecular termination with radicals entering from the aqueous phase.

It has been experimentally shown that monomer mass transfer is high enough to bring about a rapid thermodynamic equilibrium (Altarawneh *et al.*, 2008; Gugliotta *et al.*, 1995b; Mendoza *et al.*, 2000; Salazar *et al.*, 1998; Zeaiter *et al.*, 2002b). In addition, experimental data presented in this work showed that for this system, RAFT agent mass transfer is not subjected to diffusional limitation. A similar conclusion was reported in the literature (Smulders *et al.*, 2003) in which the consumption rate of RAFT agent was found to be lower than its transportation rate from the droplets through the aqueous phase to the particles. Hence the mass transfer of the RAFT agent is not rate determining step and any reacted AR will be readily replenished. Bearing this in mind, the concentration of AR in the particle phase can be calculated as a function of monomer concentration (Altarawneh *et al.*, 2008; Monteiro *et al.*, 2005).

Typical calculations, using $k_{tr}^{AR} = 196 \quad (mol/L.s)$ (Altarawneh *et al.*, 2008; Smulders *et al.*, 2003); $k_{tr}^{M} = 0.01 \quad (mol/L.s)$ (Gilbert, 1995; Zeaiter *et al.*, 2002b); average entry rate $\rho_{avg} = 0.002 \quad s^{-1}$ (Asua *et al.*, 1990; Vicente *et al.*, 2001); $C_p^{M} = 5.5 \quad (mol/L)$;

and $C_p^{AR} = rC_p^M \quad (mol/L)$ (Altarawneh *et al.*, 2008; Monteiro *et al.*, 2005; Smulders, 2002), show that the rate of transfer reaction to AR is two orders of magnitude higher than that to monomer ($k_{tr}^{AR}C_p^{AR} / k_{tr}^{M}C_p^{M} \approx 653$) and three orders of magnitude higher than termination by radical entry ($k_{tr}^{AR}C_p^{AR} / \rho_{avg} \approx 5390$). Under these circumstances, the number average molecular weight is given by:

$$Mn = \frac{k_p C_p^M}{k_{tr} C_p^{AR}} = \frac{k_p N_m / V_p}{k_{tr} N_{AR} / V_p} M_w^M = \frac{N_m}{C_{tr} N_{AR}} M_w^M \qquad \textbf{(7-30)}$$

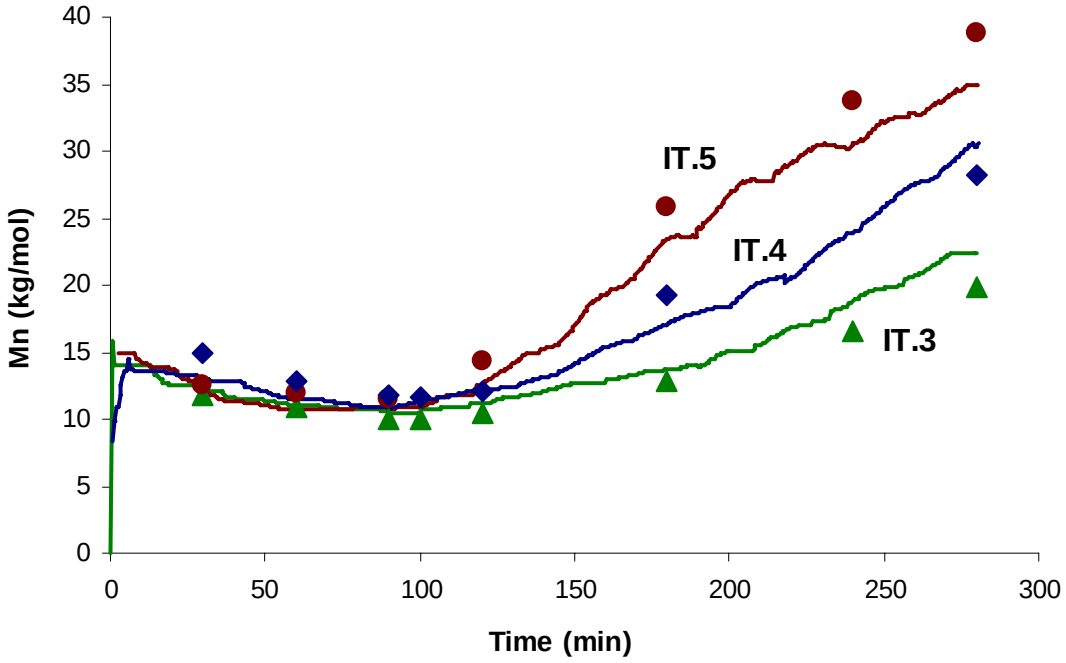

Figure 7-5: Number average molecular weight measured by GPC (symbols) and calorimetry Legend: Run IT.3 (▲); Run IT.4 (♦); Run IT.5; and calorimetry (–).

Figure 7-5 presents a comparison between the number average molecular weight of the produced polymer measured by calorimetry model and size exclusion chromatography. As the transfer to AR is the dominant chain stopping event, almost all of the produced polymeric chains are believed to carry the RAFT moity and hence the concentration of these dormant chains is approximately equal to the initial concentration of RAFT agent. Therefore, the dormant polystyrene chains possess the RAFT agent moiety and can regain radical activity upon reactivation and further polymerize with the added monomer resulting in increasing Mn.

Calorimetric measurements indicate that the increase in Mn is proportional to monomer flow rate as shown in Figure 7-5. With the concentration of the dormant polystyrene-xanthate is approximately constant, the increase in Mn is mainly due to the increase in the molar ratio of monomer to RAFT agent. Thus, it is concluded that the number average molecular weight of the polystyrene-xanthate dormant chains can be efficiently controlled by manipulating monomer flow rate. It can be seen that the prediction of the calorimetric model agrees well with the measured Mn by SEC. Thus, by using the online temperature measurements, the calorimetric model can be used as an online sensor to infer monomer conversion and polymer molecular weight.

7.7.2 Optimization results

Rate retardation is an inherent characteristic of RAFT emulsion polymerization. Such retardation is attributed to the exit of small RAFT-derived radicals generated from the transfer reaction to RAFT agent (AR). These radicals terminate in the aqueous phase unless reentry occurs. The termination of these radicals results in radical loss which alters radical flux and eventually reduces the rate of polymerization. The use of RAFT agent flow rate as a manipulated variable will result in influencing both polymerization rate and polymer molecular weight. As discussed in Chapters 5 and 6, due to the low activity of our RAFT agent (transfer constant ≈ 1) the number average molecular weight was found to be almost constant and proportional to the initial molar ratio of monomer to AR. On the other hand, without feeding in RAFT agent, the number average molecular weight was found to increase with an increased monomer concentration when operating under semi-batch mode. This behaviour is demonstrated in Figure 7-7a at different monomer flow rates. Using the initial AR concentration as the control variable would result in affecting polymer molecular weight during the batch pre-period, in which low molecular weight can be obtained by increasing AR concentration and vice versa. The effect of AR during the semi-batch period is almost negligible as the amount of the remaining AR is very low, unless extra AR is added.

The effect of RAFT agent on the polymerization rate is one of the major drawbacks in any polymerization system, and using it as a manipulating variable during the semi-

batch period is of insignificant importance. In emulsion polymerization, the concentration of monomer in the polymer particles is proportional to the reaction rate. Controlling this parameter can be done by manipulating the feed rate of monomer. On the contrary, the relation between the concentration of radicals in the polymer particles and the initiator feed is not always evident. Therefore, the initiator feed rate cannot be used to control the reaction rate. Thus, it is decided in this work to use monomer flow rate as the primary manipulating variable, where the production rate, particle size and molecular weight can all be manipulated.

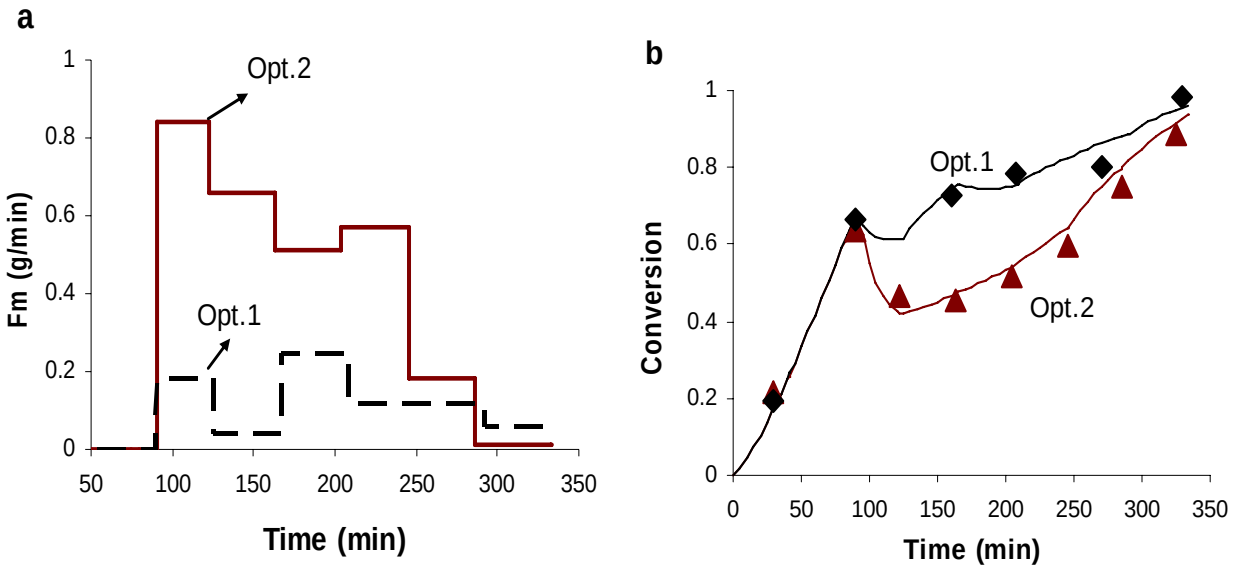

Figure 7-6: Experimental (symbols) and simulated (lines) semi-batch emulsion polymerization of styrene: (a) Optimal monomer feed rate profiles; (b) Monomer conversion. Legend: Run Opt.1 (♦); Run Opt.2 (▲); and dynamic optimization (–).

Two objective functions were studied, in terms of both monomer conversion and molecular weight. For molecular weight, maximising Mn (Opt.2) was used as the objective function. Particle polydispersity index, particle average diameter, total amount of the added monomer and the final monomer conversion were included as end-point constraints. The aim of the first optimization run (Opt.1) was to maximize monomer conversion (productivity), i.e. to minimize the reaction time and to obtain a polymer with a desired molecular weight, and particle size. Two conditions must be considered to determine the maximum reaction rate, i.e. the largest possible monomer concentration in the particle phase. These are: (i) the absence of droplet phase and (ii) the reaction rate should not exceed the maximum heat removal capability.

It is known that when the maximum swelling of the polymer particles with monomer is reached, a droplet phase forms. As the reaction rate in the polymer particles depends solely on the amount of monomer in the particles, an additional droplet phase will not increase the reaction rate, but it will act as a reservoir and enable the direct influence on the concentration in the particle phase. Thus, droplet phase is unnecessary and should be avoided. The latter condition is often neglected in trajectory optimization of emulsion polymerization, if laboratory-scale reactor is considered. Due to the high surface-volume ratio and high flow rate of the cooling medium, this condition dose not limits the reaction rate. However, for large scale reactors this condition becomes increasingly important (Gesthuisen *et al.*, 2004).

The optimal monomer feed rate to achieve high monomer conversion is given in Figure 7-6a. To achieve high productivity (Opt.1 in Fig 7-6b), the dynamic optimization suggests low monomer feed rates to ensure starved feed conditions in the absence of monomer droplets. The optimal duration to produce the desired polymer was found to be of about six hours. Figure 7-6b, shows the time evolution of monomer conversion obtained from experiment Opt.2. Initially, due to the high monomer feed rate monomer conversion drops to a low value of about 45% and then increases with a decrease in monomer feed rate to attain a value of about 88% at the end of the reaction. This is due to the fact that the sudden increase in the monomer flow rate results in monomer accumulation inside the reactor. However, the decrease in monomer conversion is short-lived as the concentration inside the particles starts to increase with monomer diffusing from the aqueous phase. As a result the reaction rate increases and the monomer conversion climbs and reaches higher values. The responses show that the highest conversion drop occurs with the highest monomer flow rate.

As depicted in Figure 7-7b, during the batch pre-period, the growth rate of particles decreases with a decrease in monomer concentration, while the Mn remains almost constant due to the low activity of the used RAFT agent. With the sudden addition of monomer during the semi-batch stage, particle growth resumed, thus, preventing broadening of the PSD and the final particle size is within the constraint range. In Opt.1, proportional to the amount of the reacted monomer, Mn increases slowly with time, and reaches a value of 26 kg/mol at 98% conversion, which is within the constraint range.

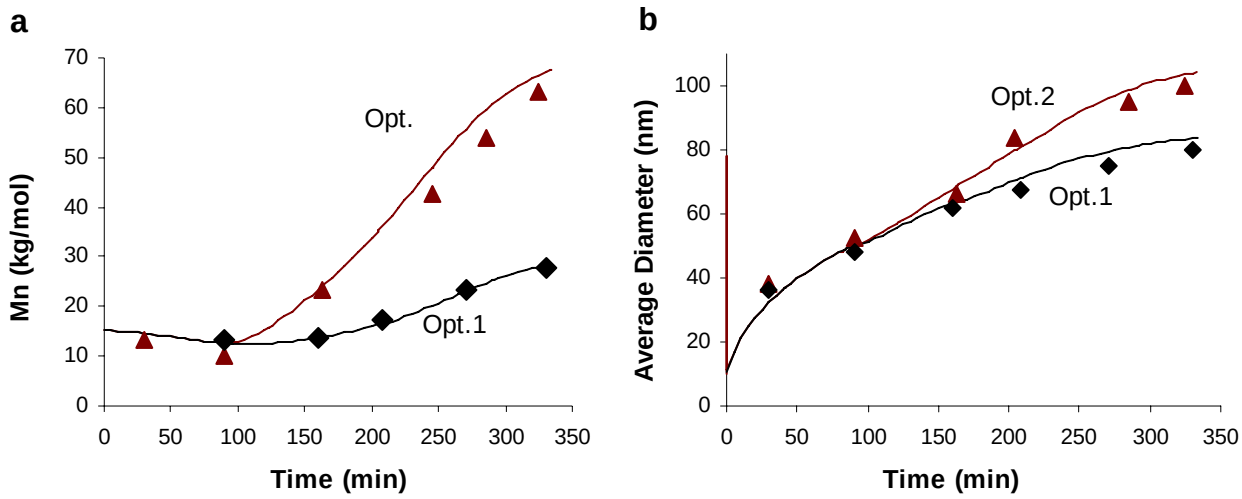

Figure 7-7: Experimental (symbols) and simulated (lines) semi-batch emulsion polymerization of styrene: (a) Number average molecular weight of the produced polymer; (b) Average particle size. Legend: Run Opt.1 (♦); Run Opt.2 (▲); and dynamic optimization (–).

Experiment Opt.2 was designed to maximize the number average molecular weight, Mn, of the produced polymer by using monomer feed rate as a control variable with conversion and particle size constraints. The polystyrene-xanthate chains produced in the batch pre-period are dormant and capable of regaining radical activity via further transfer reactions. Thus, the size of these chains increases by the addition of more monomer resulting in increasing Mn and demonstrating the living nature of these chains. The optimal monomer feed rate profile for Opt.2 is given in Figure 7-6a. It is worth noting that, in order to maximize Mn, the dynamic optimization suggests higher monomer feedrates.

Figure 7-8 presents the simulated and experimental PSD results for Opt.1 and Opt.2, after employing the calculated optimal strategies. It can be clearly seen that, the final shape of the experimental PSD is in good agreement with the simulation results. The absence of bimodality (resulting from secondary nucleation) in these distributions strongly indicates that the particle size distributions in both experiments are narrow, and the particles formed essentially fall within the 'small' size regime. The MWDs presented in Figure 7-9, were measured using double-detection size exclusion chromatography equipped with UV detector (operating at a wavelength equal to 254 nm) and a combination of RI and Viscometer detectors. The perfect overlap of the UV and RI/Visco MWD traces for both experiments strongly suggests that almost all of the polystyrene-xanthate dormant chains obtained at the end of the batch pre-period were

completely incorporated in the polymerization with the added monomer. This is another indication that the system exhibits living characteristics in which no bimodality was observed in both traces. Once again, the experimental MWD results are in good accord with our simulation results.

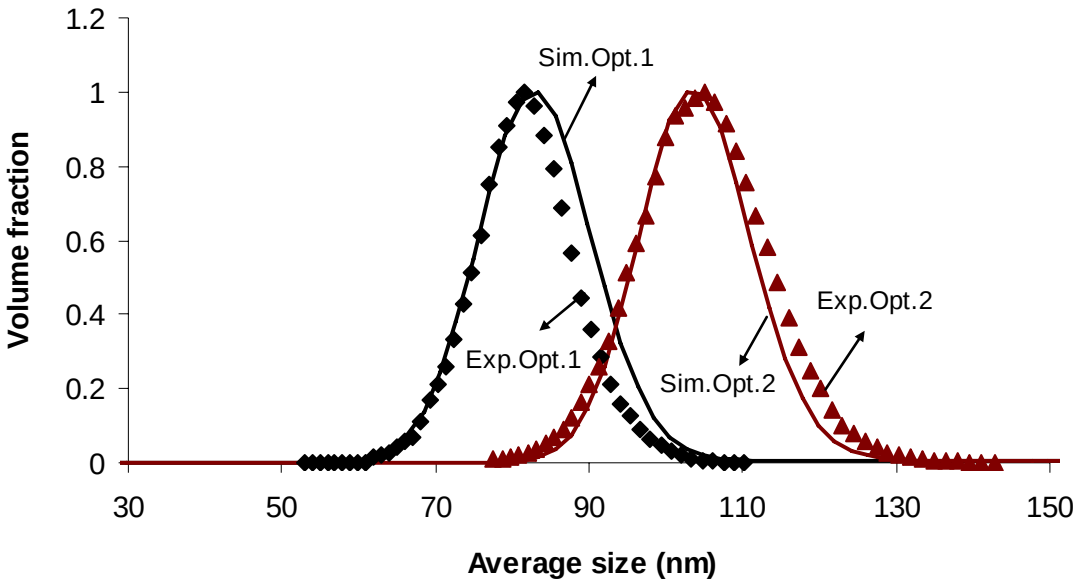

Figure 7-8: Particle size distribution (PSD) measured by PL-PSDA. Legend: Run Opt.1 (♦); Run Opt.2 (▲); and dynamic optimization (–).

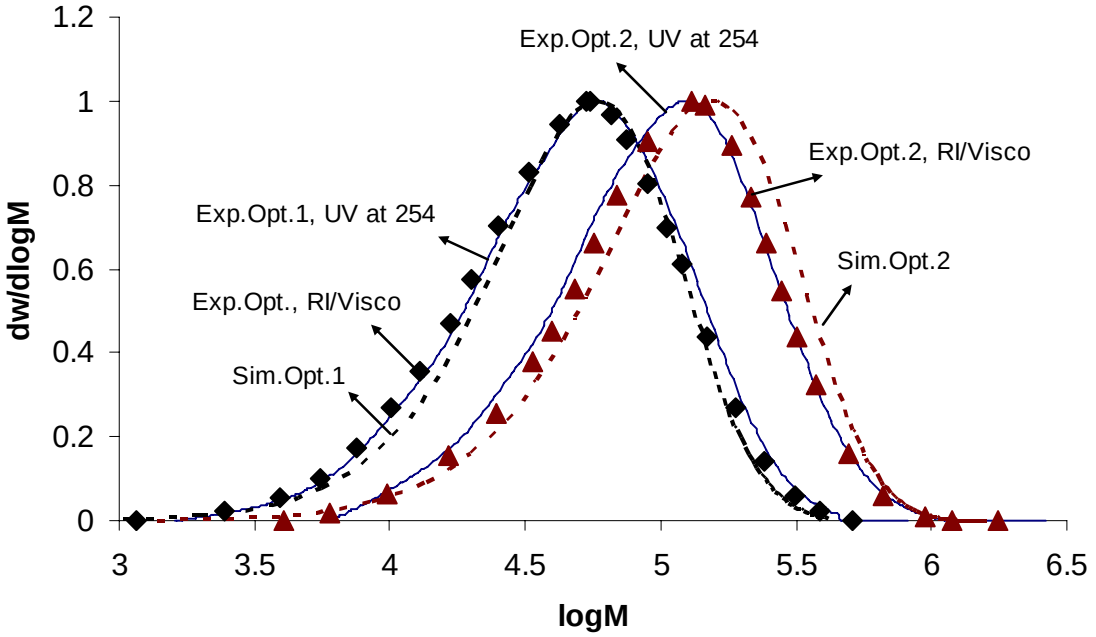

Figure 7-9: Molecular weight distribution of the produced polymer measured by double detection SEC system. Legend: Run Opt.1: RI/Visco (♦); UV (–); and dynamic optimization (···); Run Opt.2: RI/Visco UV (–); and dynamic optimization (···).

The deficiency of accurate online sensors for the measurement of polymer properties coupled with the non-linearity of the system behavior represent drawbacks of batch and semi-batch polymerization reactor control. This optimisation system was used as a case study tested against the calorimetric model on obtaining the overall monomer conversion and polymer molecular weight. The calorimetric model developed in this Chapter was used with the pre-determined values of the overall heat coefficient (U) and the heat loss parameters (α and β) to process the temperature measurements obtained online from experiment Opt.2. Monomer conversion was calculated from the gravimetric data based on the total amount of monomer at the time of sampling (method (a), instantaneous conversion) and based on the total amount of the added monomer throughout the reaction (method (b), overall conversion).

The agreement between the calorimetric and gravimetric measurements of monomer is good as shown in Figure 7-10. We conclude that the calorimetric model developed in this Chapter can be used as an accurate online sensor for inferring both of monomer conversion and polymer molecular weight. However, it is worth noting that the calorimetric model for molecular weigh estimation is valid for our system where the transfer to RAFT agent is the dominant chain stopping event.

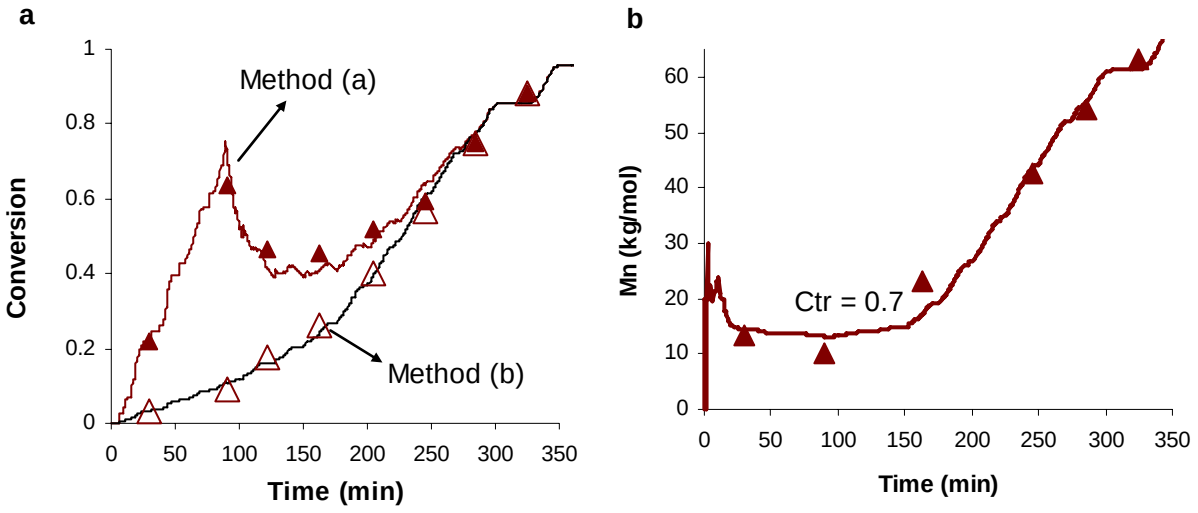

Figure 7-10: Semi-batch emulsion polymerization of styrene: (a) Monomer conversion measured by gravimetry (symbols) and calorimetry (lines); (b) Number average molecular weight of the produced polymer conversion measured by GPC (symbols) and calorimetry (line).

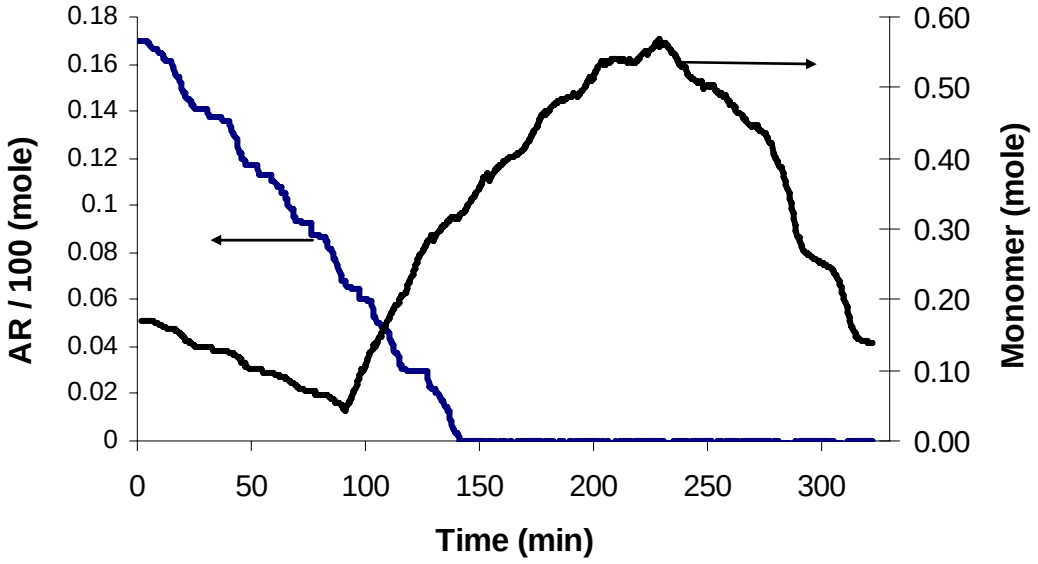

Figure 7-11: Monomer and AR concentrations in mole measured by the calorimetry model for Opt.2.

Figure 7-11 shows the calorimetric measurements of the remaining number of moles of AR and monomer with time (Opt.2). As no AR was fed into the reactor, the concentration of AR decreased with time and reached zero after approximately two hours. At higher monomer feedrates, it is quite clear that the monomer feed rate was higher than the polymerization rate as indicated by the accumulation of monomer in the reactor. As a result of the decreasing monomer feed rate, as suggested by dynamic optimization (Fig. 7-6a, Opt.2), monomer concentration decreased dramatically during the final stages of polymerization. This suggests that the polymerization rate was higher than monomer feedrate, and hence a higher monomer conversion of about 88% was obtained.

In the calorimetric model, the molecular weight was inferred by computing the concentrations of the monomer and AR. The concentration of AR is calculated using equation 7-27 which is a function of the polymerization rate, the transfer constant and the initial molar ratio of monomer to AR.

7.7.3 Sensitivity of the calorimetric model

It should be noted that the polymerization rate does not affect the evolution of Mn as discussed in Chapter 3. That is, the rate retardation has no effect on molecular weight control, but dramatically influences the kinetics of polymerization (Saricilar *et al.*, 2003). The evolution of Mn is strongly influenced by the activity of our RAFT agent. The sensitivity of the calorimetric model toward the transfer constant was tested under similar polymerization rate and initial molar ratio of monomer to AR as in Opt.1.

The transfer constant was increased by two orders of magnitude from 0.7 to 70. Under these conditions, one would expect a linear growth of the number average molecular weight with the overall conversion. It should be noted that in a real situation the polymerization with a high active RAFT agent would result in high rate retardation, and monomer conversion would be even lower than that obtained from experiment Opt.2. In Figure 7-12 the monomer conversion was calculated from the gravimetric data based on the total amount of the added monomer throughout the reaction. In this Figure, the linear growth of polymer molecular weight with conversion, in the semi-batch period, is evident as measured by the calorimetric model and agrees with theory.

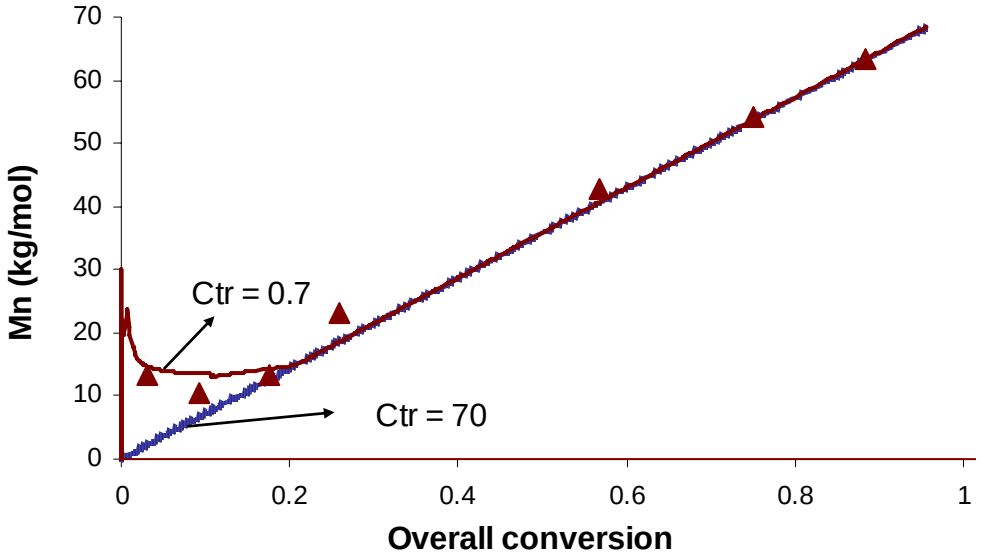

Figure 7-12: Evolution of polymer molecular weight with monomer conversion calculated based on the total amount of the added monomer throughout the reaction. Mn values were measured using SEC (symbols); and calorimetry model (–).

This would suggest that the calorimetric model can also be used for emulsion polymerizations with high activity RAFT agents to predict polymer molecular weight. Additionally, the overlap of the molecular weight profiles for the polymer produced during the semi-batch period indicates that the differences between high and low active RAFT agents in terms of polymer molecular weight can be eliminated when operating under semi-batch mode. That is, under semi-batch mode the concentration of monomer is kept low and the concentration of the dormant polymeric RAFT agent produced from the batch reaction is almost constant. This implies that monomer units are slowly added to the propagating chains, i.e. each propagating radical adds a few number of monomer units before radical activity is transferred to another radical, resulting in all propagating radicals simultaneously grow with the monomer conversion.

7.8 Conclusions

The lack of online instrumentation was the main reason for developing our calorimetry-based soft-sensor. The online soft sensor enables predicting of the key polymer properties in real-time for control of reaction to obtain desired properties. In this Chapter, a model for the online energy balance of the RAFT mediated polymerization reactor has been developed with particular attention being paid to the evolution of polymerization rate and molecular weight. The calorimetric model was used for determining the heat of reaction dynamically from temperature measurements. The rate of polymerization, which is proportional to the heat of reaction, was then estimated and integrated to obtain the overall monomer conversion. The calorimetric model developed was found to be capable of estimating polymer molecular weight via simultaneous estimation of monomer and AR concentrations. The model was validated with batch and semi-batch emulsion polymerization of styrene with and without RAFT agent. The results show good agreement between measured conversion profiles by calorimetry with those measured by the gravimetric technique. Additionally, the number average molecular weight results measured by SEC (GPC) with double detections compare well with those calculated by the calorimetric model. The sensitivity of the calorimetric model was tested towards the activity of the used RAFT agent. A linear growth of Mn with monomer conversion is one of the main characteristics of living polymerization. The model was tested for high active RAFT agent and the results were found to agree with

the theory. We conclude that semi-batch emulsion polymerization can be used to approach living polymerization with low active RAFT agent

The dynamic model presented in Chapter 4 is used to represent emulsion polymerization. The optimisation problem was formulated as a multi-objective optimisation by reformulating the multi-objective problem as a single-objective case by placing some of the objectives in the form of constraints. Results show that the optimisation procedure was able to minimize the reaction time and simultaneously obtain a polymer with desired quality (conversion, particle size and molecular weight distribution). The optimal policies obtained were tested experimentally and good agreement was obtained. The approach was found to be suitable for the advanced control of polymerization reactors, especially to implement closed-loop control of conversion and molecular weight which are crucial in enhancing the properties of the polymer produced.

7.9 References

Altarawneh, I.S.; Gomes, V.G. and Srour, M.S., 2008. The Influence of Xanthate-Based Transfer Agents on Styrene Emulsion Polymerization: Mathematical Modeling and Model Validation. *Macromolecular Reaction Engineering*, 2(1): 58.

Arzamendi, G. and Asua, J.M., 1989. Monomer addition policies for copolymer composition control in semicontinuous emulsion copolymerization. *Journal of Applied Polymer Science*, 38(11): 2019.

Arzamendi, G. and Asua, J.M., 1991. Copolymer composition control of emulsion copolymers in reactors with limited capacity for heat removal. *Industrial & Engineering Chemistry Research*, 30(6): 1342.

Asua, J.M., 2004. Emulsion polymerization: From fundamental mechanisms to process developments. *Journal of Polymer Science, Part A: Polymer Chemistry*, 42(5): 1025.

Asua, J.M.; Adams, M.E. and Sudol, E.D., 1990. A New Approach for the Estimation of Kinetic Parameters in Emulsion Polymerization Systems. I. Homopolymerization under Zero-One Conditions. *J. Appl. Polym. Sci.* , 39: 1183.

Broadhead, T.O.; Hamielec, A.E. and MacGregor, J.F., 1985. Dynamic modeling of the batch, semi-batch and continuous production of styrene/butadiene copolymers by emulsion polymerization. *Makromolekulare Chemie, Supplement*, 10-11: 105.

Choi, K.Y. and Butala, D.N., 1991 An experimental study of multiobjective dynamic optimization of a semibatch copolymerization process. . *Polymer Engineering and Science*, 31: 353.

Coen, E.M.; Gilbert, R.G.; Morrison, B.R.; Leube, H. and Peach, S., 1998. Modelling particle size distributions and secondary particle formation in emulsion polymerisation *Polymer*, 39(26): 7099.

de Buruaga, I.S.; Echevarria, A.; Armitage, P.D.; de la Cal, J.C.; Leiza, J.R. and Asua, J.M., 1997. On-line control of a semibatch emulsion polymerization reactor based on calorimetry. *AIChE Journal*, 43(4): 1069.

Dimitratos, J.; Elicabe, G. and Georgakis, C., 1994. Control of emulsion polymerization reactors. *AIChE Journal*, 40(12): 1993.

Gesthuisen, R.; Kraemer, S. and Engell, S., 2004. Hierarchical control scheme for time-optimal operation of semibatch emulsion polymerizations. *Industrial & Engineering Chemistry Research*, 43(23): 7410.

Gesthuisen, R.; Kramer, S.; Niggemann, G.; Leiza, J.R. and Asua, J.M., 2005. Determining the best reaction calorimetry technique: Theoretical development. *Computers and Chemical Engineering*, 29(2): 349.

Gilbert, R.G., 1995. Emulsion polymerization: a mechanistic approach. Academic Press, London.

Gugliotta, L.M.; Arotcarena, M.; Leiza, J.R. and Asua, J.M., 1995a. Estimation of conversion and copolymer composition in semicontinuous emulsion polymerization using calorimetric data. *Polymer*, 36(10): 2019.

Gugliotta, L.M.; Arzamendi, G. and Asua, J.M., 1995b. Choice of monomer partition model in mathematical modeling of emulsion copolymerization systems. *Journal of Applied Polymer Science*, 55(7): 1017.

Guinot, P.; Othman, N.; Fevotte, G. and McKenna, T.F., 2000. On-line monitoring of emulsion copolymerisations using hardware sensors and calorimetry. *Polymer Reaction Engineering*, 8(2): 115.

Hamielec, A.E.; MacGregor, J.F. and Penlidis, A., 1987. Multicomponent free-radical polymerization in batch, semi-batch and continuous reactors. *Makromolekulare Chemie, Macromolecular Symposia*, 10-11: 521.

Isabel Sáenz de Buruaga, A.E.P.D.A.J.C.d.l.C.J.R.L.J.M.A., 1997. On-line control of a semibatch emulsion polymerization reactor based on calorimetry. *AIChE Journal*, 43(4): 1069.

Kim, K.J. and Choi, K.Y., 1991. Online estimation and control of a continuous stirred tank polymerization reactor. *Journal of Process Control*, 1(2): 96.

Kiparissides, C. and Morris, J., 1996. Intelligent manufacturing of polymers. *Computers & Chemical Engineering*, 20: S1113.

Leiza, J.R.; Cal, J.R.d.l.; Montes, M. and Asua, J.M., 1993. On-line monitoring of conversion and polymer composition in emulsion polymerization systems. *Process Control and Quality*, 4(3): 197.

Leswin, J.; Lamb, D. and Gilbert, R.G., 2005. Particle formation kinetics in RAFT controlled emulsion polymerizations. *Polymer Preprints (American Chemical Society, Division of Polymer Chemistry)*, 46(2): 334.

McKenna, T.F.; Fevotte, G.; Graillat, C. and Guillot, J., 1996. Joint use of calorimetry, densimetry and mathematical modelling for multiple component polymerizations. *Chemical Engineering Research & Design, Transactions of the Institute of Chemical Engineers, Part A*, 74(A3): 340.

Mendoza, J.; De La Cal, J.C. and Asua, J.M., 2000. Kinetics of the styrene emulsion polymerization using n-dodecyl mercaptan as chain-transfer agent. *Journal of Polymer Science Part A: Polymer Chemistry*, 38(24): 4490.

Monteiro, M.J.; Adamy, M.M.; Leeuwen, B.J.; van Herk, A.M. and Destarac, M., 2005. A "living" radical ab initio emulsion polymerization of styrene using a fluorinated xanthate agent. *Macromolecules*, 38(5): 1538.

PSE, 2004. gPROMS Advanced User Guide,. *Process System Enterprise Ltd , London, UK*.

Salazar, A.; Gugliotta, L.M.; Vega, J.R. and Meira, G.R., 1998. Molecular Weight Control in a Starved Emulsion Polymerization of Styrene. *Ind. Eng. Chem. Res.*, 37(9): 3582.

Saricilar, S.; Knott, R.; Barner-Kowollik, C.; Davis, T.P. and Heuts, J.P.A., 2003. Reversible addition fragmentation chain transfer polymerization of 3-[tris(trimethylsilyloxy)silyl]propyl methacrylate. *Polymer*, 44(18): 5169.

Schuler, H. and Schmidt, C.U., 1992. Calorimetric-state estimators for chemical reactor diagnosis and control: review of methods and applications. *Chemical Engineering Science*, 47(4): 899.

Smulders, W.W., 2002. Macromolecular architecture in aqueous dispersions: 'living' free-radical polymerization in emulsion. Ph.D. Thesis, Technische Universiteit Eindhoven, Eindhoven, Neth.

Smulders, W.W.; Gilbert, R.G. and Monteiro, M.J., 2003. A kinetic investigation of seeded emulsion polymerization of styrene using reversible addition-fragmentation chain transfer (RAFT) agents with a low transfer constant. *Macromolecules*, 36(12): 4309.

Srour, M.H.; Gomes, V.G.; Altarawneh, I.S. and Romagnoli, J.A., 2008. Inferential Conversion and Composition Monitoring via Microcalorimetric Measurements in Emulsion Terpolymerization. *Polymer-Plastics Technology and Engineering*, 47(1): 13.

Varela De La Rosa, L.S., E. D.; El-Aasser, M. S.; Klein, A. , 1999. Emulsion polymerization of styrene using reaction calorimeter. I. Above and below critical

micelle concentration. *Journal of Polymer Science Part A: Polymer Chemistry*, 37(22): 4054.

Vassiliadis, V.S.; Pantelides, C.C. and Sargent, R.W.H., 1993. Optimization of discrete charge batch reactors. *Computers & Chemical Engineering*, 18: S415.

Vassiliadis, V.S.; Sargent, R.W.H. and Pantelides, C.C., 1994. Solution of a Class of Multistage Dynamic Optimization Problems. 1. Problems without Path Constraints. *Industrial & Engineering Chemistry Research*, 33: 2111.

Vicente, M.; BenAmor, S.; Gugliotta, L.M.; Leiza, J.R. and Asua, J.M., 2001. Control of molecular weight distribution in emulsion polymerization using on-line reaction calorimetry. *Industrial and Engineering Chemistry Research*, 40(1): 218.

Zeaiter, J.; Gomes, V.G.; Romagnoli, J.A. and Barton, G.W., 2002a. Inferential conversion monitoring and control in emulsion polymerisation through calorimetric measurements. *Chemical Engineering Journal (Amsterdam, Netherlands)*, 89(1-3): 37.

Zeaiter, J.; Romagnoli, J.A.; Barton, G.W.; Gomes, V.G.; Hawkett, B.S. and Gilbert, R.G., 2002b. Operation of semi-batch emulsion polymerisation reactors: Modelling, validation and effect of operating conditions. *Chemical Engineering Science*, 57(15): 2955.

Chapter Eight

Block Copolymerization

Chapter 8
Block Copolymerization

Abstract

This Chapter presents the application of low activity RAFT agent in emulsion polymerization for the synthesis of block copolymers. First, emulsion polymerizations of styrene, methyl acrylate and butyl acrylate were performed. Polymerizations of acrylic monomers showed higher polymerization rates as compared to styrene polymerization. Though a low active RAFT agent was used, linear growth of the number average molecular weight of the produced polymethyl acrylate and polybutyl acrylate polymers was observed. The polymer produced from the first stage of polymerization was chain-extended under batch conditions. Due to the formation of new particles during the second stage polymerization, homopolymers were produced. This resulted in adversely affecting the block copolymer produced. Nevertheless, we found that this approach is feasible for producing block copolymers.

To further optimize blocking efficiency and synthesizing block copolymers of high purity, semi-batch reactions were performed. Experimental results showed that, under semi-batch conditions, linear growth of the polymer molecular weight with conversion and low polydispersity could be successfully achieved. It was found that the choice of block sequence was important in reducing the influence of terminated chains on the distributions of polymer that were obtained. In this regard, polymerizing styrene first followed by butyl acrylate or methyl acrylate resulted in a high purity block copolymer with low polydispersity. Dual-detection and NMR spectroscopy analysis showed that the polymer produced was indeed high purity block copolymer.

8.1 Introduction

Block copolymers are macromolecules composed of sequences, or blocks, of chemically distinct repeating units. Block copolymers are useful in many applications where a number of different polymers are connected together to yield a material with hybrid

properties. Block copolymers demonstrate useful and distinct properties as compared to random copolymers and homopolymers. The synthesis of block copolymers via conventional free radical polymerization is not feasible, as the life time of a growing chain is less than a few seconds. CLFRP methods convert the serially growing polymer chains of free radical polymerization to parallel growing chains, and increase average lifetime of the active chain centers to times needed for the full conversion. In addition, after polymerization is completed, the active polymer chains can be isolated in the different dormant forms depending on the CLFRP method employed, and can be re-activated to synthesize block copolymers.

One of the major applications of RAFT mediated living polymerization is the synthesis of block copolymers by simply adding another monomer once the first polymerization stage is completed. In RAFT polymerization, a propagating chain is capped when the radical attacks the carbon-sulfur double bond of the RAFT agent. Attack of the agent by another polymer chain removes the first chain, allowing it to continue propagation. The first block consisting of monomer B is initially polymerized in the presence of RAFT agent (AR) forming a macro-RAFT agent or polymeric RAFT agent (AP_B). In the second stage of polymerization, the polymeric RAFT agent (AP_B) is used to mediate the polymerization of monomer C resulting in an AP_BP_C block copolymer. (Perrier, 2005).

Several studies exist for production of block copolymer by RAFT mediated solution, bulk, emulsion and miniemulsion polymerizations (Chong *et al.*, 1999; de Brouwer, 2000; Jin *et al.*, 2005; Kanagasabapathy *et al.*, 1999; Kanagasabapathy *et al.*, 2001; Mayadunne *et al.*, 2000; Rivera *et al.*, 2005; Save *et al.*, 2005). Since xanthate is the RAFT agent used in this work, it is then beyond the scope of this work to revise all of these studies. However, there have been specific studies using the two stages procedure (mentioned above) and xanthates as RAFT agents to prepare block copolymer, some of these studies are highlighted next.

The synthesis of block poly(butyl acrylate)-co-poly(styrene) (b-PBA-co-PSt) in emulsion polymerization was investigated by Monteiro *et al*. (2000). Butyl acrylate was polymerized in the presence of xanthate RAFT agent to prepare PBA seed latex (PBA-xanthate). In the second stage styrene monomer was added and polymerization was

carried out to give b-PBA-co-PSt polymer. Smulders et al. (2004) prepared b-PSt-co-PBA polymer in solution and emulsion polymerizations . In solution polymerization, styrene was polymerized first at 70^{o}C for 21hours to give polystyrene homopolymer (PDI ≈2) attached with xanthate. The first block homopolymer was then purified to remove the unreacted styrene and RAFT agent. According to GPC the polydispersity of the polystyrene homopolymer was close to 2. However, after purification the polydispersity was 1.4 as obtained by the GPC. This low value is probably due to the polymer purification, in which the lowest molecular weight species was removed. Butyl acrylate monomer was then added to polystyrene-xanthate homopolymer in toluene, as in the first stage the reaction was initiated using AIBN initiator at 60^{o}C and was allowed to continue for 23.5h during which high conversion (88%) was achieved. The b-PSt-co-PBA polymer produced had a polydispersity of 2.15. In emulsion polymerization, the same copolymer was produced. In the first stage, styrene monomer was polymerized under batch condition in polymethyl methacrylate seeds in the presence of xanthate RAFT agent resulting in polystyrene-xanthate particles. BA was then polymerized under semi-batch conditions into these particles to give b- PSt-co-PBA polymer with a polydispersity close to 1.3.

This work presents the synthesis of block copolymers of polystyrene with methyl and butyl acrylates in emulsion using RAFT based xanthate transfer agent (O-ethylxanthyl ethyl propionate).

8.2 Experimental

8.2.1 Materials

The RAFT agent **(O-ethylxanthyl ethyl propionate)** was synthesized in our laboratory according to the procedure described in Section 5-3-2. Water to a Milli-Q-standard was used. Methyl acrylate monomer (Sigma); Styrene and Butyl acrylate monomers, initiator (sodium persulfate), purification column, and surfactant (sodium dodecyl sulfate) were all obtained from Sigma-Aldrich (USA). All monomers were purified by passing through an inhibitor-removal column; the purification procedure was repeated two times to ensure high purity. All other chemicals were used as received.

8.2.2 Block copolymer synthesis

In this work, *ab initio* batch emulsion polymerizations were first performed in the presence of O-ethylxanthyl ethyl propionate RAFT based transfer agent to produce latex particles containing the chosen polymer attached with RAFT moiety. In the second stage, the second monomer was polymerized in the previously produced latex particles containing the macro-RAFT agent either under batch or semi-batch conditions. Semi-batch conditions were carried out under starved feed conditions where the monomer feed rate is equal to or less than the polymerization rate. All emulsion polymerization reactions (batch and semi-batch) were carried out with O-ethylxanthyl ethyl propionate (AR) under slight nitrogen pressure in a 1L laboratory reactor, described in Section 5-2.

8.2.2.1 First stage emulsion polymerization

In the first stage, polystyrene, polymethyl acrylate and polybutyl acrylate homopolymers were prepared with predetermined molecular weight. Emulsion polymerization was performed under batch conditions at a reaction temperature of 70^{o}C and 350rpm agitation speed using 450g water, 3.85g AR, 2.76g SDS, 0.2g KPS, 0.08g Buffer and 150g monomer X (X: methyl acrylate (reaction 1), butyl acrylate (reaction 2) and styrene (reaction 3)). All experiments were designed to produce polymeric latex particles containing macro-RAFT agent (A-PX, where PX is the homopolymer produced from the polymerization of monomer X and A is the RAFT moiety) with a targeted molecular weight equal to 9194 g/mol at full conversion.

8.2.2.2 Second stage emulsion polymerization

In the second stage I, the entire amount of styrene (100g) was added to 260g PMA seed latexes (at 24.63% solids) obtained from first stage I. Water (190g) and SDS (0.15g) were added to the mixture, which was then stirred overnight at 100rpm to swell. The temperature was then increased to 70^{o}C, agitation speed was increased to 350rpm and nitrogen was bubbled throughout the mixture. After 2 hours, batch emulsion polymerization of styrene in PMA seeds was then started by adding 0.15g KPS (prepared in 10g water solution at reaction temperature) under nitrogen pressure. In the second stage III, styrene was polymerized in 240g PMA seeds (24.63% solids) obtained

from the first stage I. Prior to starting the reaction, 40% of styrene, 190g water and 0.15g SDS were added to PMA seed particles and agitated overnight at 100 rpm in order to have the polymeric particles swollen with styrene. Polymerization was then started by adding 0.15g KPS solution (prepared in 10g water at reaction temperature) with continuous addition of the remaining amount of styrene under semi-batch conditions at 70^{o}C and 350rpm. The synthesis of b-PBA-co-PSt, b-PSt-co-PMA and b-PSt-co-PBA were carried out using similar procedure. Our typical procedural details are given in Tables 8-1 and 8-2.

8.3 Analytical techniques

8.3.1 Conversion and PSD analysis

Monomer conversion was gravimetrically determined offline with samples from the reactor. The PSD and average particle size were measured using a Polymer Laboratory Particle Size Distribution Analyzer (PL-PSDA Model PL-DG2). This uses the principle of packed column hydrodynamic chromatography (HDC) to separate particles in the interstitial void space created by the solid spherical column packing material. The particles eluting from the column was detected using a UV detector.

8.3.2 Molecular weight analysis

Molecular weight distribution (MWD) analyses were carried out using a high temperature chromatography system (PL-GPC 120) with a PLgel guard 5μm 50×7.5mm column connected in series with two PLgel (Mixed-C 10μm 300×7.5mm) columns (PL, Polymer Laboratories) at 40^{o}C. A known weight of the dried polymer was dissolved in a known volume of tetrahydrofuran (THF, Fluka). THF was used as the eluent at a flow rate of 1ml/min. Calibration was done using narrow-distribution polystyrene standards (with molecular weight from 580 to 7.1×10^{6}g/mol). The injection volume was 100 μL.

The conventional calibration method is the most frequently used technique for column calibration using GPC. However, the disadvantage of this method is that the MWDs obtained are always relative to the polymer standards (polystyrene standards) used for

calibration. As such, the universal calibration method was used as a more accurate means for determining MWDs for polymer samples whose chemistry and architecture may differ considerably from that of the polymer standards. The PL-GPC 120 used was upgraded and coupled to an online differential viscometer (PL-BV 400 HT) for the direct determination of the specific viscosity of the eluting polymer fractions. The combination of RI and Viscometer detectors (RI/Visco) provides accurate molecular weight determination for all polymer types based on the universal calibration. The dual detections (UV and RI/Visco) PL-GPC 120 system is powerful in monitoring the formation of block copolymers with one UV-absorbing block. Therefore, a UV detector (WellChrom Spectro Photometer K-2501) was used in conjunction with RI/Visco detectors. A PL Data stream unit was used for data acquisition and the data obtained from UV detector were processed using Cirrus^{TM} GPC software. A Cirrus^{TM} multi detector software was used to process the data obtained from the combination of RI and Viscometer detectors.

8.3.3 Block copolymer structure and composition

Nuclear Magnetic Resonance (NMR) is a branch of spectroscopy in which electromagnetic radiation (usually of radiowave frequency) is absorbed by molecules possessing nuclei with nonzero spins. NMR spectroscopy is a powerful method used in the determination of the type and structure of unknown organic compounds. The utility of NMR spectroscopy for structural characterization arises because different atoms in a molecule experience slightly different magnetic fields and therefore transitions at slightly different resonance frequencies in an NMR spectrum. Furthermore, splitting of the spectra lines arise due to interactions between different nuclei provide information about the proximity of different atoms in a molecule. The NMR can provide quantitative and qualitative information about the functional group analysis, bonding connectivity and orientation, through space connectivity, molecular conformation and chemical dynamics.

The block copolymer sample was dried under a nitrogen atmosphere at 150^{o}C in order to remove the water traces present in the sample. Then 12mg of the sample was dissolved in 1mL of deuterium chloroform ($CDCl_3$). The sample solution was then

placed in the NMR tube and the tube was loaded in the NMR spectrometer. The analysis of the sample was carried out at 35°C. A Bruker AM 400 spectroscopy (400 MHz) was used to determine the block copolymer structure and composition through ^{1}H-NMR spectra.

8.4 Results and discussion

8.4.1 First stage: homopolymer block

8.4.1.1 Monomer conversion

Table 8-1 describes the experimental conditions for the homopolymerization of methyl acrylate (reaction 1), butyl acrylate (reaction 2) and styrene (reaction 3). Figure 8-1a shows the variations in conversion with time for the employed monomers. Due to their high propagation rate coefficients and water solubilities, the highest rate of polymerization was obtained for MA (reaction 1) followed by BA (reaction 2) and the lowest for St monomer (reaction 3).

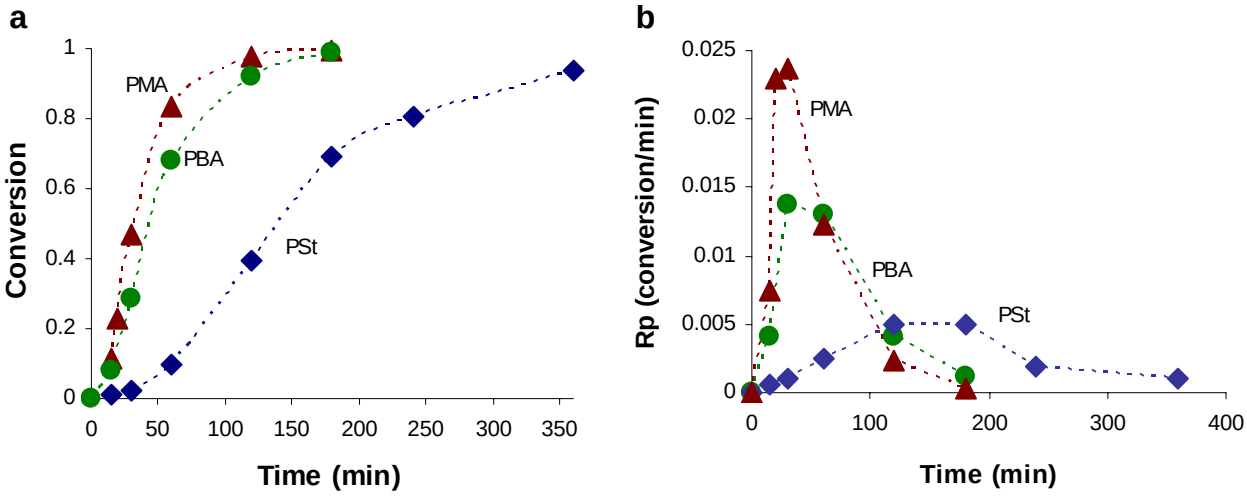

Figure 8-1: First stage batch emulsion polymerization with AR: (a) Conversion-time profiles for MA (▲), BA (●) and St (♦); (b) Polymerization rates for MA (▲), BA (●)and St (♦) in batch emulsion.

A rapid increase in Rp during the nucleation period, interval I, and an almost constant Rp during interval II were observed for the polymerization with MA and BA. During interval III a dramatic decrease in Rp was observed for MA and BA, as shown in Fig. 8-1b. For styrene polymerization, the rate of polymerization is lower than that for MA and

BA due to its low propagation rate and water solubility. The differences in the propagation rate coefficients and water solubility of the employed monomers resulted in different durations and intensities of each interval. For all polymerizations a notable inhibition (no polymerization activity for a defined period of time) was observed during the earliest stages of interval I due to the high concentration of AR. In all reactions, the rate of polymerization began to decrease at almost 60%-80% conversion.

The rate of reaction in an emulsion polymerization is a complex function of propagation rate coefficient (kp), monomer concentration in the polymer particles (Cp), number of particles (Np) and radical number per particle ($\bar{n}$). Assuming that the number of particles is almost constant and all polymerizations were carried out under similar conditions, the difference in the rate of polymerizations can be attributed to variations in kp, Cp and $\bar{n}$.

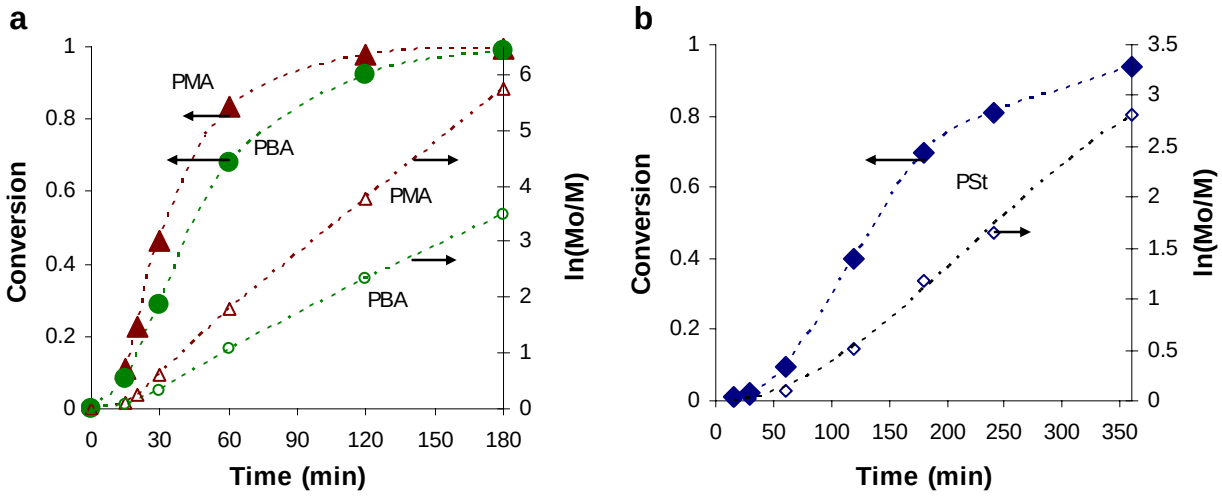

Figure 8-2: Combined monomer fractional conversion (closed symbols) and ln(Mo/M) plot (open symbols) as function of time: (a) Batch emulsion polymerization of MA and BA; (b) Batch emulsion polymerization of St.

Monomer concentration in the polymer particles, Cp, usually increases with monomer solubility in water. As such, the increase in Cp for MA (MA solubility in water = 5%) is higher than that for BA (BA solubility in water = 0.2%) and for St (St solubility in water = 0.05%). Solubility data were obtained from literature (Gilbert, 1995). Generally, the rate of polymerization cannot be ordered in terms of kinetic and thermodynamic

constants, as it strongly depends on $\bar{n}$ which is a function of the rate of radical entry into polymer particles, exit from polymer particles and termination in the polymer particles.

The first order ln(Mo/M) plot can be used as an indicator of the relative extent of initiation and termination reactions. Inspection of Fig. 8-2 indicates that after an initial inhibition period the ln(Mo/M) plots are approximately linear. It should be noted that the half-life of the initiator used in this work, KPS, is 8 hours at 70^{o}C. Thus it is unlikely that the radical flux (initiation) has significantly changed. Under this condition, any decrease in the polymerization rate as a result of increased termination would be reflected in the ln(Mo/M) plot. The linearity of the ln(Mo/M) curves indicates that there is a steady state radical concentration, which means that the rate of radical generation and the rate of radical loss are equivalent during the course of the reactions. Therefore, the number of growing chains (propagating species) is constant throughout the polymerization reactions. Thus, the linear first order plot of monomer conversion (ln(Mo/M), Fig. 8-2) suggests that bimolecular termination does not have a considerable effect on the decreased polymerization rate, and the decreased polymerization rate is most likely due to the depletion of the monomer in the particles.

8.4.1.2 Homopolymer molecular weight and MWD

The evolution of the number average molecular weight (Mn) with conversion is crucial when considering the extent of living behaviour that the system displays. As expected, due to the low transfer constant of the used RAFT agent, the evolution of polystyrene molecular weight with conversion (reaction 3) decreased and reached a value of about 9928 g/mol at 93% conversion, as depicted in Fig. 8-3a. However, Mn is still controlled and can be manipulated by changing the initial concentration of the used RAFT agent. The molecular weight resulting from the polymerizations of MA and BA are shown in Fig. 8-3a. It can be seen that the number average molecular weight progressed linearly with conversion, indicating that the chains grew in a controlled manner. The rate of growth was slightly greater for the polymerization with MA. These results are consistent with predictions (Equation 8-3, Muller equation) using the experimentally measured Ctr (1.5) for BA (Monteiro *et al.*, 2000). For MA, the transfer constant was

used as a fitting parameter and a value equal to 2 was found to provide an excellent fit with the experimental data.

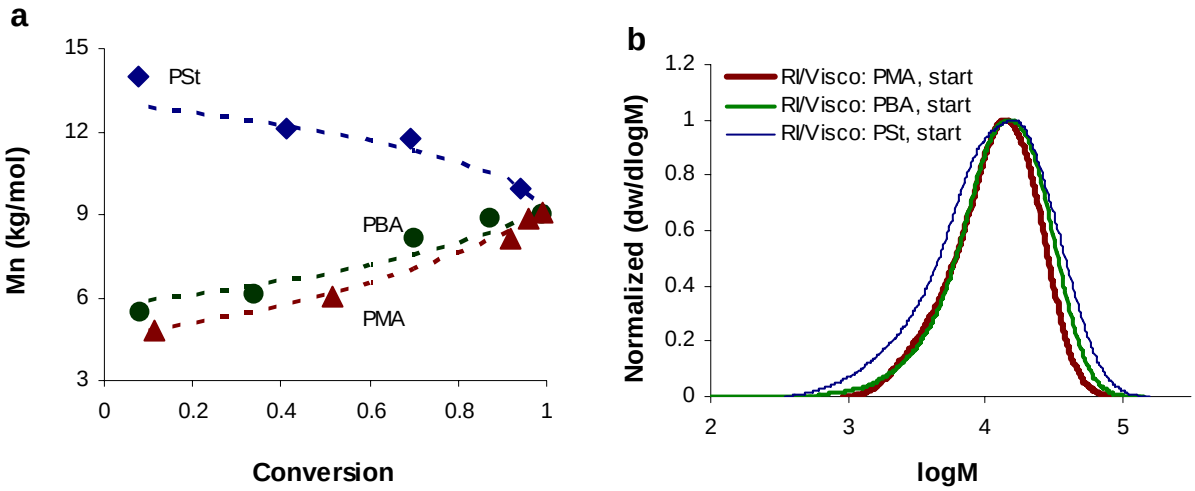

Figure 8-3: Homopolymer molecular weight and molecular weight distribution: (a) Evolution of PMA, PBA and PSt molecular weights with conversion; (b) Normalized GPC RI/Visco traces of PMA, PBA and PSt homopolymers (all samples were taken at the end of reaction).

Polymer polydispersity (PDI) started at approximately 2 and decreased to 1.87 and 1.63 for polymerization with BA and MA, respectively. While on the other hand, PDI for polymerization with styrene started at 2 at low conversion and increased to 2.17 at high conversion. The GPC chromatograms of the polymerization with the three monomers at high concentration of RAFT ([AR]/[KPS] ~ 24) are shown in Fig. 8-3b. The absence of bimodal MWD indicates that the uncontrolled aqueous phase polymerization appeared to be negligible.

8.4.1.3 RAFT agent distribution

For an effective application of RAFT in *ab initio* emulsion polymerization, two main criteria must be satisfied. First, the RAFT agent has to be fully in the reaction loci (polymer particles) and its transportation rate should be fast to ensure that all particles contain RAFT agent and hence all chains experience the same life time. Second, the RAFT agent must be distributed homogeneously among the polymer particles to prevent differences in chains produced in different particles and hence the same average chain length can be obtained in all particles (Apostolovic *et al.*, 2006). These criteria can be

fulfilled by ensuring that the nucleation rate (R_{nuc}) is much greater than the transportation rate of RAFT agent to the polymeric particles (R_{tran}) and the transportation rate of RAFT agent is much greater than the polymerization rate (R_p), i.e. $R_{nuc} >> R_{tran} >> R_p$.

First criterion:

The high nucleation rate guarantees the second requirement in which all particles will have similar chances to receive similar amount of RAFT agent. The nucleation rate can be adjusted by acting on the initiation rate or by manipulating the amount of surfactant. Another approach is to carry out the reaction in pre-prepared seed particles, seeded emulsion polymerization, as such all particles are present in the system from the very beginning of the reaction and the nucleation period is eliminated. The results from PL-PSDA measurements for PSD indicate that polybutyl acrylate, polymethyl acrylate and polystyrene seed particles (reaction 1, 2 and 3 respectively) have narrow particle size distributions (low values for polydispersity < 0.015). The narrow particle size distribution suggests that all the particles in the batch emulsion polymerizations of MA, BA and St were nucleated in a short time period and grew at similar rates by one primary nucleation mechanism. Additionally, for all reactions, a single MWD (unimodal MWD, Fig. 8-3b) is observed, indicating the absence of secondary nucleation and suggesting that the micellar nucleation is the primary nucleation mechanism.

The transportation rate (R_{tran}) of the RAFT agent is a crucial factor that strongly affects polymer molecular weight. If $R_{tran} < R_p$ then not all of the RAFT agent is incorporated in the polymerization which would result in a polymer with high molecular weight and high polydispersity. On the other hand, if R_{tran} and R_p are close to each other, then there will be continuous generation of new dormant species as the RAFT agent is transported during the entire duration of the reaction, thereby resulting in broadening of the MWD. The methodology used by Smulders (2002) to test whether the transport limitation (on the level of one particle) of the used RAFT agent plays a role has been adopted in this work. No RAFT agent will be consumed if a particle does not contain a radical, thus

only particles with one radical are considered. In one radical particle, the rate of polymerization is given by:

$$R_p = k_p C_p C_p^{rad} N_A v_p = k_p C_p \quad \textbf{(8-1)}$$

The rate of transport is a function of the RAFT agent concentration in the aqueous phase. At equilibrium, the rate of RAFT agent entry into a particle can be derived from the Smolukowski equation and is given by:

$$R_{tran} = 2\pi D_{AR} N_A d_s C_w^{AR} = 2\pi D_{AR} N_A d_s r C_w^{sat,AR} \quad \textbf{(8-2)}$$

where N_A is Avogadro's number; v_p is particle volume; r is molar ratio of RAFT to monomer in the particle; C_p^{rad} is radical concentration in one radical particle and is given by: $(1/N_A)/v_p$; D_{AR} is diffusion rate coefficient of the RAFT agent in the aqueous phase and C_w^{AR} is concentration of the RAFT agent in the aqueous phase and is given by: $rC_w^{sat,AR}$; d_s is the swollen diameter of the particle. The polymerization rate and the rate of RAFT agent consumption and transportation were calculated using the typical values of D_{AR}, k_p, C_p, k_{tr}^{AR} and $C_w^{sat,AR}$ given in Table 8-3. We found that the transportation rate of RAFT agent is three and four orders of magnitude higher than the polymerization rate for small (swollen diameter: 50nm) and large (swollen diameter: 100nm) particles, respectively. Therefore, the system under investigation apparently obeys the first criterion which is fast transport of the RAFT agent, unless the aqueous phase concentration of the RAFT agent reaches an extremely low value.

Second criterion:

The presence of thiocarbonylthio moieties (RAFT fragment, A: S=C(OEt)S-) can be examined using dual detectors of the SEC (GPC). UV and RI/Visco detectors were used to determine whether all the polymer chains have the RAFT agent moeity (homogenous distribution of RAFT agent among the particles). The UV detector was set at 300nm as the RAFT moiety (S=C(OEt)S-) absorbs strongly at this wavelength (Hartmann *et al.*,

2006), and the UV detector detects only polymer carrying a RAFT moiety, while RI/Visco is a concentration sensitive detector which detects polymers with and without RAFT moiety.

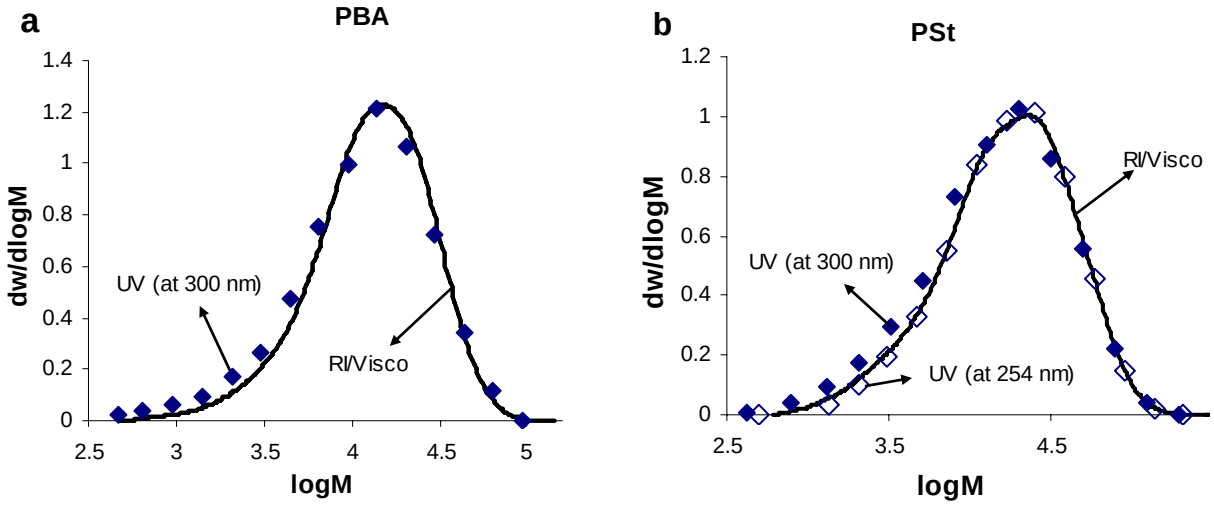

Figure 8-4: UV and RI/Visco SEC data: (a) For RAFT mediated batch emulsion polymerization of butyl acrylate prepared from reaction 2; (b) For RAFT mediated batch emulsion polymerization of styrene prepared from reaction 3.

Figure 8-4 shows an example of the overlay comparisons of the two signals which indicate whether the RAFT functionality is heterogeneously or homogenously distributed throughout the molar mass distribution curve. One of the factors affecting the UV signal is the dilution effect due to an increase in molecular weight. This results in a weaker signal at high molecular weights. At low molar mass, the UV signal observed is strong because the chains are small, resulting in a high concentration of the RAFT agent per mass of chain (Reda Fleet *et al.*, 2007). Figure 8-4 shows that the RAFT moiety was homogenously distributed in the polymerization of BA, (Fig. 8-4a) and in the polymerization of St (Fig. 8-4b), as indicated by the UV-RI/Visco overlays.

8.4.2 Second stage: Di-block copolymer

8.4.2.1 Monomer conversion

In the following, several experimental runs on polymer chain extension with another polymer (P_m) in batch and semi-batch modes are presented and discussed. The experimental recipes and results are summarized in Table 8-1 and 8-2. The first block is

the polymeric RAFT agent produced from the batch experiments (see Table 8-1) and has the following structure $S=C(OCH_2CH_3)S-P_n$, where the Z group is OCH_2CH_3, and the R group is the homopolymer block P_n (P_n is PMA (reaction 1), PBA (reaction 2) and PSt (reaction 3)). All first stage reactions (batch reactions 1, 2 and 3) were designed to produce a homopolymer block with Mn = 9194 g/mol at full conversion. Figure 8-5a shows conversion for batch emulsion polymerization of styrene in PMA and PBA, respectively.

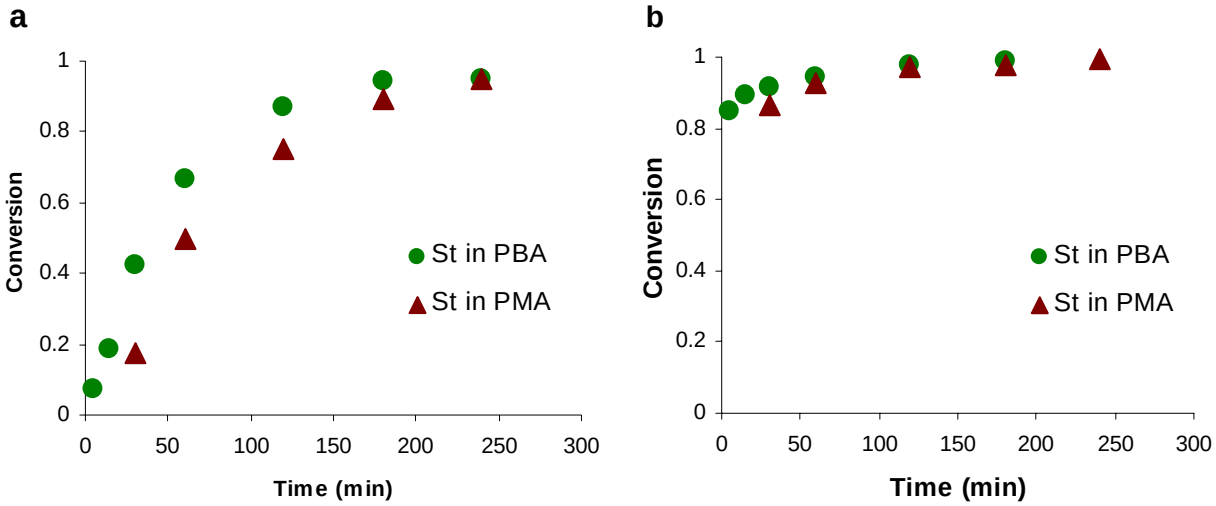

Figure 8-5: Fractional conversion of styrene: (a) Batch emulsion polymerization of styrene in PBA (●) and in PMA seed particles (▲); (b) Semi-batch emulsion polymerization of styrene in PBA (●) and in PMA seed particles (▲).

Fig. 8-5a indicates that polymerization of styrene in PMA resulted in lower conversion as compared with the polymerization in PBA, although both reactions were performed under similar conditions. We note that the difference between styrene conversions profiles can not be attributed to the exit of RAFT derived radical which is in this case a water insoluble long chain polymer. The most likely reason behind the observed low polymerization rate of styrene in PMA is the number of PMA seed particles. The average size of particles containing PMA, measured using PL-PSDA, was found to be larger (~50nm) than those containing PBA (~39.3nm). The number of PMA particles used in reaction 4 was calculated by dividing the total volume of PMA particles (mass of PMA/density of PMA) by the average volume of a particle. These calculations indicate that the number of PBA particles used in reaction 5 was two times greater than the number of PMA particles used in reaction 4. Thus, we conclude that the large

number of small PBA particles resulted in a large surface area and hence higher styrene conversion in comparison with styrene conversion in PMA particles.

Figure 8-5b presents styrene conversion when polymerized in PMA and PBA under semi-batch conditions. Again, for the same reason the instantaneous styrene conversion in PMA particles is lower than that in PBA particles during the early stages of polymerization. The difference is not as significant as in the batch experiments because the low flow rate of styrene monomer results in compensating the effect of low particle number. It is worth noting that the semi-batch reactions of styrene in PBA and in PMA were operated very close to starved conditions, since high conversions (~90%) were found over the entire period of the reactions.

8.4.2.2 Block copolymer molecular weight

Two approaches were adapted to synthesise block copolymers in batch and semi-emulsion polymerization. Firstly, the PMA and PBA produced from reactions 1 and 2 were chain-extended with polystyrene under batch (reaction 4 and 5) and semi-batch conditions (reaction 6 and 7). Secondly, the sequence of block preparation was reversed such that polystyrene was synthesised first (reaction 3). Polystyrene block was then chain extended by further polymerizing MA (reaction 8) and BA (reaction 9) with the pre-prepared PSt seed particles under semi-batch conditions. All experimental procedures and results are given in Table 8-2.

Assuming no termination and insignificant formation of the homopolymers of the second monomer, the theoretical number average molar mass of the produced block copolymer was calculated using the following equation:

$$Mn = M_n^A + \frac{m_B}{m_A}\frac{x}{(1-(1-x)^{Ctr}}M_n^A \qquad \textbf{(8-3)}$$

where m_B and m_A are initial concentrations of the second monomer and the polymeric RAFT agent (first block) respectively; M_n^A is the molar mass of the first block (polymeric RAFT agent); x is the fractional conversion and Mn is the theoretical number average molar mass of the formed block copolymer. For low reactive RAFT

agents this equation is valid because the number of polymer chains is already fixed at the start of the reaction since polymeric RAFT agents (PSt, PMA and PBA) are used, and monomer units are simply added to each chain with time. In semi-batch emulsion polymerization operated under starved feed conditions the rate of the transfer reaction is higher than the rate of the propagation reaction. This implies that the low reactive RAFT agent acts as a high reactive one with a high transfer constant. Under this condition, Equation 8-3 can be rewritten as follows:

$$Mn = M_n^A + x\frac{m_B}{m_A}M_n^A \qquad \textbf{(8-4)}$$

where (m_B / m_A) is mass ratio of the second monomer to the mass of the polymeric particles used. Figure 8-6 shows that the average molecular weight of b-PMA-co-PSt is higher than the average molecular weight of b-PBA-co-PSt, though styrene conversion in PBA particles (Fig. 8-5a) was higher than that in PMA and both reactions were carried out under similar conditions.

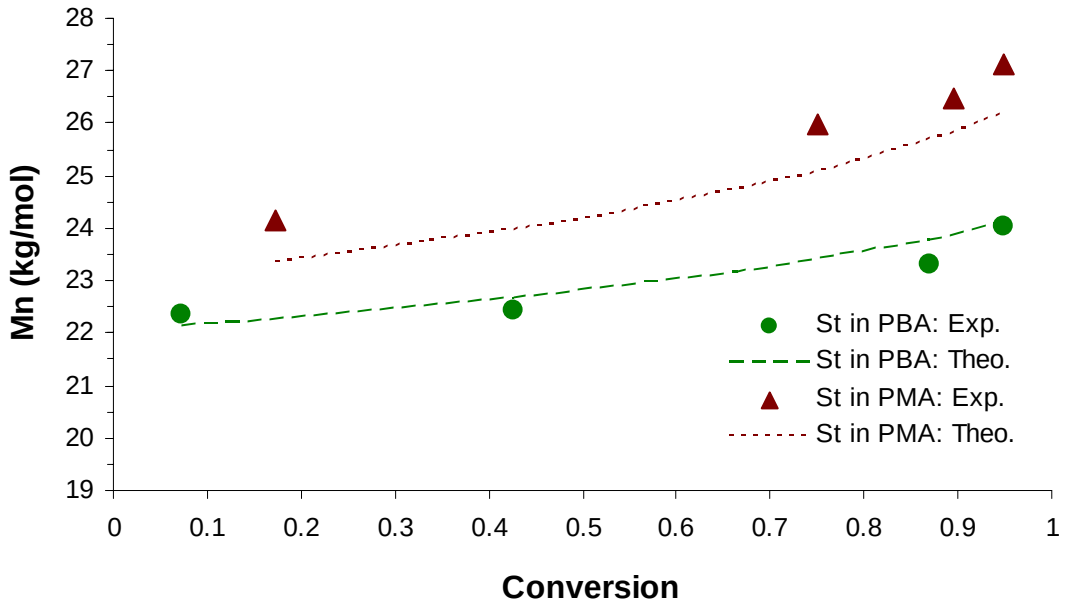

Figure 8-6: Evolution of Mn as function of conversion for the block copolymers produced from batch polymerizations of styrene in PMA and PBA seed particles.

It was shown (in the previous section) that the number of PMA seed particles used in reaction 4 was lower than the number of PBA seed particles used in reaction 5. This

implies that the amount of styrene monomer delivered into PMA particles was higher than that delivered into PBA particles. Consequently, a PMA particle will have more monomer than a PBA particle, resulting in higher Mn. Inspection of Fig.8-6 shows that Mn profiles exhibit slight linear growth with conversion during most of the reaction, characteristic of living behaviour. This is an indication there was a constant number of growing chains during the polymerizations which means there was control over molar mass during the reaction.

Using C_{tr} as a fitting parameter, similar linear growth trends were obtained with C_{tr} =1.3 for both reactions. Although both reactions showed living behavior, higher PDI values (~3.6 in reaction 4 and ~2.8 in reaction 5) were obtained. Three possible reasons have been identified:

1- The presence in polymeric RAFT seed particles of a fraction of dead chains unable to restart.
2- The continuous formation of low molecular weigh dead chains produced by termination reactions.
3- The formation of new particles, secondary nucleation, that have no RAFT agent.

The third reason, in particular, may have a significant contribution to the observed high polydispersity. As all polymeric RAFT agent chains are completely located in the pre-prepared polymeric seed particles, the new formed particles will not contain any RAFT groups as these are securely attached to polymer chains in the original population of particles. As such, polymerization in such particles produces an uncontrolled high molecular weight homopolymer (polystyrene), resulting in broadening of the molecular weight distribution and reducing the efficiency of producing a pure block copolymer. This process is confirmed by PSD (Fig. 8-7) as well as the MWD given in Fig. 8-11a and b.

The PL-PSDA measurements for PSD, presented in Fig 8-7, indicate the generation of a new crop of particles during later stages of batch emulsion polymerization of styrene in PMA (reaction 4). The main reasons behind the formation of new particles are the

relatively high monomer concentration in the aqueous phase (batch mode), the low number of PMA seed particles, and the reduced entry into glassy PMA particles.

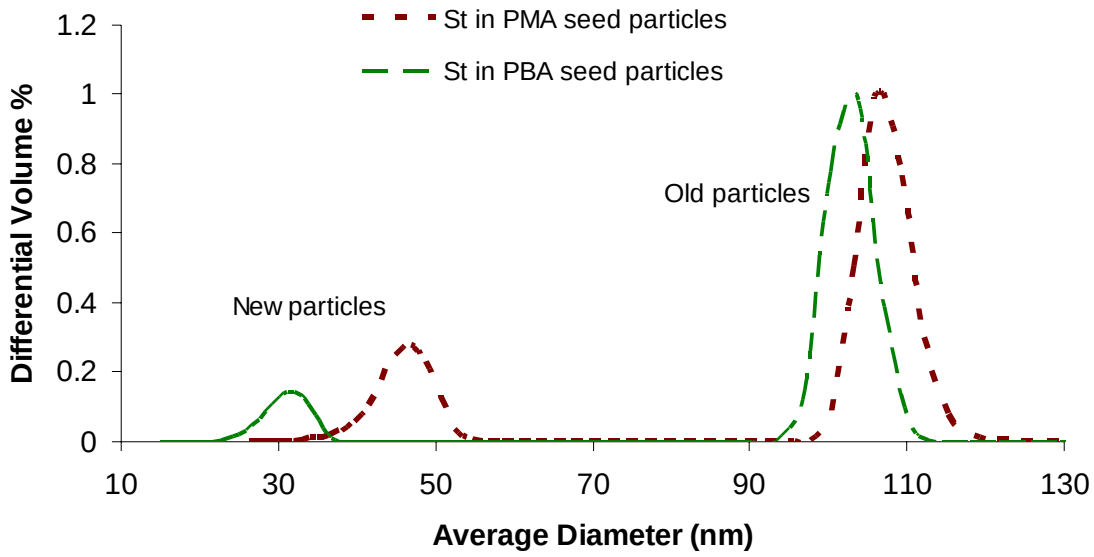

Figure 8-7: PL-PSDA measurements of PSD obtained from reactions 4 and 5, batch polymerization of styrene in PMA and PBA seed particles, respectively. All samples were taken at the end of the reaction. The primary PSD peaks (old particles) were used for normalization.

The formation of new particles was also observed in the polymerization of styrene in PBA seed particles (reaction 5) but with lower intensity than that observed in reaction 4. The relatively large average size of the new particles formed in reaction 4 strongly indicates that secondary nucleation commenced long before the end of the reaction due to the low number of PMA seed particles. This explains the higher Mn values measured by GPC compared with the predicted ones for the polymerization of styrene in PMA as shown in Fig. 8-6. This strongly suggests the formation of PSt homopolymer in the newly formed particles. In reaction 5 (batch polymerization of styrene in PBA seed particles), the small average size of the newly formed particles suggests that secondary nucleation commenced shortly before the end of the reaction, thereby indicating that the reduced entry into a glassy PBA particle is may be the main reason behind the formation of new particles in the aqueous phase.

Since the degree of living polymerization is measured by the ratio of transfer rate to propagation rate, the living nature is then governed by the value of the transfer constant (C_{tr} = ktr/kp). Due to high monomer concentration in batch polymerization, the RAFT

agent with low transfer constant used in this work cannot strictly control polymer molecular weight. This is because the rate of propagation reaction is greater than the rate of transfer reaction. Consequently, each radical can add a large number of monomer units before radical activity is transferred to another chain. Thus, a suitable way to approach living characteristics using a low active RAFT agent is to maintain low monomer concentration, thereby significantly reducing the rate of propagation reactions (Mueller *et al.*, 1995).

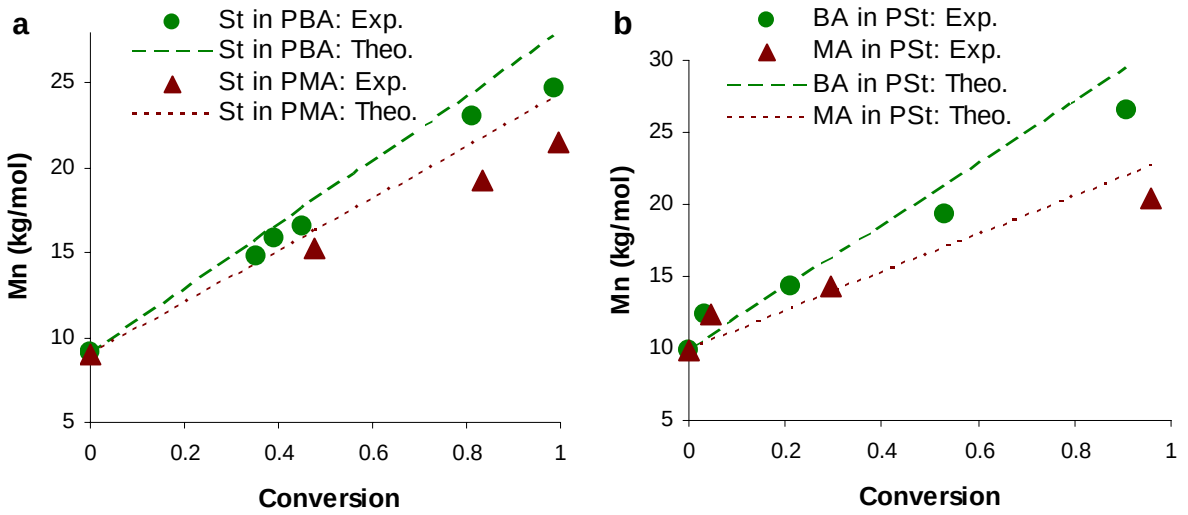

Figure 8-8: Evolution of Mn as a function of conversion for block copolymers: (a) Semi-batch polymerization of styrene in PMA and PBA seed particles, reactions 6 and 7; (b) Semi-batch polymerizations of MA and BA in PSt seed particles, reactions 8 and 9.

It is worth noting that high monomer conversions were obtained in semi-batch experiments (reactions 6, 7, 8 and 9) because monomer feedrates were close to, or less than, the polymerization rates. Under these conditions, any added monomer readily reacts, resulting in low monomer concentration. Consequently, each growing radical adds few monomer units before radical activity is transferred to another chain. This implies that all radicals, simultaneously, add monomer and grow in size with the continuous addition of monomer resulting in a low polydispersity polymer.

The significant difference between batch and semi-batch reactors in terms of living behaviour is illustrated in Fig. 8-8a and b, where the linear growth of polymer molecular weight with conversion is observed. We note that the predicted values provided in Figures 8-8a and b are only guidelines, since the termination reactions are not included

in Equation 8-3. The predicted Mn values are calculated with the same equation used for the calculation of the homopolymer seed latices. It can be seen that the predicted and measured Mn values agree well up to moderate conversions. At high conversions (> 60%), there are notable deviations and the measured Mn values for some reactions appear to level out. The lower Mn values are due to the formation of low molecular weight terminated material, which results in lowering the number average molecular weight. This is due to the reduced accessibility of the dormant polymeric RAFT agents at higher conversion, which in turn is due to the increased viscosity inside the particles. As such, the propagating radical is unable to reach the RAFT group, and therefore preferentially terminates. This is also confirmed in Fig. 8-9, where the polydispersities of the polymer produced are relatively higher than that obtained with high reactive RAFT agents (Bowes *et al.*, 2007; Reda Fleet *et al.*, 2007).

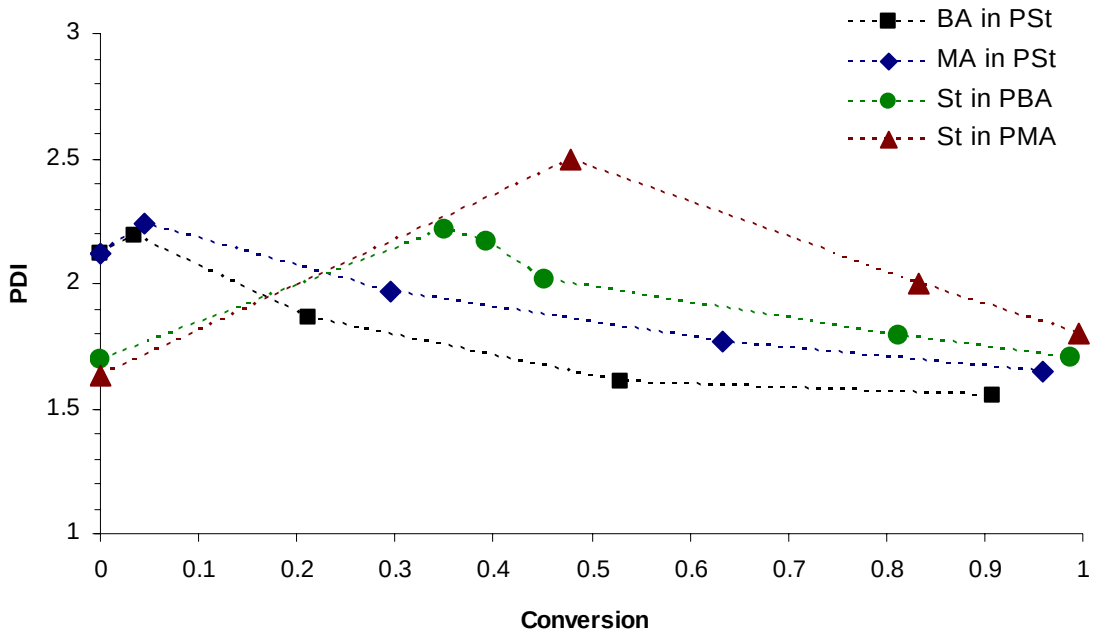

Figure 8-9: Block copolymers polydispersity indices as a function of monomer conversion.

The measured Mn was evaluated as a function of conversion using RI/Visco and UV detectors with universal calibration, for reactions 6 to 9. The linear growth of Mn as a function of monomer conversion is again a strong indication that there was a constant number of growing chains, in reactions 6, 7, 8 and 9, signifying that there was control over polymer molecular weight. Once again, the decreased polydispersity is another indication that polymerization under semi-batch conditions exhibits living characteristics as shown in figure 8-9.

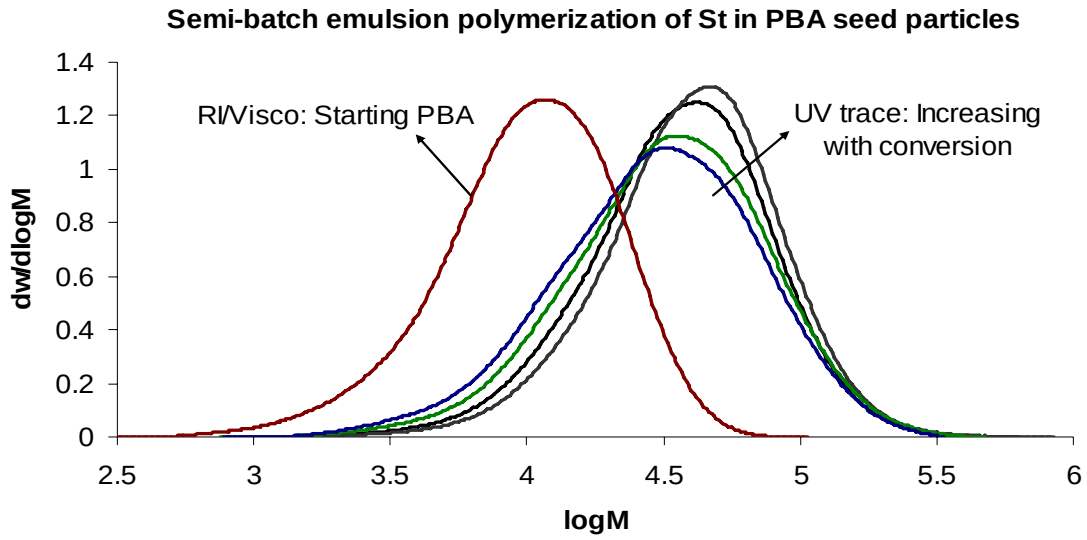

Figure 8-10: Normalized GPC chromatograms (UV at 254nm) of the chain extended PBA with styrene under semi-batch conditions, final Mn 24696 g/mol and PDI 1.70.

Figure 8-10 shows the experimental MWD profiles of the b-PBA-co-PSt polymer. An analysis of the GPC chromatograms, using UV detector at 254nm (Fig.8-10), shows a shift towards increasing molecular weights in the distributions, indicating that the added styrene monomer was successfully incorporated with the previously prepared PBA chains, a characteristic of controlled/living free radical polymerization. In each chromatogram a unimodal distribution was observed indicating negligible or no homogenous polymerization of styrene (polymerization in the aqueous phase). As UV at 254nm detects only polystyrene, useful information about the block copolymer composition can be obtained from these GPC traces. It is clear that the fraction of the second block (polystyrene) increased with conversion which indicates the incorporation of polystyrene in the block copolymer.

8.4.2.3 Block copolymer via batch emulsion polymerization

Since butyl acrylate is invisible to UV at 254 nm, the GPC UV trace can be used with this system to verify incorporation of styrene monomer. The combination of RI/Visco detectors, with universal calibration, shows the combined MWD of all polymers, whereas the UV detector (at 254 nm) only observes chains containing styrene either as a block or a homopolymer. For PMA homopolymer, a very weak UV signal at 254 nm

was observed and hence the use of UV-RI/Visco double-detection may not provide conclusive evidence of the formation of b-PSt-co-PMA and b-PMA-co-PSt polymers, since PMA slightly affects the UV signal. However, a shift of UV and RI/Visco traces toward higher molecular weights was observed when both MA and St were polymerized first (Fig. 8-12a and 8-13a, respectively) indicating the integration of the second monomer into the block copolymer. Therefore, the assumption of negligible UV absorbance by PMA is valid with insignificant error, as the PMA UV signal was very weak.

Figure 8-11 (a and b) shows the GPC UV-RI/Visco traces for b-PMA-co-PSt (Fig. 8-11a, reaction 4) and b-PBA-co-PSt (Fig. 8-11b, reaction 5). It can be seen that both PMA and PBA homopolymers formed in the first stage have low molecular weight (i.e. 8991g/mol and 9046g/mol, respectively) with low polydispersities (1.63 for PMA and 1.7 for PBA) as indicated by the starting GPC RI/Visco traces. The second stage polymerization of styrene in PMA and PBA particles produced polymers with Mn close to 27.7 and 23.6kg/mol with PDI equal to 3.6 and 2.8, respectively, as measured by GPC RI/Visco. Since MA and BA were polymerized first in reactions 4 and 5, and followed in the second stage by styrene, a shift of UV trace towards higher molecular weight does not necessarily indicate the formation of block copolymer, as both of the starting PMA and PBA are invisible and cannot be detected by UV detector.

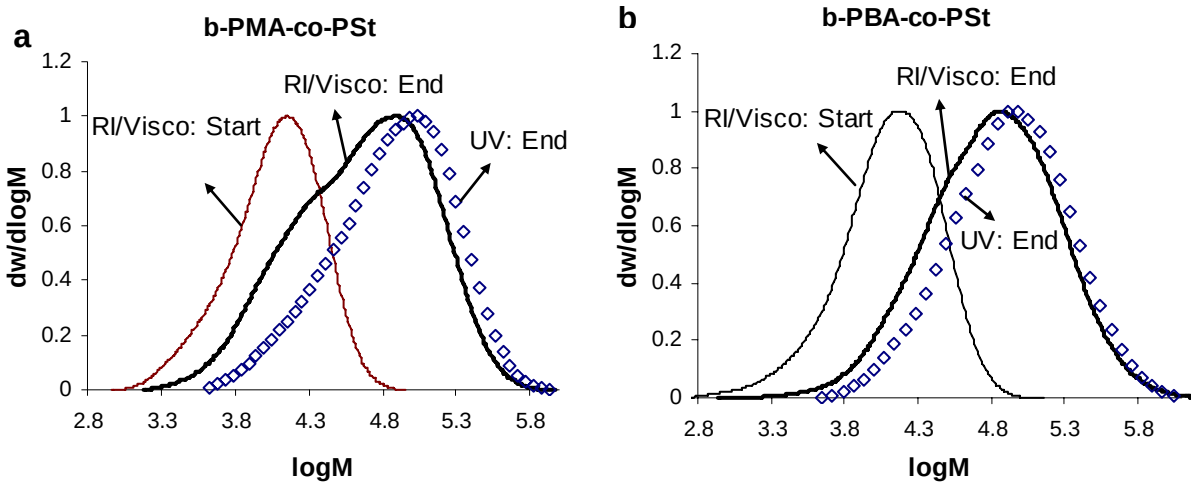

Figure 8-11: UV-RI/Visco overlay: (a) Batch polymerization of St in PMA, starting PDI = 1.63, finial PDI (RI/Visco) = 3.6, final PDI (UV) = 2.3; (b) Batch polymerization of St in PBA, starting PDI =1.7, finial PDI (RI/Visco) = 2.8, final PDI (UV) = 2.27.

However, the shift of the low molecular weight peak (RI/Visco: Start) indicates the growth of the polymer from the original seed latex, and its transformation into a block copolymer. As shown in Fig. 8-11b, the UV and the RI/Visco traces largely overlap. This indicates that most of the original PBA (polybutyl acrylate) was living and underwent addition-fragmentation chain transfer with PSt radicals to form a block copolymer (b-PBA-co-PSt) with a higher molecular weight. Similar observation is seen in Fig. 8-11a with less blocking efficiency. Because UV detector at 254nm can detect PSt (polystyrene) and not the starting polymer, further evidence about the formation of b-PMA-co-PSt and b-PBA-co-PSt in the batch experiments (reactions 4 and 5) can be obtained. If the transfer reaction between the dormant polymeric RAFT agent (PMA and PBA) and the propagating PSt radicals occurred, the Mn (measured by UV) will be higher and the polydispersity will be lower than that obtained from RI/Visco trace. It was found that Mn is 45kg/mol with PDI of 2.30 for b-PMA-co-PSt and 37kg/mol with PDI of 2.27 for b-PBA-co-PSt. This Mn is much lower than the Mn that would be obtained if no transfer reaction occurred and styrene polymerized separately by conventional uncontrolled free radical mechanism.

If all PMA and PBA co-exist in blocks, the UV trace would have been identical and overlapped with the RI/Visco signals. Under batch conditions, it is observed in Fig. 8-11 that UV and RI/Visco do not overlap, meaning that not all of the starting PMA and PBA were converted into block copolymers. The differences between UV and RI/Visco traces could be possibly due to the formation of new particles that have no dormant polymeric RAFT agent. This is evident in Fig. 8-11a which represents reaction 4 where a considerable formation of new particles was observed (Fig. 8-7). The accessibility of the dormant polymeric RAFT agent (first block) for a propagating radical is also another possible reason. It can be seen from UV and RI/Visco traces in Fig 8-11a (reaction 4) that both secondary nucleation and reduced accessibility exist. On one hand, the high molecular weight side of the UV trace suggests the formation of PSt homopolymers which support the formation of new particles. On the other hand, the low molecular weight side shows the presence of a considerable amount of low molecular weight material. This material contains the terminated low molecular weight species and the unreacted polymeric RAFT agent. The most likely reason behind the presence of this material is the reduced accessibility whereby the propagating radical is not able to reach the RAFT group and therefore preferentially terminates.

In conclusion, block copolymers were produced via batch emulsion polymerization. However, the quality of the produced block copolymer is related to the amount of terminated chains during the formation of the first block, the number of new particles formed and the accessibility of the propagating radical to the RAFT agent. Thus it is desirable to maximize the fraction of dormant chains (polymeric RAFT agent) that are able to restart polymerization when the second monomer is added, reduce or eliminate the formation of new particles and maximize the accessibility of the dormant RAFT agent for the propagating radical. The required conditions can be approached by operating under semi-batch conditions.

8.4.2.4 Block copolymer via semi-batch emulsion polymerization

A high purity block copolymer with low polydispersity cannot be obtained under batch conditions because of the previously described problems and the low transfer constant of MA, BA and styrene with xanthate. Because the rate of propagation over the rate of transfer can be decreased by maintaining low monomer concentration during semi-batch operation, it is theoretically possible to overcome the disadvantages of low active RAFT agent and a polymer with low polydispersity could be produced.

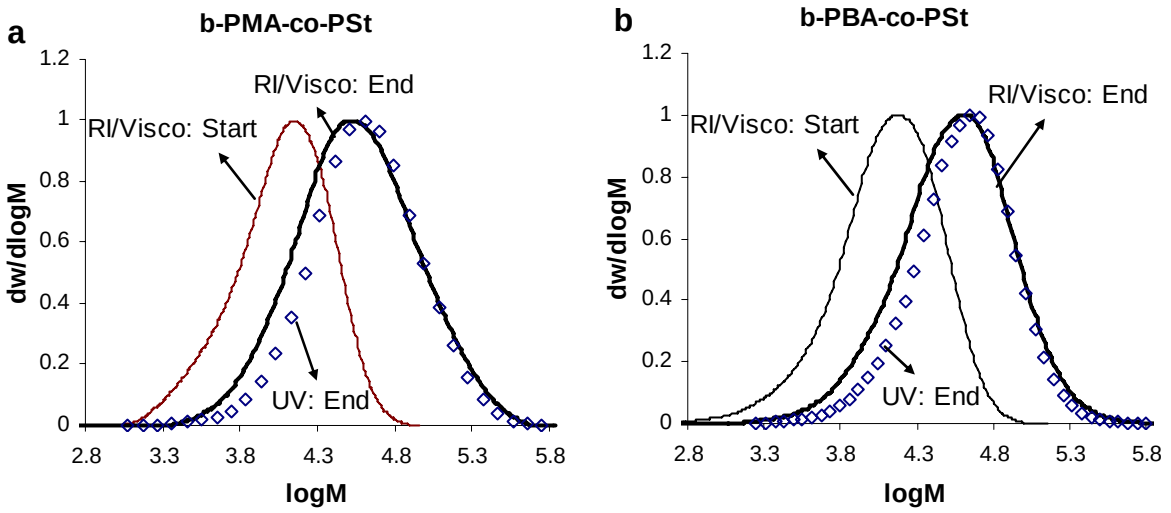

Figure 8-12: UV-RI/Visco overlay: (a) Semi-batch polymerization of St in PMA, starting PDI (RI/Visco) = 1.63, finial PDI (RI/Visco) = 2.16, final PDI (UV) = 1.8; (b) Semi-batch polymerization of St in PBA, starting PDI (RI/Visco) =1.7, finial PDI (RI/Visco) = 2.12, final PDI (UV) = 1.7.

We conducted experiments in semi-batch mode to optimize the formation of block copolymers. Figures 8-12b shows the normalized UV and RI/visco chromatograms for the produced b-PBA-co-PSt polymer from semi-batch reaction. In this reaction BA was polymerized first, and styrene was polymerized in the second polymerization stage.

The MWD of the starting PBA (reaction 7) moves to higher molecular weights with conversion, showing the living character of the original polymer. The UV-RI/Visco overlays indicate the presence of the second block (polystyrene) throughout the distribution. We observe that the low molecular weight sides of the RI/Visco and UV traces do not overlap. As the RI/Visco traces in Figures 8-12b show the presence of low molecular weight chains with finial PDI (RI/Visco) = 2.12, we conclude that these chains are unreacted PBA polymeric RAFT agents and terminated low molecular weight PBA chains. Yet, a significant amount of St monomer was successfully integrated as the second block with the first PBA block. Similar results were obtained for the polymerization of St in the PMA seed particles. Once again, deviations from ideal behavior (UV and RI/Visco do not fully overlap) are observed. This is because the monomer concentration does not approach zero and there is reduced accessibility along with side reactions such as transfer to monomer, polymer and termination. Moreover, polymerization is performed in emulsion which may result in not all polymer chains experiencing similar growth conditions as a result of compartmentalization.

Figure 8-13b shows the normalized UV and RI/Visco chromatograms for the produced b-PSt-co-PBA polymer from semi-batch reaction. It should be noted that in this reaction styrene was polymerized first and butyl acrylate was polymerized in the second polymerization stage. The UV MWD shifted, completely, towards the higher molecular weight, which indicates that a block copolymer has successfully formed. From the excellent overlays of the UV and RI/Visco MWDs we conclude that styrene polymerization followed by a highly reactive monomer results in a block copolymer of high purity with low polydispersity. This is because of the higher transfer rate of BA to PSt-xanthate compared with that of St to PBA-xanthate.

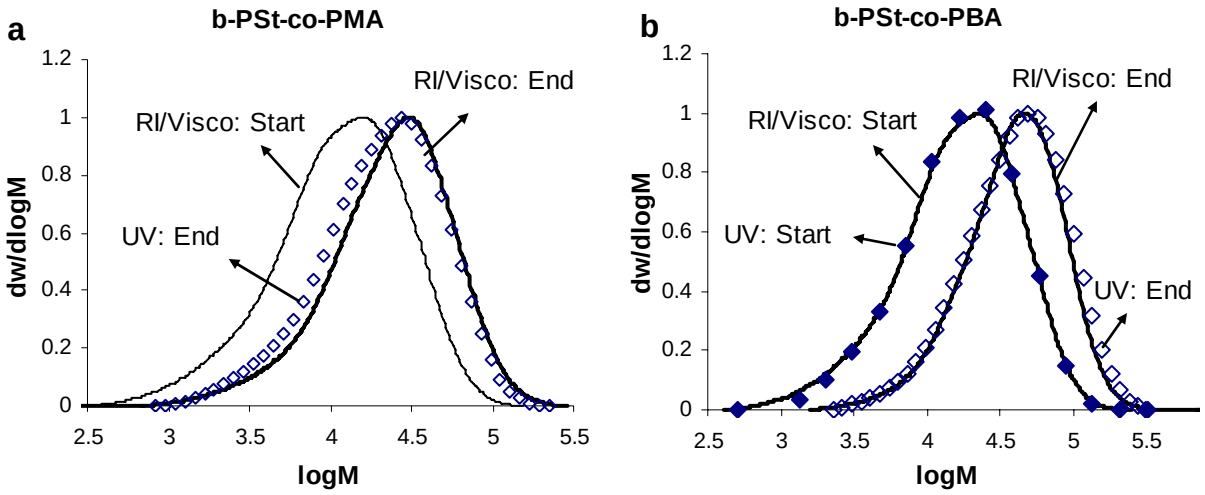

Figure 8-13: UV-RI/Visco overlay: (a) Semi-batch polymerization of St in PMA, starting PDI = 2.12, finial PDI (RI/Visco) = 2.09, final PDI (UV) = 2.15; (b) Semi-batch polymerization of St in PBA, starting PDI =2.12, finial PDI (RI/Visco) = 1.67, final PDI (UV) = 1.60.

The difference between RI/Visco PDI (1.67) and the UV PDI (1.6) is because of the side reactions which can not be completely avoided. It should be noted that an even narrower MWD will be obtained if the first block would have a narrow MWD. This is not possible with a low active RAFT agent used in the first stage. However, we observe that the polydispersities in these semi-batch polymerizations are much lower than those in batch polymerization. It is therefore expected that the block copolymers produced under semi-batch conditions are much purer.

8.4.2.5 Block copolymer structure and composition

The structure and the composition of the polymer formed were determined by Proton Nuclear Magnetic Resonance (^{1}H-NMR) spectroscopy (Bürker AM 400 MHz) at 35^{o}C with $CDCl_3$ as a solvent. The samples were dried at 150^{o}C for 1h under nitrogen atmosphere in order to remove water from the polymer. Since BA and MA both are sensitive to moisture due to hydrogen bonds with water molecules, the samples were stored in a desiccator after drying.

Figures 8-14, 8-15 and 8-16 show the ^{1}H-NMR spectrum obtained for PSt-xanthate, PMA-xanthate and PBA-xanthate homopolymers.

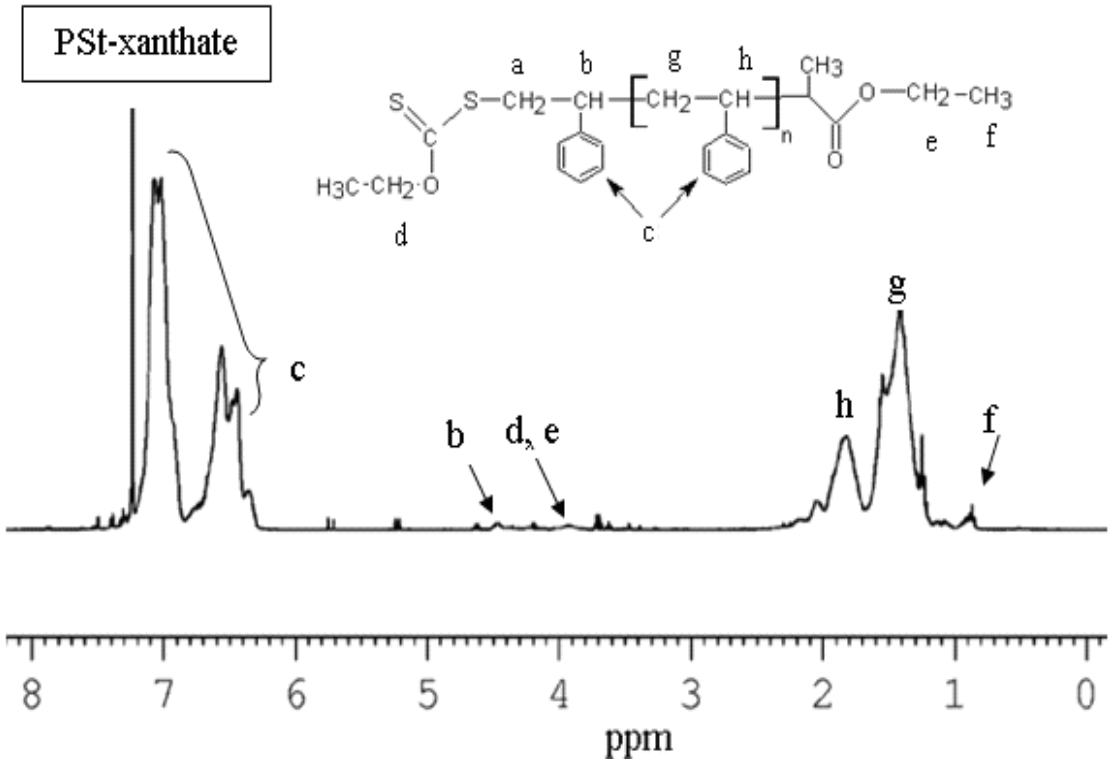

Figure 8-14: ^{1}H-NMR spectrum of polystyrene with RAFT group, sample was taken at the end of the reaction.

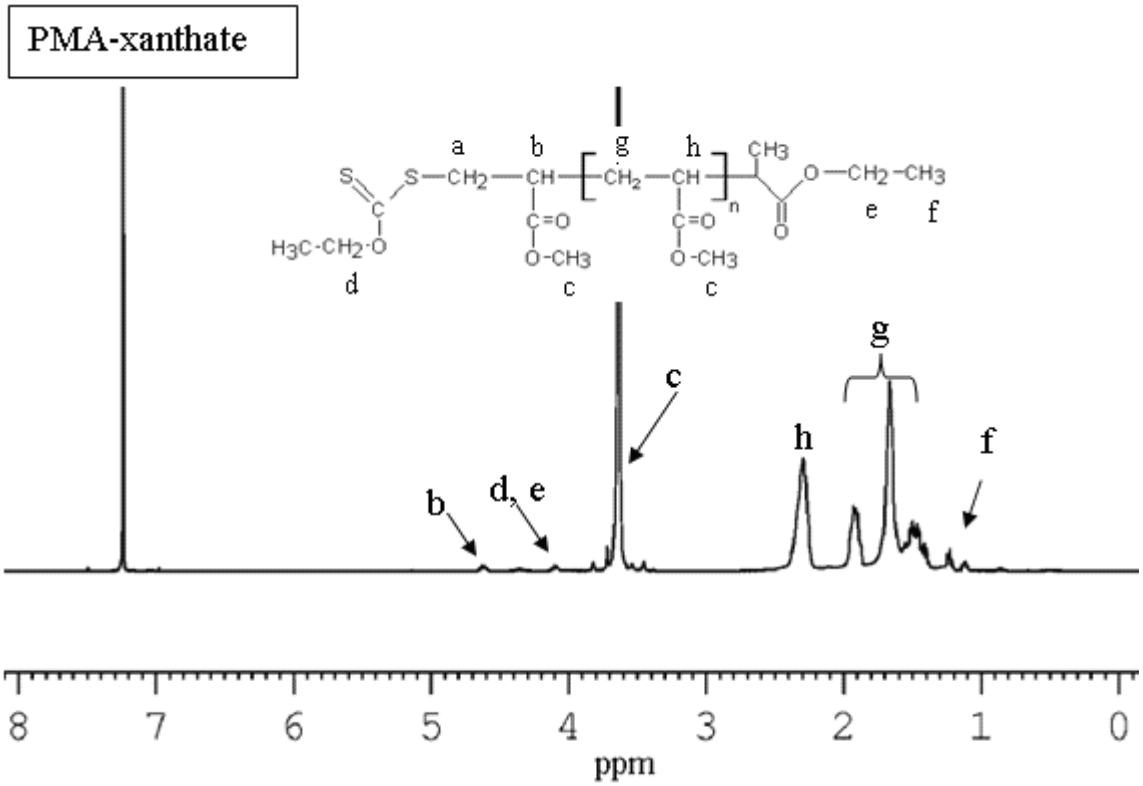

Figure 8-15: ^{1}H-NMR spectrum of polymethyl acrylate with RAFT group, sample was taken at the end of the reaction.

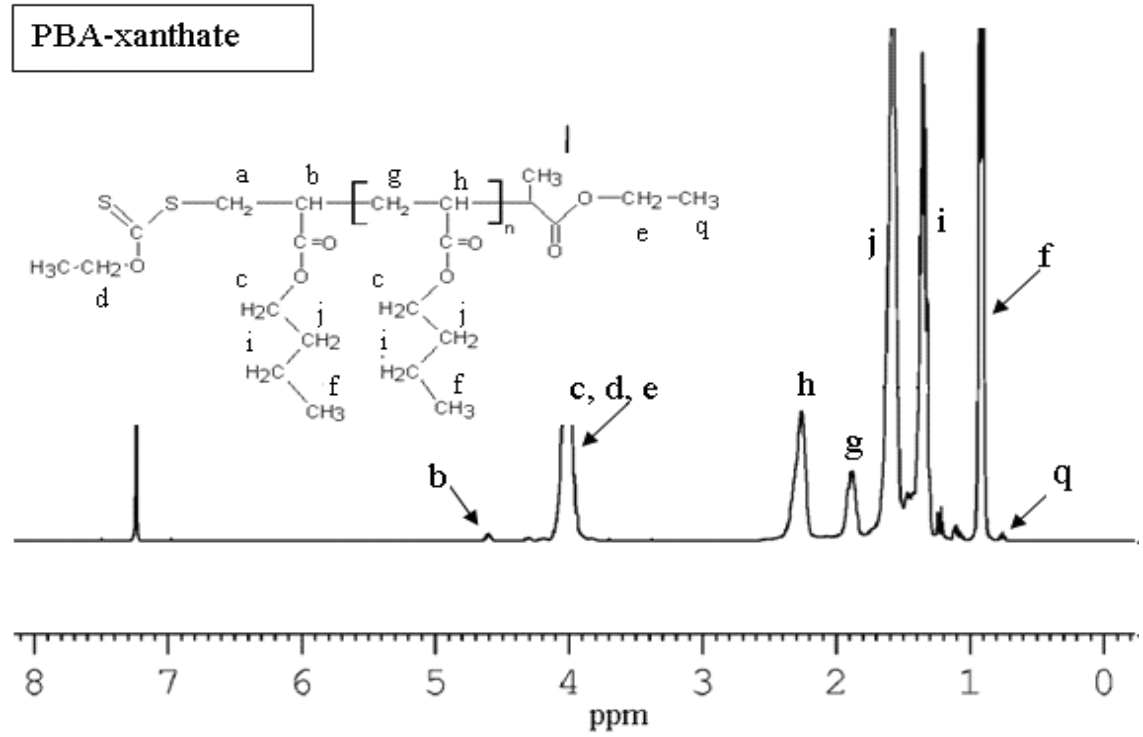

Figure 8-16: ^{1}H-NMR spectrum of polybutyl acrylate with RAFT group, sample was taken at the end of the reaction.

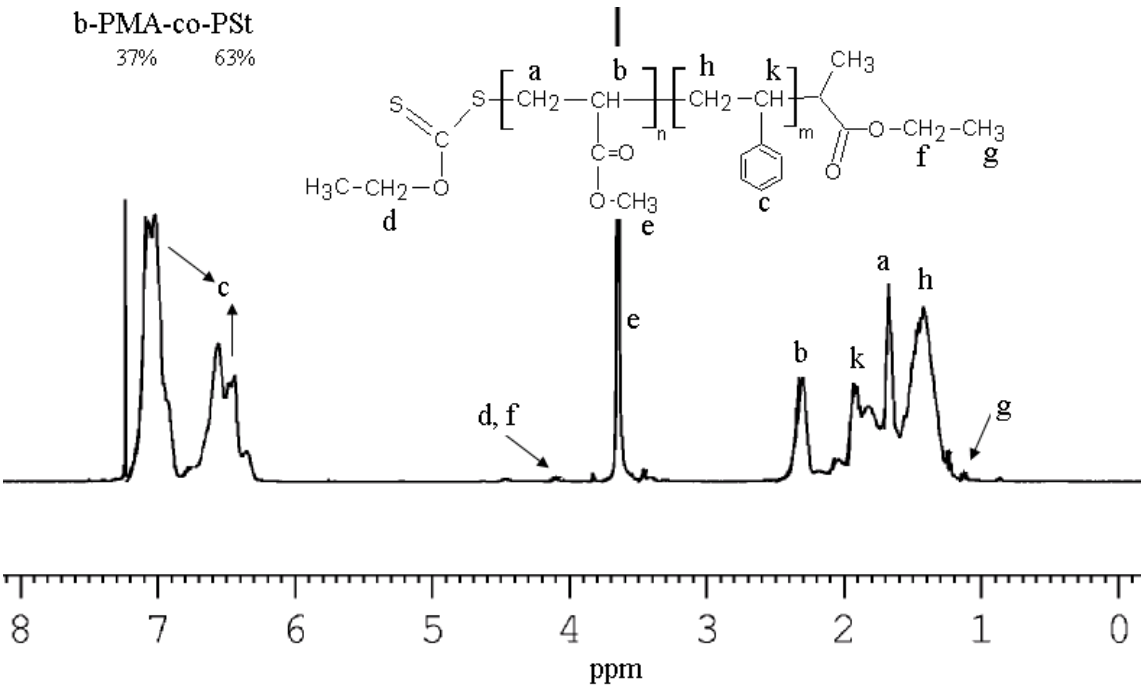

Figure 8-17: ^{1}H-NMR spectrum of b-PMA-co-PSt, MA was polymerized first and St was polymerized in the second stage under semi-batch conditions, sample was taken at the end of the reaction.

The ^{1}H-NMR spectrum of PSt-xanthate, PMA-xanthate and PBA-xanthate show the incorporation of the RAFT agent in the structure of the produced homopolymers as the signal of C**H$_3$** end group, from RAFT agent, (f in Fig. 8-14, f in Fig. 8-15 and q in Fig. 8-16) appears separately at 0.80-1.10ppm and the signal of C**H$_2$**-O protons (d, e in Figures 8-14, 15 and 16) appears at 3-90-4.10ppm. This suggests that the RAFT agent was homogenously distributed during the polymerization of St, MA and BA and support the dual-detection GPC results shown in Fig. 8-4. It is noted that in all figures (Fig. 8-14 to Fig. 8-20) the solvent, $CDCl_3$, signal appears at 7.25 ppm.

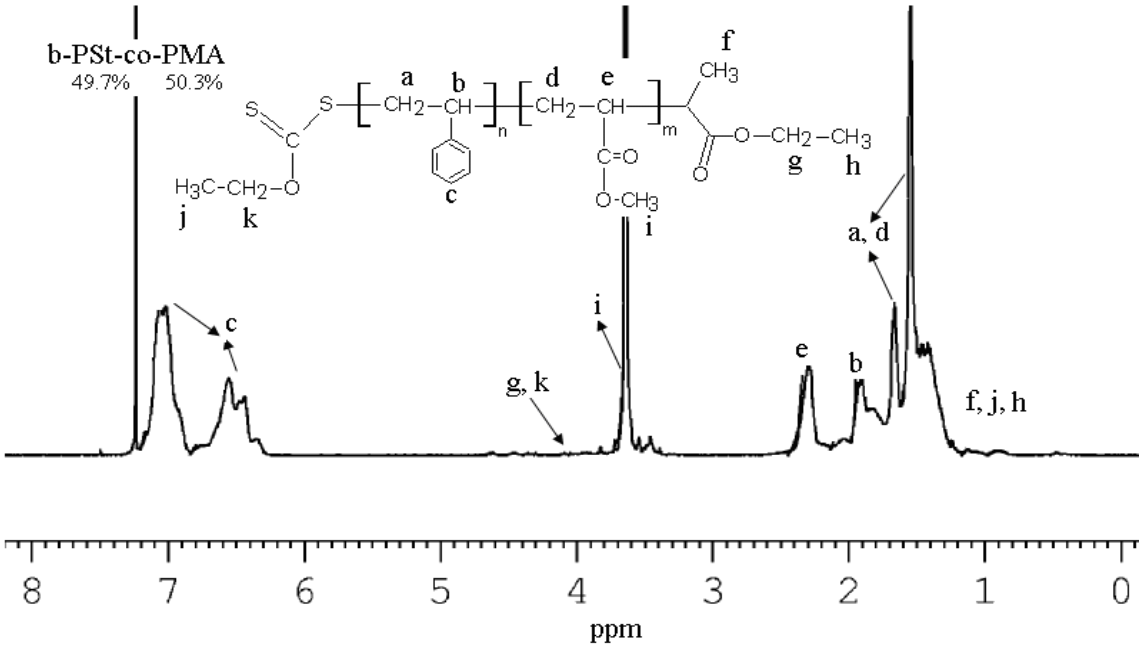

Figure 8-18: ^{1}H-NMR spectrum of b-PSt-co-PMA, St was polymerized first and MA was polymerized in the second stage under semi-batch conditions, sample was taken at the end of the reaction.

Compared with the ^{1}H-NMR spectra of PMA (Fig. 8-15) the b-PMA-co-PSt polymer produced (Fig. 8-17) has three new proton signals; at 6.25-7.22ppm, peak c, corresponding to phenyl group from styrene (at 6.25-6.84ppm for meta H from the aromatic ring and at 6.84-7.22 ppm corresponding to ortho- and para- H from the aromatic ring); at 1.8 ppm (k) for C**H** of polystyrene backbone and at 2.4 ppm (b) corresponding to C**H$_2$** absorbance of the main PSt chain. Similarly, compared with the ^{1}H-NMR spectra of PSt (Fig. 8-14) the produced b-PSt-co-PMA polymer (Fig. 8-18) has three new proton signals; at 3.65 ppm corresponding to the methyl group (OC**H$_3$**) of the methyl ester; at 1.6 ppm and at 2.3 ppm (d and e) corresponding to the absorbance

of CH_2 and CH of the main PMA chain, respectively. These results give further support that the polymer produced is a block copolymer.

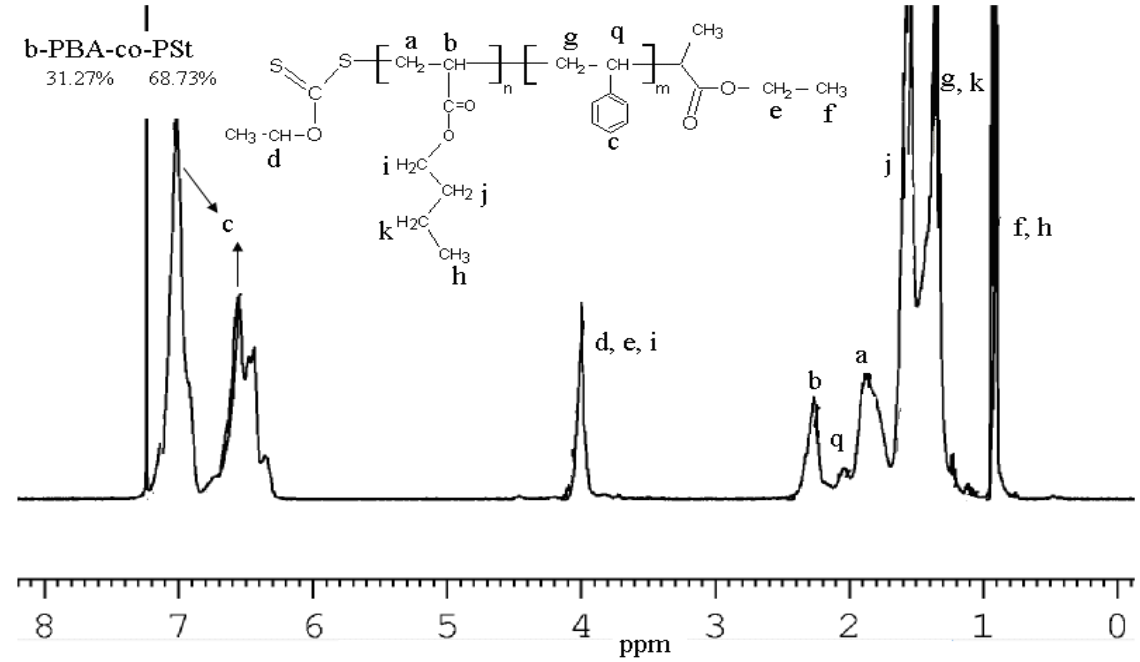

Figure 08-19: ^{1}H-NMR spectrum of b-PBA-co-PSt, BA was polymerized first and St was polymerized under semi-batch conditions, sample was taken at the end of the reaction.

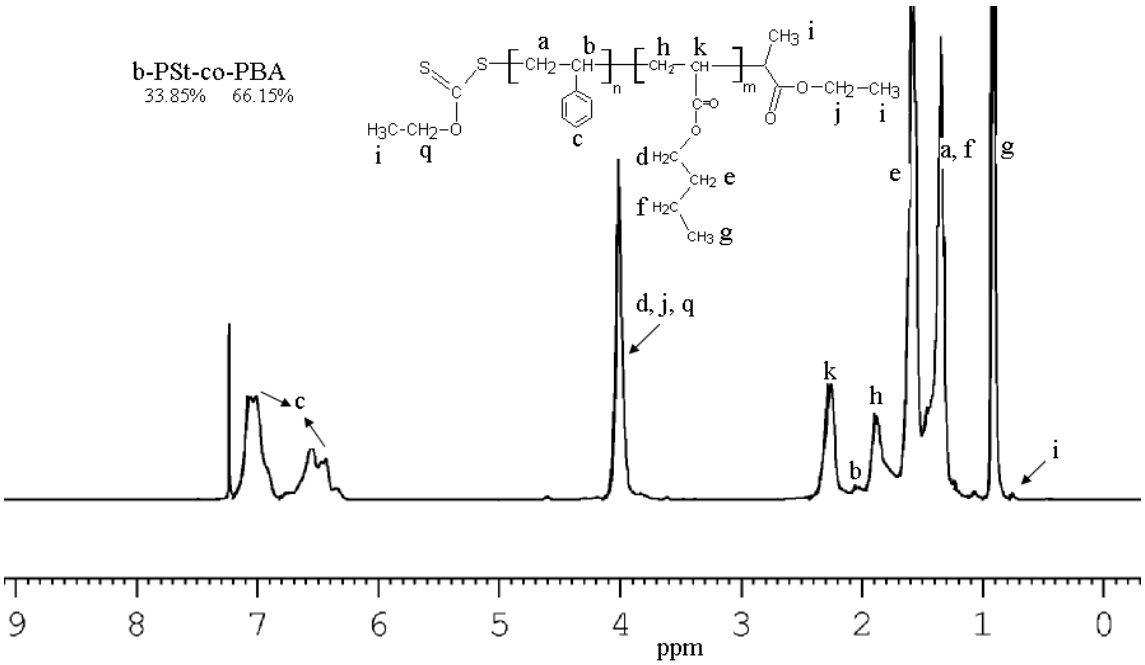

Figure 8-20: ^{1}H-NMR spectrum of b-PSt-co-PBA, St was polymerized first and BA was polymerized under semi-batch conditions, sample was taken at the end of the reaction.

Analysis of the diblock copolymer (b-PBA-co-PSt, Fig. 8-19), affords a spectrum that demonstrates the resonances of the parent PBA (first block) as indicated by the resonance of OC**H$_2$** (belonging to butyl acrylate) at 4.0 ppm, and additional resonances that correspond with polystyrene illustrated by the presence of styrene aromatic protons (Phenyl group: C$_6$**H$_5$**-) appear at 6.25-7.22 ppm. Similarly, ^{1}H-NMR spectra of b-PSt-co-PBA (Fig. 8-20) demonstrates representative peaks of the two blocks. Aromatic protons of polystyrene (C$_6$**H$_5$**-) were observed between 6.25 and 7.22 ppm and methylene oxide proton (OC**H$_2$**) was evident at 4.0 ppm.

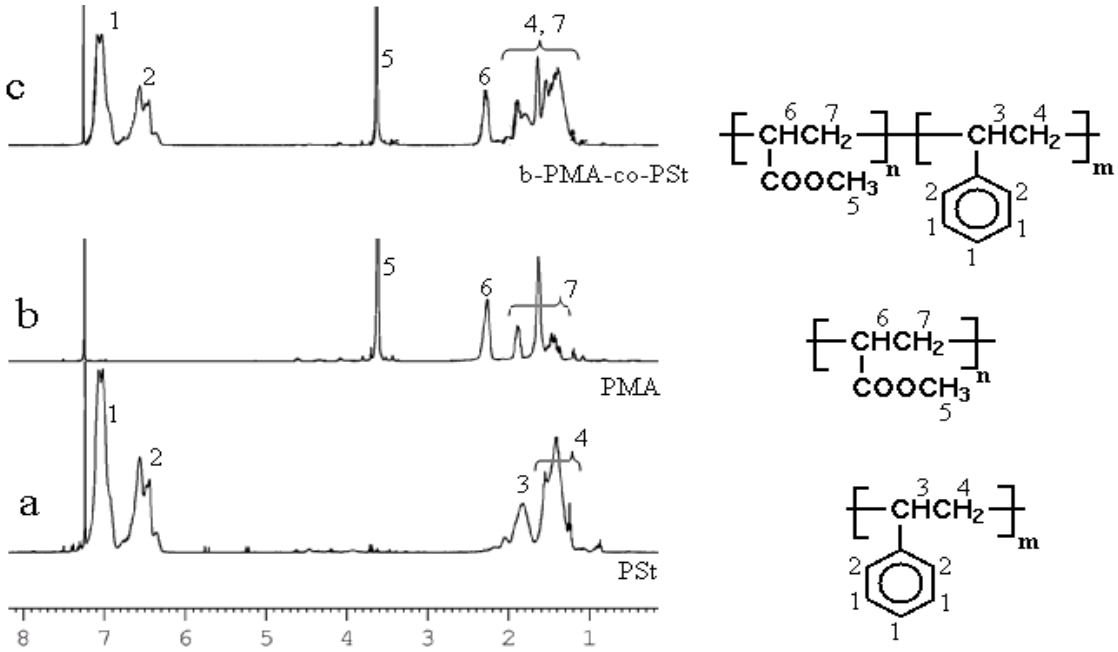

Figure 8-21: ^{1}H-NMR spectrum of PSt (a); PMA (b) and b-PMA-co-PSt (c). MA was polymerized first and St was polymerized in the second stage under batch conditions, sample was taken at the end of the reaction.

Figures 8-21 and 8-22 show the H-NMR spectra of the produced block copolymer (C) and those of the individual blocks. It was shown previously that chain extending PMA with PSt under batch conditions resulted in high polydispersity block copolymer due to the formation of PSt homopolymer in the newly formed particles (reaction 4). By carefully inspecting Fig. 8-21 and comparing it with Figures 8-17 and 8-18, it can be seen that peak 4 in Fig. 8-21a still appears in Fig. 8-21c, which may indicate the

presence of PSt homopolymer, and that not all of St monomer was incorporated in the second block.

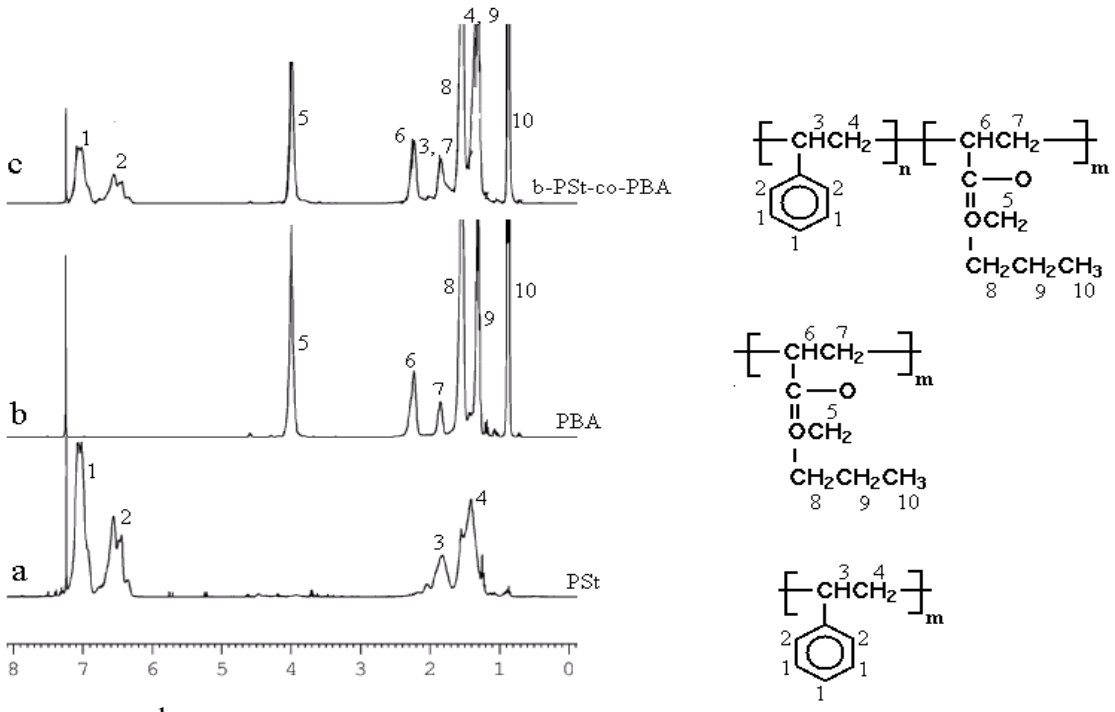

Figure 8-22: ^{1}H-NMR spectrum of PSt (a); PBA (b) and b-PSt-co-PBA (c). St was polymerized first and BA was polymerized in the second stage under semi-batch conditions, sample was taken at the end of the reaction.

Styrene, butyl acrylate and methyl acrylate mole fractions in the block copolymer, F_{St}, F_{BA} and F_{MA}, respectively, are determined from the integrals of the peaks Aar (area of the aromatic ring peak (Phenyl: C_6H_5- group) of PSt), A_{OCH_2} (area of the methylene peak (-OCH_2- group) of PBA). For b-PBA-co-PSt and b-PSt-co-PBA, peak Aar corresponds to five protons from PSt block which appears between 6.25-7.25 ppm, while peak A_{OCH_2} is assigned to the resonance of -OCH_2- group of PBA block at 4ppm. In the case of the b-PS-co-PMA and b-PMA-co-PSt block copolymers, the analysis of the copolymer composition is deduced from the integrals of the peaks Aar and A_{OCH_3} which results from the resonance of C_6H_5- group of PS and OCH_3- group (3.65 ppm) of PMA, respectively.

To evaluate the copolymer composition from the ^{1}H NMR spectrum, the following equations were used:

For b-PS-co-PBA and b-PBA-co-PSt copolymers:

$$\%PS = [\,2 \cdot A_{ar} / (2 \cdot A_{OCH_2} + 5 \cdot A_{ar})\,] \times 100$$

$$\%PBA = [\,5 \cdot A_{OCH_2} / (2 \cdot A_{OCH_2} + 5 \cdot A_{ar})\,] \times 100$$

For b-PS-co-PMA and b-PMA-co-PSt copolymers:

$$\%PS = [\,3 \cdot A_{ar} / (3 \cdot A_{OCH_3} + 5 \cdot A_{ar})\,] \times 100$$

$$\%PMA = [\,5 \cdot A_{OCH_3} / (3 \cdot A_{OCH_3} + 5 \cdot A_{ar})\,] \times 100$$

Composition results of the block copolymers produced are presented in Table 8-2. For b-PSt-co-PBA polymer, ^{1}H-NMR spectroscopy (in Fig. 8-20) shows that the copolymer exhibits the expected composition (33.15 mol-% styrene units versus 66.15 mol-% BA units), providing further evidence of the absence of homopolymer. It has been shown so far that BA is being incorporated into the polymer chains (^{1}H-NMR, Fig. 8-20) and that Mn increases with conversion according to theory (Fig. 8-8b), and that the block copolymer formed in reaction 9 contains almost exclusively RAFT end-capped chains (Fig. 8-13b).

8.5 Conclusions

The preparation of block copolymers under emulsion polymerization using low active RAFT was achieved. First, *ab initio* emulsion polymerizations of styrene, methyl acrylate and butyl acrylate were separately performed to prepare seed particles containing a low molecular weight polymer (first block) attached with xanthate. The addition of a low active RAFT agent to the butyl acrylate or methyl acrylate systems caused no significant rate retardation as compared with styrene system, while still yielding relatively good control over the polymer molecular weight. Well-defined PMA (PDI = 1.63) and PBA (PDI = 1.70) homopolymers particles were synthesized.

Low molecular weight polymers of butyl acrylate and methyl acrylate prepared in the first stage were used as the polymeric RAFT agent to polymerize styrene in the second

stage under batch and semi-batch emulsion conditions to provide well-defined block copolymers (b-PMA-co-PSt and b-PBA-co-PSt) with narrow molecular weight distributions. Under batch conditions, the formation of new particles that contain uncontrolled homopolymer resulted in high polydispersity as the produced polymer is a mixture of block copolymer located in the original particles and uncontrolled homopolymer located in the new particles along with the presence of terminated species in both types of particles. Thus, it is concluded that secondary nucleation in RAFT systems is highly undesirable and must be avoided.

The process was further optimized by performing semi-batch polymerization, in which the second monomer was gradually added to the reactor. This resulted in a block copolymer of high purity and relatively low polydispersity as compared with that produced under batch conditions. The choice of block sequence is important in reducing the influence of terminated chains on the distributions of polymers that were obtained. We found that polymerizing styrene first followed by the high active acrylate monomers resulted in much pure block copolymers with low polydispersity. This is because the transfer rate of the acrylic radical to polystyrene-xanthate dormant chain is high. Finally, it has been demonstrated that living polymerization can be approached by using semi-batch emulsion polymerization operating under starved-feed conditions.

Table 8-1: First stage emulsion polymerization recipe and experimental results.

First stage

I. Batch emulsion polymerization of methyl acrylate with AR to produce PMA-A seed particles (A: RAFT moiety S=C(OEt)S-) (Reaction 1)

Recipe		Conditions		Final results: PMA-A	
Water	450g	Temperature	70°C	Conversion	99.2%
Methyl acrylate	150g	Agitation speed	350rpm	Solid content (wt/wt)	24.53%
KPS	0.20g	Time	3 hours	Mn (calc, Eq. 8-3, Ctr ≈ 2.0)	9194
RAFT agent	3.85g	Mo/ARo	107	Mn (measured)	8991
SDS	2.76g			PDI	1.63
Buffer	0.08g			Average size: dp (nm)	49.9
				Particle number: Nc (cm^{-3})	2.12×10^{18}

II. Batch emulsion polymerization of butyl acrylate with AR to produce PBA-A seed particles (A: RAFT moiety S=C(OEt)S-) (Reaction 2)

Recipe		Conditions		Final results: PBA-A	
Water	450g	Temperature	70°C	Conversion	98.9%
Butyl acrylate	150g	Agitation speed	350rpm	Solid content (wt/wt)	24.45%
KPS	0.20g	Time	5 hours	Mn (calc, Eq 8-3, Ctr ≈ 1.5)	9194
RAFT agent	3.85g	Mo/ARo	72	Mn (measured)	9046
SDS	2.76g			PDI	1.70
Buffer	0.08g			Average size: dp (nm)	39.4
				Particle number: Nc (cm^{-3})	4.25×10^{18}

III. Batch emulsion polymerization of styrene with AR to produce PSt-A seed particles (A: RAFT moiety S=C(OEt)S-) (Reaction 3)

Recipe		Conditions		Final results: PSt-A	
Water	450g	Temperature	70°C	Conversion	94%
Styrene	150g	Agitation speed	350rpm	Solid content (wt/wt)	23.25%
KPS	0.20g	Time	6 hours	Mn (calc, Eq 8-3, Ctr ≈ 0.7)	9194
RAFT agent	3.85g	Mo/ARo	88.28	Mn (measured)	9928
SDS	2.76g			PDI	2.17
Buffer	0.08g			Average size: dp (nm)	-
				Particle number: Nc (cm^{-3})	-

Table 8-2: Second stage emulsion polymerization recipe and experimental results.

Second stage

I. Batch emulsion polymerization of styrene in PMA-A seed particles produced from first stage I to produce b-PMA-co-PSt (Reaction 4)

Recipe		Conditions		Final results: b-PMA-co-PSt-A	
PMA seeds (24.55% solids)	260g	Temperature	70°C	Conversion	88%
PMA mass	63.8g	Agitation speed	350rpm	Solid content (wt/wt)	23%
water	200g	Time	4 hours	Mn (calc, Eqs. 8-3, Ctr ≈ 1.2)	26427
KPS	0.15g	Flow rate	0.0g/min	Mn (measured, GPC)	25722
SDS	0.15g	Solid content		PDI	3.6
Buffer	0.08g	with 200 g	13.8 %	PMA % (^{1}H-NMR)	41.72
Styrene	100g	water (wt/wt)		PSt % (^{1}H-NMR)	58.28
		Nc (cm^{-3})	9.05×10^{17}	Secondary nucleation observed	

II. Batch emulsion polymerization of styrene in PBA-A seed particles produced from first stage II to produce b-PBA-co-PSt (Reaction 5)

Recipe		Conditions		Final results	
PBA latex (24.45% solids)	260 g	Temperature	70°C	Conversion	94.8%
PBA mass	63.57g	Agitation speed	350rpm	Solid content (wt/wt)	25.7
water	200g	Time	4 hours	Mn (calc, Eqs. 8-3, ≈ 1.2)	24984
KPS	0.15g	Flow rate	0.00g/min	Mn (measured, GPC)	23633
SDS	0.15g	Solid content		PDI	2.8
Buffer	0.08g	with 200 g	13.8 %	PBA % (^{1}H-NMR)	39.90
Styrene	100g	water (wt/wt)		PSt % (^{1}H-NMR)	60.10
		Nc (cm^{-3})	1.8×10^{18}	Secondary nucleation observed	

III. Semi-batch emulsion polymerization of styrene in PMA-A seed particles produced from first stage I to produce b- PMA-co-PSt (Reaction 6)

Recipe		Conditions		Final results	
PMA latex (24.62% solids)	240g	Temperature	70°C	Conversion	99.5%
PMA mass	59.1g	Agitation speed	350rpm	Solid content (wt/wt)	29.4
water	200g	Time	4 hours	Mn (calc, Eqs. 8-3 & 8-4)	24233
KPS	0.15g	Flow rate	0.25g/min	Mn (measured)	21489
SDS	0.15g	Total added St	60.6g	PDI	1.81
Buffer	0.08g	Solid content		PMA % (^{1}H-NMR)	37.0%
Initial Methyl acrylate	40g	with 200 g	12.3%	PSt % (^{1}H-NMR)	63.0%
		water (wt/wt)		Ctr used to fit Exp. Mn	>3
		Nc (cm^{-3})	8.39×10^{17}	Insignificant secondary nucleation	

IV. Semi-batch emulsion polymerization of styrene in PBA-A seed particles produced from first stage II to produce b- PBA-co-PSt (Reaction 7)

Recipe		Conditions		Results	
PBA latex (24.45% solids)	200g	Temperature	70°C	Conversion	98.8%
PBA mass	48.9g	Agitation speed	350rpm	Solid content (wt/wt)	29.6
water	200g	Time	3 hours	Mn (calc, Eqs. 8-3 & 8-4)	27710
KPS	0.15g	Flow rate	0.33g/min	Mn (measured)	24696
SDS	0.15g	Total added St	60.2g	PDI	1.70
Buffer	0.08g	Solid content		PBA % (^{1}H-NMR)	31.27%
Initial styrene charge	40 g	with 200 g	11.1 %	PSt % (^{1}H-NMR)	68.73%
		water (wt/wt)		Ctr used to fit Exp. Mn	>3
		Nc (cm^{-3})	1.4×10^{18}	No secondary nucleation	

V. Semi-batch emulsion polymerization of methyl acrylate in PSt-A seed particles produced from first stage III to produce b-PSt-co-PMA (Reaction 8)

Recipe		Conditions		Results	
PSt-A latex (17.4% solids)	503g	Temperature	70°C	Conversion	97%
PSt mass	87.9g	Agitation speed	350rpm	Solid content (wt/wt)	24.7
water	200g	Time	3 hours	Mn (calc, Eqs. 8-3 & 8-4)	22645
KPS	0.05g	Flow rate	0.33g/min	Mn (measured)	20365
SDS	0.15g	Total added MA	60.07g	PDI	1.64
Buffer	0.08g	Solid content		PMA % (^{1}H-NMR)	50.30%
Initial MA charge	40g	with 200 g	12.5 %	PSt % (^{1}H-NMR)	49.70%
		water (wt/wt)		Ctr used to fit Exp. Mn	>3
				No secondary nucleation	

VI. Semi-batch emulsion polymerization of butyl acrylate in PSt-A seed particles produced from first stage III to produce b-PSt-co-PBA (Reaction 9)

Recipe		Conditions		Results	
PSt latex (17.4% solids)	303g	Temperature	70°C	Conversion	90.8%
PSt mass	52.9g	Agitation speed	350rpm	Solid content (wt/wt)	26.9
water	200 g	Time	3.5 hours	Mn (calc, Eqs. 8-3 & 8-4)	29390
KPS	0.05g	Flow rate	0.426g/min	Mn (measured)	26541
SDS	0.15g	Total added BA	89.5g	PDI	1.47
Buffer	0.08g	Solid content		PBA % (^{1}H-NMR)	66.15%
Initial BA charge	40g	with 200 g	10.3 %	PSt % (^{1}H-NMR)	33.85%
		water (wt/wt)		Ctr used to fit Exp. Mn	>3
				No secondary nucleation	

Table 8-3: Parameters used to calculate the rate of RAFT agent transportation and consumption.

Parameter	Value	Reference
D_{AR}	$2\times10^{-7}\ dm^2/s$	(Smulders, 2002)
k_p	$2.60\times10^{2}\ mol/dm^3.s$	(Thickett and Gilbert, 2006)
$k_{tr}^{AR}\ (C_{tr}k_p)$	$1.82\times10^{2}\ mol/dm^3.s$	(Smulders *et al.*, 2003)
$C_w^{sat,AR}$	$2\times10^{-3}\ mol/dm^3$	(Smulders *et al.*, 2003)
C_p	$5.5\ \ mol/dm^3$	(Gilbert, 1995)
$r\ \ (RAFT_o/Monomer_o)$	0.01	
d_s	$5\times10^{-7}-1\times10^{-6}\ dm$	assumed

8.6 References

Apostolovic, B.; Quattrini, F.; Butte, A.; Storti, G. and Morbidelli, M., 2006. Ab initio emulsion polymerization by RAFT (reversible addition-fragmentation chain transfer) through the addition of cyclodextrins. *Helvetica Chimica Acta*, 89(8): 1641.

Bowes, A.; Mcleary, J.B. and Sanderson, R.D., 2007. AB and ABA type butyl acrylate and styrene block copolymers via RAFT-mediated miniemulsion polymerization. *Journal of Polymer Science Part A: Polymer Chemistry*, 45(4): 588.

Chong, Y.K.; Le, T.P.T.; Moad, G.; Rizzardo, E. and Thang, S.H., 1999. A More Versatile Route to Block Copolymers and Other Polymers of Complex Architecture by Living Radical Polymerization: The RAFT Process. *Macromolecules*, 32(6): 2071.

de Brouwer, H.S., M. A. J.; Klumperman, B.; Monteiro, M. J.; German, A. L. , 2000. Controlled radical copolymerization of styrene and maleic anhydride and the synthesis of novel polyolefin-based block copolymers by reversible addition-fragmentation chain-transfer (RAFT) polymerization. *Journal of Polymer Science Part A: Polymer Chemistry*, 38(19): 3596.

Gilbert, R.G., 1995. Emulsion polymerization: a mechanistic approach. Academic Press, London.

Hartmann, J.; Urbani, C.; Whittaker, M.R. and Monteiro, M.J., 2006. Effect of degassing on surfactant-free emulsion polymerizations of styrene mediated with RAFT. *Macromolecules*, 39(3): 904.

Jin, Y.; Hahn, Y.B.; Nahm, K.S. and Lee, Y., 2005. Preparation of stable polyurethane-polystyrene copolymer emulsions via RAFT polymerization process. *Polymer*, 46(25): 11294.

Kanagasabapathy, S.; Claverie, J. and Uzulina, I., 1999. Synthesis of well defined triblock copolymer by reversible addition fragmentation chain transfer (RAFT) polymerization in emulsion. *American Chemical Society, Polymer Priprints, Division of Polymer Chemistry*, 40(2): 1080.

Kanagasabapathy, S.; Sudalai, A. and Benicewicz, B.C., 2001. Reversible addition-fragmentation chain-transfer polymerization for the synthesis of poly(4-acetoxystyrene) and poly(4-acetoxystyrene)-block-polystyrene by bulk, solution and emulsion techniques. *Macromolecular Rapid Communications*, 22(13): 1076.

Mayadunne, R.T.A.; Rizzardo, E.; Chiefari, J.; Krstina, J.; Moad, G.; Postma, A. and Thang, S.H., 2000. Living Polymers by the Use of Trithiocarbonates as Reversible Addition-Fragmentation Chain Transfer (RAFT) Agents: ABA Triblock Copolymers by Radical Polymerization in Two Steps. *Macromolecules*, 33(2): 243.

Monteiro, M.J.; Sjoberg, M.; Van der Vlist, J. and Gottgens, C.M., 2000. Synthesis of butyl acrylate-styrene block copolymers in emulsion by reversible addition-fragmentation chain transfer: effect of surfactant migration upon film formation. *Journal of Polymer Science, Part A: Polymer Chemistry*, 38(23): 4206.

Mueller, A.H.E.; Yan, D.; Litvinenko, G.; Zhuang, R. and Dong, H., 1995. Kinetic Analysis of "Living" Polymerization Processes Exhibiting Slow Equilibria. 2. Molecular Weight Distribution for Degenerative Transfer (Direct Activity Exchange between Active and "Dormant" Species) at Constant Monomer Concentration. *Macromolecules*, 28(22): 7335.

Perrier, S.T., P., 2005. Macromolecular design via reversible addition-fragmentation chain transfer (RAFT)/xanthates (MADIX) polymerization. *Journal of Polymer Science Part A: Polymer Chemistry*, 43(22): 5347.

Reda Fleet; McLeary, J.B.; Grumel, V.; Weber, W.G.; Matahwa, H. and Sanderson, R.D., 2007. Preparation of New Multiarmed RAFT Agents for the Mediation of Vinyl Acetate Polymerization. *Macromolecular Symposia*, 255: 8.

Rivera, M.R.; Rodriguez-Hernandez, A.A.; Hernandez, N.; Castillo, P.; Saldivar, E. and Rios, L., 2005. Controlled/Living Free Radical Copolymerization of Styrene and Butyl Acrylate in Bulk and Emulsion with Industrial Monomers. Influence of Monomer Addition on Polymer Properties. *Ind. Eng. Chem. Res.*, 44(8): 2792.

Save, M.; Manguian, M.; Chassenieux, C. and Charleux, B., 2005. Synthesis by RAFT of amphiphilic block and comblike cationic copolymers and their use in emulsion polymerization for the electrosteric stabilization of latexes. *Macromolecules*, 38(2): 280.

Smulders, W.W., 2002. Macromolecular architecture in aqueous dispersions: 'living' free-radical polymerization in emulsion. Ph.D. Thesis, Technische Universiteit Eindhoven, Eindhoven, Neth.

Smulders, W.W.; Gilbert, R.G. and Monteiro, M.J., 2003. A kinetic investigation of seeded emulsion polymerization of styrene using reversible addition-fragmentation chain transfer (RAFT) agents with a low transfer constant. *Macromolecules*, 36(12): 4309.

Smulders, W.W. and Monteiro, M.J., 2004. Seeded emulsion polymerization of block copolymer core-shell nanoparticles with controlled particle size and molecular weight distribution using xanthate-based RAFT polymerization. *Macromolecules*, 37(12): 4474.

Thickett, S.C. and Gilbert, R.G., 2006. Rate-controlling events for radical exit in electrosterically stabilized emulsion polymerization systems. *Macromolecules*, 39(6): 2081.

Chapter Nine

Conclusions and Future Directions

Chapter 9
Conclusions and Future Directions

9.1 Conclusions

The flexibility of free-radical polymerization (FRP) and its applicability to a wide range of monomers under different reaction conditions makes it an attractive industrial technique for the production of commercial polymeric materials. However, this technique shows very little control over the molecular weight of the final product. Additionally, the synthesis of sophisticated macromolecular architectures, such as block copolymers, star polymers or comb polymers, is not possible with FRP. The necessity of having good control in polymerization systems led to the development of controlled/living free radical polymerization (CLFRP). The significant advantages of CLFRP permit the preparation of a wide range of different materials which are either difficult to prepare, or not available via other polymerization processes. Reversible addition–fragmentation chain transfer process (RAFT process) is the most flexible CLFRP technique which is able to induce living behaviour for a wide range of monomers via a range of initiation methods and at varying reaction temperatures.

Emulsion polymerization is one of the FRP techniques and is an important process for the polymer industry, as it has significant advantages over bulk and solution polymerizations. Furthermore, emulsion polymerization is a water based system and hence it is an environmentally friendly process. This thesis focuses on the application of RAFT process in emulsion polymerization, as the combination of the advantages of RAFT process and emulsion polymerization in a single process offers an ideal route for polymer production, and will lead to a wider range of macromolecular architectures.

To gain an adequate knowledge in order to incorporate RAFT mechanism in emulsion polymerization mechanism, the application of RAFT process in solution and bulk polymerizations was investigated. A mathematical model of the novel RAFT mediated free radical polymerization in homogenous systems was developed. The model was

integrated with the chain-length-dependent termination model to account for the effect of RAFT agent on the termination reaction. Careful simulations of conversion versus time were carried out for solution polymerization of styrene in toluene with a high active RAFT agent. It was found that slow fragmentation of the intermediate radical cannot be used alone to explain the observed retardation. Simulations indicated that the use of a high active RAFT agent reduces the gel effect and increases the average termination rate coefficient via reducing the molar mass distribution of the propagating radicals. Along with the intermediate radical termination, simulations also showed that the reduction in the gel effect is one of the main reasons behind the observed retardation, especially for the systems employing highly active RAFT agents.

The application of RAFT in emulsion polymerization is an important factor when it comes to industrial acceptance. Thus, the RAFT process has also been performed in *ab initio* emulsion polymerization of styrene. A mathematical model, which is the core component of this study, was developed to simulate the emulsion polymerization of styrene with low active RAFT-based transfer agent. The main objective was to develop a practical tool to predict key product properties such as monomer conversion, molecular weight distribution (MWD) and particle size distribution (PSD). The model was solved using an efficient numerical scheme suitable for online monitoring and control. A number of simulations with variable concentrations of RAFT agent, monomer, surfactant and initiator at different reaction temperatures were carried out and compared with experimental data obtained from our laboratory. Good agreement between the model predictions and experimental results were obtained. Under batch conditions, the effects of the xanthate transfer agent (AR), surfactant (SDS), initiator (SPS) and temperature were investigated. The polymerization rate (Rp), the number average molecular weight (Mn) and the particle size (r) decreased with increasing AR. Rp increased with increase in SDS and SPS, while with increase in temperature, Mn decreased, Rp increased and r increased. The observed rate retardation was attributed to the exit and re-entry of small radicals. Experimental data on polymer molecular weight suggested that the partitioning coefficient of the RAFT agent between water and polymer phases was close to that for the monomer, and hence a rapid thermodynamic equilibrium was achieved.

The model was further validated against experimental data obtained from semi-batch emulsion polymerization of styrene under variable conditions. O-ethylxanthyl ethyl propionate was used as a RAFT agent in *ab initio* semi-batch emulsion polymerization of styrene. During the period of monomer feed (second stage), Mn increased with time due to the increase in monomer-AR molar ratio in the particle. When RAFT agent was fed along with monomer, no change in the evolution of Mn with time was observed, indicating that a rapid thermodynamic partitioning was achieved. In addition, the living nature of the used RAFT agent was confirmed by the shift of the unimodal molecular weight distribution for the extended polystyrene-xanthate chains towards higher molecular weights. Thus, it was concluded that real living polymerization with low active RAFT agent can be approached by operating under semi-batch conditions. Under certain reaction conditions, secondary nucleation was observed and attributed to the frustrated entry of the z-mer into the glassy particles, accompanied by the drop in free surfactant concentration below the cmc. Up to this point, it has been concluded that secondary nucleation is highly undesirable in RAFT systems.

A calorimetric model was developed and used to determine the heat of reaction dynamically from temperature measurements. The rate of polymerization, which is proportional to the heat of reaction, was then estimated and integrated to obtain the overall monomer conversion. The calorimetric model was found to be capable of estimating polymer molecular weight via simultaneous estimation of monomer and AR concentrations. The calorimetric model was validated offline for batch and semi-batch emulsion polymerization of styrene with and without RAFT agent.

A multi-objective dynamic optimisation method for the calculation of the optimal control policies for polymer composition, PSD, MWD and Mn in a semi-batch RAFT-emulsion polymerisation was developed. The optimisation problem was formulated as a multi-objective optimisation by reformulating the multi-objective problem as a single-objective case by placing some objectives in the form of constraints. By using monomer feed rate as the primary control variable, the optimisation procedure was able to minimize the reaction time and simultaneously obtain a polymer with a desired quality (conversion, particle size and molecular weight distribution). The obtained optimal policies were validated experimentally and a good agreement was obtained.

Eventually, the knowledge gained in this study has been applied toward the creation of macromolecular architectures in aqueous dispersions in the form of block copolymers of styrene/methyl acrylate and styrene/butyl acrylate. First, *ab initio* emulsion polymerizations of styrene, methyl acrylate and butyl acrylate were performed separately to prepare seed particles containing low molecular weight polymer (first block) attached with xanthate. The produced homopolymers of PMA and PBA were then separately chain-extended by the addition of styrene in the second stage under batch and semi-batch conditions. Under batch conditions the formation of new particles that contain uncontrolled homopolymers resulted in a high polydispersity and low blocking efficiency. Thus, it was concluded that secondary nucleation in RAFT systems is highly undesirable and must be avoided.

For livingness and desirable block copolymer, optimal results were obtained when styrene was polymerized under semi-batch conditions. Under semi-batch conditions monomer was slowly added to the reactor, thereby resulting in low monomer concentration and artificially increasing the transfer rate over the propagation rate. As such, monomer units were slowly added to the first block and a high purity block copolymer was produced. The choice of block sequence is important in reducing the influence of terminated chains on the distributions of polymer that were obtained. It was found that polymerizing styrene first followed by the high active acrylate monomers resulted in a block copolymer with high purity and low polydispersity. Finally, it was demonstrated that living polymerization can be achieved by using semi-batch emulsion polymerization operating under controlled feed conditions. GPC (dual-detection) and NMR spectroscopy analysis showed that the produced polymer is indeed of high purity block copolymer.

9.2 Future Directions

During this study it was observed that polymer engineering is a vast area for research and there remains large scope for improvement in this field of study. Despite the great deal of effort and the substantial progress that have been achieved in this thesis, it is clear that there are still a number of issues to be addressed for improving the advanced operation of RAFT-emulsion polymerization processes. To expand the scope of this thesis, some of the future potential areas that deserve attention are outlined below:

1. The mathematical model developed in this work for RAFT emulsion polymerization of styrene provides by its nature the simplest way to study emulsion polymerization systems that employs RAFT process. The use of this model to study emulsion polymerization of other monomers is recommended.

2. The model was developed to account for the application of low active RAFT agents since this kind of transfer agents obeys zero-one kinetics. For high active RAFT agents the mechanism is different and termination reaction is not instantaneous, this implies that zero-one kinetics is not valid for such systems. However, it has been shown in literature that emulsion polymerization with high active RAFT agent obeys zero-one kinetics at low conversions. Thus, the model should be further modified by integrating both zero-one and pseudo-bulk kinetics, along with the inclusion of a RAFT induced exit mechanism.

3. RAFT agent transportation from monomer droplet to polymer particles through the aqueous phase is one of the main problems that hinder the application of high active RAFT agent in emulsion polymerization. Miniemulsion polymerization is considered to be one of the ideal alternatives to overcome such a problem, since the entire amount of RAFT agents is concentrated in the monomer droplets which are the location of the polymerization reaction. With this in mind, the most obvious area for future work is to extend into miniemulsion processes.

4. Despite their high economic value, it is well known that copolymerization processes are very complex in nature and thus pose a major challenge in academia and industry alike. Nevertheless, the model developed in this work can be used as a basis for the development of a RAFT-copolymerization model. Issues regarding the control of the copolymer PSD and MWD and its composition should be important targets of any future study.

5. As shown in this thesis, the high water solubility of the xanthate creates the potential for an emulsion-based system to be developed, eliminating the need for the hyrdophobe and the application of high shear. With this in mind, the system

described in this work can be considered as a promising one for industrial applications and hence a large scale investigation is an obvious areas for future work.

6. As already mentioned, CLFRP are currently most attractive as a means to create polymers of well-defined and unique architectures. With this as the objective, block copolymers of styrene/methyl acrylate and styrene/butyl acrylate were successfully produced as presented in this work. It is then of significant importance to use the technique shown in this work to produce di and tri-block copolymer of different monomers. Additionally, the formation of block copolymers, and particles with core-shell morphology could also be developed.